Co-pyrolysis of lignocellulosic biomass and plastic wastes and catalytic deoxygenation of the products over modified HZSM-5

Yehya Jaafar

Normandie Université

THESES

Pour obtenir le diplôme de doctorat

Spécialité Génie des Procédés

Préparée au sein de « l'Institut National des Sciences Appliquées de Rouen Normandie » et « Université libanaise »

Co-pyrolysis of Lignocellulosic Biomass and Plastic Wastes and Catalytic Deoxygenation of the Products over modified HZSM-5

Presented and defended by

Yehya JAAFAR

Thesis publicly defended on December 14, 2022, before the jury:		
M. Yann ROGAUME	Professeur des Universités, Université De Lorraine	Rapporteur
M. Ammar BENSAKHRIA	MCF HDR, Université de Technologie de Compiègne UTC	Rapporteur
M. Edmond ABI-AAD	Professeur des Universités, Université du Littoral Côte d'Opale	Examinateur
Mme. Chetna MOHABEER	R&D Engineer, Holcim innovation Center	Examinatrice
M. Antoine EL SAMRANI	Professeur des Universités, Université Libanaise	Co-Directeur de thèse
M. Roland EL HAGE	Professeur des Universités, Université Libanaise	Co-Directeur de thèse
M. Lokmane ABDELOUAHED	MCF HDR, INSA Rouen Normandie	Co-Encadrant de thèse
M. Bechara TAOUK	Professeur des Universités, INSA Rouen Normandie	Directeur de thèse

Thesis directed by Bechara TAOUK and co-supervised by Lokmane ABDELOUAHED, Laboratoire de Sécurité des Procédés Chimiques - LSPC and co-directed by Antoine EL SAMARANI, Laboratory of Geoscience, Georesources and Environment (L2GE) and Roland EL HAGE, Laboratory of Physical Chemistry of Materials (LCPM), EDST-PR2N (Platform for Research in NanoSciences and NanoTechnology).

INSA ROUEN NORMANDIE

ED PSIME

LSPC Laboratoire de sécurité des procédés chimiques

Plateforme de Recherche en NanoSciences et Nanotechnologie – Ecole Doctorale des Sciences et Technologie – Campus Fanar

الجامعة اللبنانية UNIVERSITE LIBANAISE

ACKNOWLEDGMENTS

First and foremost, I would like to thank God. He has given me the strength and encouragement throughout all the challenging moments of completing this dissertation. I am truly grateful for His unconditional and endless love, mercy, and grace.

I would like to express my deepest thanks to my thesis director, Bechara TAOUK, for welcoming me into the lab, for the trust and support given during the past three years, and for offering advice and encouragement. Lokmane ABDELOUAHED, you have played an outstanding role in supporting and offering the insight needed in the work done, I am so grateful. I wish to thank Antoine EL SAMRANI and Roland El HAGE my Lebanese supervisors for your continued presence, your serious and relevant scientific follow-up, and your commitment to my side throughout the thesis. To all the people who played a major role in moving the work forward: Bruno, Sylvie, Christine, Jeremy, Maria, and Ikram, thank you all!

I wish to acknowledge and thank INSA Rouen Normandie and Lebanese University for having funded this research work under the cotutelle program UL-UTT-INSA. I also wish to thank Prof. Yann ROGAUME and Dr. Ammar BENSAKHRIA for having approvingly accepted to be the rapporteurs for this Ph.D. thesis. Furthermore, I extend my gratitude to Prof. Edmond ABI-AAD and Dr. Chetna MOHABEER for taking the time and effort to be a part of my thesis jury.

I want to acknowledge and thank all my colleagues who have been a part of this journey; including all the permanent staff from LSPC and UL. I also wish to thank all the interns and students who worked on this project alongside me; Andreas and Gian. To my colleagues, Louis, Jandung, Michael, Bashar, Maxwell, Lillivet, Leonella, Minda, Laura, Alexandra, and Balkydia, thank you. To my beloved wife Hawraa, thank you for your extraordinary support, you have made countless sacrifices throughout the entire process. And last, but not least, I wish to thank my family, my mom, dad, brothers, and sister, for their exceptional love and support.

TABLE OF CONTENTS

LIST OF FIGURES

LIST OF TABLES

LIST OF ABBREVIATIONS AND SYMBOLS

Abbreviation	Definition
Fig.	Figure
GC	Gas chromatography
GC-MS	Gas chromatography-mass-spectroscopy
FID	Flame-Ionization detector
TCD	Thermal conductivity detector
^{1}H-NMR	Nuclear magnetic resonance spectroscopy
HDO	Hydrodeoxygenation
BW	Beech wood
HDPE	High-Density polyethylene
LDPE	Low-Density polyethylene
LLDPE	Linear low-density polyethylene
PE	Polyethylene
PET	Polyethylene terephthalate
PU	Polyurethane
PP	Polypropylene
PS	Polystyrene
PVC	Polyvinyl chloride
PPA	Polyphthalamide
MP	Mixed Plastic
HHV	Higher Heating Value
LHV	Lower Heating Value
PAH	Polycyclic aromatic hydrocarbon
BTX	Benzene, toluene, xylene

FT-IR	Fourier transform infrared spectroscopy
TAN	Acid number
N	Number of carbons in a given organic compound
n	Normal
ECN	Effective carbon number
TGA	Thermogravimetric analysis
Cal.	Calculated
Exp.	Experimental
n.a.	Not applicable
n.r.	Not reported
MTBE	Methyl tert-butyl ether
ETBE	Ethyl tert-butyl ether
XRD	X-ray diffraction spectroscopy
XRF	X-ray fluorescence spectroscopy
BET	Brunauer-Emmett-Teller
ICP-OES	Inductively coupled plasma optical emission spectroscopy
BJH	Barrett–Joyner–Halenda
RT	Retention Time
pH	Hydrogen potential
FCC	Fluidized catalytic cracking
SC	Semi-continuous
SEM	Scanning electron microscope

Symbol	**Symbol name**	**Unit**
m	Mass	[g]
z	Charge number	

(m/z)	Mass-to-charge ratio	[g.mol-1]
wt.%	Weight percentage	[%]
Vol%	Volume percentage	[%]
LHV	Lower heating value	[MJ.kg-1]
HHV	Higher heating value	[MJ.kg-1]
BP	Boiling point	°C
r^2	Pearson's coefficient of determination	
ID	Inner diameter	[m]
OD	Outer diameter	[m]
x_{th}	Expected weight percentage	[wt.%]
x_i	Experimental weight percentage of each product	[wt.%]
y_i	Liquid or gas yield of each plastic	[wt.%]
w_i	Weight percentage of each plastic in the plastic mix	[wt.%]
x_{th}	Expected weight percentage	[wt.%]
θ	Diffractometer angle	Degrees

ABSTRACT

The depletion of fossil fuels and the harmful consequences of greenhouse gases alongside the devastating plastics waste problem has highlighted the necessity of renewable energy and the development of new techniques to resolve the waste problem. Among the different renewable resources, biomass shows considerable potential. Lignocellulosic biomass (Beechwood (BW)) and plastic wastes (polystyrene (PS), low-density polyethylene (LDPE), high-density polyethylene (HDPE), polypropylene (PP)) can be pyrolyzed to produce liquid products that can be used as fuels or combustibles to replace fossil fuels. The objective of this thesis is to provide a detailed characterization of the products obtained from the co-pyrolysis of beechwood and thermoset plastics in a semi-continuous reactor while varying the temperature and the biomass/plastics ratio under 400 $mL.min^{-1}$ of nitrogen. As for plastic pyrolysis, they seem to crack to their basic monomers. For BW pyrolysis, the oil was rich with acids, ketones, and levoglucosan with a low energy heating value of around 18 MJ/kg and high oxygen content of around 41 wt.%. The co-pyrolysis of BW and PS yields the best results with a great reduction of oxygen to about 8 wt.% for the 50-50 BW-PS mixture. After that, a catalytic co-pyrolysis was carried out in the same reactor using several metal-modified zeolites (HZSM-5). Fe/Ni-ZSM-5 gave the best results in terms of bio-oil oxygen content and heating value.

The effect on the catalytic co-pyrolysis process of changing the pyrolysis reactor technology to a continuous fluidized bed reactor was also examined. It was found that there was a negligible difference between the 2 setups, yet the continuous bed reactor produced more oil allowing a better analysis of the latter. The oil splits into an organic and aqueous phase and the water content of each phase in all the experiments was computed to be as low as 0 to1 wt.% for the organic phase and between 50 to 70 wt.% for the aqueous phase. In the end, this work details the compositional analysis of pyrolytic and co-pyrolytic products along with their main characteristics to produce high-grade oil with the possible end-use of each product before and after catalytic treatment.

Keywords: Pyrolysis; biomass; plastics; catalyst; fluidized bed reactor; fixed bed reactor, beechwood.

RÉSUMÉ

L'épuisement des combustibles fossiles et les conséquences néfastes des gaz à effet de serre, ainsi que le problème dévastateur des déchets plastiques, ont mis l'accent sur les besoins aux énergies renouvelables et de développer de nouvelles techniques pour résoudre le problème des déchets. Parmi les différentes ressources renouvelables, la biomasse présente un intérêt considérable. La biomasse lignocellulosique (bois de hêtre (BW)) et les déchets plastiques (polystyrène (PS), polyéthylène basse densité (LDPE), polyéthylène haute densité (HDPE), polypropylène (PP)) peuvent être pyrolysés pour produire des carburants ou combustibles et remplacer les combustibles fossiles. L'objectif de cette thèse est de fournir une caractérisation détaillée des produits obtenus par la co-pyrolyse du bois de hêtre et des plastiques thermodurcis dans un réacteur semi-continu en faisant varier la température et le ratio biomasse/plastique sous 400 $mL.min^{-1}$ d'azote. En ce qui concerne la pyrolyse des plastiques, ils semblent craquer en leurs monomères de base. Pour la pyrolyse du BW, l'huile formée est riche en acides, cétones et lévoglucosane avec un faible pouvoir calorifique d'environ 18 MJ/kg et une forte teneur en oxygène d'environ 41 wt.%. La co-pyrolyse de BW et PS donne les meilleurs résultats avec une forte réduction de la teneur en oxygène à environ 8 wt.% pour le mélange 50-50 BW-PS. Ensuite, une co-pyrolyse catalytique a été réalisée dans le même réacteur en utilisant une HZSM-5 modifiée par les métaux fer et nickel. Le catalyseur Fe/Ni-ZSM-5 a donné les meilleurs résultats en termes de réduction de la teneur en oxygène et de pouvoir calorifique de la bio-huile

L'effet sur le processus de co-pyrolyse catalytique du changement de technologie du réacteur de pyrolyse en utilisant un réacteur à lit fluidisé continu a également été examiné. Il a été constaté qu'il y avait une différence négligeable entre les deux installations, mais que le réacteur à lit fluidisé continu produisait plus d'huile permettant une meilleure analyse de cette dernière. L'huile se divise en une phase organique et une phase aqueuse et la teneur en eau de chaque phase dans toutes les expériences a déterminée. Cette teneur est de 0-1 wt.% dans la phase organique et de 50-70 wt.% dans la phase aqueuse. Finalement, ce travail détaille l'analyse de la composition des produits pyrolytiques et co-pyrolytiques ainsi que leurs principales caractéristiques pour produire une huile de haute qualité avec l'utilisation finale possible de chaque produit avant et après traitement catalytique.
Mots clés : Pyrolyse ; biomasse ; plastiques ; catalyseur ; réacteur à lit fluidisé ; réacteur à lit fixe, bois de hêtre

General Introduction

GENERAL INTRODUCTION

The rapid growth of the worldwide population and advances in technology, economics, and civilization gave rise to an exponential increase in energy demand. However, the energy demand is usually met by burning fossil fuels, as shown in **Fig. 1**. Given the non-sustainability of fossil fuels and the growing concern about their devastating environmental impact resulting in greenhouse emissions, fossil fuel burning is by far the worst option. The present and expected state of greenhouse emissions will results in climate change, sea level rise, and ecosystem threats (Olabi et al., 2022). For that, the search for a new reliable renewable energy source is vital for world sustainability. Renewable energies are mainly divided into hydroelectric, solar, wind geothermal, and mainly biomass, which constitutes around 67 % of all renewable energies (World Bioenergy Association, 2020)**.** In this regard, agricultural waste based on lignocellulosic biomass plays a significant role in bio-energy generation (Mohabeer, 2018).

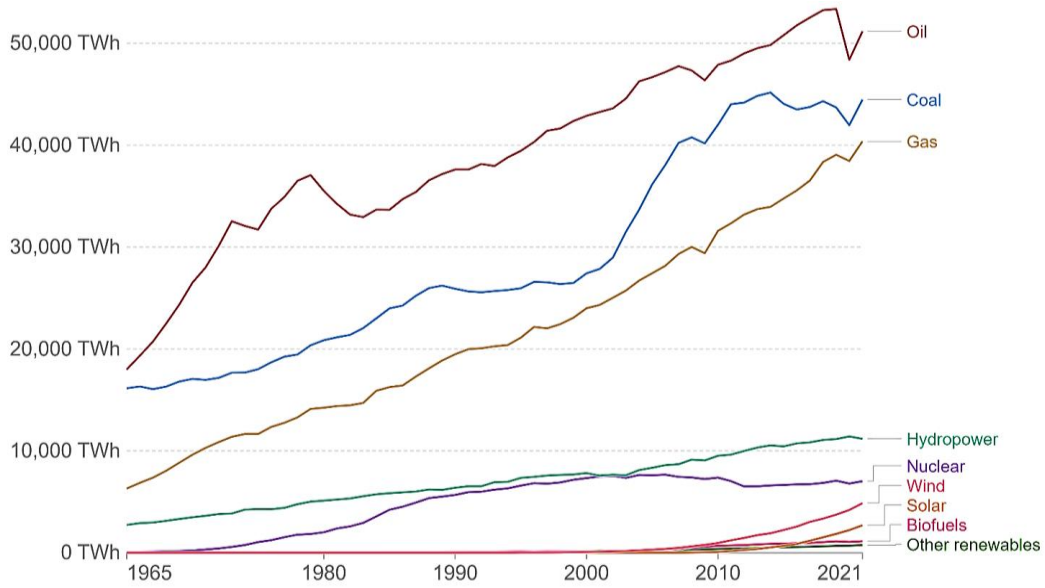

Fig. 1. Primary energy consumption by source (Ritchie et al., 2020).

Yet the term biomass in renewable energy is very general. The main focus is on the fuels derived from biomass material, which are not so abundant as the whole biomass family due to the limited technology in this area. **Fig. 2** demonstrates the evolution of the worldwide production of biofuels since the year 1990. Production seems to increase 10 folds during the past 20 years. For further development, more research is needed to exploit this renewable source.

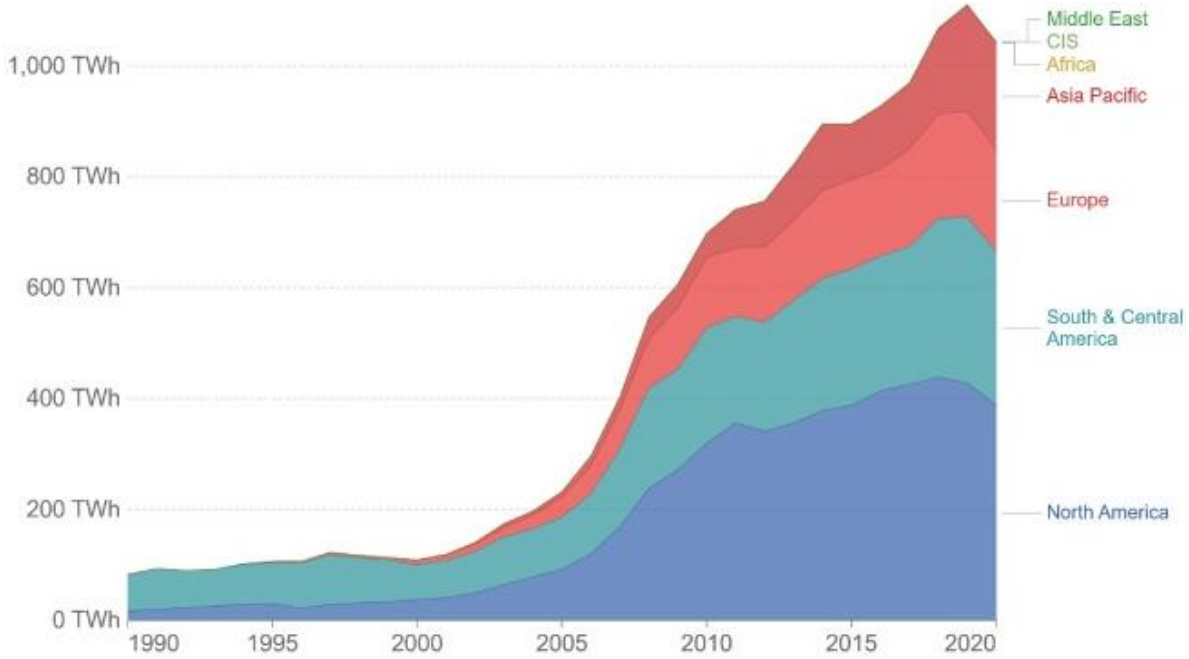

Fig. 2. Biofuel production by region (Duarah et al., 2022).

On the other side of the coin, plastics wastes seem to have the same behavior as energy demand. However, the increase in plastic demand is accompanied by serious environmental problems, especially on marine life (A Alabi et al., 2019). Studies have shown that 15 % to 40 % of municipal plastic waste (MPW) flows into the ocean through rivers (Seo and Park, 2020). The most famous and terrifying example is the Great Pacific Garbage Patch (GPGP), an accumulation of plastic particles in the Pacific, between the U.S. states of Hawaii and California. According to the latest estimations (Lebreton, 2018), the size of the GPGP is approximately 1.6 million km^2,

which is around 2.5 times the area of France. MPW has serious environmental effects and hazardous implications on the marine ecosystem. The previously described problems could be reduced or tackled by the use of pyrolysis.

Biomass and plastics are constituted from polymers that can be thermally cracked to produce various chemicals which can be used as petrochemical or fuels. The process is called pyrolysis. Yet the pyrolysis of biomass alone yields low-quality bio-oil having very high oxygen and water content of about 35-40 wt.% and 15-30 wt.% respectively; thus, also having very low calorific value (16-19 MJ/kg) (Zhang et al., 2007). So, co-feeding biomass with a hydrocarbon-rich source like plastics during pyrolysis may have a good effect on improving the quality of the oil produced (Abnisa and Wan Daud, 2014).

The present work has been funded by INSA ROUEN NORMANDIE and the Lebanese University. The main aim is to provide a detailed study of the pyrolysis and co-pyrolysis of lignocellulosic biomass and plastics with deep analysis and possible end-use of the obtained products. Also, the effect of the catalyst and pyrolysis technology was thoroughly investigated. The detailed description of the present research work is transcribed into five chapters:

Chapter 1 presents a brief literature review of the different aspects of biomass and plastic catalytic co-pyrolysis. The various technologies governing biomass and plastic co-pyrolysis are presented. Then, the co-pyrolysis process is detailed and a comprehensive literature review is given. In the end, a set of the catalyst used for catalytic co-pyrolysis is also elaborated.

In **Chapter 2,** thermoset plastics such as polystyrene (PS), low-density polyethylene (LDPE), high-density polyethylene (HDPE), polypropylene (PP), and their mixture underwent intermediate isothermal pyrolysis at 450 °C, 500 °C, 550 °C, and 600 °C inside a tubular semi-continuous reactor under an inert nitrogen atmosphere. The liquid pyrolytic oil samples recovered

in each case were analyzed through gas chromatography-mass spectrometry (GC-MS) and flame ionization detector (GC-FID) to identify and quantify the different products formed. The compounds were grouped into chemical families and the heating value of the products was computed. A glance at the possible end-use of each oil was investigated along with a principal component analysis (PCA) on the pyrolytic oil to visualize the global trend of the data.

Chapter 3 investigate the co-pyrolysis of lignocellulosic biomass (beech wood (BW)), with polypropylene, high- and low-density polyethylene, polystyrene, and their mixture as synergistic effects on liquid oil production inside a tubular semi-continuous reactor under an inert nitrogen atmosphere is also studied. The liquid oil recovered was analyzed using gas chromatography methods. Beechwood to plastic ratio and operating temperature were varied. A deep study of synergy on the heating value, oxygen content, and the concentration of each family inside the oil was thoroughly conducted.

The purpose of **Chapter 4** is to investigate whether the catalytic co-pyrolysis of beech wood with polystyrene has a synergistic and catalytic effect on liquid oil production. For this purpose, a tubular semi-continuous reactor under an inert nitrogen atmosphere was used. Several zeolite catalysts were modified by incipient wetness impregnation using iron and/or nickel. The liquid oil recovered was analyzed using GC-MS for the identification of the liquid products, and GC-FID for their quantification. Effects of catalyst type, beechwood to polystyrene ratio, and operating temperature were investigated.

Finally, **Chapter 5** presents a continuous setup for the catalytic co-pyrolysis using a fluidized bed reactor. This chapter has comprehensively investigated the co-pyrolysis of BW and PS mixtures over iron and nickel modified zeolite in a fluidized bed reactor. The influence of different parameters such as metal loading of the zeolite catalyst (1.4 % Fe- 1.4 % Ni and 5 % Fe-

5 % Ni), biomass/plastic ratio (1:3, 1:1, 3:1), and pyrolysis temperature (450-600 °C) on the quality and quantity of co-pyrolysis oil was investigated. The heating value, water content, oxygen content, and concentration of each chemical family were computed.

References

A Alabi, O., I Ologbonjaye, K., Awosolu, O., E Alalade, O., 2019. Public and Environmental Health Effects of Plastic Wastes Disposal: A Review. https://doi.org/10.23937/2572-4061.1510021

Abnisa, F., Wan Daud, W.M.A., 2014. A review on co-pyrolysis of biomass: An optional technique to obtain a high-grade pyrolysis oil. Energy Convers. Manag. 87, 71–85. https://doi.org/10.1016/j.enconman.2014.07.007

Duarah, P., Haldar, D., Patel, A.K., Dong, C.-D., Singhania, R.R., Purkait, M.K., 2022. A review on global perspectives of sustainable development in bioenergy generation. Bioresour. Technol. 348, 126791. https://doi.org/10.1016/j.biortech.2022.126791

Lebreton, L., 2018. Evidence that the Great Pacific Garbage Patch is rapidly accumulating plastic. Nature 22 03, 7.

Mohabeer, C.C.D., 2018. Bio-oil production by pyrolysis of biomass coupled with a catalytic de-oxygenation treatment (These de doctorat). Normandie.

Olabi, A.G., Obaideen, K., Elsaid, K., Wilberforce, T., Sayed, E.T., Maghrabie, H.M., Abdelkareem, M.A., 2022. Assessment of the pre-combustion carbon capture contribution into sustainable development goals SDGs using novel indicators. Renew. Sustain. Energy Rev. 153, 111710. https://doi.org/10.1016/j.rser.2021.111710

Ritchie, H., Roser, M., Rosado, P., 2020. Energy. Our World Data.

Seo, S., Park, Y.-G., 2020. Destination of floating plastic debris released from ten major rivers around the Korean Peninsula. Environ. Int. 138, 105655. https://doi.org/10.1016/j.envint.2020.105655

World Bioenergy Association, 2020. GLOBAL BIOENERGY STATISTICS 2020.

Zhang, Q., Chang, J., Wang, T., Xu, Y., 2007. Review of biomass pyrolysis oil properties and upgrading research. Energy Convers. Manag. 48, 87–92. https://doi.org/10.1016/j.enconman.2006.05.010

CHAPTER 1:

Literature Review

1. LITERATURE REVIEW

1.1. Introduction

Today, fossil fuels contribute more than 80% of the world's demand for primary energy. Their consumption is increasing and prices are rising (Eisentraut, 2010). In this context, renewable energies are becoming increasingly important. Wood is one of the main sources of renewable energy (Jölli and Giljum, 2005), but often used in an inefficient and unsustainable way ("FAOSTAT"; Karampinis et al., 2012), which leads to increased deforestation issues. The development of modern methods of conversion of biomass into energy, with high yields, is crucial and must be based on by-products from agriculture, industry, or agri-food industry. On the other hand, the reserves of fossil fuels are finite and will be depleted in the future. There are some controversial studies regarding the availability of fossil fuels. New energy reports predict that because of new technologies like hydraulic fracturing (Fracking), oil and other fossil fuel resources will grow significantly in the next decades (Reuters, 2015). In their annual energy report, the British petroleum company, BP, calculated the period according to the reserves-to-production (R/P) ratio of 50 years (B.P., 2018); the time in years in which the oil reserves will last in the case that the consumption rate will also remain constant. So, the availability of fossil fuels as an energy source is still in question for the short run. On the other hand, energy dependence on fossil fuels has a serious environmental impact on the increase of greenhouse emissions and critical pollutants (-SOx and NOx) (Perera and Nadeau, 2022; US EPA, 2017). Therefore, the development of new renewable fuels and technologies is necessary.

The use of renewable energies is increasing year by year. A major part of renewable energy sources (67 %) is considered to be biomass, as shown in **Fig. 1.1.** Biomass could be used via

several techniques which would be further discussed later on. One of the techniques is pyrolysis to produce liquid bio-oil.

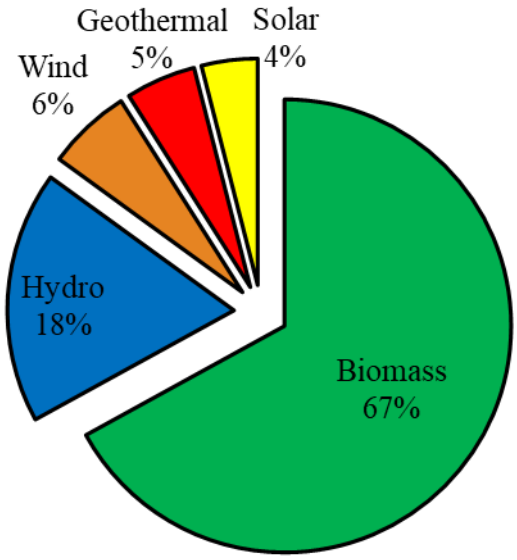

Fig. 1.1 Word-wide renewable energy distribution in 2018 (World Bioenergy Association, 2020)

In this regard, bio-oil derived from agricultural residue, and food waste can serve as a promising new renewable and reliable carbon-neutral biofuel. Pyrolysis has been considered an effective route for biomass valorization where the desired product is a liquid bio-oil, which can be used as a fuel or fuel substitute for petro-sourced products after treatment (Abnisa, 2013; Czernik and Bridgwater, 2004; Vo et al., 2022; Zhang, 2016). Furthermore, it has been industrialized for large-scale pyrolysis of tires, plastics, and rubbers into valuable products, especially liquid pyrolysis oil, in several countries around the globe, such as Lebanon, Indonesia, India, Kuwait, etc. (Doing group, 2022; Huayin Renewable Energy, 2022; Mingjie group, 2022). However, due to biomass' oxygenated nature, 43 wt.% oxygen (Yan et al., 2009), the produced bio-oil consequently will be almost entirely dominated by oxygenated compounds (Rahman et al., 2021).

The high oxygen content causes a relatively low calorific value, high viscosity, corrosion, and unstable bio-oil (Qi, 2007), inappropriate for direct use. Various approaches have been applied to improve bio-oil quality, mainly catalytic deoxygenation, steam reforming, esterification, and hydrodeoxygenation (Bridgwater, 2012). An alternate, more practical approach lies via co-pyrolysis (Abnisa and Wan Daud, 2014). Co-pyrolysis describes the thermo-chemical decomposition of organic material with two different feedstocks at the same time to improve the quality and quantity of the produced liquid oil. It has been shown that the composition, the nature of biomass and synthetic polymers, and the pyrolysis conditions have a great influence on the performance, chemical structure, and physical properties of the products (Ansari et al., 2021; Mortezaeikia et al., 2021; Wang, 2021).

On the other hand, the economics of catalytic pyrolysis of biomass has been investigated by several researchers (B. Li et al., 2015; Thilakaratne et al., 2014; Vasalos et al., 2016). The studies showed that selling the bio-oil produced at a rate of $ 3-4 per gallon makes the process economically feasible with an internal rate of return of 10 %. However, economic feasibility plays a small part in the transition to bio-fuels. Worldwide collaboration and commitment would play a major part in this transition.

In this regard, this chapter reviews the catalytic co-pyrolysis process from several points of view, starting from feedstock characteristics and conversion techniques, co-pyrolysis definition and chemistry with the reactors used, and ultimately describing catalytic co-pyrolysis and demonstrating the catalysts used. Consequently, recent progress in the experimental studies on both the non-catalytic pyrolysis and catalytic co-pyrolysis of biomass with polymers is also summarized with an emphasis on the liquid yield and quality.

1.2. Biomass

1.2.1. Biomass composition

The term "biomass" is defined as any material with biological origin. This origin can be of plant origin (food, agricultural, and forestry residue) and animal origin (animal corpses, meat residue). In this case, the main interest lies in the plant origin, which includes organic wastes originating from forestry and agricultural residue, such as wood and vegetal matter. It is a sustainable and renewable energy source; it uses the infinitive power of the sun by converting it through photosynthesis into a carbon-neutral energy source (Czernik and Bridgwater, 2004). In comparison to other renewable energy sources like wind or solar energy, biomass has the advantage that it is easily stored, consequently diminishing the intermittency problem of renewable energies. The energy forms generated from biomass are present in all forms: solid, liquid, and gas.

Lignocellulosic biomass is the most abundant and renewable non-edible biomass (e.g., grass, wood, energy crops, forestry, and agricultural residues) (Ge et al., 2018). In Europe, there are approximately 1.84×10^{12} tons of biomass mainly composed of hydrocarbon molecules with oxygen in the form of three main polymers: cellulose, hemicelluloses, and lignin (**Fig. 1.2**). The typical composition and elemental analysis of lignocellulosic biomass are present in **Table 1.1** and **Table 1.2.**

Table 1.1: Composition of dry biomass (Mohabeer et al., 2018).

Biomass	Cellulose (wt. %)	Hemicellulose (wt. %)	Lignin (wt. %)
Hardwood	45-50	20-25	20-25
Softwood	35-50	25-30	27-30

Cellulose $(C_6H_{10}O_5)_n$, the most abundant polymer on the planet, is considered to be a linear homopolysaccharide made up of glucose monomers (D-glucopyranose) linked together by β-(1,4) glycosidic bonds (Klemm et al., 2005). The repeating unit, composed of the association of two glucose, is called cellobiose. It is linear, partially crystalline, and represents around 35-50 wt.% of all lignocellulosic biomass. Hemicellulose is a branched biopolymer with different monomer units, representing 20-30 wt.% of lignocellulosic biomass. It is responsible for the stability of the cell membrane and the cell walls with its sticky properties (Kaltschmitt et al., 2009). It is usually built out of 50 to 200 monomer units (Klass, 1998), with acetyl groups as the most prevalent group. Pentose such as xylose subunits is the main constituent of hemicellulose in hardwood. In softwood, it consists of glucose, mannose, and galactose subunits (hexose). Lignin is a much-branched, three-dimensional aromatic polymer, which is often building boundaries with cellulose to a lignocellulose complex in the cell wall of plants, especially of woody biomass (Klass, 1998). The three components represent approximately 95 % of dry biomass, where the distribution of the quantity of each component depends strongly on the type of biomass.

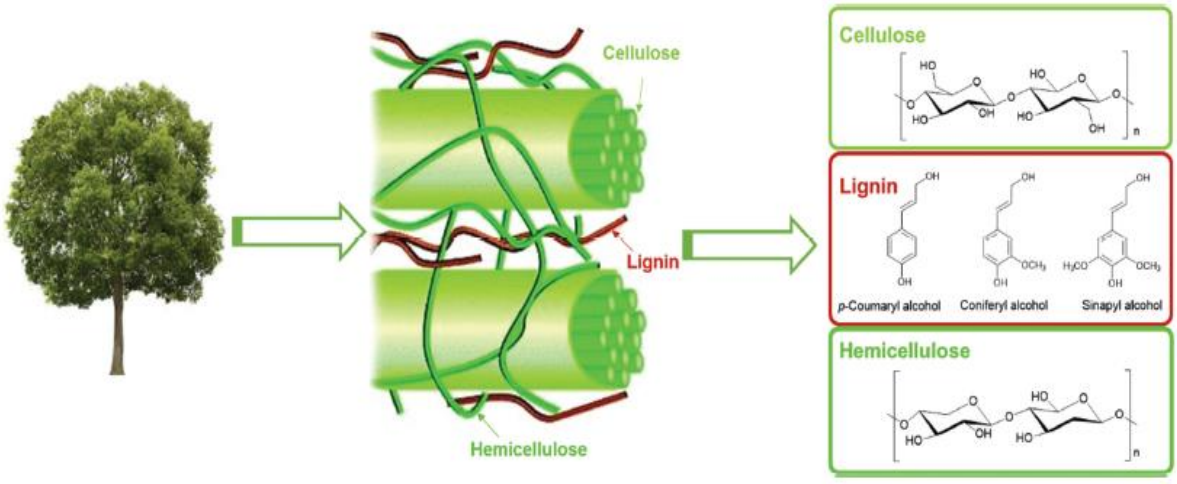

Fig. 1.2 Overview of the structure of cellulose, lignin, and hemicellulose, adapted from (Zhang, 2016)

As for the elemental analysis, biomass mainly consists of carbon, hydrogen, and oxygen, which represent about 95 wt.%, covering the 3 previously discussed biopolymers. Furthermore, the remaining 5 wt.% are mainly the macro-and micronutrients like nitrogen, potassium, calcium, phosphorous, sulfur, magnesium, etc. Minerals and other inorganic matter known as ashes are also naturally present in the lignocellulosic biomass where the content differs from one biomass to another. In addition, woody biomass contains certain amounts of extractives such as waxes and fats in the form of fatty acids, glycerol, and terpenes that give the plant special odor and antiseptic properties (Stevanovic, 2007).

Table 1.2. Elemental composition of dry biomass (Kaltschmitt et al., 2009)

Element	**C**	**H**	**O**	**N**	**P**	**K**	**Na**	**S**	**Ca**	**Si**	**Mg**	**others**
Quantity (wt.%)	42-47	6	40-44	1-5	<0,8	<5	<0,5	<3	<5	<3	<1	<1

1.2.2. Biomass conversion

Biomass can be principally converted through thermochemical and biochemical routes. An overview of the possible pathways of biomass valorization is present in **Fig. 1.3.**

Thermochemical conversion describes the transformation of biogenic energy sources into energy. This could be either realized directly through complete oxidation, or indirectly through chemical modification to synthesize liquid, solid, or gaseous secondary energy sources. Thermochemical conversion can be categorized into four main methods: combustion for direct heat and energy application, gasification for the production of syngas (mixture of CO and H_2), hydrothermal gasification for wet biomass under supercritical conditions to produce synthetic gas (CH_4, CO_2, and H_2), and pyrolysis, which yields liquid oil, solid char, and incondensable gases (Kruse, 2009; Ram and Mondal, 2022).

Biochemical conversion is a very selective process that uses biological catalysts (enzyme, bacteria, etc.); for instance, transesterification by lipase (Bridgwater, 2012), aerobic digestion (composting), anaerobic digestion for the production of methane gas, and fermentation for the production of ethanol, etc. This thesis is targeted toward pyrolysis due to its feasibility and efficient conversion into a liquid oil that is easy to handle, transport, and store (Cimenti and Hill, 2009).

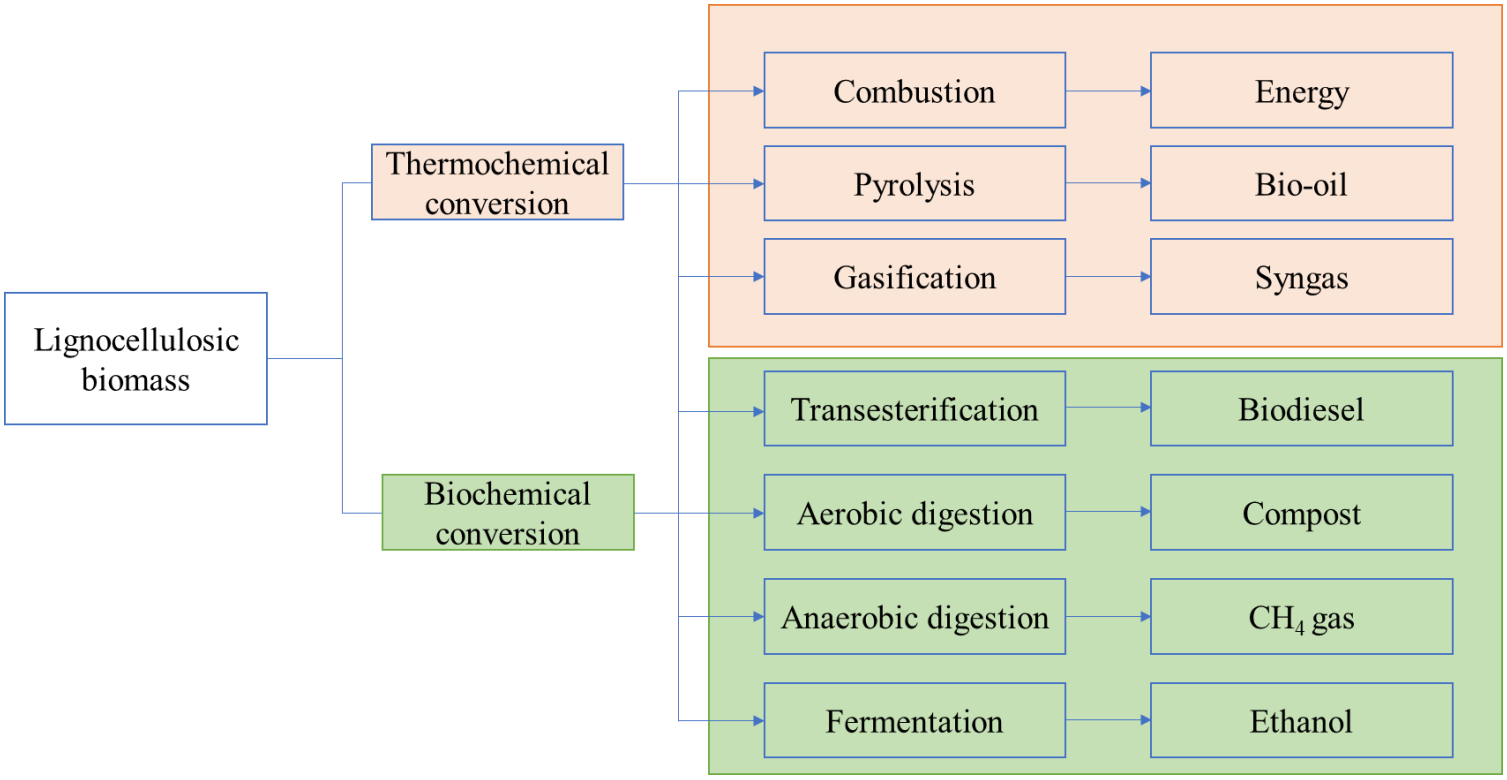

Fig. 1.3 Biomass transformation pathway

1.2.3. Biomass pyrolysis

The word pyrolysis comes from “Pyro” which means fire and “lysis” which refers to cutting. Pyrolysis describes a thermochemical transformation process of biomass into energetic products (Buderus and Schmidt, 2015). Unlike combustion and gasification of biomass, pyrolysis is realized in a lack of oxygen (inert atmosphere), so the transformation is not described as an oxidation process. The process takes place at high temperatures (300-700 °C), which lead to the thermal decomposition of the biomass into smaller molecules, mainly hydrocarbon chains with oxygen groups (e.g. acids, phenols, ketones, carbohydrates, etc.)(Buderus and Schmidt, 2015). Thus, pyrolysis of biomass describes the transformation of low energetic biomass to higher

energetic secondary compounds. It produces a variety of non-condensable gases, condensable vapor, and solid char.

Pyrolysis can be classified into three types (Dhyani and Bhaskar, 2018):

1) **Slow pyrolysis** is one of the oldest treatments of biomass and is known to be the classical technique. It is mainly used at low temperatures (300-500 °C) and long contact time for the production of charcoal that was used in the past mainly for metal smelting.
2) **Intermediate pyrolysis** is carried out in the range of 300-600 °C. The chemical reaction is more controlled with moderate retention times.
3) **Fast pyrolysis** aims towards the optimization of liquid yield by controlling process parameters, mainly reaction temperature and vapor residence time. Pyrolysis temperatures vary between 450 and 600 °C, coupled with a short residence time of fewer than two seconds.

The difference between each pyrolysis classification is present in **Fig. 1.4**. The gaseous phase contains mostly carbon dioxide (CO_2), carbon monoxide (CO), hydrogen (H_2), and methane (CH_4) with small proportions of C_2 to C_4 compounds (Kaltschmitt et al., 2009).

Liquid oils contain a wide carbon range of compounds described as hydrocarbons, acids, alcohols, esters, carbonyls, phenols, furans, sugars, and nitrogenous compounds (Zhang et al., 2015). Liquid production is the main scope of this process. It shows easy storage and handling and has high densities and high energy efficiency. Furthermore, it can be used for already-built machines that work on petroleum fuel where no retrofitting is required.

Char is the non-volatile product of pyrolysis (fixed carbon and ash). It consists of carbonaceous materials and ashes, which are usually burned or gasified for direct energy recovery. It is the most energetic product, constituting about 25 % of the feed energy, compared to 4 % for

gases. Therefore, there is around 15-30 % total energy loss from the feed to produce bio-oil. In general, pyrolysis requires 15 % of the total feed energy to carry out pyrolysis (Cai et al., 2017).

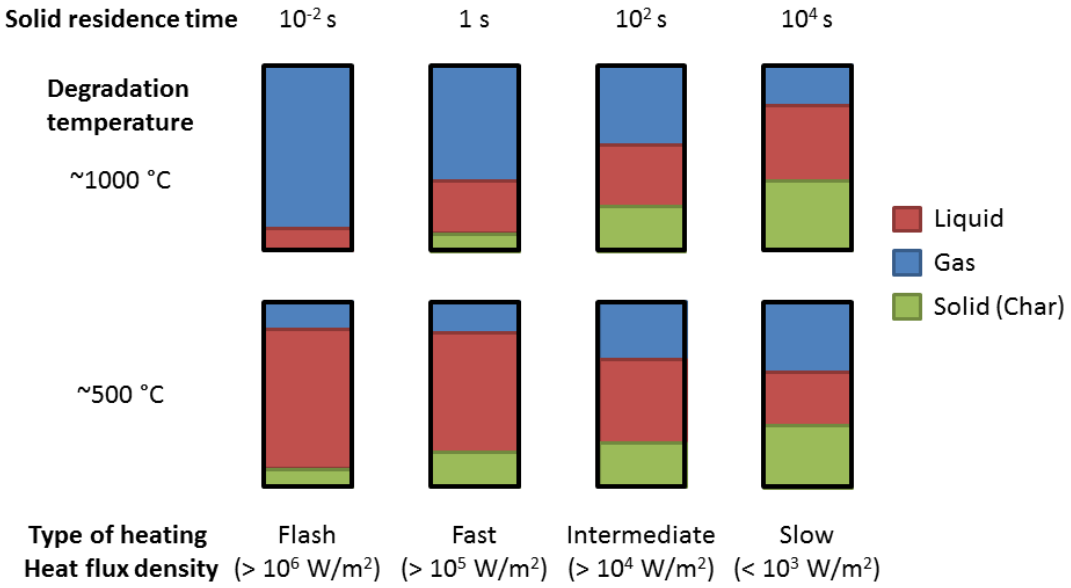

Fig. 1.4 Pyrolysis processes classification (Mohabeer et al., 2018).

The main ambition of pyrolysis is the production of sustainable, abundant, and renewable pyrolysis oil, which can replace the use of liquid fossil fuels. Indeed, the combustion of pyrolysis oil causes emissions like carbon dioxide, which is considered a greenhouse gas, but in contrast to fossil fuels, the pyrolysis process can be considered a part of the natural biogenic carbon cycle, so they do not cause new emissions, i.e., carbon neutral emissions; the CO_2 liberated during the combustion of the bio-oil was the CO_2 absorbed by the plant to grow.

Yet, the bio-oil should undergo further treatment. In contrast to catalytic cracking, co-pyrolysis has shown promise for future application in the industry because of its attractive performance/cost ratios (Abnisa and Wan Daud, 2014). Ultimately, it can further consume plastic waste and decrease their disposal, especially for plastics that are challenging to recycle, such as polystyrene (Anuar Sharuddin et al., 2016).

For that, a detailed analysis of the possible plastic sources along with their pyrolysis technologies is further investigated in the upcoming section.

1.3. Plastics

1.3.1. Plastic composition

The invention of plastic has been reported as a major breakthrough that facilitated people's life. It is light, durable, resistant to corrosion, and low cost. Plastics serve as a good substitute for materials such as wood, ceramics, and metals in various applications. On the other hand, polymers can be merged with other compounds to form composite materials which are getting remarkable attention due to their growing applications (Mahesh et al., 2021).

Plastic is an expression for various kinds of synthetic, organic polymers with a high molecular mass. It consists mainly of long carbon-hydrogen chains but it can also contain: oxygen as polyethylene terephthalate (PET), nitrogen as polyurethane (PU), or halogens as polyvinyl chloride (PVC). The quantity of oxygen, however, is much lower than in biomass. This has an important effect on the combustion potential of the two materials. The most commonly used plastics are high-density polyethylene (HDPE), light-density polyethylene (LDPE), polypropylene (PP), polyvinylchloride (PVC), polyethylene terephthalate (PET), polyphthalamide (PPA), and polystyrene (PS); with their contribution discussed in **Fig. 1.5**. The different structures of the most produced plastics are present in **Fig. 1.6**.

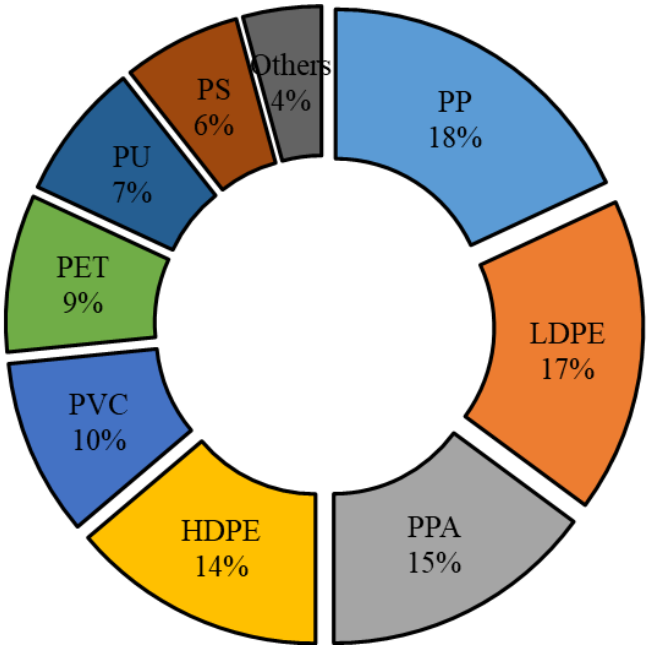

Fig. 1.5 Types of plastics produced worldwide. Adapted from (Rabnawaz et al., 2017)

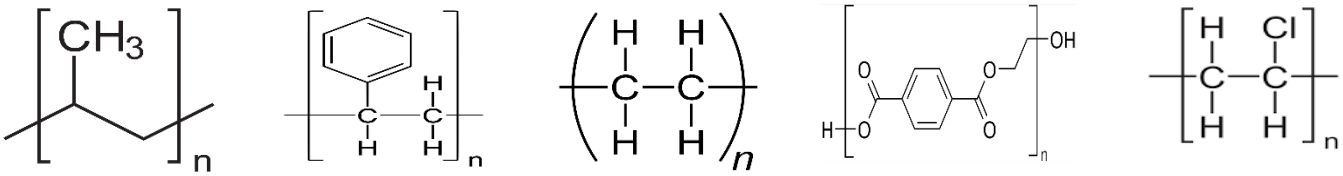

Fig. 1.6 The molecular formula of major thermoplastic plastics

Worldwide plastic production is rising as a function of time from 1.5 Mt in 1950 up to 367 Mt in 2020. It is expected to double again in the next 20 years and almost quadruple by 2050 ("Statista," 2022). Consequently, plastic waste is also rising over the years. The rate of generation of municipal plastic waste (MPW) and municipal solid waste (MSW) has increased at a rate of 5% and 3.2 to 4.5 % per year respectively (Tang et al., 2018), whereas the increase in recycling is only 3 % annually (Silvarrey and A.N., 2016). Plastic landfilling has certain drawbacks as the plastics are non-biodegradable, which leads to about 4 % loss of valuable petroleum products in addition to the high energy waste (40 MJ/kg for hydrocarbonaceous plastics) (Silvarrey and A.N., 2016). In Europe, around 50 % of plastic is recovered (Wong et al., 2015).

Recycling can be carried out by four primary technologies as classified by (Siddiqui, 2009):

1) **Primary recycling** (no heat treatment) is the processing of plastics scraping into similar types of products from which they have been generated, using standard plastics processing methods. This process remains the most used as it ensures simplicity and low cost, dealing only with the recycling of clean uncontaminated single-type waste.
2) **Secondary or mechanical recycling** is where the polymer is separated from its associated contaminants and can be readily reprocessed into granules by conventional melt extrusion. The main disadvantage of this type of recycling is the deterioration of product properties in every cycle.
3) **Tertiary or chemical/thermal recycling** involves the transformation/degradation of polymeric materials through heat or chemical agents to yield a variety of products ranging from the starting monomers to oligomers or mixtures of other hydrocarbon compounds. The resulting raw materials are then reprocessed into plastic materials or other products of the oil refining process. The most used tertiary recycling methods are pyrolysis and gasification.
4) **Quaternary recycling** or energy recovery by incineration is an effective way to reduce the volume of organic materials by recovering the latent energy content of plastic materials by incineration.

Pyrolysis has been recognized as an ideal approach for recovering energy and getting high-value products. It is considered a substitute for conventional recycling in many cases with less sorting and labor cost. Furthermore, recycling deteriorates the mechanical properties of the plastic due to the continuous heat treatment and the irremovable addition of additives (antioxidants, colorants, UV stabilizers, etc.) that sever the quality of recycled plastics. For instance, just one

PVC bottle in a batch of 10,000 PET bottles can ruin the entire melt (Basak, 2009). Pyrolysis is a technique that produces no waste stream and where all byproducts are used. Pyrolysis holds several advantages over gasification as it produces liquid products under lower temperatures making it suitable for handling, transportation, and direct use in boilers without any major retrofitting (Akhtar et al., 2018).

1.3.2. Plastic pyrolysis

Pyrolysis of plastic describes also the decomposition of the feedstock in an inert atmosphere where a secondary energy source is produced. Like in the pyrolysis of biomass, the goal of this process is to obtain a high-grade oil. Because of the composition of plastic, which contains mostly hydrogen and carbon, the oxygen content of the produced bio-oil is notably lower. The process is mostly realized in a temperature range between 400 and 700 °C. In the pyrolysis of polymers, the macromolecular structures of the plastic are cracked into oligomers or monomer units (Abnisa and Wan Daud, 2014). The decomposition of the plastic is caused as a consequence of the free radical mechanism based on three steps: i) initiation, ii) propagation, and iii) termination. Each pyrolyzed polymer is mainly reduced to its basic monomers, dimers, and trimers. For instance, the product of PS is reduced mainly to styrene. HDPE and LDPE produce linear chain hydrocarbons in contrast to PP, where the oil is rich in branched hydrocarbons.

Plastics can deliver high hydrogen percentages and unsaturated double bonds that could have positive synergy when mixed together with biomass during pyrolysis. This is the main objective of the thesis which will be emphasized further in the upcoming sections.

In **Table 1.3,** the composition of the pyrolytic oil produced through the pyrolysis of different polymers can be seen. It is remarkable, that the variety of products is very high and that there are some notable differences between the single types of polymers. As already mentioned,

the main components of the pyrolysis of HDPE, LDPE, and PP are olefins and paraffins, whereas the main products of the process with PVC and PS are mostly aromatic compounds. It is also remarkable that the number of products containing oxygen is quite small except for PET, which has a positive effect on the combustion value of pyrolytic oil, achieved between 40 and 47 MJ/kg (Syamsiroa, 2014).

Plastics can deliver high hydrogen percentages and unsaturated double bonds that could have positive synergy when mixed together with biomass during pyrolysis. This is the main objective of the thesis and it will be emphasized further in the upcoming sections.

Table 1.3 Composition of pyrolytic oil produced through pyrolysis of different types of plastic (Anuar Sharuddin et al., 2016; Ballice and Reimert, 2002; Liu et al., 2000)

PET	**HDPE/LDPE**	**PVC**	**PP**	**PS**
1-Propanone	1-Hexene	Azulene	Toluene	Benzene
Benzoic acid	Cyclohexene	1-Methyl-naphthalene	2,4-Dimethyl-1-pentene	Toluene
Biphenyl	1-Heptene	Biphenyl	1-Heptene	Ethylbenzene
Diphenylmethane	1-Octene	1-Ethyl-naphthalene	2,4-Dimethyl-1-heptene (Trimer)	Xylene
4-Ethylbenzoic acid	1-Nonene	9H-Fluorene	Benzene	Styrene (Monomer)
4-Vinylbenzoic acid	1-Decene	2,7-Dimethyl-naphthalene	2,4,6-Trimethyl-1-nonene	α-Methylstyrene
Fluorene	1-Undecene	1,6-Dimethyl-naphthalene,	3,3-Dimethyl-1-butene	2,4-Diphenyl-1-butene (Dimer)
Benzophenone	1-Tridecene	1,7-Dimethyl-naphthalene	Xylene	Naphthalene
				2,4,6-Triphenyl-1-hexene (Trimer)

1.4. Co-pyrolysis

As discussed before, the quality of the bio-oil produced from biomass can be improved via co-pyrolysis. Hence, co-pyrolysis of lignocellulosic biomass with plastic waste will be discussed hereupon. A general overview of the co-pyrolysis scale-up process is described in **Fig.1.7**. Other combinations of feedstocks for co-pyrolysis which are examined in literature are e.*g*., biomass and coal. The product of the pyrolysis process, the bio-oil, has various applications: In burners and boilers, medium-speed diesel engines, turbines or to produce some chemicals (Czernik and Bridgwater, 2004).

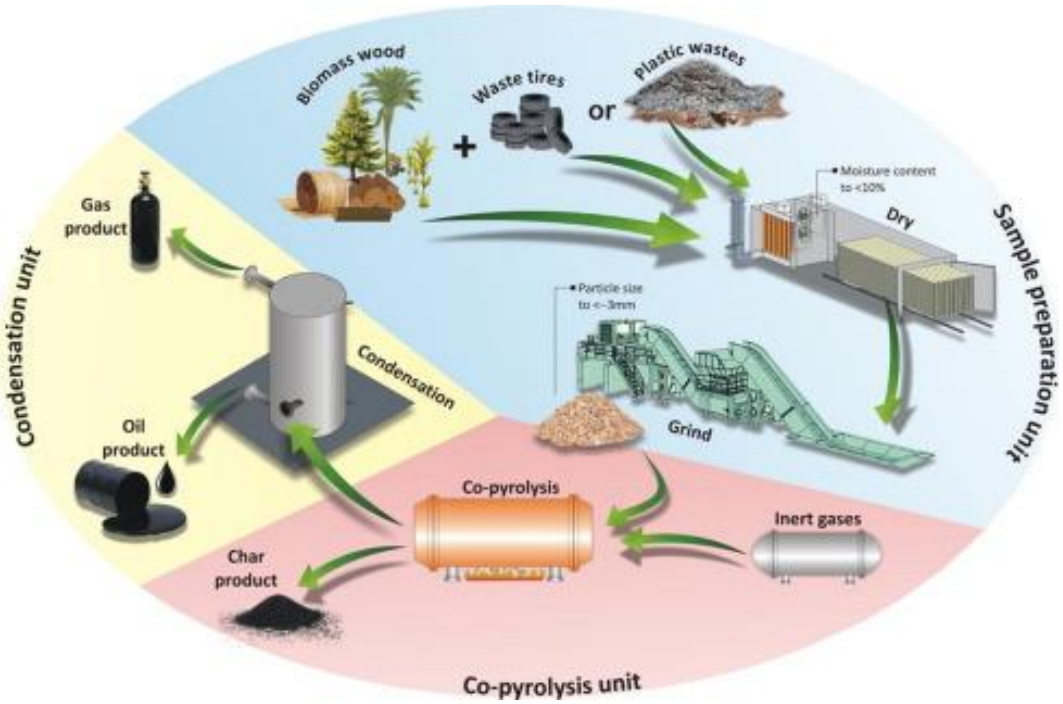

Fig.1.7 Co-pyrolysis scale-up procedure (Abnisa and Wan Daud, 2014).

Simplicity and effectiveness are especially important in developing techniques to produce the ideal synthetic liquid fuel. In this regard, the co-pyrolysis of biomass can be a technique that shows promising results by meeting these two criteria. Many studies have shown that biomass co-pyrolysis has successfully improved the oil quantity and quality without any improvement in the

overall process (Ansari et al., 2021; Mortezaeikia et al., 2021; Wang, 2021). A previous study (Önal et al., 2012) has shown that the yield of oil obtained from incorporating plastic was higher than that obtained with woody biomass alone. A higher calorific value was obtained which comes from hydrocarbon polymers consisting of paraffins (Iso-paraffins, olefins, naphthenes, and aromatics, and a non-condensable gas with a high calorific value) (Önal et al., 2012). The idea of blending oil from biomass with oil from plastic (or waste tires) seems impossible and may increase operating costs. Oil from biomass cannot be completely mixed with oil from plastic or tire waste because of the polar nature of the biomass pyrolytic oil. If these oils are mixed, an unstable mixture forms, which breaks (phase separation) after a short time. If biomass and plastic (or waste tires) pyrolysis occur independently or separately, more energy is required and the cost of oil production will significantly increase. The co-pyrolysis technique is found to be more reliable to produce homogenous pyrolysis oil than the blending oil method. The interaction of radicals during the co-pyrolysis reaction can promote the formation of a stable pyrolysis oil that avoids phase separation (Abnisa and Wan Daud, 2014).

Önal et al. (2012) mentioned that several radical reactions during co-pyrolysis can be formed as follows: de-polymerization, formation of monomers, favorable and unfavorable H-transfer reactions, intermolecular hydrogen transfer (formation of paraffin and dienes), isomerization via vinyl groups and termination by disproportionation or recombination of radicals (Önal et al., 2012).

1.4.1. Co-pyrolysis mechanism

In comparison to the mechanism of biomass pyrolysis (trans-glycosylation and cyclo-reversion) and plastic waste pyrolysis (radical mechanism with initiation, propagation, and

termination), the mechanism of co-pyrolysis of the two components is more complex. The reason for this is the various chemical structures and therefore, a bigger range of product formation.

Marin et al. (2002) have proposed a mechanism for the co-pyrolysis of wood biomass and plastic waste mixtures. Analysis has shown, that at a low temperature of around 300 °C, the thermal degradation of biomass starts, followed by the degradation of HDPE (high-density polyethylene), whereby free radicals from the biomass degradation initiate the de-polymerization. In the first step, the addition of biomass leads to a solid formation. In the second step, the degradation of polyolefin takes place caused by the radicals of biomass. While the degradation of the polymer takes place, there are some interactions between the formed radicals and the solid form, which leads to the formation of alkadienes (Marin et al., 2002).

In this step, the synergetic effect of the co-pyrolysis of biomass and plastic can be observed, because it leads to an acceleration of the decomposition of biomass in the HDPE. Consequently, the amount of residue at the end of the reaction is reduced (Rotliwala and Parikh, 2011). Because of the free radicals and the hydrogen transfer from polyolefin chains to biomass-derived radicals lead to higher stability of the bio-oil as well as the quantity of the condensable fraction in the product (Önal et al., 2012). Thus, the yield and quality of bio-oil improve due to the co-pyrolysis of biomass with plastic waste in comparison to single pyrolysis. Some researchers suggest hydrogen abstraction by biomass-derived oxygenates to stabilize the latter compounds; the presence of PE could enhance the stabilization of some oxygenated compounds. (Kumagai et al., 2019, 2016). A further explanation of the hydrogen abstraction is further described in **Fig. 3.4 (chapter 3).**

1.4.2. Co-pyrolysis reactors

The most common reactors to perform co-pyrolysis of biomass and plastic waste are a fixed bed (or packed bed), circulating fluidized bed, and auger reactors. Other reactors are used in pyrolysis, as ablative, conical spouted bed, and rotating cone reactors. The choice of the reactor also plays a role in the quality and quantity of the pyrolysis oil. The influence will be also discussed later in the optimization of the co-pyrolysis process. In this part, the different kinds of reactors will be presented and their characteristics will be explained.

Fixed-bed reactor

Fixed bed reactors and fluidized bed reactors **(Fig. 1.8 (a) and (b))** are quite similar in their construction. The advantage of a fixed bed is that there is no need for gas filtration afterward, but the fixed solids generate friction and consequently lead to heat generation. Furthermore, these types of reactors are simple and easier to operate, especially when using plastics, since plastics are challenging to continuously feed at high temperatures. Plastics will melt and clog the entrance since they have relatively low melting points of around 100 °C (Chmiel, 2006). Pyrolysis could be modified by the use of a catalyst; the catalyst could be *in-situ* (mixed with feed) or *ex-situ* (independent reactor), which will be discussed further on in the catalyst part.

Fluidized-bed reactor

The principle of a fluidized bed reactor **(Fig. 1.8 (b))** is that the reactant passes through a bed of solid, heterogeneous fluidization agents in continuous fluidization, such as sand, biomass, plastics, or a catalyst. Fluidization permits excellent temperature stability with an increased mass transfer due to the increase in surface area of contact. Fluidization with sand/catalyst and inert gas has a huge surface area but less contact between the different feedstock, reducing the synergetic effect. Furthermore, char must be rapidly removed since it has a catalytical effect that would reduce

oil yields. So, separation systems such as cyclones and particulate matter control are very critical and essential due to high solid loading and aerosol production.

Auger reactor

The auger reactor **(Fig. 1.8 (c))**, which is a compact continuous reactor is quite different in comparison to the two previous reactors. It is an extruder shape reactor that can achieve the maximum intimate contact between feeds, resulting in maximum synergetic effect, disregarding whether it is positive or negative, which makes it the best for multiple feeds. In this reactor, a heat carrier can be introduced, like sand or steel shot, and the heat transfer takes place directly on the interface between the feedstock material and the heat carrier. During the process, the heat carrier and the feedstock are moved in loops with the auger and at the end of the reactor, the solid and volatile products are obtained (Kaltschmitt et al., 2009). It can be double screw with sand as a heat carrier. It is economical since it is simple with low carrier gas flow, thus capital and operating costs will dramatically decrease. Furthermore, the control of biomass residence time is simple, and gas outlets can be added to reduce vapor residence time with solid residence varying from 11 s to 12 min.

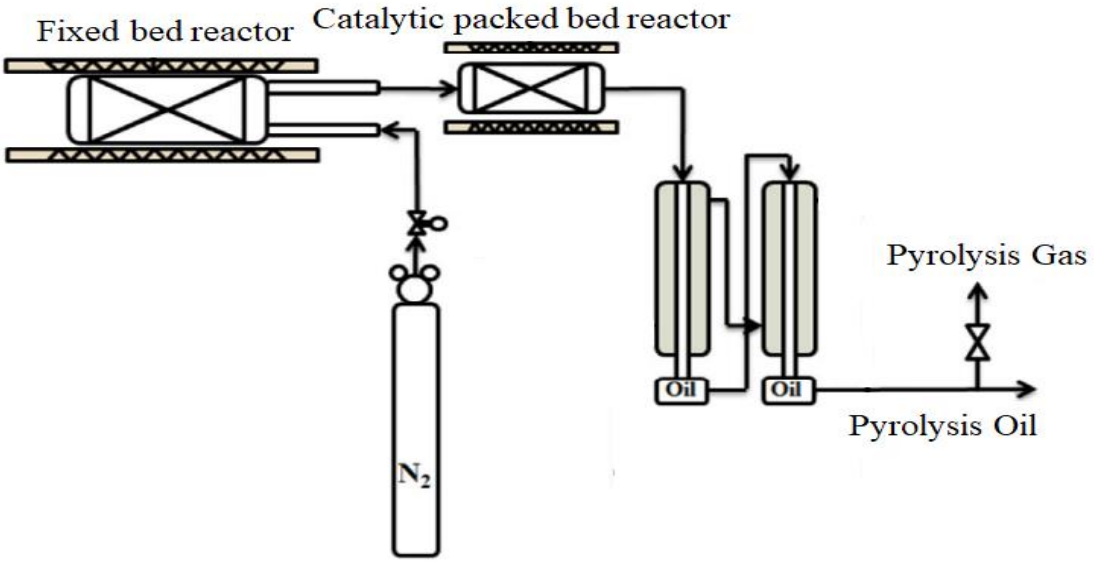
Fixed bed reactor
Catalytic packed bed reactor
Pyrolysis Gas
Oil
Oil
Pyrolysis Oil
N_2

(a)

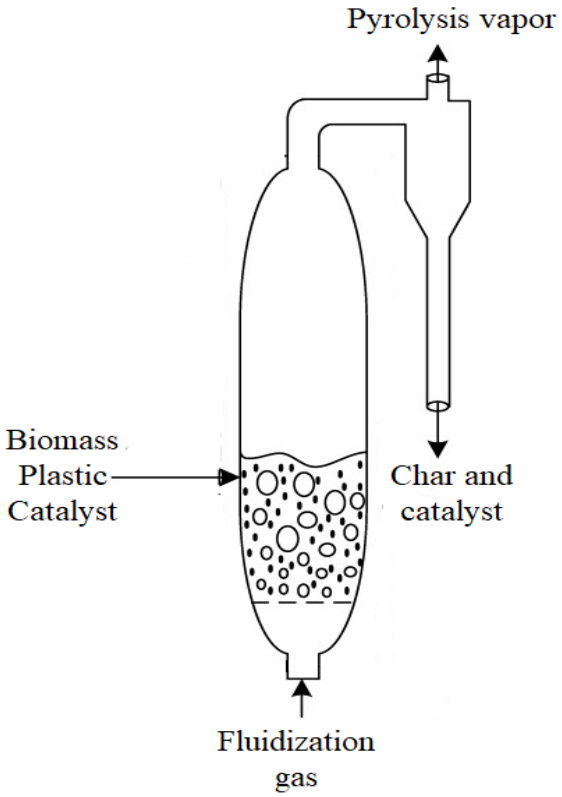
Pyrolysis vapor
Biomass
Plastic
Catalyst
Char and
catalyst
Fluidization
gas

(b)

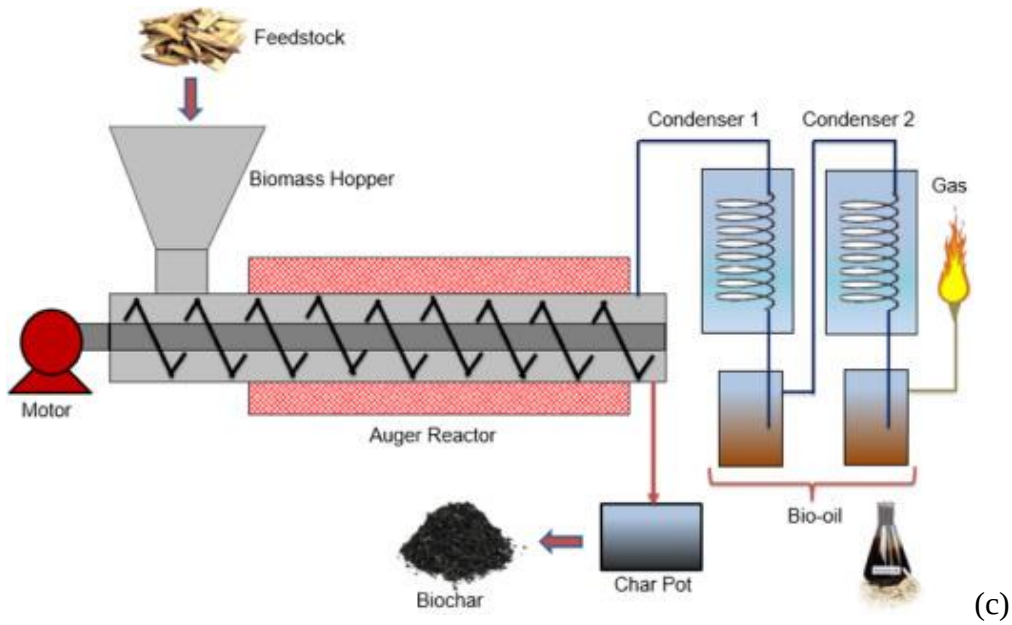

(c)

Fig. 1.8 Schematics of the reactors used: (a) fixed bed reactor, (b) fluidized bed reactor, (c) auger reactor (Campuzano et al., 2019)

To conclude, the fixed bed reactors show the simplest cost-wise possible scale-up reactor. Their simple operation has a great advantage in reducing the total cost of the operation thus making the operation feasible. The fluidized bed reactor has the drawback of the high operating cost of fluidization, however, it could be used to treat the produced bio-oil by catalytic cracking as done in the refineries (Speight, 2019). The auger reactor shows some promise since it has the advantage of introducing multiple feeds thus an improved interaction, yet there exist few scale-up experiments on such a reactor.

1.4.3. Pyrolysis products

Similar to the pyrolysis of biomass or plastic waste, the products of co-pyrolysis can be divided into three groups: solid, liquid, and gaseous components.

Solid products

As a result of co-pyrolysis, a black solid layer product can be usually inside the reactor which consists mostly of char. The quantity of the latter in regular co-pyrolysis, which is in the range of 5-15 wt.%, relies on the process parameters. The elemental composition is mainly carbon, oxygen, and hydrogen with an HHV of about 30 MJ/kg (Xue et al., 2015). The char can be used as an energy source in combustion with coal, in incineration, or as an adsorbent. Active carbon can be produced from the char to increase its surface area (Venderbosch and Prins, 2010), which then can be added to the soil as fertilizers to absorb both organic and inorganic like heavy metals and pesticides. Moreover, it can be used to sequestrate carbon back into the soil, limiting global warming (Brassard et al., 2017).

Gaseous products

The gaseous phase produced in co-pyrolysis, more specifically the non-condensable of the vapor part, contains mostly CO, CO_2, H_2, CH_4, C_2H_4, C_2H_6, C_3H_6, C_3H_8, and also little quantities of other hydrocarbon molecules. The quantity of the gaseous phase is approximately between 13-25 wt. %. However, the actual composition and quantity depend strongly on the process parameters, such as the temperature, heating rate, retention time, the ratio as well as the choice of biomass and plastic (Abnisa and Wan Daud, 2014). Gases are usually used as an energy source for the pyrolysis process, although they can be used for other chemical purposes due to their olefinic nature.

Liquid products

The liquid phase of the co-pyrolysis process is the most interesting product of this work. Often speaking about the liquid phase, the word “bio-oil” is used. It is obtained through condensation of the condensable part of the gases exiting the reactor during and after the process.

The main interest is the application of co-pyrolysis oil as a fuel. Therefore, it should possess a high combustion potential as well as a high heating value. The main parameters to characterize liquid fuels are density, viscosity, calorific value (HHV or LHV), and surface tension, in addition to char level and particle size effects, which should be accounted for the storage and transportation of the liquid oil.

Bio-oil in general is a brown-black viscous liquid. The quantity of the liquid phase in co-pyrolysis varies strongly depending on the process parameters but has an orientation value between 40-60 wt.% (Abnisa et al., 2013). The properties of the bio-oil can be analyzed by different methods like ^{1}H-NMR, GC, or IR.

For instance, Abnisa et al. (2013) studied the chemical and physical properties of bio-oil from the co-pyrolysis of palm shells with polystyrene at 600 °C. A summary of their results analyzing the characteristics can be seen in **Table 1.4.**

Table 1.4 Physical and chemical properties of bio-oil by co-pyrolysis of palm shell and polystyrene (Abnisa et al., 2013).

Properties	**Value**	**Unit**
Viscosity at 50 °C	8.3	cP
pH	2.8	
Density at 24 °C	1058	kg/m^3
High heating value (HHV)	40.3	MJ/kg
Water content	1.9	%
Elemental composition (wet basis)		
C	81.3	wt%
H	7.8	wt%
N	0.4	wt%
O (by differences)	10.5	wt%

As can be seen, the pyrolytic oil has a low pH value (2.8) and high viscosity value of about 8.3 cP, compared to water with a viscosity of 0.55 cP at 50 °C. Instead, the density at room temperature is very similar compared to the value of water at 1000 kg/m^3.

The bio-oil consists mainly of carbon, hydrogen, and oxygen in different structures and contains more than 300 oxygenated compounds (Zhang et al., 2015). However, the oxygen content in co-pyrolysis bio-oil is lower than that produced in biomass pyrolysis. This shows the synergetic effect of co-pyrolysis and explains the high heating value of 40 MJ/kg that is obtained. Co-pyrolytic oil constitutes of several major families which are:

- Furans
- Carboxylic acids
- Carbohydrates
- Esters
- Phenols and alcohols
- Aldehydes and ketones
- Hydrocarbons (aromatics, alkanes, alkenes, alkadiene)
- Water

Usually, if the water content is high, the oil would be separated into 2 phases: an aqueous phase and an organic phase. Water can be beneficial in decreasing the viscosity, increasing stability, and reducing the combustion temperature and NO_x emissions, despite its effectiveness in the decrease of the calorific value (Venderbosch and Prins, 2010).

1.4.4. Co-pyrolysis state of the art

A synergetic effect is the main factor responsible for all improvements in oil quality and quantity. Generally, the research is focused on the study of the interactive effects of the used

feedstock. Some common findings in co-pyrolysis studies are discussed in this section. Synergistic effects can be achieved through radical interactions during the co-pyrolysis reaction. Besides, data on the presumed positive or negative synergy depend on pyrolysis duration, the type and contact of components, temperature, and heating rate, removal or equilibrium of formed volatiles, the addition of solvents, catalysts, and hydrogen donors (Johannes et al., 2013; Sharypov et al., 2002), and more importantly, the ratio between biomass and plastics (Abnisa et al., 2013). A handful of different feedstock combinations and operating conditions done in the literature will be discussed in the upcoming section. A summary of the main results is presented in **Table 1.5.**

Co-pyrolysis of different biomass with hydrocarbonaceous polymers (LDPE, HDPE, PP, PS).

Several studies were carried out describing the co-pyrolysis of lignocellulosic biomass and plastic. However, different conclusions were revealed. Some suggest an increase in oxygen content, while others suggest a decrease and an improvement in the quality of the oil to be used as fuel. Kumagai et al. (2016) investigated the interaction of beech wood (BW) and polyethylene (PE) during co-pyrolysis in a horizontal tube reactor at 350 °C. The heating rate was chosen to be 10 °C.min^{-1}. The results showed an increase in oxygenated compounds such as methoxyphenols (guaiacols) and levoglucosan of about 55 % and 65 % at a BW-PE mixture of 40-60, respectively. Furthermore, the study stated that hydrogen abstraction from PE stabilized levoglucosan radicals and other oxygenated compounds, thus increasing their percentages. A more recent study by Kumagai et al. (2019) investigated the pyrolysis of BW with PE to enhance the production of methoxy phenols and levoglucosan at 350 °C. The latter interactions were further verified and an increase in the yield of levoglucosan and methoxyphenols of about 70 % and 40 %, respectively were observed. However, for aromatic polymers, Özsin and Pütün, (2018) examined the co-pyrolysis of polystyrene (PS) with walnut shells and peach stones in a fixed bed reactor under a

temperature range of 400-700 °C. The results showed an elevated oxygen content of about 20 wt.% for the 50-50 biomass-plastics mixtures for both biomasses under study, compared to 30 wt.% for the biomass alone.

On the other hand, Abnisa et al. (2014) studied the effect of polystyrene to palm shell ratio on the liquid yield and characteristics in a fixed bed reactor with a heating rate of 10 °C.min^{-1} at 500 °C. The results yielded a high heating value of 40 MJ/kg and low oxygen content of around 4 wt.% for the liquid using a palm shell to polystyrene ratio of 40:60. Kumar and Srinivas (2020) conducted at 510 °C the co-processing of groundnut shells with PP in a vertical fixed bed reactor at a heating rate of 10 °C.min^{-1}. The experiments produced more valuable chemicals like toluene and xylene at equal mixing ratios. The total yield of monoaromatics and olefins reached a maximum of about 73 wt.% for a 50:50 biomass-to-PP ratio at 510 °C. When the biomass was co-fed with PS, more valuable styrene monomers and ethylbenzene were found in the product at intermediate mixing ratios.

Co-pyrolysis of biomass with different polymers (PET and PVC).

Ephraim et al. (2018) studied the co-pyrolysis of polystyrene and polyvinyl chloride (PVC) with poplar wood (PW), to investigate the synergistic effect of PVC content on product yield, gas species yield, and heating value. The experiments were performed using a fixed-bed reactor with 10 g of the sample placed in a quartz crucible, heated to 750 °C with a rate of 20 °C.min^{-1} under a nitrogen atmosphere (33 mL.min^{-1}). For experiments with PVC, two impinger bottles containing aqueous solutions of KOH were placed to trap HCl gas. Results show that PVC has a largely positive synergy on char yield with a maximum value of 8 wt.% at 30 wt.% PVC content.

Concerning oil and gas production, PVC showed a significant positive synergy on oil yield with a maximum value increase of 11 wt.% from the calculated yield at 50 wt.% PVC content,

which was linked to a strong negative synergy in gas production. Furthermore, by comparing the distribution of chloride species in the products of co-pyrolysis with PVC, using experimental and theoretical methods, results show that the negative synergy in HCl yield observed was mainly due to the dissolution of HCl in the water fraction of the condensed oil phase, rather than the formation of chlorinated organic compounds.

Özsin and Pütün (2018) investigated the co-pyrolysis of waste lignocellulosic biomass and plastics to find out whether the quality of pyrolysis products was improved. For the sake of yield and compositional comparison, three polymers (polyethylene terephthalate, polystyrene, and polyvinyl chloride) and two biomasses (walnut shells and peach stones) were tested in a fixed bed reactor. In each trial, the reactor was fed with 10 g of raw material (or blended at 50 wt. %). The pyrolysis experiments were performed to study the effect of pyrolysis temperature in the range of 400-700 °C. The liquid products were recovered by washing the traps and the connection lines with dichloromethane (CH_2Cl_2). The maximum bio-oil yield in pyrolysis was obtained at 500 °C, reaching a value of 21 wt.% for walnut shell and 18 wt. % for peach stone pyrolysis. Thus, co-pyrolysis experiments were performed at this temperature. Based on the experimental findings, blending polyethylene terephthalate, polystyrene, and polyvinyl chloride into biomass affected product yield substantially. Results showed a significant effect on the chemical structure of tars after co-pyrolysis, and tar yield increased up to 50 wt.%, while enhancing the quality of the tars and chars.

Table 1.5 Summaries of studies on co-pyrolysis of biomass mixed with plastics.

Biomass	Type of plastics	Type of reactor	T (°C)	Biomass alone Yield (wt.%)	Mixture materials (1:1 ratio) (wt.%)	Extra yield (wt.%)	Biomass Alone (MJ/kg)	Mixture materials (1:1 weight ratio) (MJ/kg)	References
Palm shell	PS	Stainless steel SC*	500	46.1	61.6	15.5	HHV=11.94	HHV=38.0	(Abnisa et al., 2014)
Pine cone	LDPE	Glass reactor SC	500	47.5	63.9	16.4	HHV =n.d	HHV =46.3	(Brebu et al., 2010)
	PP		500		64.1	16.6		HHV=45.6	
	PS		500		69.7	22.2		HHV=46.4	
Willow	PHB	Stainless steel SC	450	50.1	64.2	14.5	HHV=16.1	HHV=20.2	(Cornelissen et al., 2009, 2008a, 2008b)
	PLA				51.3	2.5		HHV=18.5	
	Bepearls				52.8	2.7		HHV=19.1	
	Solanyl				59.2	9.1		HHV=15.7	
	Potato starch				51.5	1.4		HHV=19.2	
Potato skin	HDPE	Stainless steel SC	500	23.0	39.0	16.0	HHV=32.0	HHV=45.6	(Önal et al., 2012)
Fir sawdust	Waste electrical and electronic equipment	Drop tube reactor	500	46.3	62.3	16.0	Not reported	Not reported	(Liu et al., 2013)
Wood chip	Block polypropylene	Quartz U-tube SC	500	39.3	63.1	23.8	HHV=19.9	HHV=45.0	(Jeon et al., 2011)
Pine Residue	(56%PE,17% PS and 27% PP)	Stainless steel autoclave	400	32.0	53.0	21.0	HHV=20.0	HHV=45.0	(Paradela et al., 2009)
Cellulose	PS	Vertical Pyrex	500	45.5	58.8	13.3	Not reported	Not reported	(Rutkowski and Kubacki, 2006)
Gasoline		HHV=43.9							(Ayanoğlu and Yumrutaş, 2016)
Diesel		HHV=42.7							

* SC: Semi-continuous

1.5. Catalytic co-pyrolysis

The obtained oil from co-pyrolysis requires further treatment to reduce the oxygen content. The most common technique to achieve this goal is the use of catalysts. There exist two different types of catalytic processes which are used for deoxygenation: hydrodeoxygenation (HDO) and catalytic cracking.

HDO uses conventional refinery hydrotreatment to gain the desired hydrocarbon product under the high pressure of hydrogen gas. The expensive catalysts used and challenging operating conditions with high hydrogen consumption make this technique economically and technically challenging (Elliott, 2007; Wang et al., 2013).

Catalytic cracking is a process that uses a solid catalyst to further crack the pyrolytic vapor under atmospheric pressure in an inert and hydrogen-free environment. Upgrading the bio-oil is done directly on the pyrolytic volatiles during pyrolysis by the use of a catalyst. Two catalyst configurations exist; in-situ and ex-situ. In-situ is conducted by feeding the raw material with the catalyst mixed all together. However, when the catalyst is placed downstream of the reactor, in the volatile zone, ex-situ configuration is attained.

One of the most commonly used catalysts is the zeolite ZSM-5. Several researchers supported the performance of zeolites, especially ZSM-5, in terms of deoxygenation potential and aromatic selectivity due to their acidity and pore size (Xue et al., 2016; Zhang et al., 2015, 2014). Deoxygenation occurs on the active sites of the catalyst via 3 main pathways: decarboxylation, decarbonylating, and dehydration (Xue et al., 2016). Decarboxylation mainly targets acid, thus releasing CO_2, decarbonylating targets carbonyl functional groups, while phenols and alcohols are deoxygenated by dehydration.

The main interest of using a catalyst in co-pyrolysis is the reduction of the oxygen content and thus, the increase of the heating value of the pyrolysis oil. To achieve this goal, there are many different methods in existence. Catalytic pyrolysis shows a low aromatic yield associated with high coke formation. This could be the consequence of the oxygen-enriched and hydrogen-deficient nature of biomass.

This hydrogen deficiency is characterized by a ratio called H/C_{eff} mass ratio **(Eq. 1.1)** which can predict the profile of catalytic co-pyrolysis (Zhang et al., 2015).

$$H/C_{eff} = \frac{H - 2O - 2S - 3N}{C} \qquad \textbf{Eq. 1.1}$$

H, O, S, N, and C are the respective mass percentages of hydrogen, oxygen, sulfur, nitrogen, and carbon within the given raw material.

H/C_{eff} for biomass is usually low (<0.3); Zhang et al. (2015) showed that this ratio must be greater than unity to attain low coking with high aromatic yield. The hydrogen deficiency of most biomass can be compensated by co-feeding processes with a hydrogen-rich source such as plastics or alcohol (Zhang et al., 2014). It has been shown that co-feeding biomass with synthetic polymers in catalytic pyrolysis could influence positively the performance of pyrolysis and the quality of products formed (Xue et al., 2016; Zhang et al., 2015). This addition could mimic hydrodeoxygenation by supplying the needed hydrogen at atmospheric pressure with minor modifications and an attractive performance/cost ratio.

The main catalysts used are HZSM-5, Γ-Al_2O_3, LOSA-1, HY, spent FCC, MCM-41, etc., and they could be further modified by certain metals to improve their activity. The characterization is essential for comparison between catalysts and to make sure the catalyst will work. Some characterization methods include (Bradley et al., 2010):

- **XRD** patterns: usually used to analyze crystallinity.
- **Scanning Electron Microscopy (SEM)**: gives a three-dimensional and topographic image of the catalyst and can detect the various atom distribution on a given surface of the catalyst.
- **Infrared Spectroscopy (IR):** tests the structure of the catalyst and other functional groups, and can be combined with the adsorption/desorption of probe molecules (pyridine, ammonia) to determine weak Lewis and Bronsted acid sites.
- **NMR** (^{29}Si,^{27}Al,^{1}H): helps get silicon and aluminum content thus determining, the SiO_2/Al_2O_3 ratio.
- **Nitrogen physisorption:** the micro-, meso-, and macro-sized pore dimension and size are determined including BET surface area.
- **Thermogravimetric analysis (TGA)** analysis to test thermal stability

1.5.1. Reactions and Mechanism

In terms of the reactions and steps for catalytic co-pyrolysis, they are quite similar to catalytic pyrolysis. The reaction mechanism of catalytic co-pyrolysis can be relatively complex due to the various types of materials introduced into the process. The catalytic co-pyrolysis mechanism can be grouped into two main interactions:

1) between biomass and polymers during thermal degradation, and
2) between the pyrolytic volatiles at the catalytic sites.

The focus will be on hydrocarbonaceous plastics since the objective is to reduce oxygen content. It is not practical to improve oxygen reduction by using an oxygenated plastic like PET. For this, the reaction pathway can be divided into 2 sets of plastic families: olefinic (LDPE, HDPE, and PP) and aromatics (PS). For the catalytic co-pyrolysis of biomass and plastic model compounds, polyolefins, it was observed that there was a positive synergy for aromatic production

in the co-feeding of cellulose and polyolefins. Cellulose-derived oxygenates could react with light olefins to produce aromatics (Chi et al., 2018; Dorado et al., 2014).

Fig.1.9 presents the reaction pathway for the conversion of cellulose and polyolefins into aromatic products in the catalytic co-pyrolysis over the ZSM-5 catalyst. It can be seen that furans (e.g., furan and furfural) derived from cellulose can interact with light olefins (ethylene and propylene) evolved from PE/PP to produce aromatics (e.g., BTX (benzene, toluene, and xylene)) through Diels–Alder reactions followed by dehydration reaction (Cheng and Huber, 2012).

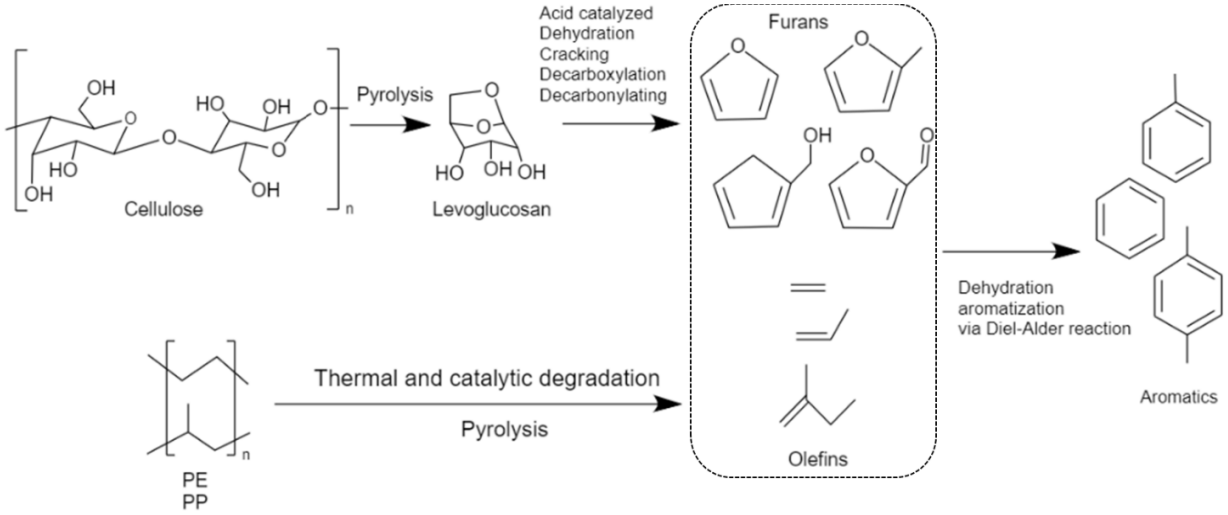

Fig.1.9 Aromatic production pathway from the catalytic co-pyrolysis of cellulose with olefinic polymers in the presence of the ZSM-5 catalyst; adapted from (Chi et al., 2018; Dorado et al., 2014)

In contrast to PP and PE, PS cannot produce olefins to interact with furan derivates to produce single-ring aromatic compounds. Yet, the interactions can follow a different pathway to produce polycyclic aromatic hydrocarbons (PAH), such as naphthalene. Generally, naphthalenes can be produced through the Diels–Alder condensation, dehydration of the benzene ring with furans, along with a cascaded alkylation of the aromatic ring and the intermediate allene. A detailed suggested mechanism is presented in **Fig.1.10**. Styrene is a major product of the thermal

degradation of PS and could undergo successive alkylation with allene derived from furans to form indene in the presence of the catalyst. As such, the indene produced could further react with allene to produce naphthalene.

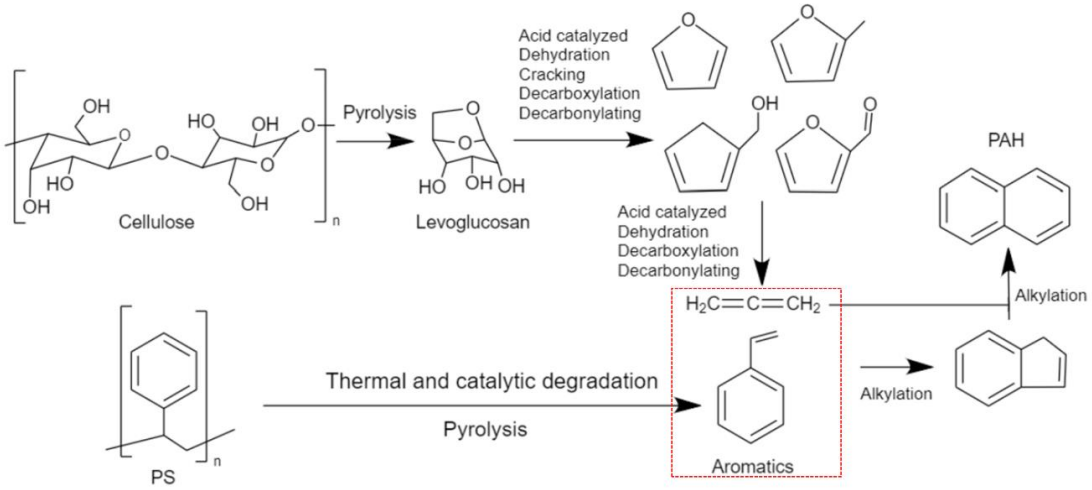

Fig.1.10. Reaction pathway of catalytic co-pyrolysis of polystyrene and biomass under ZSM-5, adapted from (Cheng and Huber, 2012 and Dorado et al., 2015).

The above-stated mechanisms describe only cellulose decomposition. For one of the other lignocellulosic biomass components, hemicellulose could be eliminated through a sequence of dehydration, decarbonylation, and decarboxylation reactions to generate furan compounds in the thermal degradation and then interact with the plastic-free radicals (Ren et al., 2012). Hence, the mechanism could be comparable to that of cellulose. On the other hand, unlike cellulose and hemicellulose, lignin is usually decomposed into phenolic compounds. However, the existence of free radicals from the plastic polymers could enhance the hydrogen transfer reaction, thus improving the decomposition of these phenolic compounds into hydrocarbon compounds (Serrano et al., 2005). The hydrogen from the thermal degradation of plastics was provided to biomass-derived oxygenates, that in turn acted as strong hydrogen acceptors, suppressing char formation.

1.5.2. State of art of catalytic co-pyrolysis

It is indicated that the liquid products from the non-catalytic pyrolysis of biomass with polymers cannot be used as liquid fuels, even though some properties (e.g., HHV and oxygen content) of liquid products have been improved to a large extent. To obtain advanced products, a catalyst should be introduced into the co-pyrolysis so that the carbon efficiency of aromatics can be enhanced and coke formation can be correspondingly reduced. To date, few studies have pointed out that the catalytic co-pyrolysis of biomass with plastics could significantly improve the carbon yield of target aromatics. The summary of representative studies on the catalytic co-pyrolysis of biomass with plastics is shown in **Table 1.6.**

Most of the previous studies focused on cellulose as a model compound of lignocellulosic biomass to investigate the catalytic co-pyrolysis with plastics. For instance, Li et al. (2013) carried out the catalytic co-pyrolysis of LDPE with cellulose. Results showed that the co-pyrolysis produce more aromatics (47 wt.%) than catalytic pyrolysis of cellulose alone accompanied by a lower coke formation. Most of the produced aromatics were valuable monocyclic aromatics such as toluene and xylene. As such, the difference among LDPE, PP, and PS in the catalytic co-pyrolysis over ZSM-5 was also investigated by Li et al., (2014). During co-feeding with cellulose, the reaction had a high selectivity towards petrochemicals, such as aromatics and olefins with a lower yield of solid residues (coke/char). It was clear that cellulose with LDPE showed more pronounced synergy because of the Diels–Alder reaction between cellulose-derived furans and LDPE-derived linear olefins during catalytic co-pyrolysis.

Table 1.6 Summary of studies on the catalytic co-pyrolysis of biomass with plastics.

Type of materials		Reaction conditions					Results		Ref.
Biomass	Plastics	Catalyst	SiO_2/Al_2O_3 (S_{BET} m^2/g)	Biomass/ Plastic	Temp. (°C)	Reactor	Aromatic yield (wt. %)	Aromatic selectivity	
Cellulose	LDPE	HZSM-5	25 (395)	1:1	650	Pyroprobe	48	Toluene and xylenes	(Li et al., 2013)
Cellulose	LDPE	HZSM-5	25 (372)	1:1	590	Curie-point pyrolyzer	34	BTX	(Zhou et al., 2014)
		B/HZSM-5	25 (163-315)				31	Xylenes and toluene	
Cellulose	LDPE	HZSM-5	25 (395)	2:1	550	Pyroprobe	48	Toluene and xylenes	(Li et al., 2014)
	PP						38	Toluene and PAH	
	PS						54	Benzene and PAH	
Cellulose	LDPE	HZSM-5	50 (387-396)	1:0.4–1:1.45	250–500	Microwave pyrolyzer	36–46	Xylenes and trimethylbenzene	(Zhang et al., 2016)
Cellulose	LLDPE	HZSM-5	30 (405)	1:1	500-600	Micro pyrolyzer	12–33	Toluene and xylenes	(Kim et al., 2016)
		HY	30 (780)				10–17	Toluene and xylenes	
	PP	HZSM-5	30 (405)				8–27	Toluene and xylenes	
		HY	30 (780)				9–15	Xylenes and other mono-aromatics	
Milled wood	PE	HZSM-5	30 (405)	1:1	500	Micro-pyrolyzer	15	BTX	(Xue et al., 2016)
Pine sawdust	PE	Spent FCC	1.4 (243)	1:4–4:1	400–650	Fluidized bed reactor	15–38	Benzene and naphthalene	(Zhang et al., 2014)
		LOSA-1	3.9 (220)	1:1	600		43	Benzene and toluene	
		Γ-Al_2O_3	0 (135)				26	Benzene and naphthalene	
		Sand	n.a				20	Benzene and toluene	
	PP	Spent FCC	1.4 (243)				35	Benzene and naphthalene	
	PS	Spent FCC	1.4 (243)				47	Benzene and naphthalene	
Switchgrass	LDPE	HZSM-5	23 (425)	1:1	650	Micro pyrolyzer	7	Xylene and toluene	(Dorado et al., 2014)
	HDPE						6	*X*ylene and toluene	
	PP						10	*X*ylene and toluene	
	PET						10	*X*ylene toluene, and naphthalene	

Moreover, Dorado et al. (2015) aimed to produce fuels from the catalytic co-pyrolysis of switchgrass with plastics (LDPE, HDPE, PP, PS, and PET) in the presence of the HZSM-5 catalyst. Results showed that the enhancement of aromatic hydrocarbons took place with aliphatic polymers (PE and PP) and PET, presenting a remarkable increase in the aromatic yield. In contrast with ZSM-5-based catalysts, Kim et al. (2016) have made efforts to study the effect of the zeolite pore structure on aromatic production during catalytic co-pyrolysis. The catalytic co-pyrolysis of linear low-density polyethylene (LLDPE) or PP with cellulose was carried out in the presence of an HZSM-5 or HY catalyst. Results showed that the synergistic aromatic production was better under HY for both LLDPE and PP.

On the other hand, several researchers discussed the metal impregnation of zeolites with metals to improve the performance of the catalyst. Yao et al. (2015) investigated the catalytic co-pyrolysis of pine wood with low-density polyethylene in a semi-continuous pyroprobe. The catalyst was mixed with the feed with a catalyst-to-feed ratio of 15 at 550 °C. The study used ZSM-5 as a base catalyst and modified it with nickel (Ni) and phosphorus (P) then with phosphorous alone, 2 % P-ZSM-5, and 3 %/2 % P/Ni-ZSM-5. Results showed an increase of olefins and aromatics from 43 wt.% for conventional ZSM-5 to about 53-54 wt.% for P- and P/Ni-ZSM-5, respectively. Lin et al. (2015**)** did a similar modification of ZSM-5. The study investigated the performance of P-ZSM5 through the catalytic co-pyrolysis of poplar wood and high-density polyethylene in a quartz pyroprobe with P-loadings varying from 0 to 10 wt.%. The effect of several parameters was studied, such as heating rates, temperature, residence time, and catalyst-to-feedstock ratio. It was found that the parent ZSM-5 favored aromatic production whereas the modified P-ZSM-5 favored the formation of light aliphatic hydrocarbons. Another approach was carried out by J. Li et al. (2015); the authors studied the catalytic co-pyrolysis of pine wood and low-density polyethylene using a gallium-modified zeolite in a semi-continuous

microreactor at 550 °C. An increase of monoaromatics of 5 % Ga-ZSM-5 compared to the parent ZSM-5 by about 5 wt.% was shown.

In the end, the best catalyst that showed the best activity based on previous studies could be HZSM-5 modified by certain metals. One of these metals would be nickel since it showed good improvement in the catalyst. Other metals could be co-impregnated with nickel to further improve their performance.

1.6. Recapitulation

The pyrolysis process has the potential to play an important role in the generation of energy sources regarding the heating value. More precisely, the use of co-pyrolysis of biomass and plastic feedstock seems to possess a synergetic effect which makes the produced bio-oil more suitable for further application. In addition, using lignocellulosic biomass as a source of fuel and petrochemicals reduces the dependence on petroleum fuels and mitigates global warming. Furthermore, by using waste polymers as co-reactant, waste disposal and handling in landfills are reduced, which can also solve environmental hazards and play a role in energy security.

Catalytic-co-pyrolysis is not only concerned with increasing carbon yield and decreasing oxygen content, but it also leads to dramatic coke reduction boosting catalysts' lifetime. Catalytic cracking under the zeolite-based catalyst has shown to be the best/economic route in the catalytic process.

1.7. References

Abnisa, F., 2013. Co-pyrolysis of palm shell and polystyrene waste mixtures to synthesis liquid fuel. Fuel 108, 311–318.

Abnisa, F., Daud, W.M.A.W., Sahu, J.N., 2014. Pyrolysis of mixtures of palm shell and polystyrene: An optional method to produce a high-grade of pyrolysis oil. Environmental Progress & Sustainable Energy 33, 1026–1033. https://doi.org/10.1002/ep.11850

Abnisa, F., Wan Daud, W.M.A., 2014. A review on co-pyrolysis of biomass: An optional technique to obtain a high-grade pyrolysis oil. Energy Conversion and Management 87, 71–85. https://doi.org/10.1016/j.enconman.2014.07.007

Abnisa, F., Wan Daud, W.M.A., Ramalingam, S., Azemi, M.N.B.M., Sahu, J.N., 2013. Co-pyrolysis of palm shell and polystyrene waste mixtures to synthesis liquid fuel. Fuel 108, 311–318. https://doi.org/10.1016/j.fuel.2013.02.013

Akhtar, A., Krepl, V., Ivanova, T., 2018. A Combined Overview of Combustion, Pyrolysis, and Gasification of Biomass. Energy Fuels 32, 7294–7318. https://doi.org/10.1021/acs.energyfuels.8b01678

Ansari, K.B., Hassan, S.Z., Bhoi, R., Ahmad, E., 2021. Co-pyrolysis of biomass and plastic wastes: A review on reactants synergy, catalyst impact, process parameter, hydrocarbon fuel potential, COVID-19. Journal of Environmental Chemical Engineering 9, 106436. https://doi.org/10.1016/j.jece.2021.106436

Anuar Sharuddin, S.D., Abnisa, F., Wan Daud, W.M.A., Aroua, M.K., 2016. A review on pyrolysis of plastic wastes. Energy Conversion and Management 115, 308–326. https://doi.org/10.1016/j.enconman.2016.02.037

Ayanoğlu, A., Yumrutaş, R., 2016. Rotary kiln and batch pyrolysis of waste tire to produce gasoline and diesel like fuels. Energy Conversion and Management 111, 261–270. https://doi.org/10.1016/j.enconman.2015.12.070

Ballice, L., Reimert, R., 2002. Classification of volatile products from the temperature-programmed pyrolysis of polypropylene (PP), atactic-polypropylene (APP) and thermogravimetrically derived kinetics of pyrolysis. Chemical Engineering and Processing: Process Intensification 41, 289–296. https://doi.org/10.1016/S0255-2701(01)00144-1

Basak, A., 2009. Environmental Studies [WWW Document]. URL https://books.google.com.lb/books?id=yElrhPSIq-wC&pg=PA156&lpg=PA156&dq=PVC+bottle+in+a+batch+of+10,000+PET&source=bl&ots=5mptFry2BB&sig=ACfU3U1PK_HgezEViH6T8CoHuk2TEHElIQ&hl=en&sa=X&ved=2ahUKEwiE7vycnvj3AhVCy6QKHUyfBZQQ6AF6BAgpEAM#v=onepage&q=PVC%20bottle%20in%20a%20batch%20of%2010%2C000%20PET&f=false (accessed 5.24.22).

B.P., 2018. BP Statistical Review of World Energy 2018.

Bradley, S.A., Broach, R.W., Mezza, T.M., Prabhakar, S., Sinkler, W., 2010. Zeolite Characterization, in: Zeolites in Industrial Separation and Catalysis. John Wiley & Sons, Ltd, pp. 85–171. https://doi.org/10.1002/9783527629565.ch4

Brassard, P., Godbout, S., Raghavan, V., 2017. Pyrolysis in auger reactors for biochar and bio-oil production: A review. Biosystems Engineering 161, 80–92. https://doi.org/10.1016/j.biosystemseng.2017.06.020

Brebu, M., Ucar, S., Vasile, C., Yanik, J., 2010. Co-pyrolysis of pine cone with synthetic polymers. Fuel 89, 1911–1918.

Bridgwater, A.V., 2012. Review of fast pyrolysis of biomass and product upgrading. Biomass Bioenergy 38, 68–94.

Buderus, J., Schmidt, B., 2015. Grundlagen der organsichen Chemie. Walter de Gruyter GmbH, Dortmund.

Cai, J., He, Y., Yu, X., Banks, S.W., Yang, Y., Zhang, X., Yu, Y., Liu, R., Bridgwater, A.V., 2017. Review of physicochemical properties and analytical characterization of lignocellulosic biomass. Renewable and Sustainable Energy Reviews 76, 309–322. https://doi.org/10.1016/j.rser.2017.03.072

Campuzano, F., Brown, R.C., Martínez, J.D., 2019. Auger reactors for pyrolysis of biomass and wastes. Renewable and Sustainable Energy Reviews 102, 372–409. https://doi.org/10.1016/j.rser.2018.12.014

Cheng, Y.-T., Huber, G.W., 2012. Production of targeted aromatics by using Diels–Alder classes of reactions with furans and olefins over ZSM-5. Green Chem. 14, 3114. https://doi.org/10.1039/c2gc35767d

Chi, Y., Xue, J., Zhuo, J., Zhang, D., Liu, M., Yao, Q., 2018. Catalytic co-pyrolysis of cellulose and polypropylene over all-silica mesoporous catalyst MCM-41 and Al-MCM-41. Science of The Total Environment 633, 1105–1113. https://doi.org/10.1016/j.scitotenv.2018.03.239

Chmiel, H., 2006. Bioprozesstechnik. Spektrum Akademischer Verlag, München.

Cimenti, M., Hill, J.M., 2009. Direct Utilization of Liquid Fuels in SOFC for Portable Applications: Challenges for the Selection of Alternative Anodes. Energies 2, 377–410. https://doi.org/10.3390/en20200377

Cornelissen, T., Jans, M., Stals, M., Kuppens, T., Thewys, T., Janssens, G.K., Pastijn, H., Yperman, J., Reggers, G., Schreurs, S., Carleer, R., 2009. Flash co-pyrolysis of biomass:

The influence of biopolymers. Journal of Analytical and Applied Pyrolysis, Pyrolysis 2008 85, 87–97. https://doi.org/10.1016/j.jaap.2008.12.003

Cornelissen, T., Jans, M., Yperman, J., Reggers, G., Schreurs, S., Carleer, R., 2008a. Flash co-pyrolysis of biomass with polyhydroxybutyrate: Part 1. Influence on bio-oil yield, water content, heating value and the production of chemicals. Fuel 87, 2523–2532.

Cornelissen, T., Yperman, J., Reggers, G., Schreurs, S., Carleer, R., 2008b. Flash co-pyrolysis of biomass with polylactic acid. Part 1: Influence on bio-oil yield and heating value,Fuel.

Czernik, S., Bridgwater, A.V., 2004. Overview of Applications of Biomass Fast Pyrolysis Oil. Energy Fuels 18.

Dhyani, V., Bhaskar, T., 2018. A comprehensive review on the pyrolysis of lignocellulosic biomass, in: Renew. Energy, 1st International Conference on Bioresource Technology for Bioenergy, Bioproducts & Environmental Sustainability. pp. 695–716. https://doi.org/10.1016/j.renene.2017.04.035

Doing group, 2022. manufacturers Tire pyrolysis plant,pyrolysis plant,pyrolysis oil plant,pyrolysis tyre/plastic to oil [WWW Document]. URL https://www.doinggroup.com/ (accessed 8.25.22).

Dorado, C., Mullen, C.A., Boateng, A.A., 2015. Origin of carbon in aromatic and olefin products derived from HZSM-5 catalyzed co-pyrolysis of cellulose and plastics via isotopic labeling. Applied Catalysis B: Environmental 162, 338–345. https://doi.org/10.1016/j.apcatb.2014.07.006

Dorado, C., Mullen, C.A., Boateng, A.A., 2014. H-ZSM5 Catalyzed Co-Pyrolysis of Biomass and Plastics. ACS Sustainable Chem. Eng. 2, 301–311. https://doi.org/10.1021/sc400354g

Eisentraut, A., 2010. Sustainable Production of Second-Generation Biofuels: Potential and Perspectives in Major Economies and Developing Countries. OECD, Paris. https://doi.org/10.1787/5kmh3njpt6r0-en

Elliott, D.C., 2007. Historical Developments in Hydroprocessing Bio-oils. Energy Fuels 21, 1792–1815. https://doi.org/10.1021/ef070044u

Ephraim, A., Pham Minh, D., Lebonnois, D., Peregrina, C., Sharrock, P., Nzihou, A., 2018. Co-pyrolysis of wood and plastics: Influence of plastic type and content on product yield, gas composition and quality. Fuel 231, 110–117. https://doi.org/10.1016/j.fuel.2018.04.140

FAOSTAT [WWW Document], n.d. URL https://www.fao.org/faostat/en/#data (accessed 5.19.22).

Ge, X., Chang, C., Zhang, L., Cui, S., Luo, X., Hu, S., Qin, Y., Li, Y., 2018. Chapter Five - Conversion of Lignocellulosic Biomass Into Platform Chemicals for Biobased Polyurethane Application, in: Li, Y., Ge, X. (Eds.), Advances in Bioenergy. Elsevier, pp. 161–213. https://doi.org/10.1016/bs.aibe.2018.03.002

Global plastic production 1950-2020 [WWW Document], 2022. . Statista. URL https://www.statista.com/statistics/282732/global-production-of-plastics-since-1950/ (accessed 6.27.22).

Huayin Renewable Energy, 2022. Pyrolysis Plant For Solid Wastes Recycling. Huayin Renewable Energy. URL https://huayinre.com/pyrolysis-plant/ (accessed 8.25.22).

Jeon, M.-J., Choi, S.J., Yoo, K.-S., Ryu, C., Park, S.H., Lee, J.M., Jeon, J.-K., Park, Y.-K., Kim, S., 2011. Copyrolysis of block polypropylene with waste wood chip. Korean J. Chem. Eng. 28, 5.

Johannes, I., Tiikma, L., Luik, H., 2013. Synergy in co-pyrolysis of oil shale and pine sawdust in autoclaves. Journal of Analytical and Applied Pyrolysis 104, 341–352. https://doi.org/10.1016/j.jaap.2013.06.015

Jölli, D., Giljum, S., 2005. Unused biomass extraction in agriculture, forestry and fishery.

Kaltschmitt, M., Hartmann, H., Hofbauer, H., 2009. Energie aus Biomasse: Grundlagen, Techniken und Verfahren. s.l. : Springer 2. Auflage.

Karampinis, E., Grammelis, P., Zethraeus, B., Andrijevskaja, J., Kask, Ü., Kask, L., Hoyne, S., Phelan, P., Casini, L., Picchi, G., Sandak, A., Sandak, J., 2012. BISYPLAN: The Bioenergy System Planners Handbook. European Biomass Conference and Exhibition Proceedings 20th EU BC&E-Milan 2012, 2462–2464. https://doi.org/10.5071/20thEUBCE2012-5AV.3.52

Kim, B.-S., Kim, Y.-M., Lee, H.W., Jae, J., Kim, D.H., Jung, S.-C., Watanabe, C., Park, Y.-K., 2016. Catalytic Copyrolysis of Cellulose and Thermoplastics over HZSM-5 and HY. ACS Sustainable Chem. Eng. 4, 1354–1363. https://doi.org/10.1021/acssuschemeng.5b01381

Klass, D.L., 1998. Biomass for renewable energy, fuels and chemicals. Academic Press, San Diego.

Klemm, D., Heublein, B., Fink, H.-P., Bohn, A., 2005. Cellulose: Fascinating Biopolymer and Sustainable Raw Material. Angewandte Chemie International Edition 44, 3358–3393. https://doi.org/10.1002/anie.200460587

Kruse, A., 2009. Hydrothermal biomass gasification. The Journal of Supercritical Fluids, 20th Year Anniversary Issue of the Journal of Supercritical Fluids 47, 391–399. https://doi.org/10.1016/j.supflu.2008.10.009

Kumagai, S., Fujita, K., Kameda, T., Yoshioka, T., 2016. Interactions of beech wood–polyethylene mixtures during co-pyrolysis. Journal of Analytical and Applied Pyrolysis 122, 531–540. https://doi.org/10.1016/j.jaap.2016.08.012

Kumagai, S., Fujita, K., Takahashi, Y., Nakai, Y., Kameda, T., Saito, Y., Yoshioka, T., 2019. Beech Wood Pyrolysis in Polyethylene Melt as a Means of Enhancing Levoglucosan and Methoxyphenol Production. Sci Rep 9, 1955. https://doi.org/10.1038/s41598-018-37146-w

Li, B., Ou, L., Dang, Q., Meyer, P., Jones, S., Brown, R., Wright, M., 2015. Techno-economic and uncertainty analysis of in situ and ex situ fast pyrolysis for biofuel production. Bioresource Technology 196, 49–56. https://doi.org/10.1016/j.biortech.2015.07.073

Li, J., Yu, Y., Li, X., Wang, W., Yu, G., Deng, S., Huang, J., Wang, B., Wang, Y., 2015. Maximizing carbon efficiency of petrochemical production from catalytic co-pyrolysis of biomass and plastics using gallium-containing MFI zeolites. Applied Catalysis B: Environmental 172–173, 154–164. https://doi.org/10.1016/j.apcatb.2015.02.015

Li, X., Li, J., Zhou, G., Feng, Y., Wang, Y., Yu, G., Deng, S., Huang, J., Wang, B., 2014. Enhancing the production of renewable petrochemicals by co-feeding of biomass with plastics in catalytic fast pyrolysis with ZSM-5 zeolites. Applied Catalysis A: General 481, 173–182. https://doi.org/10.1016/j.apcata.2014.05.015

Li, X., Zhang, H., Li, J., Su, L., Zuo, J., Komarneni, S., Wang, Y., 2013. Improving the aromatic production in catalytic fast pyrolysis of cellulose by co-feeding low-density polyethylene. Applied Catalysis A: General 455, 114–121. https://doi.org/10.1016/j.apcata.2013.01.038

Lin, X., Zhang, Z., Sun, J., Guo, W., Wang, Q., 2015. Effects of phosphorus-modified HZSM-5 on distribution of hydrocarbon compounds from wood–plastic composite pyrolysis using Py-GC/MS. Journal of Analytical and Applied Pyrolysis 116, 223–230. https://doi.org/10.1016/j.jaap.2015.09.007

Liu, W.-J., Tian, K., Jiang, H., Zhang, X.-S., Yang, G.-X., 2013. Preparation of liquid chemical feedstocks by co-pyrolysis of electronic waste and biomass without formation of polybrominated dibenzo-p-dioxins. Bioresource Technology 128, 1–7. https://doi.org/10.1016/j.biortech.2012.10.160

Liu, Y., Qian, J., Wang, J., 2000. Pyrolysis of polystyrene waste in a fluidized-bed reactor to obtain styrene monomer and gasoline fraction. Fuel Processing Technology 63, 1, 45–55.

Mahesh, V., Joladarashi, S., M.Kulkarni.2020, S., 2021. A comprehensive review on material selection for polymer matrix composites subjected to impact load. Defence Technology. https://doi.org/10.1016/j.dt.2020.04.002

Marin, N., Collura, S., Sharypov, V.I., Beregovtsova, N.G., Baryshnikov, S.V., Kutnetzov, B.N., Cebolla, V., Weber, J.V., 2002. Copyrolysis of wood biomass and synthetic polymers mixtures. Part II: characterisation of the liquid phases. Journal of Analytical and Applied Pyrolysis 65, 41–55. https://doi.org/10.1016/S0165-2370(01)00179-6

Mingjie group, 2022. Pyrolysis Plant-Products-Henan Mingjie Environmental Equipment Co., Ltd [WWW Document]. URL https://www.mingjiegroup.com/products/products_9_1.html?gclid=CjwKCAjwu5yYBhAjEiwAKXk_eOeKLfmREXhKz3dbQe5x6Kv6VZxweRHvJTvFugyAHBRWRsCDpTqjshoCpgkQAvD_BwE (accessed 8.25.22).

Mohabeer, C.C.D., 2018. Bio-oil production by pyrolysis of biomass coupled with a catalytic de-oxygenation treatment (These de doctorat). Normandie.

Mortezaeikia, V., Tavakoli, O., Khodaparasti, M.S., 2021. A review on kinetic study approach for pyrolysis of plastic wastes using thermogravimetric analysis. Journal of Analytical and Applied Pyrolysis 160, 105340. https://doi.org/10.1016/j.jaap.2021.105340

Önal, E., Uzun, B.B., Pütün, A.E., 2012. An experimental study on bio-oil production from co-pyrolysis with potato skin and high-density polyethylene (HDPE). Fuel Processing Technology 104, 365–370. https://doi.org/10.1016/j.fuproc.2012.06.010

Özsin, G., Pütün, A.E., 2018. A comparative study on co-pyrolysis of lignocellulosic biomass with polyethylene terephthalate, polystyrene, and polyvinyl chloride: Synergistic effects and product characteristics. Journal of Cleaner Production 205, 1127–1138.

Paradela, F., Pinto, F., Gulyurtlu, I., Cabrita, I., Lapa, N., 2009. Study of the co-pyrolysis of biomass and plastic wastes. Clean Techn Environ Policy 11, 115–122. https://doi.org/10.1007/s10098-008-0176-1

Perera, F., Nadeau, K., 2022. Climate Change, Fossil-Fuel Pollution, and Children's Health. New England Journal of Medicine 386, 2303–2314. https://doi.org/10.1056/NEJMra2117706

Praveen Kumar, K., Srinivas, S., 2020. Catalytic Co-pyrolysis of Biomass and Plastics (Polypropylene and Polystyrene) Using Spent FCC Catalyst. Energy Fuels 34, 460–473. https://doi.org/10.1021/acs.energyfuels.9b03135

Qi, Z., 2007. Review of biomass pyrolysis oil properties and upgrading research. Energy Conversion and Management 48, 1, 87–92.

Rabnawaz, M., Wyman, I., Auras, R., Cheng, S.A., 2017. Roadmap towards green packaging:current status and future outlook for polyesters in the packaging industry. Green Chem 18, 1–3.

Rahman, M.H., Bhoi, P.R., Saha, A., Patil, V., Adhikari, S., 2021. Thermo-catalytic co-pyrolysis of biomass and high-density polyethylene for improving the yield and quality of pyrolysis liquid. Energy 225, 120231. https://doi.org/10.1016/j.energy.2021.120231

Ram, M., Mondal, M.K., 2022. Chapter 13 - Biomass gasification: a step toward cleaner fuel and chemicals, in: Gurunathan, B., Sahadevan, R., Zakaria, Z.A. (Eds.), Biofuels and Bioenergy. Elsevier, pp. 253–276. https://doi.org/10.1016/B978-0-323-85269-2.00008-3

Ren, S., Lei, H., Wang, L., Bu, Q., Chen, S., Wu, J., Julson, J., Ruan, R., 2012. Biofuel production and kinetics analysis for microwave pyrolysis of Douglas fir sawdust pellet. Journal of Analytical and Applied Pyrolysis 94, 163–169. https://doi.org/10.1016/j.jaap.2011.12.004

Reuters, 2015. The earth is not running out of oil and gas, BP says. The Telegrapgh.

Rotliwala, Y.C., Parikh, P.A., 2011. Thermal degradation of rice-bran with high density polyethylene: A kinetic study. Korean Journal of Chemical Engineering 28, 3, 788–792.

Rutkowski, P., Kubacki, A., 2006. Influence of polystyrene addition to cellulose on chemical structure and properties of bio-oil obtained during pyrolysis. Energy Conversion and Management 47, 716–731. https://doi.org/10.1016/j.enconman.2005.05.017

Serrano, D.P., Aguado, J., Escola, J.M., Rodríguez, J.M., San Miguel, G., 2005. An investigation into the catalytic cracking of LDPE using Py–GC/MS. Journal of Analytical and Applied Pyrolysis, Pyrolysis 2004 74, 370–378. https://doi.org/10.1016/j.jaap.2004.11.026

Sharypov, V.I., Marin, N., Beregovtsova, N.G., Baryshnikov, S.V., Kuznetsov, B.N., Cebolla, V.L., Weber, J.V., 2002. Co-pyrolysis of wood biomass and synthetic polymer mixtures. Part I: influence of experimental conditions on the evolution of solids, liquids and gases. Journal of Analytical and Applied Pyrolysis 64, 15–28. https://doi.org/10.1016/S0165-2370(01)00167-X

Siddiqui, M.N., 2009. Conversion of hazardous plastic wastes into useful chemical products. Journal of Hazardous Materials 167, 728–735. https://doi.org/10.1016/j.jhazmat.2009.01.042

Silvarrey, L.S.D., A.N., 2016. Phan,Kinetic study of municipal plastic waste,International. Journal of Hydrofgen Energy 4I, 16352–16364.

Speight, J.G., 2019. Chapter 9 - Catalytic Cracking Processes, in: Speight, J.G. (Ed.), Heavy Oil Recovery and Upgrading. Gulf Professional Publishing, pp. 357–421. https://doi.org/10.1016/B978-0-12-813025-4.00009-X

Stevanovic, T., 2007. Le monde merveilleux des extractibles du bois.

Syamsiroa, M., 2014. Fuel Oil Production from Municipal Plastic Wastes in Sequential Pyrolysis and Catalytic Reforming Reactors. Energy Procedia 47, 180-188 3.

tang, Y., Huang, Q., Sun, K., Chi, Y., Ya, J., 2018. Co-pyrolysis characteristics and kinetic analysis of organic food waste and plastic. Bioresource Technology 249, 16–23.

Thilakaratne, R., Brown, T., Li, Y., Hu, G., Brown, R., 2014. Mild catalytic pyrolysis of biomass for production of transportation fuels: a techno-economic analysis. Green Chem. 16, 627–636. https://doi.org/10.1039/C3GC41314D

US EPA, O., 2017. Greenhouse Gases [WWW Document]. URL https://www.epa.gov/report-environment/greenhouse-gases (accessed 8.22.22).

Vasalos, I.A., Lappas, A.A., Kopalidou, E.P., Kalogiannis, K.G., 2016. Biomass catalytic pyrolysis: process design and economic analysis. WIREs Energy and Environment 5, 370–383. https://doi.org/10.1002/wene.192

Venderbosch, R., Prins, W., 2010. Fast pyrolysis technology development. Biofuels, Bioproducts and Biorefining 4, 178–208. https://doi.org/10.1002/bbb.205

Vo, T.A., Tran, Q.K., Ly, H.V., Kwon, B., Hwang, H.T., Kim, J., Kim, S.-S., 2022. Co-pyrolysis of lignocellulosic biomass and plastics: A comprehensive study on pyrolysis kinetics and characteristics. Journal of Analytical and Applied Pyrolysis 163, 105464. https://doi.org/10.1016/j.jaap.2022.105464

Wang, H., Male, J., Wang, Y., 2013. Recent Advances in Hydrotreating of Pyrolysis Bio-Oil and Its Oxygen-Containing Model Compounds. ACS Catal. 3, 1047–1070. https://doi.org/10.1021/cs400069z

Wang, Z., 2021. Co-pyrolysis of waste plastic and solid biomass for synergistic production of biofuels and chemicals-A review. Progress in Energy and Combustion Science 51.

Wong, S.L., Ngadi, N., Abdullah, T.A.T., Inuwa, I.M., 2015. Current state and future prospects of plastic waste as source of fuel: A review. Renewable and Sustainable Energy Reviews 50, 1167–1180. https://doi.org/10.1016/j.rser.2015.04.063

World Bioenergy Association, 2020. GLOBAL BIOENERGY STATISTICS 2020.

Xue, Y., Kelkar, A., Bai, X., 2016. Catalytic co-pyrolysis of biomass and polyethylene in a tandem micropyrolyzer. Fuel 166, 227–236. https://doi.org/10.1016/j.fuel.2015.10.125

Xue, Y., Zhou, S., Brown, R.C., Kelkar, A., Bai, X., 2015. Fast pyrolysis of biomass and waste plastic in a fluidized bed reactor. Fuel 156, 40–46. https://doi.org/10.1016/j.fuel.2015.04.033

Yan, W., Acharjee, T.C., Coronella, C.J., Vásquez, V.R., 2009. Thermal pretreatment of lignocellulosic biomass. Environmental Progress & Sustainable Energy 28, 435–440. https://doi.org/10.1002/ep.10385

Yao, W., Li, J., Feng, Y., Wang, W., Zhang, X., Chen, Q., Komarneni, S., Wang, Y., 2015. Thermally stable phosphorus and nickel modified ZSM-5 zeolites for catalytic co-pyrolysis of biomass and plastics. RSC Adv. 5, 30485–30494. https://doi.org/10.1039/C5RA02947C

Zhang, B., Zhong, Z., Ding, K., Song, Z., 2015. Production of aromatic hydrocarbons from catalytic co-pyrolysis of biomass and high density polyethylene: Analytical Py–GC/MS study. Fuel 139, 622–628. https://doi.org/10.1016/j.fuel.2014.09.052

Zhang, H., Nie, J., Xiao, R., Jin, B., Dong, C., Xiao, G., 2014. Catalytic Co-pyrolysis of Biomass and Different Plastics (Polyethylene, Polypropylene, and Polystyrene) To Improve Hydrocarbon Yield in a Fluidized-Bed Reactor. Energy Fuels 28, 1940–1947. https://doi.org/10.1021/ef4019299

Zhang, X., 2016. Catalytic co-pyrolysis of lignocellulosic biomass with polymers: a critical review. Green Chemistry 18, 15, 4131–4314.

Zhang, X., Lei, H., Zhu, L., Qian, M., Zhu, X., Wu, J., Chen, S., 2016. Enhancement of jet fuel range alkanes from co-feeding of lignocellulosic biomass with plastics via tandem

catalytic conversions. Applied Energy 173, 418–430. https://doi.org/10.1016/j.apenergy.2016.04.071

Zhou, G., Li, J., Yu, Y., Li, X., Wang, Y., Wang, W., Komarneni, S., 2014. e. Applied Catalysis A: General 487, 45–53. https://doi.org/10.1016/j.apcata.2014.09.009

CHAPTER 2:

Co- Pyrolysis of common plastics and their mixtures to produce valuable petroleum-like products

2. PYROLYSIS OF COMMON PLASTICS AND THEIR MIXTURES TO PRODUCE VALUABLE PETROLEUM-LIKE PRODUCTS

2.1. Introduction

This chapter aims to investigate isothermal pyrolysis and analyze the chemical distribution of the gaseous and liquid products of polystyrene, low-density polyethylene, high-density polyethylene, and polypropylene pyrolysis as a function of temperature, and study the possible end-use of each pyrolytic oil. The use of such polymers in pyrolysis is attributed to two main reasons. First, the latter polymers constitute over 55 % of worldwide plastics production (Schwarz et al., 2019), thus constituting a major part of the plastics waste problem. The second reason lies in the fact that the studied polymers are hydrocarbons, thus the produced pyrolysis oil and gases would be oxygen-free, hence having better heating value and quality. On the other hand, the pyrolysis of hydrocarbon mixed plastic with a detailed product classification has not yet been thoroughly studied and could be of great importance since it reduces sorting, labor, and transportation cost. For that, a typical mixture of the latter plastics was prepared according to their contribution to Europe's plastic wastes (34 wt.% PP, 32 wt.% LDPE, 21 wt.% HDPE, and 13 wt.% PS) ("PlasticsEurope," 2021). The pyrolysis of the mixed plastics (MP) was studied and any interaction was further highlighted. The originality of this work is linked to the statistical correlations that have been established between the families, the compounds of each pyrolytic oil, and between the different pyrolytic oils obtained using principal component analysis (PCA). A part of this study was published in the journal of *Polymer Degradation and Stability (Jaafar et al., 2022).*

2.2. Materials and methods

2.2.1. Materials

The influence of different parameters on the quantity and quality of pyrolysis gaseous and liquid products were investigated, by using different feedstocks as well as different

temperatures. For the experiments, four of the most common plastics: HDPE, LDPE, PP, and PS, supplied by Goodfellow company, were mechanically milled and sieved to an average particle size of 2 mm, **Table 2.1** and **Table 2.2** illustrate the properties of all plastics used in this study. As can be seen, no plastic contains oxygen and the plastic yielded mainly volatile components upon pyrolysis. The four polymers consist only of hydrogen and carbon in different ratios. The repeating unit of HDPE and LDPE is ethylene, yet the main difference lies within the structure. HDPE is less branched than LDPE, consequently with higher density. PP has a repeating unit of propylene, and finally, PS is the only polymer in this study with aromatic monomer styrene. The elemental analysis of the four plastics was carried out using a CHN elemental analyzer Flash 2000 (Thermofisher Scientific) with logical exploitation EAGER 300. Thermogravimetric (TGA) measurements were achieved using an SDT/Q600-TA analyzer. The proximate analysis was made at a heating rate of 5 °C.min^{-1} under a nitrogen flow rate of 50 mL·min^{-1} and atmospheric pressure.

Table 2.1. Characteristics of used plastics (Goodfellow company)**.**

Name	Repeating unit [a]	LHV (MJ/kg) [a]	Density (kg/m^3) [a]	Ultimate analysis (wt.%) [b]	
				% C	% H
HDPE	-($CH_2CH_2)_n$-	44-46.2	952-965	85.9	14.1
LDPE	-($CH_2CH_2)_n$-	44-46.2	917-932	85.9	14.1
PP	-(CH_2-$CH(CH_3))_n$-	44-46.2	898-908	85.9	14.1
PS	-($CH(C_6H_5)$-$CH_2)_n$-	40.1-42.1	1040-1050	92.6	7.4

[a] The repeating unit and density were extracted from the supplier's datasheet

[b] Elemental composition computed using elemental analysis

Table 2.2. Proximate analysis of used plastic.

Name	Moisture (wt.%)	Fixed Carbon (wt.%)	Volatile (wt.%)	Ash (wt.%)
HDPE	-	-	100	-
LDPE	-	-	100	-
PP	-	-	100	-
PS	-	0.3	99.7	-

2.2.2. Methods

2.2.2.1. Pyrolysis experimental setup

Intermediate pyrolysis was carried out in a semi-continuous tubular reactor. It was composed of a quartz tube (ϕ= 50 mm, L=1050 mm) inserted horizontally in a tubular furnace. A stainless-steel sample carrier "spoon" was inserted from one end of the reactor, while the other end was connected to a condenser and a cold bath for liquid collection. Nitrogen gas of 99.995 % purity was used as carrier gas; which was regulated using a mass flowmeter. Furthermore, two steel heating jackets present around the quartz tube were adjusted to 300 °C and placed at the entrance and exit of the reactor to avoid oil pre-condensation. The exit of the tube was connected to a refrigerant circuit and a cold bath both set to a constant temperature of 5 °C. The round bottom flask was connected to a Tedlar gas bag for non-condensable gas collection.

Fig. 2.1 illustrates the layout of the reactor used. The pyrolysis experiments were conducted at temperatures of 450 °C, 500 °C, 550 °C, and 600 °C for each raw material. These temperatures were used to clearly cover the effect of temperature in the most used pyrolysis temperature range. For one specific experiment, before the introduction of a sample, an oxygen-free environment is achieved by injecting a constant nitrogen flow of 400 $mL.min^{-1}$ for at least 20 min. Under such nitrogen flow, the gas residence time was computed to be around 15-20 s. The furnace is then set at the required temperature with a heating rate of 20 $°C.min^{-1}$. About 3 g of plastic sample was placed into the sample carrier, which was situated at the entrance of the reactor until the desired temperature was reached and an inert environment was established. After stabilization, the sample carrier was placed in the middle of the reactor for 20 min. The isothermal pyrolysis reaction was roughly carried out in the first 5 min but was kept for 20 min to assure that the volatile compounds have been entirely evacuated from the reactor. Ultimately, the solid product remained in the sample carrier as residue, whereas the volatile products evaporated and were carried with the gas flow through the condenser. In the condenser, the

liquid condenses, whereas the non-condensable gas was collected in a Tedlar gas bag for gas chromatography analysis. After the reaction time of 20 min, the heater was turned off and the valve of the gas bag was closed and directed to the vent. Nitrogen continued to flow until the reactor was cooled down below 150 °C to permit the collection of a solid char without the risk of self-ignition. After cooling, n-hexane with 95% purity was used to recover the liquid product. The plastics alone and their mixture (MP) were pyrolyzed at four different temperatures in the tubular furnace and as per the conditions mentioned before. For a typical experiment, the procedure was repeated 3 times with an error computed to be around 1 % while the error on temperature could reach around 5 °C.

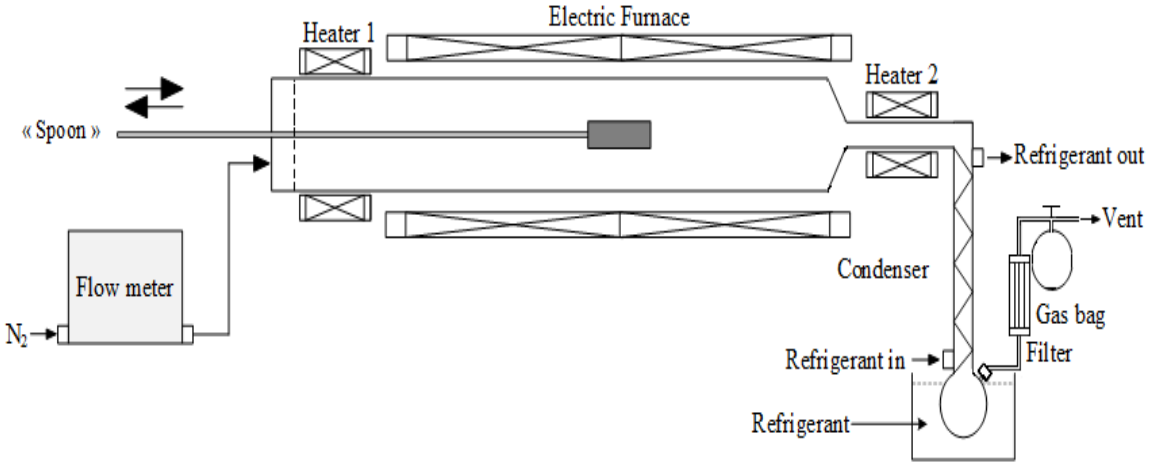

Fig. 2.1. Schematic setup of the tubular reactor.

2.2.2.2. GC analysis of non-condensable gases

To carry out the analysis of the non-condensable product, the pyrolysis gas, a Perkin Elmer® Clarus 580 gas chromatograph with argon as the carrier gas was used. The instrument possessed both, a flame-ionization detector (FID) and a thermal conductivity detector (TCD). The instrument included a Shincarbon St 100 120 column (1 m × 1 mm ID (inside diameter) × 1/16 in OD (outside diameter), a methanizer, and a hydrogen generator. The temperature of the oven was regulated from 100 to 180 °C. The TCD allowed analyzing components such as H_2 and N_2,

whereas the FID determined the carbonated components. CO and CO_2 were converted by the methanizer before passing to the FID.

2.2.2.3. GC-MS analysis for liquid products

The identification of the liquid products was realized in a gas chromatograph-mass spectrometer instrument GC-MS (Perkin Elmer Mass spectrometer Clarus® SQ 85), with a VF-1701 ms (Agilent) (60 m × 0.25 m × 0.25 µm film thickness). The carrier gas used for analysis was helium with a constant flow of 1 $mL.min^{-1}$. The detector temperature was set to 250 °C. The temperature of the oven was held for 4 min at 45 °C then heated to 240 °C for 20 min with a heating rate of 4 $°C.min^{-1}$. For each analysis, 1µL of the sample was injected at 250 °C (split ratio 30:1). For the detection of the constituents, full scan mode was used and the MS electron ionization was 70 eV. For the identification of the analyzed compounds, Varian WS (WorkStation) and NIST 2.3 software were used. Kovats's retention indices of the identified components were calculated and compared to their reference value for identity confirmation.

2.2.2.4. GC-FID analysis for liquid products

A GC-FID Scion 456-GC Bruker instrument was used to quantify the components. The column was the same as the one used for the GC-MS with the same temperature program. At first, the solvent was injected through the GC-FID to ensure that the impurities were eluted before recording the first pyrolytic compound. The identified compounds were then classified into different hydrocarbon fractions. A pure reference compound was used for each family for calibration. Standard solutions of each of these reference compounds were prepared and diluted with n-hexane. Four-point straight-line calibration curves (with $r^2>0.99$) were established for these pure compounds, which were used to quantify the different compounds. For each family, the calibration curve of the reference compounds was used to derive the quantities of all the compounds in the same family. The method used considers the structural and molecular differences between the compounds and the reference compound, which would lead to the

variation of the response factor. The relative response factors were corrected using the Effective Carbon Number method (ECN) (Scanlon and Willis, 1985).

2.2.2.5. Lower-heating value (LHV) of gaseous and liquid products

The LHV of the pyrolysis gas was computed by the average sum of the individual value of each component in the gaseous mixture. The heating value of each component was extracted from Perry's Chemical Engineers' handbook (Perry et al., 1997). However, the LHV and HHV of the pyrolytic oil were computed using Dulong equation per ***Eq. 2.1*** & ***Eq. 2.2*** (Marlair et al. 1999):

$$HHV_{fuel} = 33.8\, x_C + 144.2\, x_H - 18.03\, x_O \quad (MJ/kg) \quad \textbf{Eq. 2.1}$$

$$LHV_{fuel} = HHV_{fuel} - 21.96\, x_H \quad (MJ/kg) \quad \textbf{Eq. 2.2}$$

x_C, x_H, and x_O are the respective weight percentage of carbon, hydrogen, and oxygen.

2.2.2.6. Principal Component Analysis (PCA)

PCA is a transformation in which many original dimensions are transformed into another coordinate system with fewer dimensions; in most cases 2 dimensions (Esbensen et al., 2002). Thus, this technique allows the representation of a cloud of data onto a single graphic. XLSTAT® was used in this study for the analysis and evaluation of data. This software automatically generates all the correlations and figures that are subjected to further investigation. The different families and compounds in each family were taken as variables, whereas the various pyrolytic oil recovered under the different experimental conditions were the sample. PCA score plots, loading plots, and Pearson correlation matrices were established to deeply comprehend the covariations between the different pyrolytic oils under study (Mohabeer et al., 2017). A detailed introduction and application of PCA to multivariate data can be found in Esbensen et al. (Esbensen et al., 2002).

2.3. Results and discussion

2.3.1. TGA analysis

The TGA and DTG thermograms are shown in **Fig. 2.2**. The DTG curves show that each polymer is characterized by a one-step decomposition (one smooth peak). All the polymers have similar DTG curves, yet they are temperature-shifted from each other. This implies that the studied plastic polymers crack similarly, yet each has different thermal stability, PS being the least temperature stable, followed by PP then LDPE, and HDPE.

Based on TGA curves, each polymer was completely degraded, highlighting the absence of any char formation or the presence of inorganic residues (residue (%) = 0 after 500°C). Results also showed that pyrolysis started for PP, LDPE, and HDPE at a temperature around 390 °C (T_{onset}) and ended at 495 °C (T_{final}) (470 °C for PP) with a maximum degradation rate temperature of 470 °C (T_{max} for LDPE and HDPE and 450 °C for PP). However, PS seemed to crack at a lower temperature; cracking reactions began at 350 °C and ended at 440 °C, with a maximum degradation rate temperature of 400 °C.

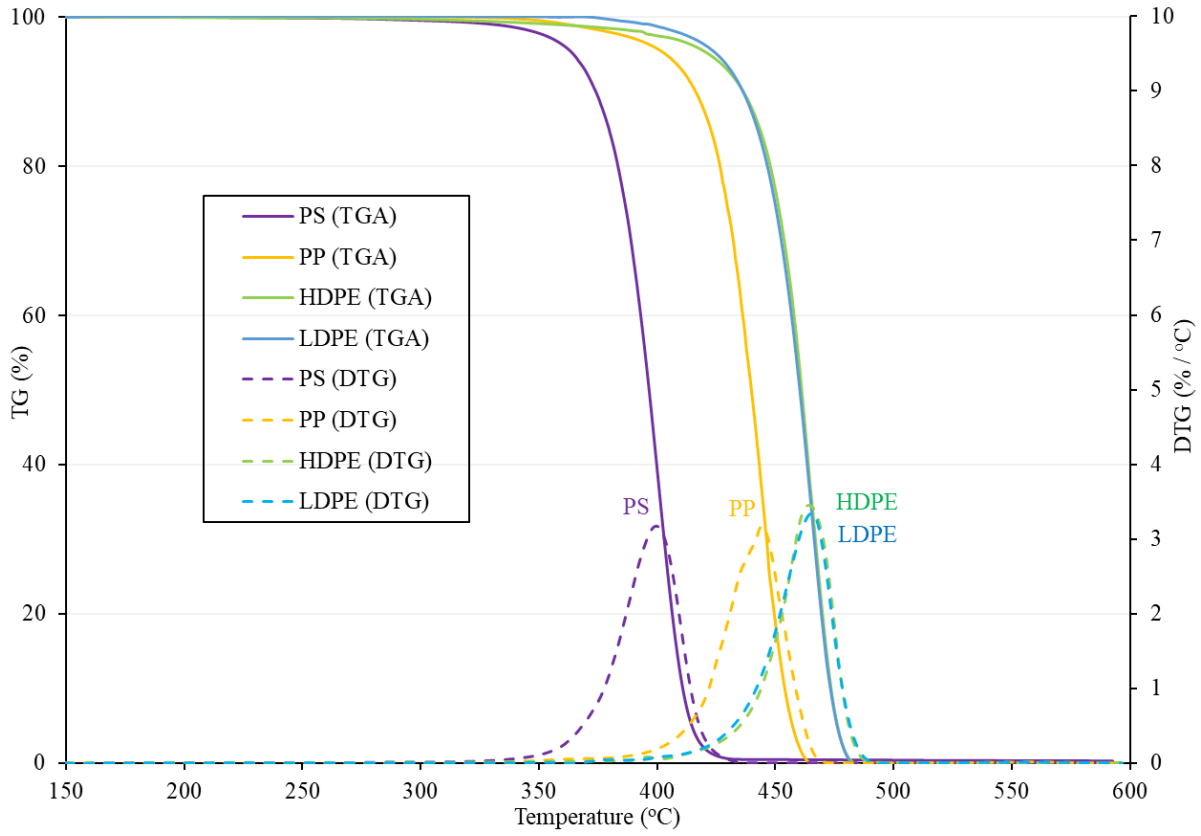

Fig. 2.2. TG and DTG analysis of the used plastics at 5 °C.min^{-1} heating rate.

2.3.2. Non-condensable gas analysis

Pyrolysis of low and high-density polyethylene

Gas component analysis was carried out for the pyrolysis of the four different plastics and their mixture at different temperatures. LDPE and HDPE showed similar gas compositions due to the chemical similarity of the two polymers. The main gases that were produced were propane, ethane, and methane as alkanes; ethylene and propylene as alkenes, serving as the dominant compounds, as shown in **Table 2.3**. Furthermore, a sharp increase in ethylene and methane gas was observed, implying the enhancement of cracking reaction as temperature increases, which was in agreement with the results obtained by Elordi et al. (2011). On the other hand, total alkanes and alkenes in both pyrolytic gases varied from 54 % and 40 % to 32 % and 59 %, respectively as the temperature varied from 450 °C to 600 °C. The gas composition found in this work was different from that observed by Onwudili et al. (2009). The authors reported that paraffinic gases were dominant at higher temperatures whereas olefinic gases dominated the gas products at lower temperatures. However, other published work, Conesa et al. (1997) corroborate this current study as more olefins were observed in the gas in a fluidized bed reactor at 800 °C.

As for product yield distribution (**Table 2.3**), liquid products dominated LDPE and HDPE products with a yield reaching around 99 wt.%. Increasing the pyrolysis temperature enhanced the gas yield while it decreased the liquid yield. For instance, HDPE and LDPE started at a slightly different liquid yields of 99 wt.% and 98 wt.%, then the two liquid yields converged to approximately the same yield of 90 wt.% at 600 °C. Thus, similar behavior is observed for LDPE and HDPE in the yield and gas composition, however, HDPE yielded no char whereas LDPE yields a small amount of char of around 0-1 wt.% that can be related to the structural differences between the two plastics.

Pyrolysis of polypropylene

Throughout pyrolysis, PP seemed to be reduced to its basic monomer propylene. Propylene dominated the gas products with a maximum concentration of 70 % at 450 °C decreasing afterward to 47 % at 600 °C. **Table 2.3** shows the composition of the PP pyrolytic gas components as a function of temperature. Methane and ethylene gas are enhanced by the temperature increase at the expense of propylene, which exhibited the opposite behavior. On the other hand, regarding the product yield, the maximum liquid yield was around 98 wt.% at 450 °C, which then decreased to 86 wt.% followed by an increase in the gas yield to 14 wt.% at 600 °C. This behavior can be explained by the enhancement of homogeneous cracking reactions that favors lighter products (Sharuddin et al., 2016).

Pyrolysis of polystyrene

For polystyrene, it's clear that the quantities of hydrogen and ethylene are the most elevated as shown in **Table 2.3**. However, for the very low gas yield of quantities close to 0 wt.%, the analysis of the gas component is not very accurate. The negligible gas yield detected agrees with the results of Liu et al. (2000) and Bouster et al. (1989). The aromatic structure of this plastic can explain the high liquid yield that was obtained. The aromatic ring is more challenging to break, thus, limiting gas yield and maximizing liquid production to almost 100 wt.% within the present experimental conditions.

On the other hand, pyrolytic gas of mixed polymers (MP) was rich in hydrogen, and the individual gas component of the mixed polymers with a reduced liquid yield. As for the lower heating value (LHV) of the pyrolytic gas, it is notable that this value was high and invariant relative to temperature and type of plastic used, ranging from 43 to 51 MJ/kg, which is comparable to that of natural gas with an LHV of 45-53 MJ/kg. The latter can be due to the dominance of light-carbon compounds with similar calorific values.

Table 2.3. Composition of gas products and the yield of gas, liquid, and char of plastic pyrolysis as a function of temperature.

Plastic	Temperature ±5 °C	Gas component (vol %)						Yield (wt.%)		
		H_2	CH_4	C_2H_4	C_2H_6	C_3H_6	C_3H_8	Gas	Liquid	Char
LDPE	450	5.8	12.5	15.3	18.4	25.0	23.1	1.1	97.3	1.6
	500	3.6	16.6	27.2	15.8	23.7	13.2	2.3	97.3	0.4
	550	4.3	19.1	33.6	13.1	23.4	6.6	5.3	94.7	-
	600	5.4	20.4	36.0	11.2	23.4	3.6	10.1	89.9	-
HDPE	450	5.3	8.9	13.8	13.4	27.3	25.6	0.6	99.4	-
	500	7.0	13.8	24.4	12.8	23.6	11.6	1.9	98.1	-
	550	4.6	18.2	34.0	12.0	24.5	5.7	5.2	94.8	-
	600	5.8	18.8	34.6	10.0	24.4	3.1	10.1	89.9	-
PP	450	1.9	8.6	1.8	14.5	69.5	3.7	2.4	97.6	-
	500	1.6	10.6	5.8	15.5	63.4	3.3	4.2	95.9	-
	550	2.8	15.4	11.5	15.0	52.6	2.7	10.9	89.1	-
	600	3.8	19.0	13.7	14.0	46.9	2.6	13.8	86.2	-
PS	450	37.3	12.7	44.7	5.3	-	-	0.0	100.0	-
	500	39.1	13.6	45.3	2.1	-	-	0.0	100.0	-
	550	41.8	13.8	37.1	1.5	5.8	-	0.1	99.9	-
	600	41.3	17.3	34.8	1.4	5.0	0.1	0.1	99.9	-
MP	450	14.8	10.9	9.2	13.7	40.7	10.7	2.2	97.8	-
	500	8.3	14.6	18.8	13.9	37.3	7.2	4.7	95.3	-
	550	15.2	16.6	22.5	11.8	30.1	3.7	11.2	88.8	-
	600	15.5	19.2	24.4	10.8	27.5	2.7	20.5	79.5	-

* The gas analysis of PS is not accurate due to the very low gas yield

2.3.3. Identification and quantification of pyrolytic components in oil

The first step in pyrolytic oil analysis was performed by GC-MS analysis. Individual peaks were identified for the four plastics alone; 246 compounds were identified for PP,183 for HDPE and LDPE, and 118 for PS. **Fig. 2.3** illustrates a typical chromatogram for the HDPE pyrolytic oil.

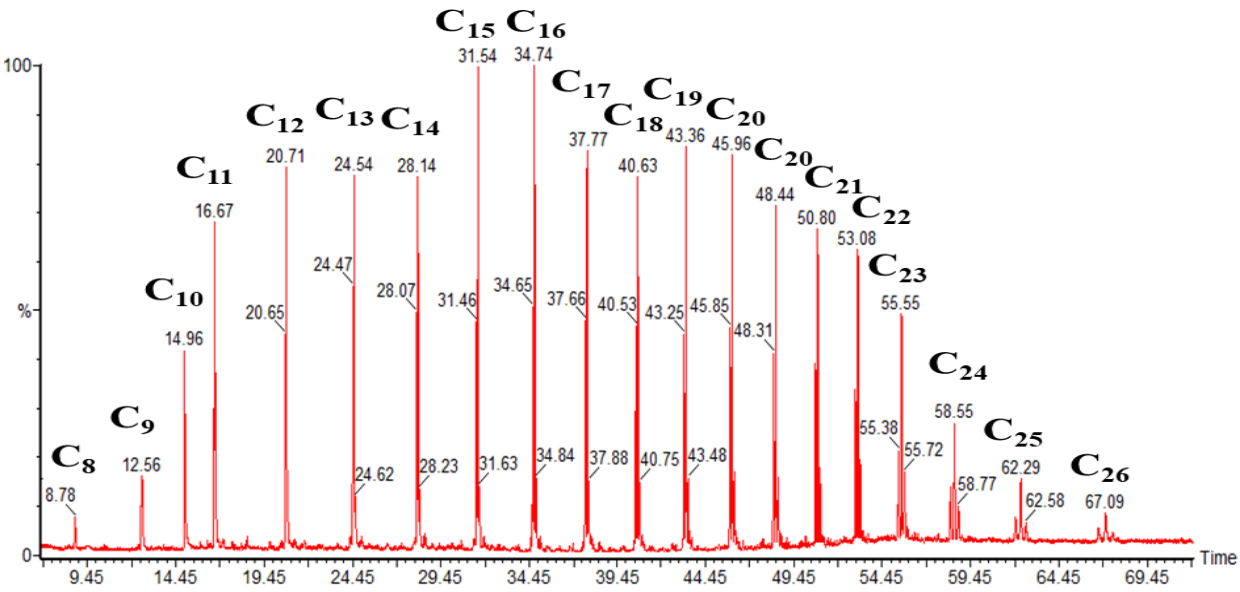

Fig. 2.3. GC-MS chromatogram of HDPE pyrolytic oil at 450 °C.

After the identification of individual peaks, quantification of each compound was performed. Thus, the products were grouped into 17 families for PP, HDPE, and LDPE summarizing the main components of liquid petroleum-derived products (BTX, gasoline, diesel, and fuel oil). Regarding PS, 5 families were created, summarizing the set of aromatic compounds produced. Families and major products for calibration are illustrated in **Table 2.4**.

The families were grouped based on structural and molecular similarities of compounds ranging from C7 to C28:

- + Diolefins compounds having at least 2 double bonds
- Gasoline compounds with C<12
- Diesel compounds with $12 \leq C \leq 20$
- Fuel oil compound with C >20

Table 2.4. List of families and major products in the plastic pyrolytic oil identified by GC-MS.

Plastic	Retention time (min)	Chemical family	Reference compound
PP HDPE LDPE	10.2*	Iso-paraffin Gasoline	4-Methylheptane
	10.2	Iso-paraffin Diesel	4-Methylheptane
	12.1	BTX	Toluene
	12.8	Naphthene Gasoline	1,3,5-Trimethylcyclohexane
	12.8	Naphthene Diesel	1,3,5-Trimethylcyclohexane
	19.4	Paraffin Gasoline	Decane

	21.6	Aromatic Gasoline	1,2,4-Trimethylbenzene
	23.4	Olefin Gasoline	1-Undecene
	25.5	Acetylene Gasoline	1-Undecyne
	27.1	Paraffin Diesel	Dodecane
	27.1	Olefin Diesel	1-Dodecene
	29.1	Acetylene Diesel	1-Dodecyne
	33.8	Aromatic Diesel	Cyclohexylbenzene
	33.9	+Diolefin Gasoline	1,13-Tetradecadiene
	33.9	+Diolefin Diesel	1,13-Tetradecadiene
	35.0	PAH	1-Methylnaphthalene
	55.5	Fuel Oil	Tetracosane
PS	12.1	BTX	Toluene
	17.9	Styrene monomer	Styrene
	21.3	Mono-aromatics (Low BP)	α-Methylstyrene
	40.8	Di-aromatics (Medium BP)	Bibenzyl
	49.4	Tri-Aromatics (High BP)	1-Phenylnaphthalene

* GC-FID retention time

Pyrolysis of low and high-density polyethylene

Pyrolysis of LDPE and HDPE produces an oil consisting mainly of linear chain paraffins and olefins. The chromatogram revealed a series of consecutive three major triplet peaks of linear aliphatic 1,(N-1)-alkadiene, 1-alkene, and n-alkane of the same carbon number (N) as shown in **Fig. 2.3**. The triplet products were also deduced by Kim et al. (2017) and Dorado et al. (2014) without mentioning the double bond position of the diolefins. Olefinic compounds were the main compounds of PE pyrolytic oil, which is reasonable and expected for a typical cracking reaction. Both HDPE and LDPE pyrolytic oil showed similar composition with similar products with a slight increase of higher molecular weight compounds for HDPE with a major product of 1-henicosene; a high molecular weight olefin. **Table 2.5** shows the major products derived from the pyrolysis of HDPE and LDPE in the liquid phase.

Table 2.5. List of the major products in HDPE/LDPE pyrolytic oil.

Retention time (min)	C_{number}	Pyrolysis products		
11.3*	C_8	Octane		
15.2	C_9	Nonane	1-Nonene	
19.3	C_{10}	Decane	1-Decene	1,9-Decadiene
23.3	C_{11}	Undecane	1-Undecene	1,10-Undecadiene

27.1	C_{12}	Dodecane	1-Dodecene	1,11-Dodecadiene
30.6	C_{13}	Tridecane	1-Tridecene	1,12-Tridecadiene
33.8	C_{14}	Tetradecane	1-Tetradecene	1,13-Tetradecadiene
36.9	C_{15}	Pentadecane	1-Pentadecene	1,14-Pentadecadiene
39.7	C_{16}	Hexadecane	Cetene	1,15-Hexadecadiene
42.4	C_{17}	Heptadecane	1-Heptadecene	1,16-Heptadecadiene
44.8	C_{18}	Octadecane	1-Octadecene	1,17-Octadecadiene
47.1	C_{19}	Nonadecane	1-Nonadecene	1,18-Nonadecadiene
49.2	C_{20}	Eicosane	1-Eicosene	1,19-Eicosadiene
51.2	C_{21}	Heneicosane	1-Henicosene	1,20-Henicosadiene
53.0	C_{22}	Docosane	1-Docosene	1,21-Docosadiene
54.9	C_{23}	Tricosane	1-Tricosene	1,22-Tricosadiene
56.9	C_{24}	Tetracosane	1-Tetracosene	1,23-Tetracosadiene
59.3	C_{25}	Pentacosane	1-Pentacosene	1,24-Pentacosadiene
62.2	C_{26}	Hexacosane	1-Hexacosene	1,25-Hexacosadiene
65.7	C_{27}	Heptacosane	1-Heptacosene	1,26-Heptacosadiene
69.9	C_{28}	Octacosane	1-Octacosene	1,27-Octacosadiene

* GC-FID retention time

Regarding the product distribution shown in **Fig. 2.4**, the fuel oil fraction was the dominant family in both HDPE and LDPE, with a percentage of 57 wt.% and 46 wt.% followed by the diesel olefinic fraction of 17 wt.% and 25 wt.%, respectively. LDPE pyrolytic oil was rich in compounds in the diesel fraction of 38 wt.% compared to 30 wt.% of that of HDPE. The gasoline fraction was also dominant for LDPE at 15 wt.% compared to 12 wt.% for HDPE. It seems that the derived oil is rich in low molecular weight straight olefins in the gasoline and diesel range. About 36 wt.% were found in LDPE along with a lower amount of 25 wt.% in HDPE, which can be due to the enhanced ramification in LDPE. On the other hand, negligible amounts of aromatics (<0.5 wt.%) and no iso-paraffins were detected in both the pyrolysis of LDPE and HDPE, which was corroborated by Marcilla et al. (2009), where no aromatics and no branched paraffins were detected by the authors for both LDPE and HDPE. Furthermore, for a better comparison with the latter study, the total amount of paraffins and 1-olefins was computed. The composition was 26 wt.% (19 wt.%) and 54 wt.% (60 wt.%) respectively for

HDPE (LDPE). This was similar to the study of Marcilla et al. (2009), where the weight fraction of total paraffins and 1-olefins were 37 wt.% (33 wt.%) and 44 wt.% (51 wt.%) for HDPE (LDPE), respectively, at 550 °C. It should be noted that both studies showed more olefinic compounds production for LDPE than HDPE being one of the few differences between the 2 plastics that can be due to their dissimilar structure.

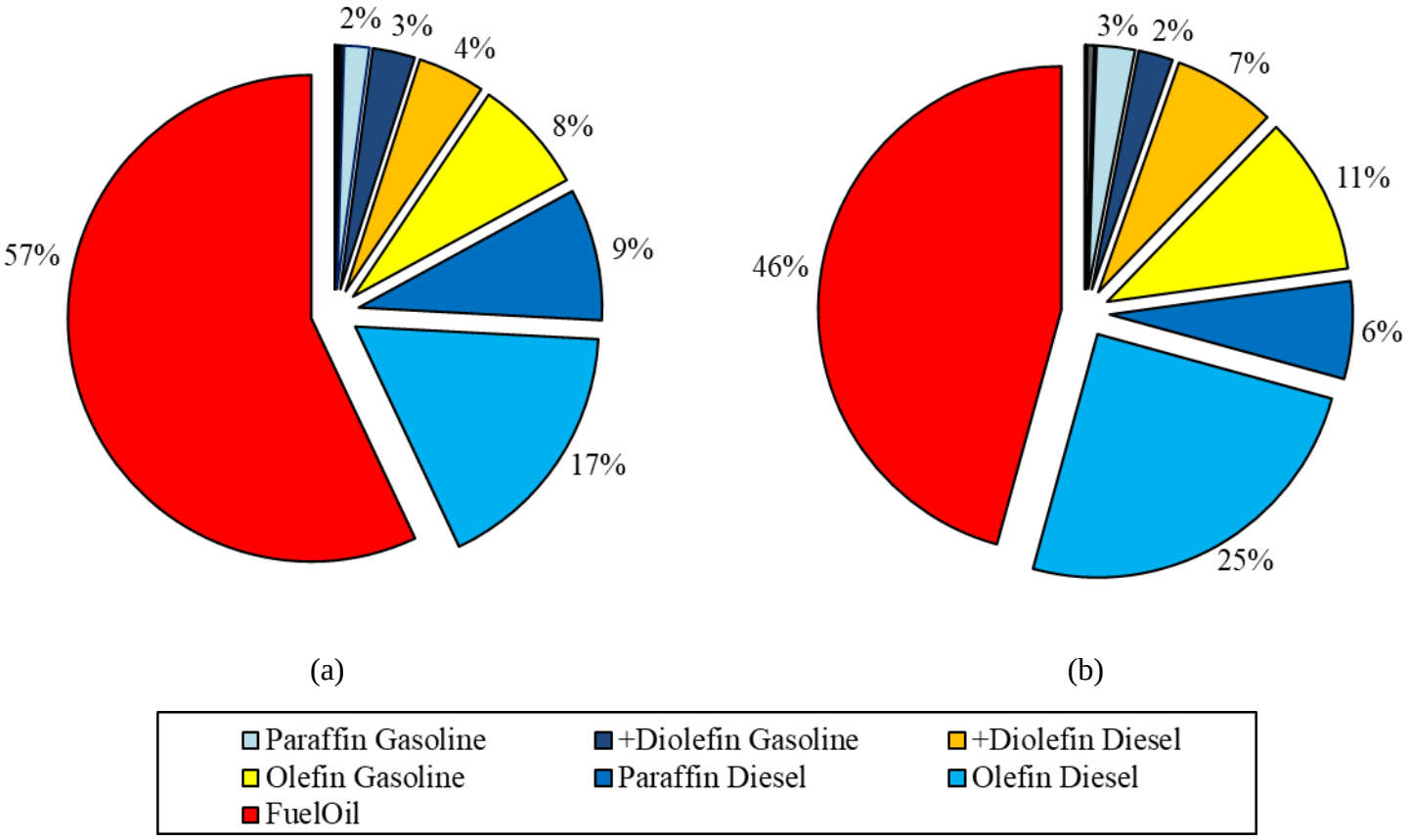

Fig. 2.4. Chemical distribution (wt.%) of species in the pyrolytic oil of (a): HDPE, (b): LDPE at 600 °C (wt.%).

The lower heating value was computed and summarized in **Table 2.6**. For each pyrolytic oil, no variation of the LHV as per temperature was observed. This could be because the families were converted with comparable conversion rates alongside the chemical similarities between the different compounds, consequently making the LHV almost identical at different temperatures. The LHV of both HDPE and LDPE pyrolytic oil was around 47 MJ/kg, which was higher than that of conventional petroleum fuels, as shown in **Table 2.6**.

Based on these observations, it seems that PE showed three major peaks of straight-chain alkene, alkane, and alkadiene, with approximate proportions of 3.4, 1.5, and 1, respectively. Despite its high LHV, the oil produced is not suitable for automotive fuel due to the high concentration of fuel oil and olefinic compounds. However, it contained valuable products of linear straight chain series of n-alkanes 1-alkenes and alkadiene that can be separated and used in the petrochemical industry.

Table 2.6. Comparison between pyrolytic oil and conventional fuel.

Name	LHV (MJ/kg)	Ref.
HDPE	46.6	This work
LDPE	46.6	
PP	46.2	
PS	40.5	
MP	45.0	
Gasoline	43.4-46.5	(Boundy and Davis, 2010)
Kerosene	43.0-46.2	
Diesel	42.8-45.8	

Pyrolysis of polypropylene

Polypropylene pyrolysis yields a set of branched aliphatic compounds with the dominance of olefinic compounds. For the gaseous composition, the propylene monomer was the major component, but in the oil fraction, the main product was propylene trimer, 2,4-dimethyl-1-heptene, representing about 20 wt.%. This compound was also identified by Ballice and Reimert (2002), without mentioning the percentage yield. The oil was mainly divided into three main fractions, as seen in **Fig. 2.5**: fuel oil, olefins in the gasoline range, and olefins in the diesel range consisting of 29 wt.%, 27 wt.%, and 21 wt.%, respectively. The pyrolytic oil showed also a low aromatic concentration of around 4 wt.% in total, of which 2 wt.% were BTX compounds, toluene mainly. However, it was low in straight-chain hydrocarbons, which can be due to the

branched nature of polypropylene, which makes the formation of straight hydrocarbons after cracking challenging. The set of major products in PP pyrolytic oil is presented in **Table 2.7**.

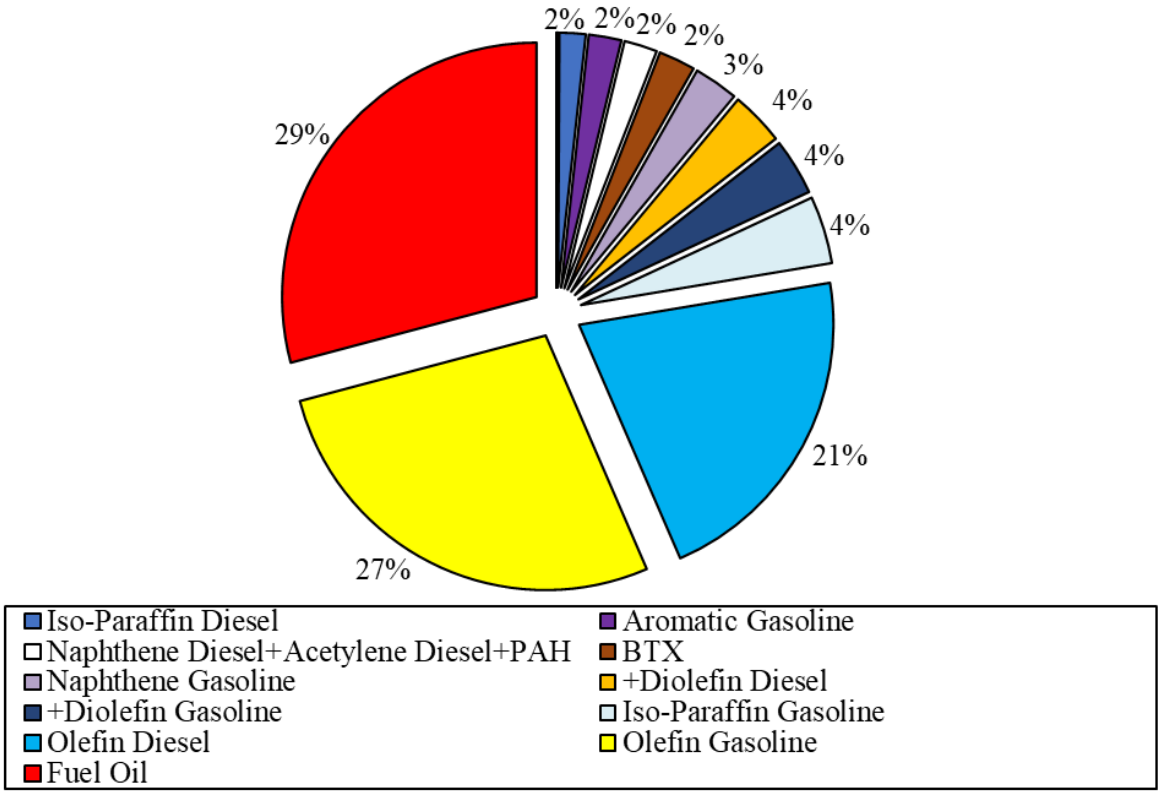

Fig. 2.5. Chemical distribution of species in PP pyrolytic oil at 600 °C (wt.%).

The pyrolytic oil from polypropylene can serve as an alternative fuel in many applications due to the variety of products, the high LHV value of 46 MJ/kg, and the difficulty of investing in petrochemicals. However, due to the high olefinic nature, the oil can only be used as gasoline or diesel fuel only after treatment (Adiwar and Batts, 1995; Pereira and Pasa, 2006).

Table 2.7. List of the major products in PP pyrolytic oil.

Retention time (min)	Pyrolysis products
12.1*	Toluene
13.2	2,4-Dimethyl-1-heptene
13.8	3,3,5-Trimethylcyclohexane
15.1	1,2,3,4,5-Pentamethylcyclopentane
16.2	p-Xylene
19.6	2,6-DimethylNonane
22.6	5-Ethyl-1-nonene
22.8	1-Undecene
24.6	8-Methyl-1-undecene
30.7	(Z)-3-Tetradecene
31.2	(Z)-7-Tetradecene

44.8	2-Methyl-7-octadecyne
47.6	3,7,11,15-Tetramethyl-2-hexadecene
62.0	1,3,5-Trimethyl-2-octadecylcyclohexane

* GC-FID retention time

Pyrolysis of polystyrene

Concerning polystyrene, its cracking yielded a set of mono, di, and tri-aromatic compounds, predominantly styrene. The major compounds with their corresponding families are listed in **Table 2.8**. All the compounds detected were aromatics as benzene, toluene, ethylbenzene, styrene, α-methyl styrene, bibenzyl, 2,4-diphenyl-1-butene (styrene dimer), and 1,3,5-triphenylcyclohexane (styrene trimer).

These compounds were also detected by Liu et al. (2000), Onwudili et al. (2009), and Demirbas (2004). However, indene, m-terphenyl, and p-terphenyl were additional compounds identified and not observed in previous studies. On the other hand, Liu et al. (2000) stated that polystyrene was reduced mainly to its basic monomers having the trimer as 2,4,6-triphenyl-1-hexene, whereas in this study, the cyclic form of the trimer (1,3,5-triphenylcyclohexane) was observed; this can be due to the higher stability of cyclic hydrocarbons over olefinic hydrocarbon.

Table 2.8. List of the major products in PS pyrolytic oil.

Fractions	Retention time (min)	Pyrolysis products
Mono-aromatics (Low BP)	8.7	Benzene (BTX)
	12.1	Toluene (BTX)
	15.8	Ethylbenzene
	17.9	Styrene (Monomer)
	21.2	α-Methylstyrene
	24.4	Indene
Di-aromatics (Medium BP)	33.6	Naphthalene
	40.6	1,2-Diphenylethane (Bibenzyl)
	45.5	2,4-Diphenyl-1-butene (Dimer)
	46.1	(E)-Stilbene
Tri-Aromatics (High BP)	49.0	1-Phenylnaphthalene
	49.1	o-Terphenyl
	49.6	2-Methylphenanthrene
	51.8	2-Phenylnaphthalene
	55.5	m-Terphenyl
	56.6	p-Terphenyl
	62.2	1,3,5-Triphenylcyclohexane (Trimer)

Fig. 2.6 shows the mass percentage of each family in PS pyrolytic oil, where styrene and BTX are removed from the mono-aromatics compounds and displayed independently for a more comprehensive analysis purpose. Results show that PS was reduced mainly to its principal monomer styrene reaching around 60 wt.% at 600 °C, which was higher than that obtained by Demirbas (2004), 50 wt.% at 875 K (~602 °C). Di-aromatics, mainly 2,4-diphenyl-1-butene (Dimer), followed styrene with a mass percentage of 24 wt.%. Furthermore, Liu et al. (2000) found that mono-, di-, and tri-aromatic fractions showed a percentage of around 87 wt.%, 12 wt.%, and 0.1 wt.% at 600 °C, respectively, compared to 69 wt.%, 24 wt.%, and 6 wt.% in this study. These observations can be an indication that higher molecular compounds are more favored under these operating conditions.

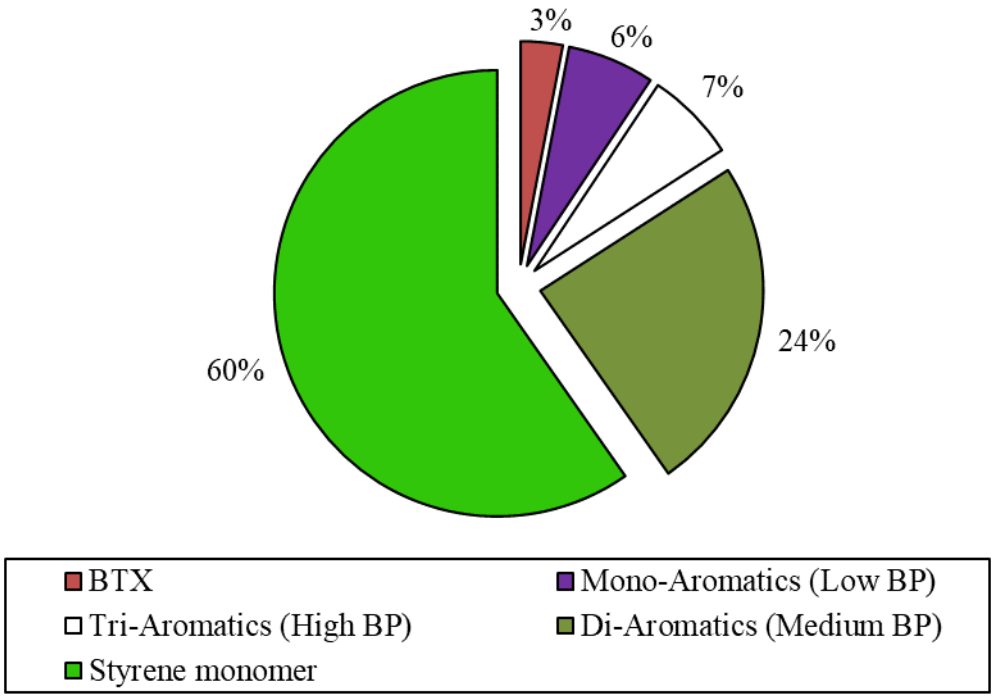

Fig. 2.6. Chemical distribution of species in PS pyrolytic oil at 600 °C (wt.%).

Ultimately, in this type of pyrolytic oil, the use of the oil as fuel is considered an economic and product loss due to the high content of valuable aromatic compounds that can be used afterward in petrochemical industries. On the other hand, it has a lower LHV of 41 MJ/kg relative to other petroleum fuels.

Pyrolysis of mixed plastic

Mixed plastic pyrolysis yielded a set of compounds derived from the individual plastic without any new remarkable ones. The main compound in the pyrolytic oil was styrene which was derived from polystyrene. Furthermore, the oil was mainly divided into four main fractions as seen in **Fig. 2.7**, fuel oil, olefins in the gasoline and diesel range, and styrene consisting of 19 wt.%, 16 wt.%, 17 wt.%, and 16 wt.%, respectively. The remarkable make-up in the oil regarding the high aromatic concentration and the high heating value of 45 MJ/kg from the aliphatic compounds can make the pyrolytic oil ideal as fuel. Monoaromatics covers 22 wt.% of the pyrolytic oil, divided between styrene, BTX, and other single-cycle aromatics. Consequently, the pyrolytic oil can be fractionated by distillation into gasoline with a high aromatic content of about 50 wt.%, greatly increasing the octane number; to diesel oil with low aromatic concentration, thus an enhanced cetane number; lastly, to fuel oil for burners.

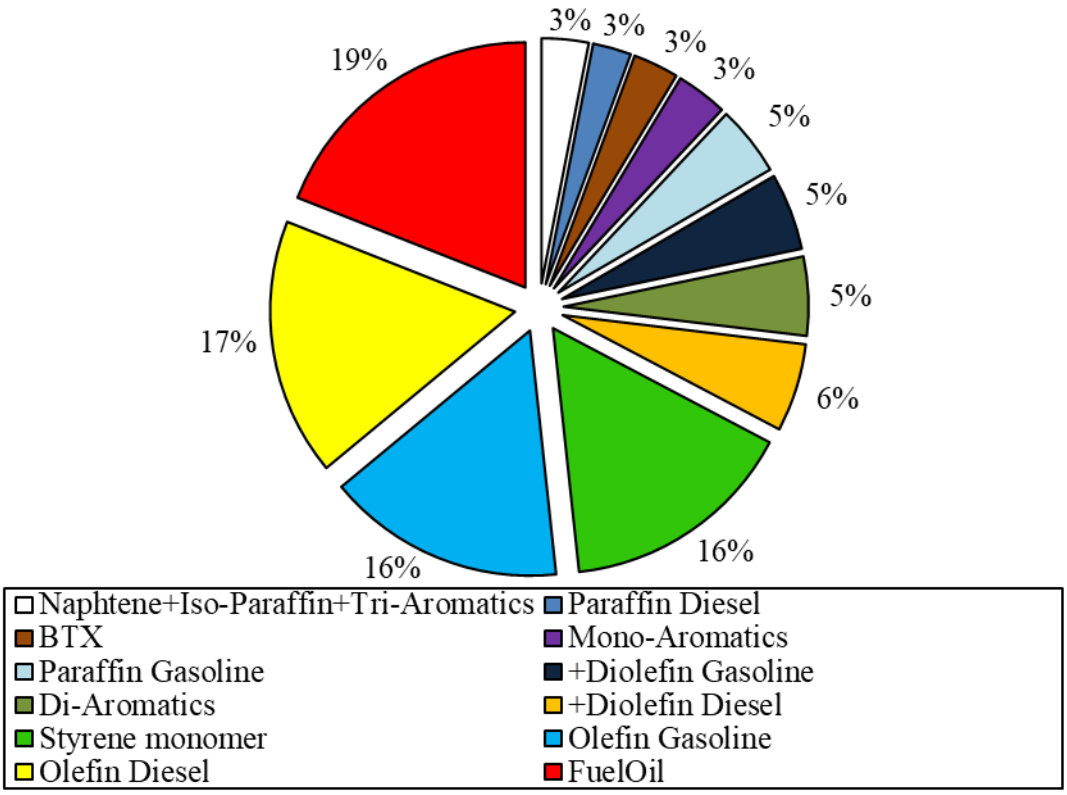

Fig. 2.7. Chemical distribution of species in MP pyrolytic oil at 600 °C (wt.%).

2.3.4. Effect of temperature on liquid product distribution

To delve deeper into the relationship between different chemical families and the pyrolytic temperature,

Table 2.9 and **Table 2.10** and **Fig. 2.8** and **Fig**. **2.9**, were established for each type of plastic pyrolyzed. The effect of temperature could be observed relative to the variation in the percentage of chemical families at different temperatures.

Pyrolysis of low- and high-density polyethylene

LDPE and HDPE product evolution with temperature is present in

Table 2.9. As shown, the pyrolytic behavior of LDPE and HDPE was somehow similar. Both LDPE and HDPE showed similar trends in the families as a function of temperature. Firstly, regarding the fuel oil fraction, both LDPE and HDPE witnessed a stable percentage of this fraction of around 64-66 wt.% for the temperature range of 450-550 °C, then this fraction decreased to 57 wt.% and 46 wt.%, respectively, at 600 °C. This can be explained by the triggering of the cracking of high molecular weight compounds in this fraction at 600 °C, especially paraffinic compounds such as octacosane, heptacosane, hexacosane, pentacosane tetracosane, tricosane, docosane, and heneicosane. The total paraffinic compounds in the fuel oil section contributed to the main decrease in this family, the percentage yield of fuel oil paraffins was fixed at around 28 wt.% for temperatures 450-550 °C then it decreased to 10 wt.% at 600 °C. The decrease in paraffinic compounds was also observed by Onwudili et al. (2009), where the total alkanes decreased from 46 wt.% to 18 wt.% in a temperature range of 425-500 °C.

For temperature optimization, the desired product is to be identified first. If it is going to be burned as fuel directly, the lowest 450 °C is recommended to reduce process energy

expenditure. For petrochemicals, which is preferable, the economic value of each special product must be specified to optimize the process parameters.

Pyrolysis of polypropylene

The families derived from PP pyrolytic oil are shown in

Table 2.9. The trends of PP families were realized to be different from that of the other plastics under study. BTX and aromatics were mainly produced at high temperatures (600 °C). The behavior of other families is almost unclear. However, adding up the families by structure could show an optimum behavior at 500 °C. For instance, for olefins in the diesel and gasoline range, the trend seems to fluctuate, but when grouped as an olefinic class, a minimum concentration was attained of 44 wt.% at 500 °C. Furthermore, the maximum concentration of total naphthenes and the minimum concentration of total iso-paraffins were obtained at 500 °C with around 9 wt.% and 3 wt.% respectively. On the other hand, the study of Demirbas (2004), showed a maximum concentration of naphthenes with 24 wt.% and 2 minimum concentrations of olefins and paraffins of 25 wt.% and 40 wt.%, respectively, at 800 K (527 °C). The difference in the values between the two studies especially for paraffins and naphthenes could be due to the different operating conditions of non-isothermal pyrolysis and reactor setup.

Table 2.9. Evolution of PE and PP pyrolytic oil composition relative to temperature (wt.%).

Chemical Families	LDPE				HDPE				PP			
	Operating Temperature (°C) ±5 °C											
	450	500	550	600	450	500	550	600	450	500	550	600
Paraffin Gasoline	2.4	1.5	2.3	2.5	1.9	1.0	0.8	1.7	-	-	-	-
Iso-Paraffin Gasoline	-	-	-	-	-	-	-	-	2.7	2.3	2.8	4.3
Olefin Gasoline	4.7	5.1	4.4	10.6	3.4	3.3	3.6	7.6	28.0	21.2	21.2	27.4
+Diolefin Gasoline	0.7	0.8	0.3	2.3	0.3	0.5	0.6	2.8	2.3	1.8	1.9	3.6
Naphthene Gasoline	-	-	-	-	-	-	-	-	2.3	7.9	1.6	2.8
Aromatics Gasoline	-	-	-	-	-	-	-	-	0.2	0.3	0.8	2.1
Paraffin Diesel	11.0	9.0	10.5	6.5	10.6	8.2	6.4	8.8	-	-	-	-
Olefin Diesel	13.4	17.3	14.5	25.0	15.2	16.3	18.9	17.2	26.5	22.3	25.8	21.1
+Diolefins Diesel	2.0	3.1	1.9	6.9	2.0	3.4	5.0	4.5	2.1	7.8	3.4	3.4
Naphthene Diesel	-	-	-	-	-	-	-	-	1.9	1.5	1.7	1.1
BTX	-	-	-	-	-	-	-	-	0.0	0.1	0.3	2.3
Fuel Oil	64.5	62.9	65.9	45.7	66.7	67.1	64.7	57.0	31.7	32.9	38.3	29.2

The application of pyrolytic oil in PP is mainly as fuel, as discussed before. The oil can be fractionated to get 3 main fractions relative to carbon number and boiling point: gasoline, diesel, and heavy fraction. However, more energy is required at higher temperatures to obtain the same LHV. So other parameters must be studied to run optimization such as carbon range and octane number. For instance, the optimum temperature could be at 600 °C since more gasoline is produced and more compounds that boost the octane number are present, such as aromatics, olefins, and iso-paraffins.

Pyrolysis of polystyrene

As a general recap, as temperature increases, the cracking reactions will be enhanced, thus lighter molecular-weight products will be produced. **Fig. 2.8** shows the evolution of the main polystyrene families as a function of pyrolysis temperature. Regarding PS, the percentage of styrene increased from 40 wt.% to 60 wt.% when the temperature rose from 450 °C to 600 °C. As for other families, BTX started to form at temperatures above 550 °C, reaching a concentration of 3 wt.% at 600 °C, with a tendency to increase at higher temperatures. The same behavior was deduced for all the other families, while the percentages of di-aromatic decreased

drastically from 50 wt.% to 24 wt.%. Mono-aromatic concentration increased only slightly, however, it was notable since BTX and styrene were excluded from the mono-aromatic family.

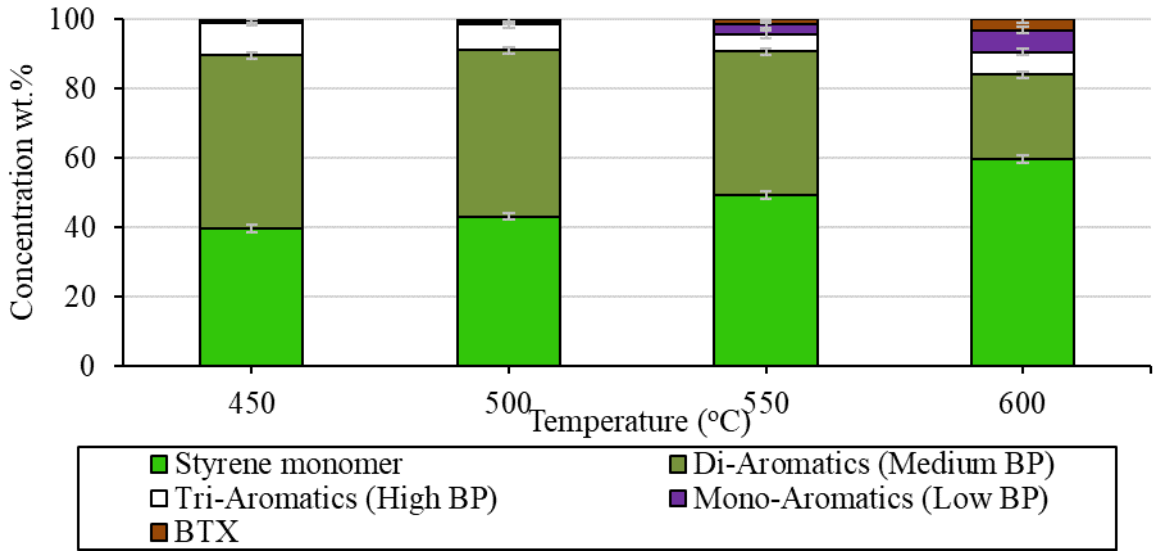

Fig. 2.8. The main components of PS pyrolysis oil as a function of temperature.

For further investigation, the evolution of the three monomers was demonstrated relative to temperature in **Fig. 2.9**. Styrene dimer and trimer showed an opposite trend as styrene monomer; which can be explained by the enhancement of cracking reactions. Ultimately the best temperature for polystyrene cracking would be 600 °C, due to the dramatic increase of BTX, styrene monomer, and other mono-aromatic compounds that have desirable demand in the petrochemical industries. On the other hand, polystyrene is light and bulky; it can be blown easily, leaving litter during collection, and requiring a high transport cost. Moreover, it is likley to be in direct contact with food, so it is hard to recycle directly (Anuar Sharuddin et al., 2017). As a way to circumvent this problem, pyrolysis can be used to reduce PS to its basic monomer, then use the monomer after separation to produce high-quality PS (Hussain et al., 2010). The remaining mono-aromatic compounds could be blended inside the gasoline pool to boost the octane number.

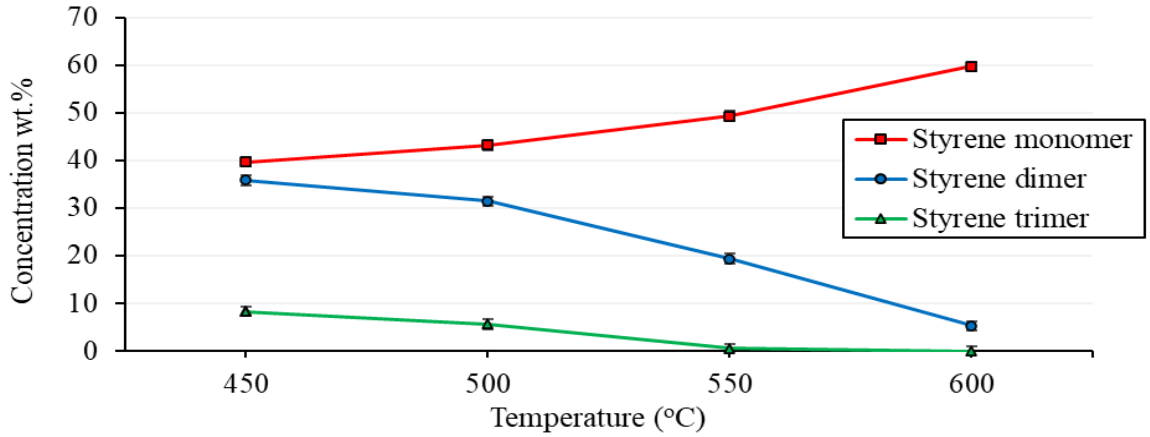

Fig. 2.9. The evolution of styrene monomer, dimer, and trimer in PS pyrolytic oil as a function of temperature.

Mixed plastic interaction

The families derived from MP pyrolytic oil are shown in **Table 2.10**. To deeply understand the interaction between plastics, an expected weight percentage for each set of products (x_{th}) was computed based on the weighted average sum of the independent plastics. The expected weight fraction was computed using ***Eq. 2.3***, where x_i is the weight fraction of the desired product, y_i is the liquid or gas yield of the independent plastics, and w_i is the weight percentage of each plastic in the plastic mix.

$$x_{th} = \frac{\sum x_i y_i w_i}{\sum y_i w_i} \qquad \textbf{Eq. 2.3}$$

Concerning the plastic mixture gas analysis, the behavior of each component versus temperature was like that of the individual plastics. However, a high gas yield and a lower liquid yield were recorded at high temperatures. For further analysis, the expected values have been calculated in **Table A.5**. The results showed an increase in ethylene and hydrogen gas and a decrease in propylene when plastics were mixed experimentally. The latter could imply, along with the higher gas yield, the presence of a synergetic effect between the different plastics, which is discussed extensively afterward.

MP pyrolytic oil composition followed the typical trend of cracking reaction, which is the increase of lighter hydrocarbons with the increase in temperature. However, one should note

that interaction between plastics when mixed exists. **Table 2.10** shows that mixing plastics favored lighter compounds at the expense of heavier ones. For instance, the expected value of fuel oil at 600 °C was around 36 wt.% compared to the experimental value of 19 wt.%. This decrease was met with the increase of light compounds such as styrene, olefins in the gasoline and diesel range, and diaromatics. This could indicate that plastics interact in a way that enhances the cracking of each polymer without the production of any significant new compounds. This hypothesis could be reinforced by the decrease in oil yield and increase in gas yield and lighter gaseous components. The variation of the product yield was also stated by Sharuddin et al. (2016), where lower liquid yield was observed for mixed plastic pyrolysis. Ultimately, the best temperature for mixed plastic cracking would be 600 °C due to the drastic increase of aromatic compounds and light hydrocarbons, which is more desirable for any possible end-use.

Table 2.10. Evolution of MP pyrolytic oil composition as a function of temperature (wt.%).

Chemical Families	Operating Temperature (°C) ±5 °C			
	450	500	550	600
Paraffin Gasoline	3.2 **(1.2)**	3.0 **(0.7)**	3.0 **(0.9)**	4.6 **(1.2)**
Olefin Gasoline	12.3 **(11.7)**	13.8 **(9.4)**	14.8 **(9.1)**	15.7 **(13.9)**
+Diolefin Gasoline	1.1 **(1.1)**	2.1 **(1.0)**	3.4 **(0.8)**	5.1 **(2.5)**
Paraffin Diesel	4.9 **(5.8)**	4.2 **(4.7)**	3.6 **(4.8)**	2.5 **(3.9)**
Olefin Diesel	18.6 **(16.4)**	18.1 **(16.5)**	19.2 **(17.0)**	17.0**(18.5)**
+Diolefin Diesel	1.5 **(1.8)**	2.7 **(4.3)**	4.7 **(2.8)**	5.8 **(4.2)**
Fuel Oil	28.1 **(45.4)**	27.9 **(45.3)**	24.9 **(47.5)**	19.0 **(36.1)**
BTX	0.8 **(0.0)**	0.9 **(0.1)**	1.3 **(0.3)**	3.0 **(1.4)**
Styrene monomer	12.2 **(5.3)**	12.2 **(5.8)**	12.1 **(6.9)**	15.6 **(8.6)**
Mono-Aromatics	0.7 **(0.1)**	1.2 **(0.2)**	2.3 **(0.7)**	3.4 **(1.6)**
Di-Aromatics	11.6 **(6.7)**	9.4 **(6.4)**	6.5 **(5.8)**	5.2 **(3.5)**
Tri-Aromatics	0.5 **(1.3)**	0.6 **(1.0)**	0.7 **(0.7)**	0.2 **(1.1)**

In bold ( ) indicates the expected values

To better visualize mixing influence, the families were grouped into the most important ones. The experimental concentration versus the calculated concentration was established in **Fig. 2.10** to clearly identify the most affected family and to know the importance of plastic interaction.

The heavy fraction (fuel oil) was the most affected with a dramatic decrease in its experimental concentration. On the other hand, the case was the opposite for both aromatics and gasoline, where a positive influence and an increase in concentration were observed. This observation could be considered proof of degradation potential increasing when plastics are mixed. Some families were not greatly affected by the mixing, which are the diesel fractions and PAH (mainly di-aromatics). This can be because these families have the same carbon range and they are midway between light and heavy compounds so any transformation in these families to lighter compounds was compensated by the transformation from the heavy family. This is of great advantage since mixing plastics favors lighter compounds at the expense of heavy compounds and favors aromatic production which boosts the quality of the oil.

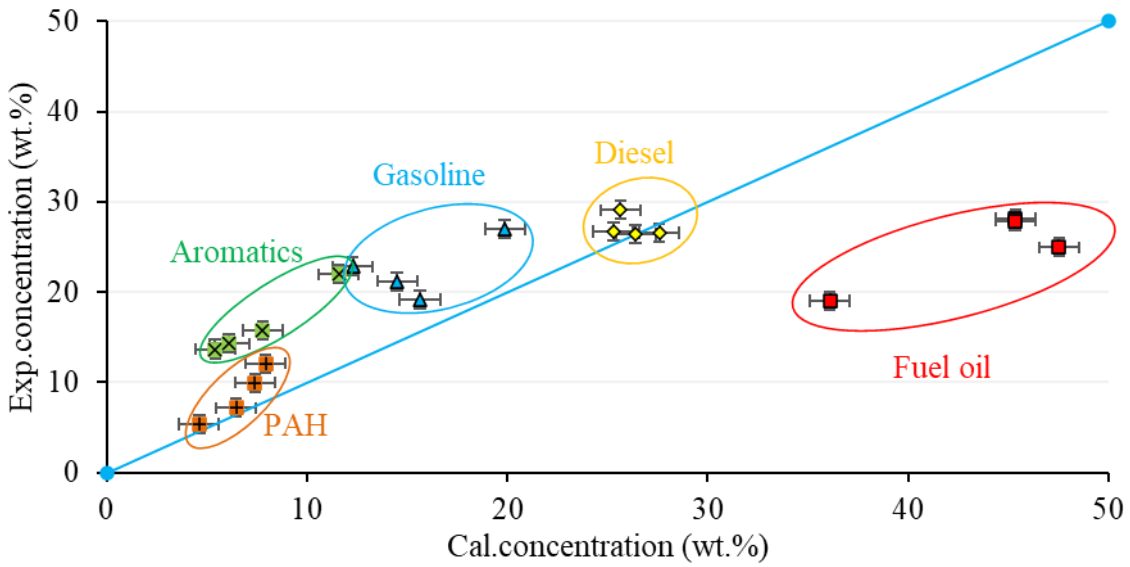

Fig. 2.10 Distribution of the major families relative to the experimental and calculated concentrations (wt.%)

2.3.5. Principal Component Analysis

PCA analysis was utilized to study the correlations and to check the global behavior of the different plastics under study. PCA has the goal to detect similarities and correlations between variables (Boukaous et al., 2018). PCA was reduced to one orthogonal variable and the first two principal components, F1 and F2. The first two principal components (F1 and F2)

described respectively 44 % and 29 % of the variability observed between the different pyrolytic oil with temperature. The analysis of the existence of correlations between each variable is carried out by the projection of the cloud of points into an orthogonal space (F1 and F2) as in **Fig. 2.11**. Usually, the two axes have no physical meaning, yet they ensure the maximum recovery and representation of information onto a 2D orthonormal plane.

Fig. 2.11 (a) demonstrates the scatter of the different experiments on the principal component axis. The set of 4 points in the scatter plot for each sample represents the evolution of the different families and plastic pyrolytic oil with temperature. Points clustering together shows tight correlations and similar behavior in the different experiments. For instance, the harmony between the experiments of LDPE and HDPE was further reassured, grouping into one confined cluster on the PCA score plot. However, the experiments on polypropylene and polystyrene clustered away showing a significant difference between the pyrolytic oil of PP, PS, and PE.

However, for the mixed plastics, the experiments clustered almost barry center-wise relative to the other plastics pyrolyzed alone. This means that each cluster of plastics attracts the MP cluster relative to its percentage in the mixture, which could be the reason why the MP cluster is closer to PE and PP than PS. On the other hand, the differences between the experimental and calculated values of MP were reassured. The calculated MP clusters were closer to that of PE plastics which yielded the majority of heavy compounds, yet the experimental MP cluster was closer to PP and PS which yielded lighter compounds along with aromatics.

One should also note that all points (S4, P4, L4, H4, M_e4, and M_c4) were relatively different from the rest of their corresponding clusters, showing the pyrolytic behavior at 600 °C was unlike the rest. From this outcome, one could say that at 600 °C and above, the behavior

of pyrolysis shifts in another direction than that of lower temperatures of 450-550 °C, which could be because that high temperature can arouse disorder.

Fig. 2.11 (b) demonstrates the loading plots of variables which are, in this case, the different chemical families. The parameters in the loading plot are considered representative if the radius is closer to the circle. Otherwise, the information is deformed and holds no physical meaning. The plot shows which families were best correlated with each other and which have the greatest influence on the principal component. For instance, vectors with small acute angles reflect a positive correlation, diagonally opposite vectors show a negative correlation, yet orthogonal vectors reveal independence or no correlation. **Fig. 2.11 (b)** showes that families with the same molecular structure possess a strong positive correlation with each other: 1) gasoline and diesel paraffins; 2) gasoline/diesel olefins and +diolefins; 3) gasoline and diesel iso-paraffins; 4) gasoline and diesel naphthenes and 5) aromatic compounds.

Ultimately, from the loading plot **Fig. 2.11 (b)**, the variables that most alter the principal component could be deduced. Olefins, iso-paraffins, diesel paraffins, styrene, di- and tri-aromatics, and fuel oil have the greatest influence on the first principal component F1, which was not surprising since these families were the most dominant in the pyrolytic oil.

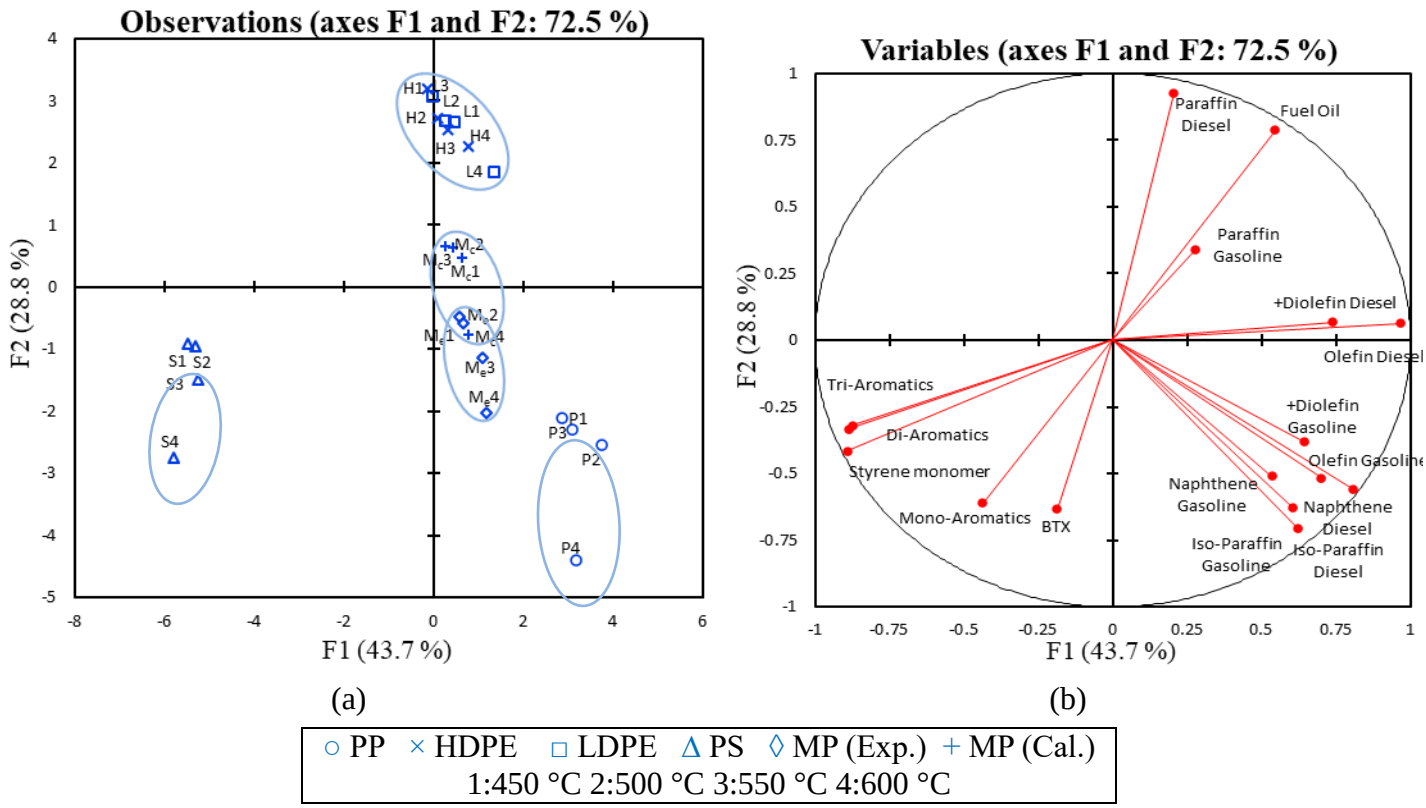

Fig. 2.11. (a): Score plot of experiments (b): Loading plot of families

Correlations between different variables from a set of samples were assessed. Detailed R-values (Pearson) were computed between the families for each plastic and between the major compounds in each family. Correlations are summarized in **Table A.3 (a), (b), (c), (d) and (e)**.

Low and high-density polyethylene pyrolytic oil

The correlation test showed the similarity in HDPE and LDPE pyrolytic oil with minor variations. As for the different families, olefins and diolefins in the gasoline and diesel ranges were strongly correlated in both types of plastics (R=0.83 to 0.99), which can be explained by the profound similarity between the two families. On the other hand, fuel oil fraction was negatively correlated with both temperature (R=-0.73 to -0.87) and the latter families (-0.97 to -0.99). It can thus be said that the heavier compounds were cracked into olefinic compounds as the temperature rises.

Delving deeper inside the families, for both LDPE and HDPE in the gasoline range, nonane, decane, and undecane were positively correlated with each other and negatively correlated with

temperature. However, 1-nonene, 1-decene, and 1-undecne exhibited a strong positive correlation with each other and a positive correlation with temperature. However, for diesel, there was some difference between the two pyrolytic oils. LDPE pyrolytic oil demonstrated that all the compounds in the paraffinic family were correlated with each other, from C_{12} to C_{20} with R=0.93 to 0.99, which was also the case with the olefinic family with R=0.9 to 0.99. On the other hand, HDPE showed two strongly correlated groups of paraffinic and olefinic compounds: group C_{12} to C_{16}, which was negatively correlated with temperature, and the C_{17} to C_{19} group, showing a positive correlation with temperature. In the final group, the heavy hydrocarbons (fuel oil), results showed a tight positive correlation between diolefins with temperature, yet, olefins and paraffins were positively correlated between the same group but negatively correlated with temperature.

Polypropylene pyrolytic oil

Polypropylene pyrolytic oil showed a strong positive correlation between aromatics and BTX compounds (R=0.98), and a positive correlation within branched paraffins in the diesel and gasoline range (R=0.97). However, the independence of fuel oil and olefins in the gasoline range on temperature was observed ($R \approx 0.08$).

Polystyrene pyrolytic oil

Globally, aromatics with a single ring structure (mono-aromatics, styrene, and BTX) showed a strong positive correlation with temperature (R= 0.94 to 0.97), unlike that of di-aromatics that demonstrated a strong negative relationship (R= -0.92) with temperature. A detailed analysis of the di-aromatic family found that the dimer has a strong negative correlation with temperature (R= -0.98), which was in contrast with that of (E)-stilbene in a positive correlation with temperature (R= 0.95). In the end, the tri-aromatic showed a negative correlation with temperature (R= -0.78), the trimer following the family trend of a negative correlation with temperature (R= -0.96).

Mixed Plastics pyrolytic oil

The families in mixed plastic were divided into two main groups relative to their correlations with temperature. The families between the same group were positively correlated with each other. For instance, gasoline olefins and diolefins, diesel diolefins, and monoaromatics were strongly correlated with temperature (R= 0.99). On the other hand, diesel paraffins and iso-paraffins, di-aromatics, and fuel oil were negatively correlated with temperature (R= -0.92 to -0.99). Furthermore, a negative correlation seemed to exist between di-aromatics and tri-aromatics with styrene, which may suggest that the polycyclic aromatic compounds were converted to styrene and other single aromatic compounds.

In the end, energy evaluation is a key factor in this type of study. It seems important to establish an energy balance for a better evaluation of the heat required to produce 1 kg of, for example, plastic oil compared to other resources such as bio-oil or syngas from biomass pyrolysis or gasification (Reyes et al., 2021a, 2021b, 2021c). In addition, the energy balance allows us to determine the equivalent energy required to obtain an equivalent mass of the current fuel.

2.4. Conclusion

Plastic pyrolysis has been considered an effective route to plastic waste management to convert waste plastics to valuable hydrocarbon products. At first, plastic pyrolysis showed mainly the reduction of plastics to their simple monomers. The pyrolysis of polyethylene (HDPE and LDPE) showed similar behavior in pyrolysis. For instance, GC analysis showed consecutive triplet series of linear aliphatic hydrocarbons at each carbon number, alkane, 1-alkene, 1, (N-1)-alkadiene. Both plastics yielded high molecular weight compounds in the majority. On the other hand, PP, LDPE, and HDPE pyrolytic oil were rich in olefinic compounds. PP pyrolytic oil was constituted mainly of branched aliphatic hydrocarbons divided into three main fractions: gasoline olefins, diesel olefins, and fuel oil, with the major product as propylene trimer, 2,4-dimethyl-1-heptene.

Contrastingly, the case was quite different for PS. The pyrolytic oil was constituted totally of aromatic compounds ranging from mono to tri aromatic hydrocarbon. Styrene was the main product covering up to 60 wt.%. For MP, interactions exist between the plastics polymers thus favoring lighter compounds. However, to fully benefit from the pyrolytic oil, a simple parameter such as temperature could be manipulated for process optimization.

The LHV was computed for each pyrolytic oil to have better insight into the end-use of each product. High gas and liquid heating values were recorded at around 47 MJ/kg, except for PS pyrolytic oil, having a relatively lower liquid heating value of around 41 MJ/kg. LDPE, HDPE, and PS pyrolytic oil could serve as essential raw materials in petrochemical industries. Whereas PP and MP pyrolytic oil are more likely to be used as fuel or blended with conventional automotive fuel. However, treatment is necessary especially for PP, as improving the cetane number by hydrotreatment or by one-time hydrocracking to reduce the fuel oil fraction to the diesel fraction. As to using it like gasoline, a low octane number would cause a problem due to the deficiency in aromatic compounds. As a result, the oil requires catalytic reforming. Nevertheless, mixed plastics showed an advantage, since it contains lighter compounds along with higher concentrations of aromatics that are more preferred and desired. So, the use of mixed plastic alters the quality of the pyrolytic oil with an acceptable decrease in the liquid yield which can be of great influence cost-wise without any catalyst intervention. As such, most liquid products formed would be ideal to be used or blended as conventional fuels, with the gases burned for energy. The use of mixed plastic pyrolysis can be an effective route to tackle the plastic waste problem with the minimum cost possible. Ultimately, plastic waste pyrolysis is seen as an effective way of managing the critical environmental problems that the world is facing.

2.5. References

Adiwar, Batts, B.D., 1995. The effect of aliphatic olefins on the stability of diesel fuel (No. CONF-941022-Vol.2). USDOE Assistant Secretary for Fossil Energy, Washington, DC (United States). Office of Technical Management.

Anuar Sharuddin, S.D., Abnisa, F., Wan Daud, W.M.A., Aroua, M.K., 2017. Energy recovery from pyrolysis of plastic waste: Study on non-recycled plastics (NRP) data as the real measure of plastic waste. Energy Convers. Manag. 148, 925–934. https://doi.org/10.1016/j.enconman.2017.06.046

Anuar Sharuddin, S.D., Abnisa, F., Wan Daud, W.M.A., Aroua, M.K., 2016. A review on pyrolysis of plastic wastes. Energy Convers. Manag. 115, 308–326. https://doi.org/10.1016/j.enconman.2016.02.037

Ballice, L., Reimert, R., 2002. Classification of volatile products from the temperature-programmed pyrolysis of polypropylene (PP), atactic-polypropylene (APP) and thermogravimetrically derived kinetics of pyrolysis. Chem. Eng. Process. Process Intensif. 41, 289–296. https://doi.org/10.1016/S0255-2701(01)00144-1

Boukaous, N., Abdelouahed, L., Chikhi, M., Meniai, A.-H., Mohabeer, C., Bechara, T., 2018. Combustion of Flax Shives, Beech Wood, Pure Woody Pseudo-Components and Their Chars: A Thermal and Kinetic Study. Energies 11, 2146. https://doi.org/10.3390/en11082146

Boundy, R.G., Davis, S.C., 2010. Biomass Energy Data Book: Edition 3 (No. ORNL/TM-2011/43). Oak Ridge National Lab. (ORNL), Oak Ridge, TN (United States). https://doi.org/10.2172/1008840

Bouster, C., Vermande, P., Veron, J., 1989. Evolution of the product yield with temperature and molecular weight in the pyrolysis of polystyrene. J. Anal. Appl. Pyrolysis 15, 249–259. https://doi.org/10.1016/0165-2370(89)85038-7

Conesa, J.A., Font, R., Marcilla, A., 1997. Comparison between the Pyrolysis of Two Types of Polyethylenes in a Fluidized Bed Reactor. Energy Fuels 11, 126–136. https://doi.org/10.1021/ef960098w

Demirbas, A., 2004. Pyrolysis of municipal plastic wastes for recovery of gasoline-range hydrocarbons. J. Anal. Appl. Pyrolysis 72, 97–102. https://doi.org/10.1016/j.jaap.2004.03.001

Dorado, C., Mullen, C.A., Boateng, A.A., 2014. H-ZSM5 Catalyzed Co-Pyrolysis of Biomass and Plastics. ACS Sustain. Chem. Eng. 2, 301–311. https://doi.org/10.1021/sc400354g

Elordi, G., 2011. Product Yields and Compositions in the Continuous Pyrolysis of High-Density Polyethylene in a Conical Spouted Bed Reactor. Ind. Eng. Chem. Res. 50, 6650–6659.

Esbensen, K.H., Guyot, D., Westad, F., Houmoller, L.P., 2002. Multivariate Data Analysis: In Practice : an Introduction to Multivariate Data Analysis and Experimental Design. Multivariate Data Analysis.

Goodfellow, n.d. Supplier of materials for research and development [WWW Document]. URL https://www.goodfellow.com/uk/en-gb (accessed 10.2.22).

Hussain, Z., Khan, K.M., Hussain, K., 2010. Microwave–metal interaction pyrolysis of polystyrene. J. Anal. Appl. Pyrolysis 89, 39–43. https://doi.org/10.1016/j.jaap.2010.05.003

Jaafar, Y., Abdelouahed, L., Hage, R.E., Samrani, A.E., Taouk, B., 2022. Pyrolysis of common plastics and their mixtures to produce valuable petroleum-like products. Polym. Degrad. Stab. 195, 109770. https://doi.org/10.1016/j.polymdegradstab.2021.109770

Kim, Y.-M., Jae, J., Kim, B.-S., Hong, Y., Jung, S.-C., Park, Y.-K., 2017. Catalytic co-pyrolysis of torrefied yellow poplar and high-density polyethylene using microporous HZSM-5 and mesoporous Al-MCM-41 catalysts. Energy Convers. Manag. 149, 966–973. https://doi.org/10.1016/j.enconman.2017.04.033

Liu, Y., Qian, J., Wang, J., 2000. Pyrolysis of polystyrene waste in a fluidized-bed reactor to obtain styrene monomer and gasoline fraction 11.

Marcilla, A., Beltrán, M.I., Navarro, R., 2009. Thermal and catalytic pyrolysis of polyethylene over HZSM5 and HUSY zeolites in a batch reactor under dynamic conditions. Appl. Catal. B Environ. 86, 78–86. https://doi.org/10.1016/j.apcatb.2008.07.026

Marlair, G., Cwiklinski, C., Tewarson, A., 1999. An analysis of some practical methods for estimating heats of combustion in fire safety studies. Interflam 99 Jun 1999 Edimbourg U. K. Ineris-00972167.

Mohabeer, C., Abdelouahed, L., Marcotte, S., Taouk, B., 2017. Comparative analysis of pyrolytic liquid products of beech wood, flax shives and woody biomass components. J. Anal. Appl. Pyrolysis 127, 269–277. https://doi.org/10.1016/j.jaap.2017.07.025

Onwudili, J.A., Insura, N., Williams, P.T., 2009. Composition of products from the pyrolysis of polyethylene and polystyrene in a closed batch reactor: Effects of temperature and residence time. J. Anal. Appl. Pyrolysis 86, 293–303. https://doi.org/10.1016/j.jaap.2009.07.008

Pereira, R.C.C., Pasa, V.M.D., 2006. Effect of mono-olefins and diolefins on the stability of automotive gasoline. Fuel 85, 1860–1865. https://doi.org/10.1016/j.fuel.2006.01.022

Perry, D.W., H., R., Green, 1997. Perry's Chemical Engineers', Handbook 7th. ed.

Plastics - the Facts 2021 [WWW Document], 2021. URL https://www.plasticseurope.org/fr/resources/publications/1804-plastics-facts-2019 (accessed 5.15.20).

Reyes L, Abdelouahed L, Buvat JC, Campusano B, Devouge-Boyer C, Taouk B, 2021. Energetic study of beech wood gasification in fluidized bed reactor under different gasification conditions (vol 164, pg 23, 2020). Chem. Eng. Res. Des. 166, 267–267. https://doi.org/10.1016/j.cherd.2020.12.015

Reyes, L., Abdelouahed, L., Campusano, B., Buvat, J.-C., Taouk, B., 2021a. Exergetic study of beech wood gasification in fluidized bed reactor using CO2 or steam as gasification agents. Fuel Process. Technol. 213, 106664. https://doi.org/10.1016/j.fuproc.2020.106664

Reyes, L., Abdelouahed, L., Mohabeer, C., Buvat, J.-C., Taouk, B., 2021b. Energetic and exergetic study of the pyrolysis of lignocellulosic biomasses, cellulose, hemicellulose and lignin. Energy Convers. Manag. 244, 114459. https://doi.org/10.1016/j.enconman.2021.114459

Scanlon, J.T., Willis, D.E., 1985. Calculation of Flame Ionization Detector Relative Response Factors Using the Effective Carbon Number Concept. J. Chromatogr. Sci. 23, 333–340. https://doi.org/10.1093/chromsci/23.8.333

Schwarz, A.E., Ligthart, T.N., Boukris, E., van Harmelen, T., 2019. Sources, transport, and accumulation of different types of plastic litter in aquatic environments: A review study. Mar. Pollut. Bull. 143, 92–100. https://doi.org/10.1016/j.marpolbul.2019.04.029

CHAPTER 3:

Co-pyrolysis of plastic polymers and biomass: Effect of beech wood/plastic ratio and temperature on enhanced oil production in a semi-continuous pyrolyzer

3. CO-PYROLYSIS OF PLASTIC POLYMERS AND BIOMASS: EFFECT OF BEECH WOOD/PLASTIC RATIO AND TEMPERATURE ON ENHANCED OIL PRODUCTION IN A SEMI-CONTINUOUS PYROLYZER

3.1. Introduction

The previous chapter discussed the individual pyrolysis of plastics and the possible end-use of each product. However, the objective lies in improving the quality of bio-oil from the pyrolysis of lignocellulosic biomass. As demonstrated in the literature, co-pyrolysis seems a promising low-cost technique for the latter purpose.

This chapter describes and investigates the synergy between biomass and plastics, by classification of the products into families and evaluating the synergy for each family. The objective of this study is to evaluate the co-pyrolysis of certain types of municipal plastic waste as high-density polyethylene (HDPE), low-density polyethylene (LDPE), polypropylene (PP), polystyrene (PS), and their mixture (MP); according to their contribution to Europe's average plastic wastes (34wt.% PP, 32wt.% LDPE, 21wt.% HDPE, and 13% PS) ("PlasticsEurope," 2021), with beech wood (*Fagus sylvatica*) (BW) as lignocellulosic forestry residue, for the production of pyrolytic oils of improved quality. BW is used in this study since it is by far the most used hardwood in Europe (Klein et al., 2016), hence producing a lot of beech sawdust. For that, BW must be included in any attempt to study the potential of bio-oil production as an alternative fuel. The influence of plastic types, mixture percentage, and pyrolysis temperature on the quantity and quality of co-pyrolysis oil was investigated. At first, plastics (PS, PP, LDPE, PE, MP) pyrolysis findings were used from the previous chapter and BW was pyrolyzed and studied independently. Then a mixture of these plastic polymers with beech wood was prepared and pyrolyzed to test and verify the synergetic effects of biomass and plastic co-pyrolysis compared to the pyrolysis of the single feedstock.

3.2. Materials and methods

3.2.1. Materials

The virgin plastics (HDPE, LDPE, PP, and PS) were the same used before and beech wood was supplied by ETS Lignex Company (Patornay, France) with an average particle size of 0.4 mm; the two materials were mixed and homogenized well before being used. The elemental analysis and proximate analysis of BW were done by the same apparatuses as mentioned before in **Chapter 2.** The obtained data are presented in **Table 3.1.**

Table 3.1. Ultimate and proximate analysis of used biomass (wt.%).

BW	Ultimate analysis			
	% C	% H	% O	
	47.4	6.1	46.5	
	Proximate analysis			
	Moisture	Fixed Carbon	Volatile	Ash
	5.7	17.5	75.9	0.9

3.2.2. Methods

3.2.2.1. Pyrolysis experimental setup

The same reactor configuration was used as in the previous chapter (**Chapter 2 Section 2.2.2.1)**. About 3 g of plastic and biomass sample was placed into the sample carrier at the entrance of the reactor until the temperature reaches the desired value. The liquid oil was collected from the condenser and the round bottom glass using acetone as solvent. The non-condensable gases were retained in the Tedlar gas bag and the char remains in the sample holder. A list of all the experiments done is summarized in **Table 3.2**.

Table 3.2. Summary of the performed experiments under different operating conditions.

Reaction	Feedstock	BW percentage (wt.%)	Temperature (°C)
Pyrolysis	BW	100	500
	HDPE	-	
	LDPE	-	
	PP	-	
	PS	-	
	MP	-	
Co-pyrolysis	BW-HDPE	25-50-75	
	BW-LDPE	25-50-75	
	BW-PP	25-50-75	
	BW-PS	25-50-75	
	BW-MP	25-50-75	
	BW-PS	50	450-500-550-600

3.2.2.2. Liquid oil and non-condensable gases analysis

The technique used for the liquid and gas product analysis has been already detailed previously (**Chapter 2**, **sections 2.2.2.2, 2.2.2.3, 2.2.2.4, 2.2.2.5**)

3.2.2.3. Synergy between biomass and plastics

The synergy between biomass and plastics has been tested over the families of the liquid oil produced, where the expected or theoretical concentrations (x_{theo}) were computed based on the weighted average sum of each feedstock and their corresponding liquid or gas yield. The expected percentages were calculated using **Eq. 3.1**, where m_{theo} is the expected mass of the desired product in the oil, and m_{total} is the total expected mass of the liquid oil. The equation is developed further to compute the expected masses. x_p *and* x_b are the desired product mass percentage, y_p *and* y_b are the pyrolytic liquid or gas yield, and w_p and w_b are the weight percentage of the biomass and plastic in the biomass-plastic mix respectively. The significance of this equation is that the values could be compared directly to the experimental values. If $x_{exp}>x_{theo}$, the synergy is positive for that product, if $x_{exp}<x_{theo}$, negative synergies, and finally if $x_{exp}\approx x_{theo}$, no synergy.

$$x_{theo} = \frac{m_{theo}}{m_{total}} = \frac{x_p y_p w_p + x_b y_b w_b}{y_p w_p + y_b w_p}$$ **Eq. 3.1**

x; y; w; mass percentage of the desired product from individual pyrolysis; corresponding liquid or gas yield from individual pyrolysis; weight percentage of each feedstock in the mix.

3.3. Results and discussion

3.3.1. TGA analysis

The TGA and DTG of BW compared to the used plastics are shown in **Fig. 2.2**. The TGA of co-pyrolysis is similar to the combination of the individual curves since the interactions were between the volatile phase. Furthermore, BW degradation reached a plateau of about 20 %, indicating the stability of the fixed carbon obtained (char) in the absence of oxygen. The fixed carbon corroborated the presence of char in the pyrolysis of BW and its absence in the pyrolysis of plastics. On the other hand, the DTG of BW showed that BW cracked through several steps, with several optimal points compared to one optimum with plastics. This can imply the presence of biopolymers within BW (cellulose, hemicelluloses, and lignin) each having different thermal stability, thus cracking at different temperatures (Anca-Couce et al., 2020). The degradation started at around 200 °C and ended at around 380 °C, with a maximum degradation temperature of 350 °C, making biomass less thermally stable than plastics.

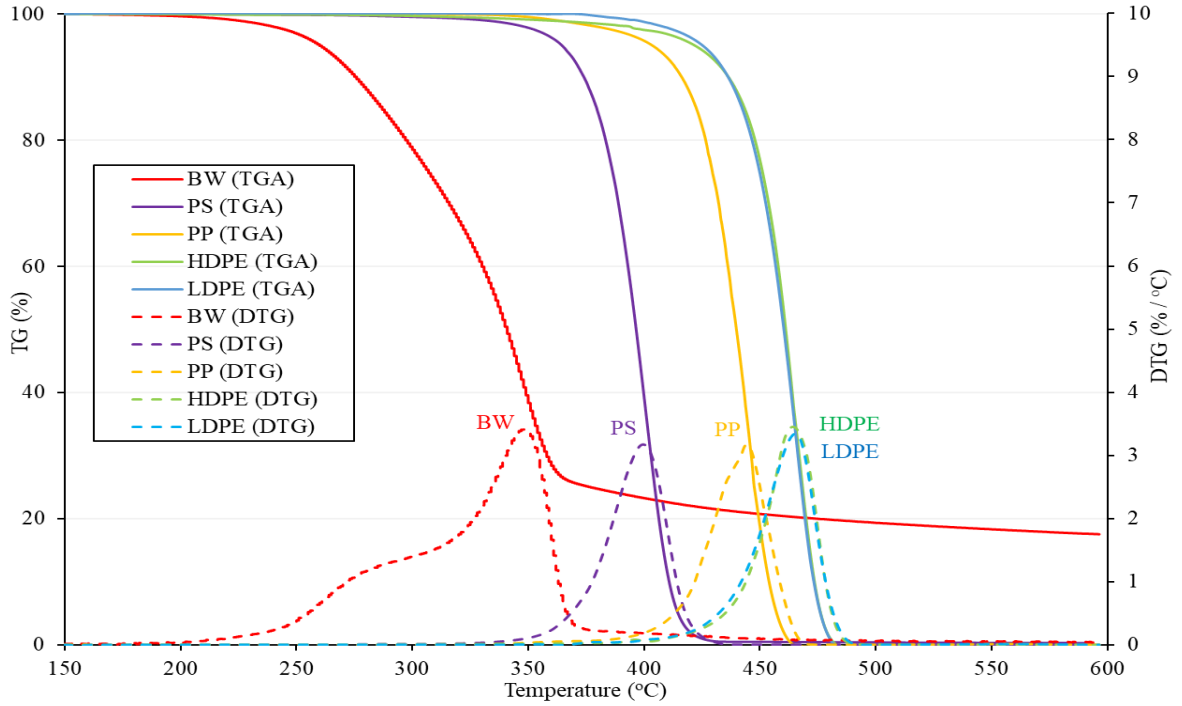

Fig. 3.1. TG and DTG thermograms of the used plastics and BW at 5 °C.min^{-1} heating rate.

3.3.2. Identification and quantification of pyrolytic components in oil

At first, GC-MS analysis was carried out for alone and mixed feedstocks to clearly identify the compounds in each pyrolytic oil obtained at 500 °C. For instance, 246 compounds were identified for PP, 183 for HDPE and LDPE, 118 for PS, and 97 for BW. The compounds identified from plastics are all hydrocarbons, in contrast to the oxygenated compounds in BW bio-oil. After that, co-pyrolysis liquid oil was investigated via GC-MS for all BW-plastic feedstock combinations in order to check the presence/absence of any new compounds. **Fig. 3.2** illustrates a typical chromatogram of BW bio-oil at 500 °C. The chromatogram shows a series of major compounds present in BW bio-oil. The compounds were mainly distributed as acetic acid, 1-hydroxy-2-propanone, levoglucosan, and guaiacol derivatives.

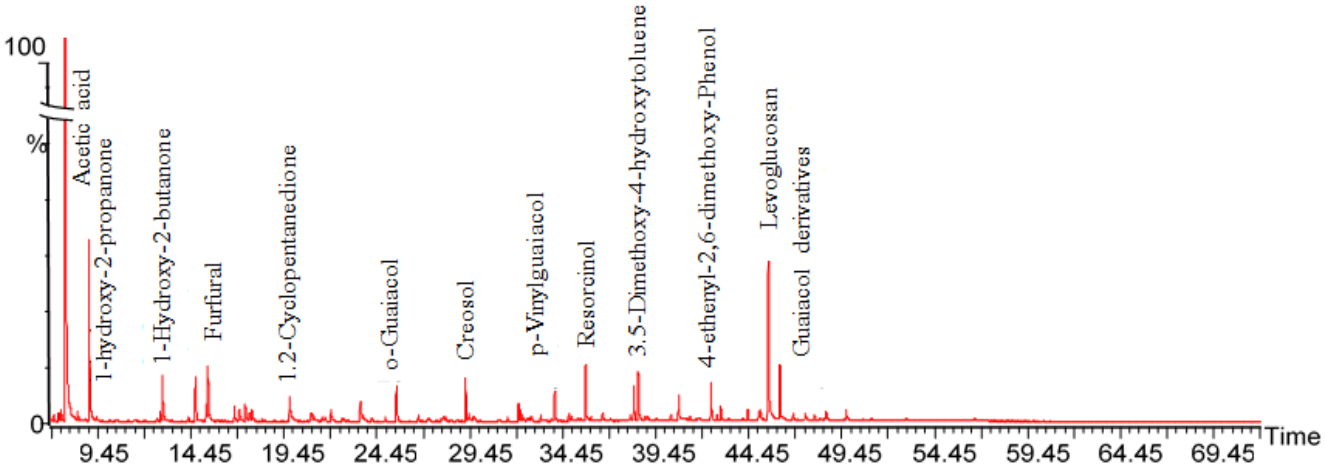

Fig. 3.2. GC-MS chromatogram of BW bio-oil obtained at 500 °C.

After identification, quantification of the identified compounds was achieved. For this motive, the products were grouped into 13 families divided between oxygenated compounds and hydrocarbons (Jaafar et al., 2022; Mohabeer et al., 2017). The families with their corresponding reference compounds for calibration are illustrated in **Table 3.3.**

Table 3.3. List of families and major products in the co-pyrolytic oil identified by GC-MS.

Retention time (min)		Chemical family	Reference compound
BW	6.63*	Furans	Furan
	11.15	Carboxylic acids	Acetic acid
	18.39	Esters & Ethers	Allyl butyrate
	19.52	Aldehydes	Furfural
	21.63	Ketones	2-methyl-2-cyclopenten-1-one
	31.82	Phenols	p-cresol
	41.74	Guaiacols	4-methylcatechol
	42.74	Nitrogenates	Benzamide
	49.58	Carbohydrates	Levoglucosan
Plastics	12.13	Aromatics	Toluene
	28.41	Olefins	1-Dodecene
	35.33	Paraffins	Tetradecane
	40.76	PAH	Bibenzyl

* GC-FID retention time

Pyrolysis of BW

BW pyrolysis was studied alone to have a better understanding of the effect of co-pyrolysis on BW. BW bio-oil was mainly comprised of carboxylic acids, carbohydrates, and ketones with respective concentrations of 36 wt.%, 18 wt.%, and 15 wt.%, as shown in **Fig. 3.3**. The results follow the same tendency observed by Mohabeer et al. (2017), who obtained 35

wt.% of carboxylic acid, 8 wt.% carbohydrates, and 14 wt.% ketones at 500°C. This implicates the acidic nature of BW bio-oil. Other biomasses showed acidity which was slightly lower than that of BW. For instance, flax shive bio-oil exhibited around 28 wt.% carboxylic acids under similar conditions (Mohabeer et al., 2017). To delve deeper into the nature of this biomass, it was considered that BW is composed of 42 wt.% cellulose, 37 wt.% hemicellulose, and 19 wt.% lignin (Gucho et al., 2015). Consequently, one could conclude that the major constituents (79 wt.%) of BW are polysaccharides (cellulose and hemicelluloses), which would explain the domination of carbohydrates and acids on the liquid bio-oil since they are the dominant species in the independent pyrolysis of cellulose and hemicelluloses, respectively (Zhao et al., 2017).

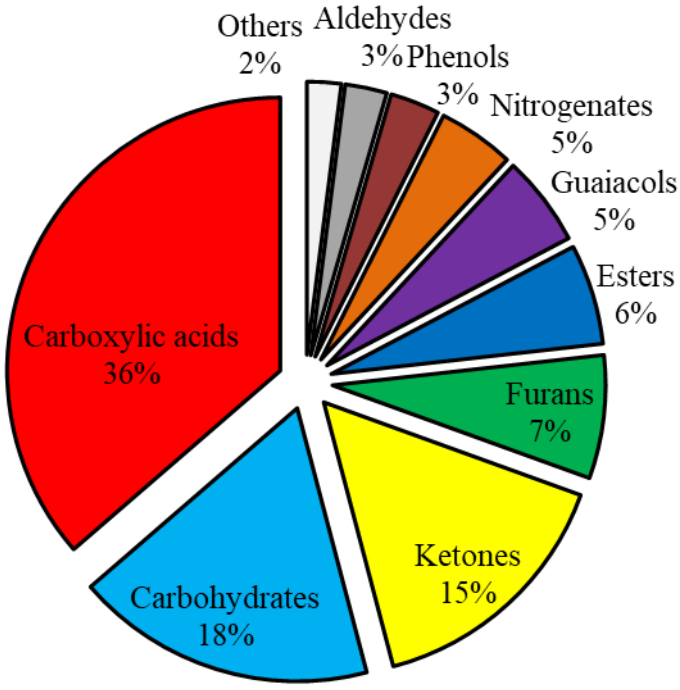

Fig. 3.3. Chemical families in BW pyrolytic oil at 500°C.

Co-pyrolysis of BW-HDPE/LDPE

Investigating the synergetic effect between BW and plastics was firstly achieved by a qualitative analysis identifying any new-formed or absent compounds in the co-pyrolysis oil. For that, **Table 3.4, Table A.6,** and **Table A.7** were established to better visualize the trends. Results show the main liquid products in plastic pyrolysis, BW pyrolysis, and plastic-BW co-

pyrolysis. As mentioned in a previous study, Jaafar et al. (2022) and the previous chapter, HDPE and LDPE pyrolytic oil were mainly comprised of successive linear chain aliphatic compounds. After co-pyrolysis of BW-HDPE, new compounds were produced as 5-hexene-2-one and acetyloxy acetic acid; countered by propanedioic acid for BW-LDPE. This difference between the 2 polymers can be due to the different structural interactions during pyrolysis. LDPE is more branched than HDPE, which results in weaker intermolecular force so the degradation is easier (Uddin et al., 1997). This can induce a slightly different pathway of interactions between BW. However, the overall quality of the 2 liquid oils was similar. On the other hand, some compounds vanished as 2,5-dimethylfuran and 1.2-ethanediol, monoacetate. This can reassure the presence of the synergetic effect between the plastic and BW. Yet, whether the interaction is positive or negative, a quantitative analysis will be investigated further on.

Regarding the product yield, whether gas, liquid, or char was not significantly affected during co-pyrolysis. The yield was almost the average sum between the product yields of the individual feedstocks.

Table 3.4. List of the major products (>0.4 wt %) in BW-LDPE and BW-HDPE pyrolytic oil.

Compounds	Percentages (wt %)				
	BW	BW-LDPE (50-50)	BW-HDPE (50-50)	LDPE	HDPE
Furan	2.7	2.5	2.9	-	-
5-hexen-2-one	-	2.6	1.8	-	-
2,5-dimethylfuran	3.6	-	-	-	-
Acetic acid	33.6	20.1	18.7	-	-
1-hydroxy-2-propanone	8.0	5.3	4.2	-	-
1.2-ethanediol, monoacetate	3.5	-	1.9	-	-
Propanedioic acid	-	1.6	-	-	-
Acetyloxy acetic acid	-	-	1.9		-
Furfural	2.1	1.4	0.8	-	-
1.2-cyclopentanedione	1.8	1.2	1	-	-
Levoglucosan	8.4	4.5	9.9	-	-
Decane	-	0.7	0.6	2.2	1.5
1-Decene	-	2.0	1.7	5.6	3.8

Undecane	-	1.2	1.2	2.9	2.4
1-Undecene	-	2.6	2.8	5.0	4.4
Dodecane	-	1.4	1.3	2.5	2.4
1-Dodecene	-	2.2	2.5	4.0	4.0
Tridecane	-	1.1	1.1	2.3	2.2
1-Tridecene	-	2.3	2.4	3.7	3.8
1-Tetradecene	-	2.2	2.5	3.8	3.9
1-Pentadecene	-	1.9	2.3	3.4	3.5
Cetene	-	1.5	1.9	2.7	2.9
1-Heptadecene	-	1.4	1.7	2.5	2.7
1-Octadecene	-	1.3	1.7	2.4	2.6
Gas yield	15.0	6.2	6.7	2.3	2.1
Liquid yield	65.0	83.1	84.0	97.3	97.9
Char yield	20.0	10.7	9.3	0.4	-

Co-pyrolysis of BW-PP/PS

As for BW-PP, several new compounds were formed during co-pyrolysis (**Table A.6**) as 1-Propen-2-ol, acetate, and 3,5-hexadien-2-ol. Other compounds did not appear as 2.5-dimethyl furan which also vanished for BW-PE. On the other hand, no new compounds were formed (**Table A.7**) for BW-PS although other compounds did not appear for the 50-50 mixture.

3.3.3. Synergy of co-pyrolysis

The synergetic effect is better observed in **Fig. 3.5-Fig. 3.7,** where both the theoretical values and experimental values of the most relevant family of each BW-plastic mix are shown. The theoretical curves showed a non-linear trend due to the presence of two variables: concentration of the family and the liquid yield, thus equation **Eq. 3.1** is not linear.

Co-pyrolysis of BW-HDPE/LDPE

Fig. 3.5 shows the variation of the major chemical families as a function of BW content for both experimental and theoretical values. Based on these results, it is evident to say that as BW content increased, oxygenated compounds increased, and aliphatics would decrease. As it could be seen, there are around 7 wt.% more carbohydrates found in the experimental liquid oil

than the theoretical one for the 50-50 mixture. This increase in some oxygenated compounds such as carbohydrates; mainly levoglucosan, and acids were observed for all BW contents. From here, one could derive a conclusion that the addition of PE to BW enhances the production and stabilization of such compounds. This outcome is in accordance with Kumagai et al. (2019 and 2016) who stated there was an increase of levoglucosan and a decrease of methoxy phenol (guaiacols) during the co-pyrolysis of BW and PE. The latter study mentioned that this can be due to the hydrogen exchange mechanism between the olefinic structure and the oxygenated compounds. This behavior can be explained further by **Fig. 3.4**, where the hydrogen abstraction from the olefinic polymers stabilizes levoglucosan radicals thus suppressing their degradation.

However, Yang et al. (2016) studied various biomass different than BW and claimed that more hydrocarbons and less oxygenated compounds were produced. This was not the case in this study and the studies of Kumagai et al. (2016,2019). This can be related to the effect of the biomass nature/composition and operating conditions.

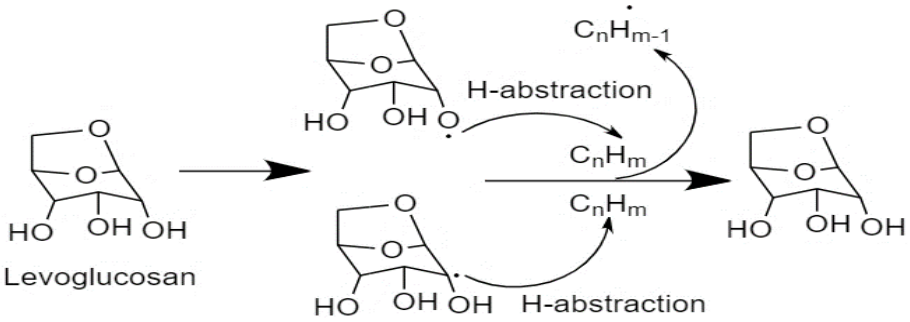

Fig. 3.4 Scheme of suggested interactions between levoglucosan and polyolefins based (Kumagai et al., 2016).

BW-PE pyrolysis showed a negative synergy with more acids and carbohydrates from the theoretical value. The oil has an elevated LHV of around 31 MJ/kg for the 50-50 mix but it has a high oxygen content of around 24 wt.%, as mentioned in **Table 3.5**. Having the same behavior, LDPE and HDPE cannot be used via co-pyrolysis to improve the quality of BW bio-oil for fuel purposes. For this, both HDPE and LDPE can be used in co-pyrolysis to increase these oxygenated compounds to be extracted later on.

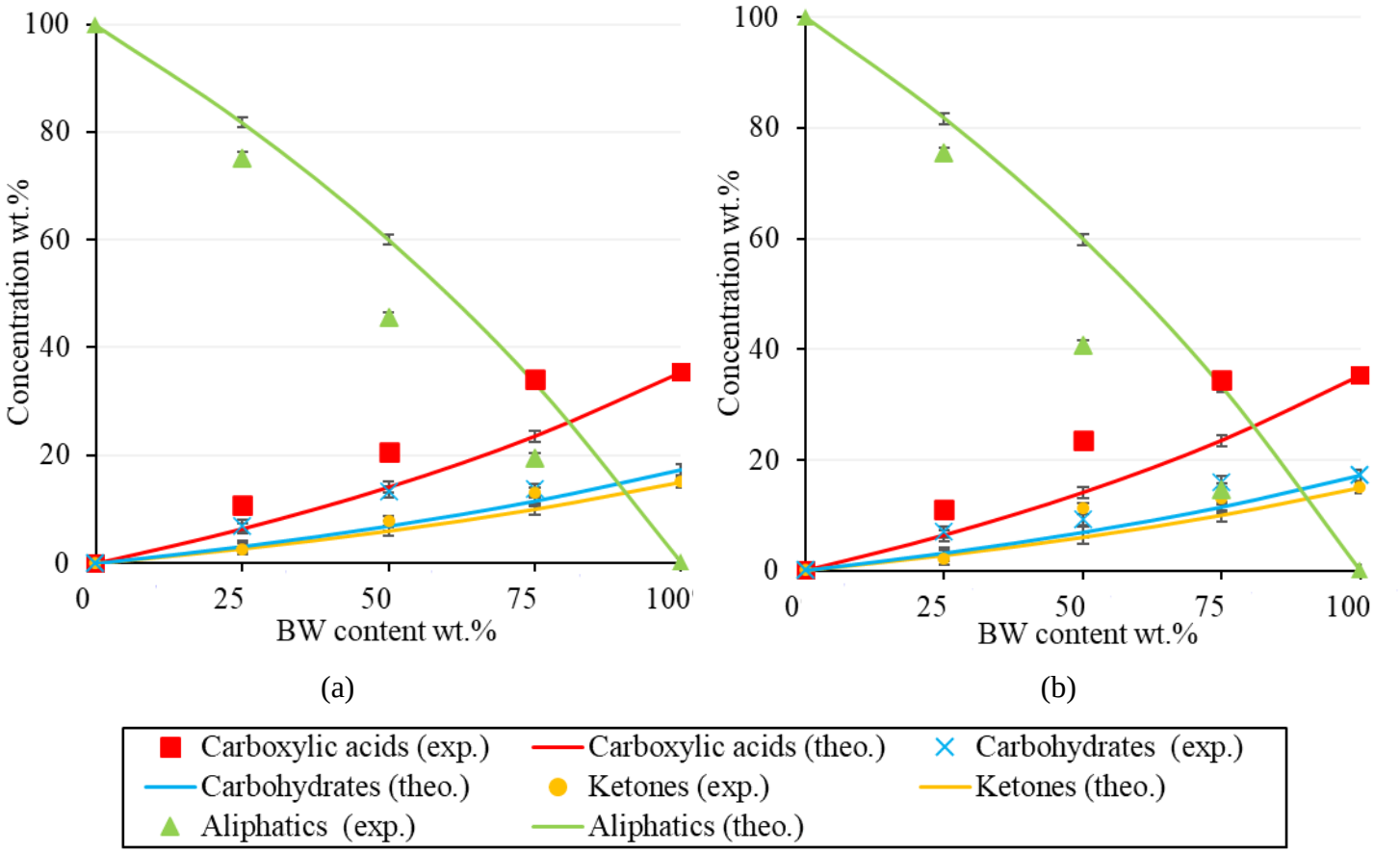

Fig. 3.5. Distribution of the major families of (a): BW-HDPE and (b): BW-LDPE liquid oil as experimental and theoretical concentrations relative to BW content (wt.%).

Co-pyrolysis of BW-PP/MP

The co-pyrolysis of BW-PP showed a slightly similar behavior as BW-PE due to the similarity of the 2 polymers in their olefinic nature. However, the effect here is not as evident as in PE. **Fig. 3.6** shows that for a BW content of 25 wt.% and 50 wt.%, there were little to no major interactions between the 2 feedstocks. However, the effect of the hydrogen abstraction (Kumagai et al., 2019) was further observed for the 75 wt.% of beech wood where the amount of carbohydrates increased by about 10 wt.% over the theoretical value. This can be a result from the branched olefinic structure of PP, that can form tertiary radicals, which are more stable than secondary and primary ones (Liu, 2021). The latter could make the radical resist the interaction until a severe condition is acquired, namely upon reaching the threshold of 75 wt.% of BW in the mixture. The increase in carbohydrates can be at the expense of methoxy phenols and aliphatic hydrocarbons; mainly olefinic, which decreased in this case from the theoretical

value of 4 wt.% to 1 wt.% and from 32 wt.%, to 16 wt.%, respectively at the 75-25 BW/plastic ratio. As for the heating value, the liquid oil has an elevated LHV of around 33 MJ/kg and a high oxygen content of around 20 wt.%, making the oil unsuitable for combustion purposes without further treatment. However, the oil from the co-pyrolysis of PE and PP with BW could be used to extract valuable chemicals such as levoglucosan. Levoglucosan is considered to be the most important product in lignocellulosic biomass pyrolysis (Dai et al., 2020). It is mainly used in the production of biodegradable polymers and is used in the synthesis of chiral pharmaceutical products (Longley and Fung, 1993). So, the incorporation of biomass with olefinic polymers could be useful in boosting the selectivity of biomass degradation towards levoglucosan.

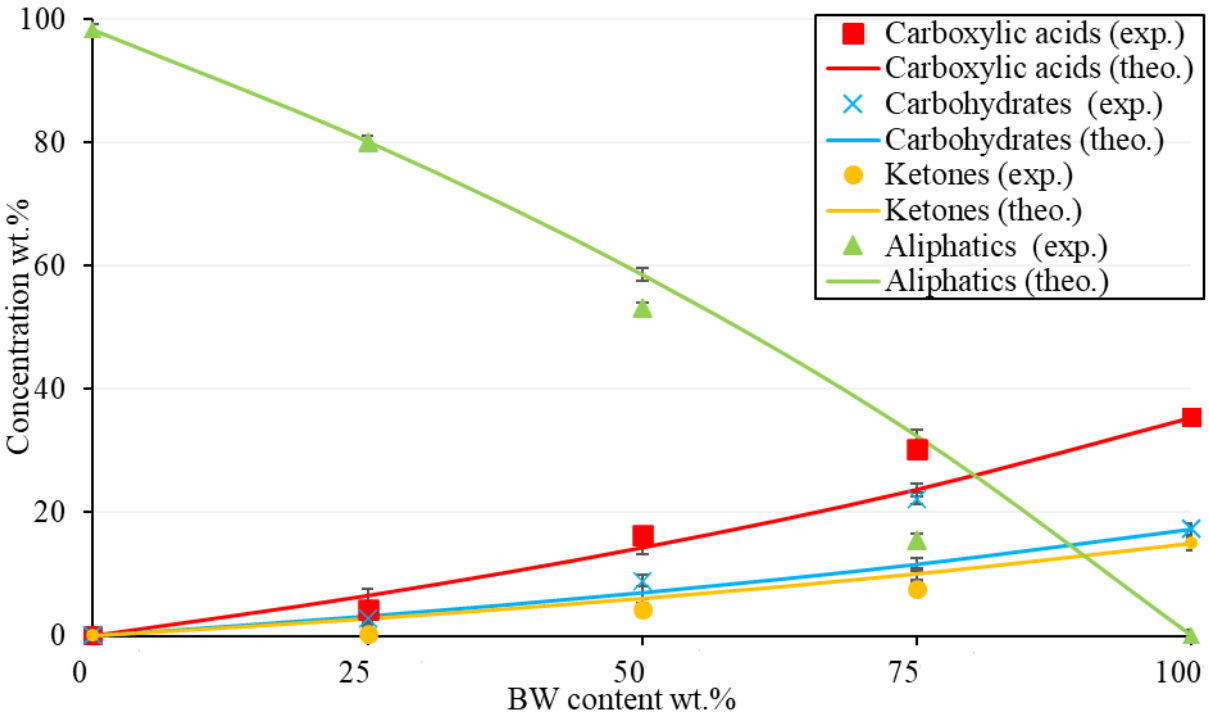

Fig. 3.6. Distribution of the major families of BW-PP liquid oil as experimental and theoretical concentrations relative to BW content (wt.%).

On the other hand, a mixture of plastics was prepared to test their effect on BW bio-oil production. As it is shown in **Fig. 3.7,** the liquid oil contains aromatics that were not affected negatively, such as aliphatic compounds. The liquid oil behavior was similar to that of PP and PE since they are the main constituents in the MP (around 87 wt.%). However, the liquid oil

showed a high aromatics concentration of around 16 wt.% with a high oxygen content of around 20 wt.% for a 50-50 mix. The mixing of plastic is preferable to be pyrolyzed alone rather than co-pyrolysis with BW which was proved in a previous study (Jaafar et al., 2022).

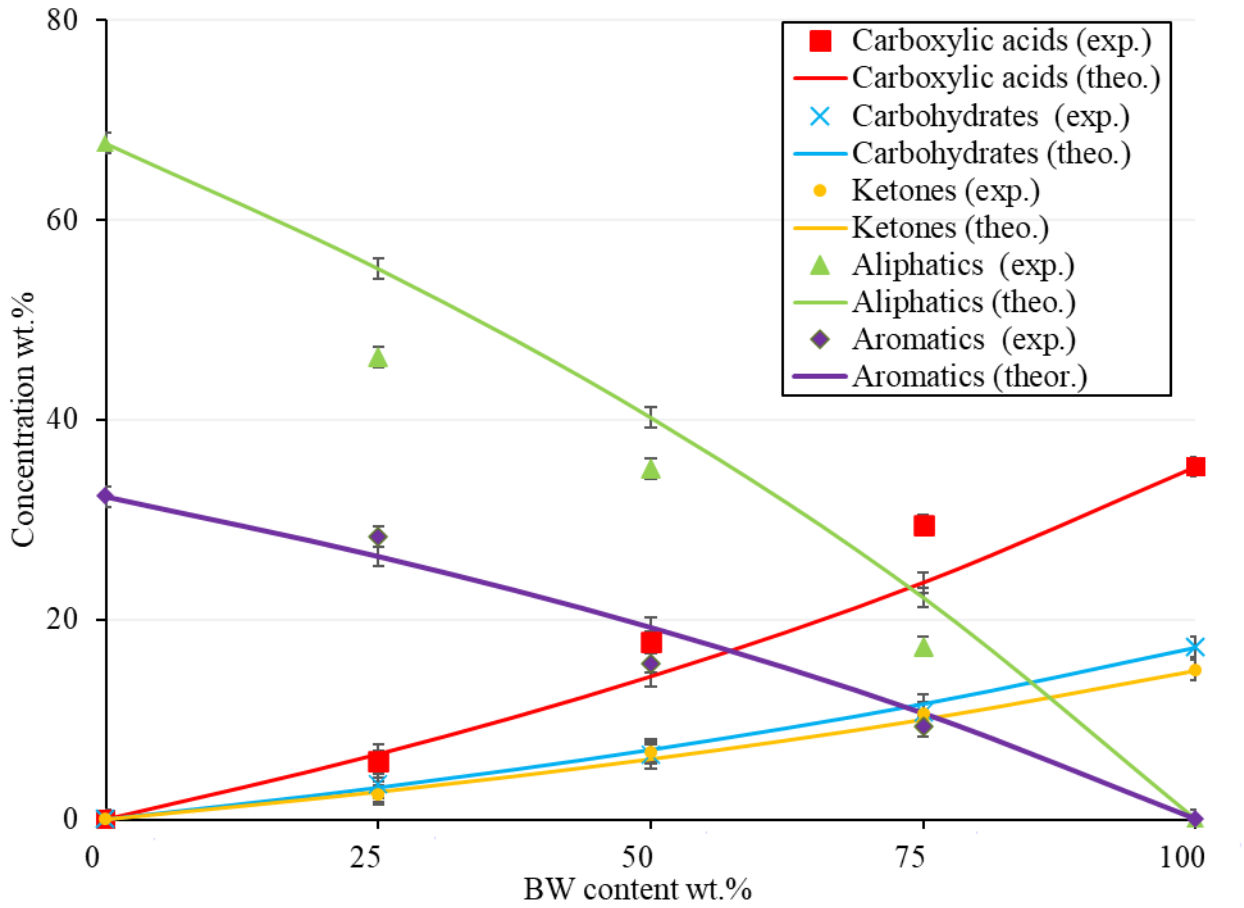

Fig. 3.7. Distribution of the major families of BW-MP liquid oil as experimental and theoretical concentrations relative to BW content (wt.%).

Co-pyrolysis of BW-PS

The case of BW-PS co-pyrolysis was quite different from the other plastics. It showed a significant increase in aromatic compounds and a decrease in acids. This positive interaction showed an increase of about 20 wt.% of aromatics in the liquid oil from the expected percentage. This increase was greatly realized for the 50-50 mixture where the increase of aromatics was about 22 wt.% instead of 13 wt.% and 20 wt.% for the 25 wt.% and 75 wt.% BW content, as shown in **Fig. 3.8**. From here, one can deduce that the interactions between plastics and biomass were the strongest for high BW content. This was also shown for other polymers

such as PP and PE, where the interaction was the strongest at 75 wt.% BW content. This also supports the main goal of co-pyrolysis which is improving the quality of liquid oil from biomass pyrolysis.

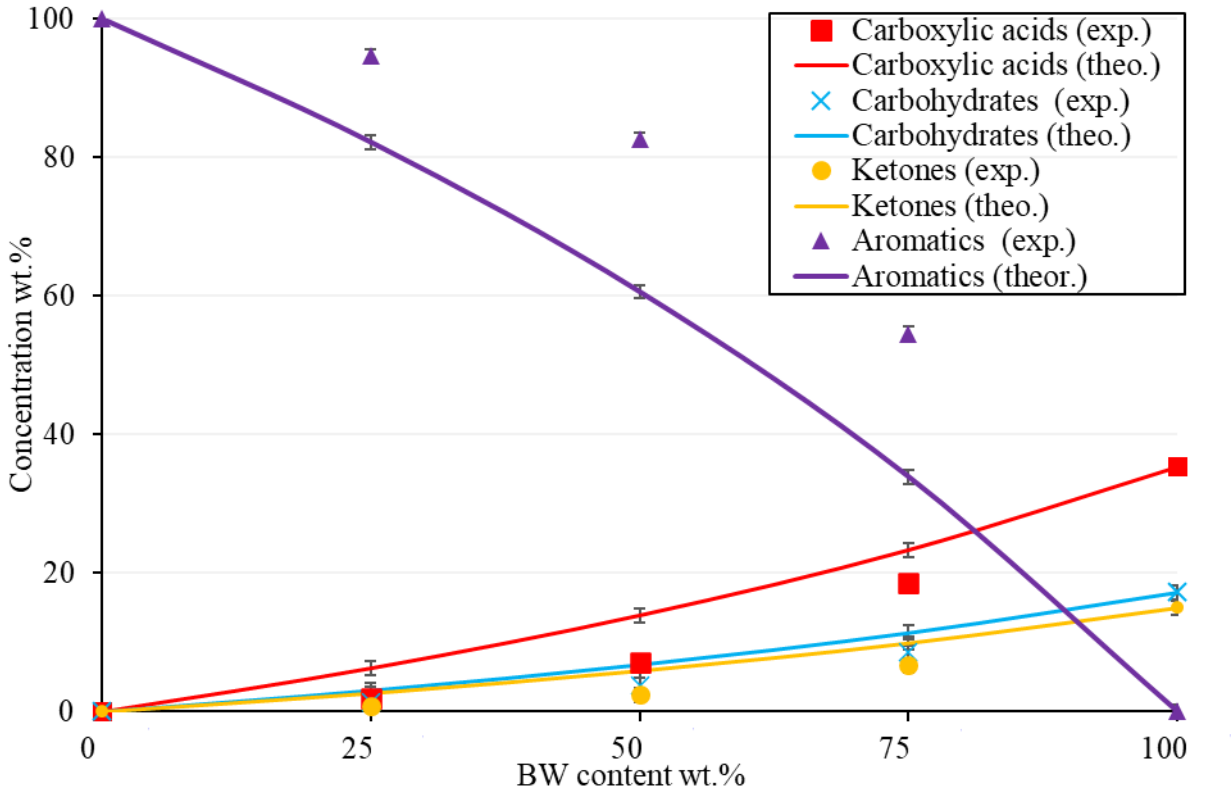

Fig. 3.8. Distribution of the major families of BW-PS liquid oil as experimental and theoretical concentrations relative to BW content (wt.%).

To compare the co-pyrolysis of BW with all plastics, **Fig. 3.9** was established. LDPE was excluded from the graph since it showed similar behavior as HDPE. The difference between the various plastic pyrolytic oil is present in a previous study (Jaafar et al., 2022). It can be shown that all plastics experienced some interactions with BW. Both the olefinic polymers exhibited an increase in oxygenated compounds, such as levoglucosan and a decrease in the olefinic compounds. The decrease was specially recorded for PE where about 15 wt.% less aliphatic compounds were formed for the 50-50 BW/plastics mix. However, for PS, the effect was reversed. More aromatic compounds and fewer acids and carbohydrates with a decrease of about 7 wt.% and 3 wt.% respectively were produced. The positive synergy and

improvement of liquid oil quality corroborated the work of Brebu (2010) and Abnisa (2013, 2014), who stated that the synergy of lignocellulosic biomass with PS yielded a liquid oil of higher heating value and lower oxygen content. Due to that, BW-PS was investigated further.

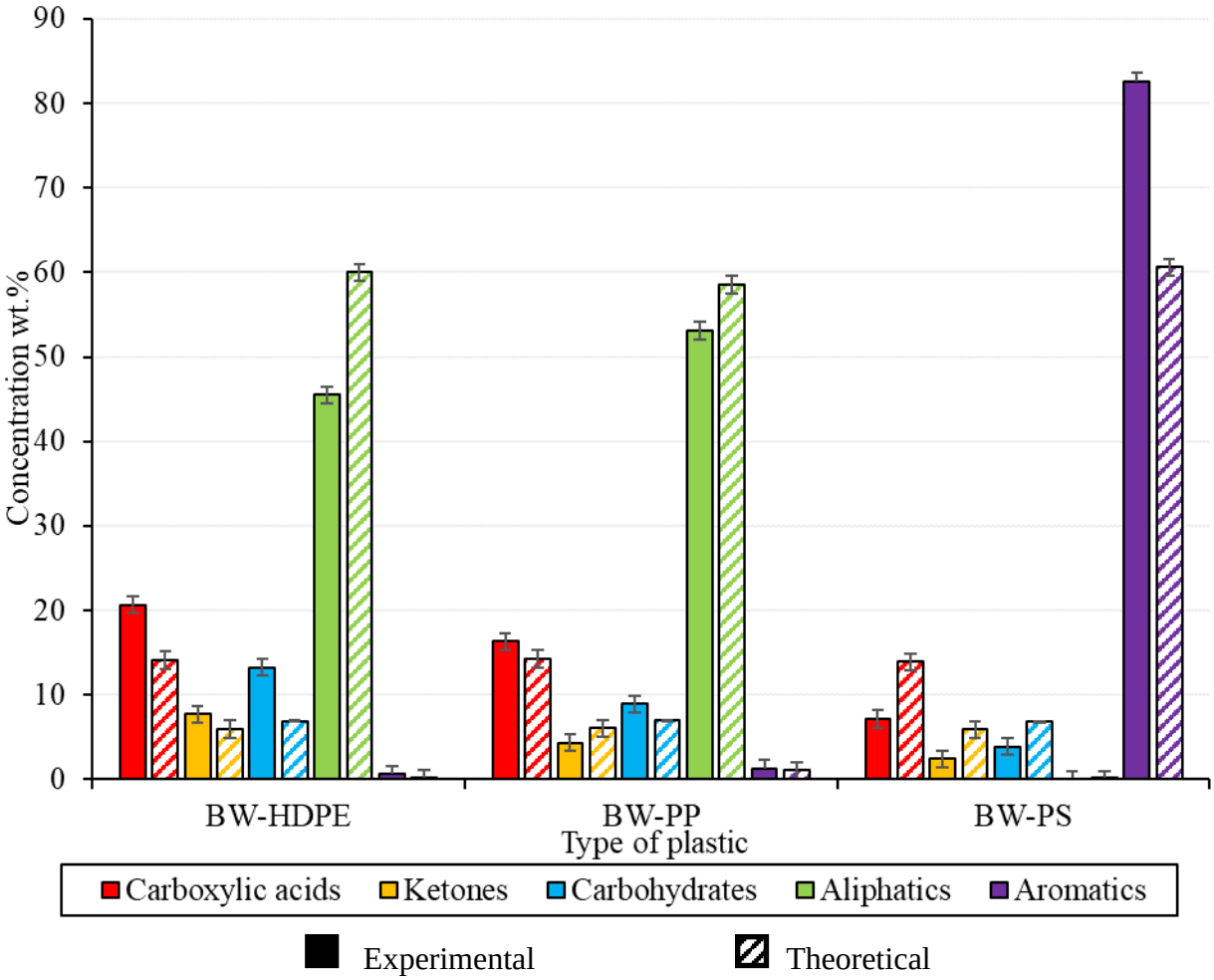

Fig. 3.9. Synergy comparison between the different polymers studied with a 50-50 BW/plastic ratio at 500 °C.

3.3.4. BW-PS pyrolytic oil

To explore more deeply the quality of BW-PS liquid oil, a pie chart was developed to represent the concentration of each family in the liquid oil, as shown in **Fig. 3.10**. The liquid oil was mainly made up of aromatics; mainly styrene, polycyclic hydrocarbons, and carboxylic acids of respective concentrations of 68 wt.% 15 wt.%, and 7 wt.%. Other families were also present such as carbohydrates, ketones, and furans. The heating value and oxygen content of BW bio-oil were around 18 MJ/kg and 41 wt.% respectively. Yet, the LHV of BW-PS (50-50)

liquid oil increased significantly to be around 36 MJ/kg, which is slightly lower than that of styrene pyrolytic oil alone (41 MJ/kg) and that of diesel (around 45 MJ/kg), as shown in **Table 3.5**. Regarding the oxygen content, the liquid oil oxygen content was reduced significantly as shown in **Fig. 3.11**, yet it is still slightly elevated and treatment becomes easier via catalytic deoxygenation (Mohabeer et al., 2019a, 2019b), or hydrodeoxygenation (Wang et al., 2021).

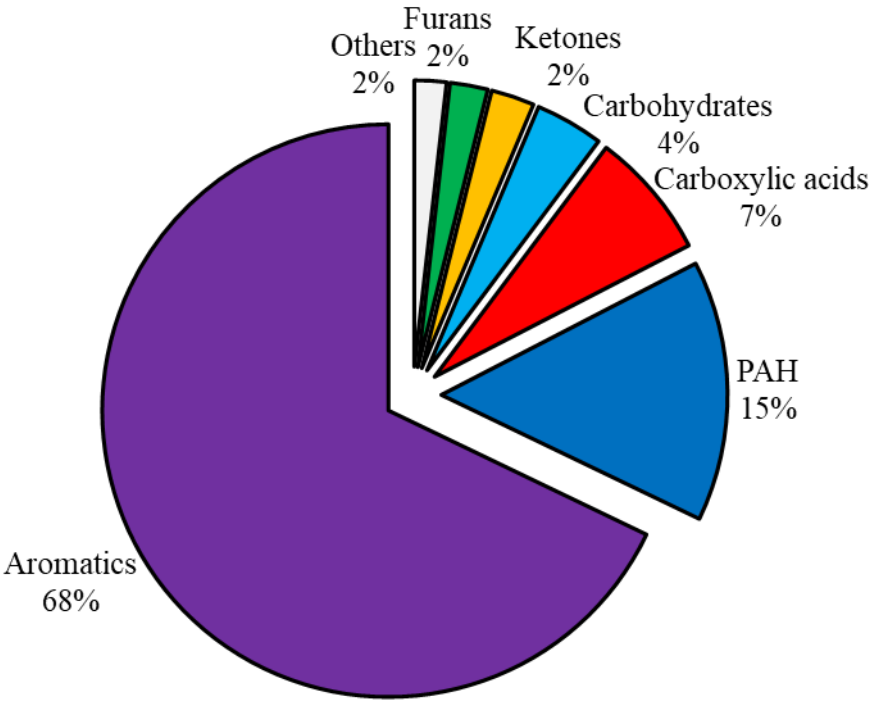

Fig. 3.10. Chemical families in BW-PS 50-50 liquid oil obtained at 500 °C.

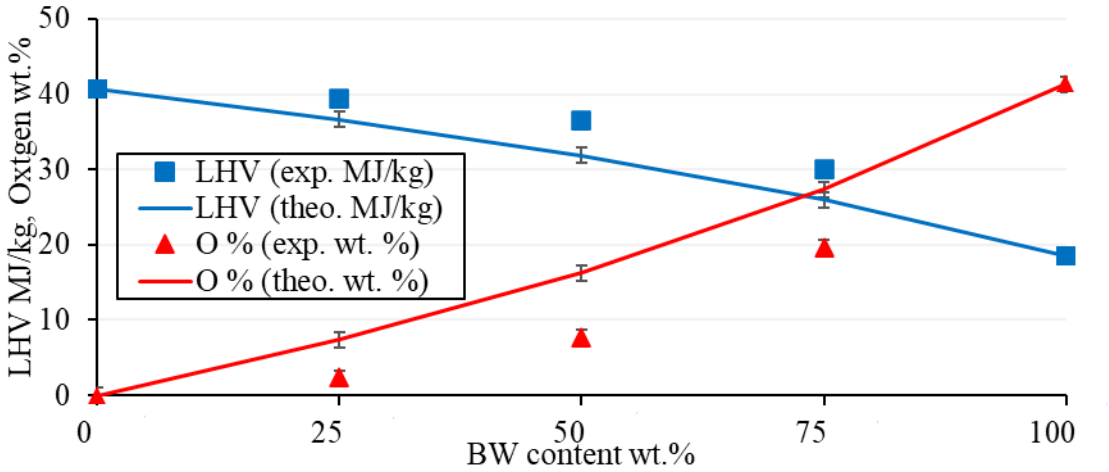

Fig. 3.11. The evolution of LHV (MJ/kg) and O % (wt.%) in BW-PS liquid oil as per BW content at 500 °C.

Regarding the quality of the liquid oil produced from BW-PS, it showed the highest heating value amongst the BW-Plastic mix, yet, it yielded the lowest LHV compared to independent plastic pyrolysis, as shown in **Table 3.5**. The heating value approached that of conventional fuel oil. Additionally, the oxygen content dropped from 41 wt.% (BW) to just 8 wt.% (PS-BW 50-50). BW-PS mix showed the highest increase in the heating value of around 98% and a remarkable decrease in the oxygen content of about 81 % from the other plastic/BW mix. The decrease in the oxygen content is remarkable, making the oil one step closer to being acceptable as bio-fuel. However, if the oxygen content has to be further reduced, upgrading would then be easier by catalytic deoxygenation, for example. The oxygen content should be slightly decreased to a level of 3 wt.%, compared to the limitation of the gasoline oxygen content of about 3 wt.%, which is gained from the addition of ethers (MTBE and ETBE) to boost the octane number ("U.S. energy facts explained," 2022). On the other hand, lignocellulosic bio-oil is considered to have no significant environmental hazards (Bridgwater, 2012); which is important, especially when used as a commodity, where there might be hazardous spills. In this case, PS-derived aromatics have, to an extent, health and environmental hazard issues, nevertheless, gasoline has a high aromatic concentration and is handled with basic and modest precautions. Ultimately, one could draw that blending between 30-50 wt.% of the derived liquid oil to the gasoline pool could be a great tool to further boost the octane number without adding ethers to gasoline and without any significant change in the calorific value. This blending would decrease gasoline production from refineries, thus reducing environmental problems by utilizing a carbon-neutral feedstock (biomass); also, it can lower refinery operating and fixed

costs, and it could help tackle PS's disposal problem, which is challenging to recycle due to its light weight.

Table 3.5. Comparison within the pyrolytic oils and between conventional fuels.

Name	LHV (MJ/kg)		LHV change (%)	O % (wt.%)		O % change (%)	Ref.
BW	18.4	**n.a.**	n.a.	41.3	**n.a.**	n.a.	This work
HDPE	46.6[a]	**30.5[b]**	+ 65.8[c]	- [a]	**23.4[b]**	− 43.3[c]	
LDPE	46.6	**30.1**	+ 63.6	-	**22.5**	− 45.5	
PP	46.2	**33.2**	+ 80.4	-	**19.5**	− 52.8	
PS	40.6	**36.5**	+ 98.4	-	**7.8**	− 81.1	
MP	44.6	**31.6**	+ 71.7	-	**20.4**	− 50.6	
Gasoline	43.4-46.5			~ 2.7			(Anuar Sharuddin et al., 2017; Imam and Capareda, 2012; "U.S. energy facts explained," 2022)
Kerosene	43.0-46.2			n.a.			
Diesel	42.8-45.8			~ 1.8			

[a] LHV/O% of pure component pyrolytic oil

[b] LHV/O% of 50-50 plastic-BW mixture pyrolytic oil

[c] Change in LHV/O% of 50-50 plastic-BW mixture oil relative to BW bio-oil

To delve deeper into the relationship between the properties and chemical families of the liquid oil and temperature, **Table 3.6** was established. The effect of temperature could be seen relative to the concentrations of the main chemical families. The effect of temperature on the oxygenated compounds was not that evident. There were no major variations of the biomass chemical families with temperature within the studied interval. This can be due to the mechanism of biomass pyrolysis, which is a series of endo/exothermic reactions, making the temperature effect not that straightforward (Demirbas, 2009). However, for aromatics, the trend seemed to have an optimum point at 500 °C. The trend of aromatics seemed to decrease from 72 wt.% to 68 wt.% as the temperature rose from 450 °C to 500 °C then increases to 73 wt.% at 600°C. The trend of aromatics is opposed to that of polycyclic aromatic hydrocarbons. The heavy aromatics showed the opposite trend as aromatics, showing that PAHs are transforming to aromatics and vice versa as temperature rises. On the other hand, liquid and gas yields slightly

increased with temperature at the expense of char production yet the increase was not remarkable, especially when taking into consideration the experimental error of about 1 %. Ultimately, the heating value and oxygen content did not change since they are mainly controlled by the oxygenated compounds, which in this case are invariant. Consequently, the best operating temperature would be 450 °C, where the operating cost is lower at low temperatures.

Table 3.6. Evolution of BW-PS (50-50) liquid oil composition and properties relative to temperature (wt.%).

Chemical Families	Operating Temperature (°C) ±5°C			
	450	500	550	600
Carboxylic acids	7.6	7.2	7.2	7.0
Ketones	3.3	2.4	3.1	2.9
Furans	1.7	2.1	1.8	1.9
Carbohydrates	2.8	3.9	3.3	2.9
Aromatics	72.2	67.9	69.8	73.4
PAH	8.6	14.7	11.8	9.3
Gas yield	4.7	5.0	5.7	5.8
Liquid yield	83.7	84.7	84.3	85.2
Char yield	11.7	10.3	10.0	9.0
O %	8.0	7.8	7.8	7.4
LHV*	36.4	36.5	36.5	36.8

***** Lower heating value (MJ/kg)

3.4. Conclusion

The co-pyrolysis of beech wood and plastics creates a good opportunity for the valorization of a widely known forestry product and the reduction in plastic waste. This study examined the synergetic effect between a certain kind of lignocellulosic biomass and hydro-carbonaceous plastics. It has been found that several compounds were newly formed or disappeared during co-pyrolysis.

After deeper analysis, olefinic polymers (PE and PP) showed a negative synergetic effect with beech wood, where an increase in oxygenated compounds was observed. However, the case was different for polystyrene, where an aromatic-rich oil was produced with a relatively

high heating value and lower oxygen content, as expected. To fully benefit from the pyrolytic oil, a simple parameter such as temperature could be manipulated for process optimization.

The temperature effect showed no significant change in the quality of the liquid oil, so a lower temperature is advised to limit energy expenditure. Contrastingly, the oxygenated chemical compounds along with the LHV and oxygen content showed no variation as per temperature. The heating value of the liquid oil of BW-PS was around 36 MJ/kg, which is relatively high. On the other hand, oxygen content has decreased significantly to about 8 wt.%, so if treatment was essential, it becomes easier by deoxygenation or hydrodeoxygenation to further reduce the oxygen content. Yet, the liquid oil could be still blended directly into gasoline with high proportions to reduce its production and boost the octane number at the same time.

3.5. References

Abnisa, F., 2013. Co-pyrolysis of palm shell and polystyrene waste mixtures to synthesis liquid fuel. Fuel 108, 311–318.

Abnisa, F., Daud, W.M.A.W., Sahu, J.N., 2014. Pyrolysis of mixtures of palm shell and polystyrene: An optional method to produce a high-grade of pyrolysis oil. Environ. Prog. Sustain. Energy 33, 1026–1033. https://doi.org/10.1002/ep.11850

Anca-Couce, A., Tsekos, C., Retschitzegger, S., Zimbardi, F., Funke, A., Banks, S., Kraia, T., Marques, P., Scharler, R., de Jong, W., Kienzl, N., 2020. Biomass pyrolysis TGA assessment with an international round robin. Fuel 276, 118002. https://doi.org/10.1016/j.fuel.2020.118002

Anuar Sharuddin, S.D., Abnisa, F., Wan Daud, W.M.A., Aroua, M.K., 2017. Energy recovery from pyrolysis of plastic waste: Study on non-recycled plastics (NRP) data as the real measure of plastic waste. Energy Convers. Manag. 148, 925–934. https://doi.org/10.1016/j.enconman.2017.06.046

Brebu, M., 2010. Co-pyrolysis of pine cone with synthetic polymers. Fuel 89, 1911–1918.

Bridgwater, A.V., 2012. Review of fast pyrolysis of biomass and product upgrading. Biomass Bioenergy 38, 68–94.

Dai, L., Wang, Y., Liu, Y., He, C., Ruan, R., Yu, Z., Jiang, L., Zeng, Z., Wu, Q., 2020. A review on selective production of value-added chemicals via catalytic pyrolysis of lignocellulosic biomass. Sci. Total Environ. 749, 142386. https://doi.org/10.1016/j.scitotenv.2020.142386

Demirbas, A., 2009. Pyrolysis mechanisms of biomass materials. Energy Source Part 31, 1186–93.

Gucho, E.M., Shahzad, K., Bramer, E.A., Akhtar, N.A., Brem, G., 2015. Experimental Study on Dry Torrefaction of Beech Wood and Miscanthus. Energies 8, 3903–3923. https://doi.org/10.3390/en8053903

Imam, T., Capareda, S., 2012. Characterization of bio-oil, syn-gas and bio-char from switchgrass pyrolysis at various temperatures. J. Anal. Appl. Pyrolysis 93, 170–177. https://doi.org/10.1016/j.jaap.2011.11.010

Jaafar, Y., Abdelouahed, L., Hage, R.E., Samrani, A.E., Taouk, B., 2022. Pyrolysis of common plastics and their mixtures to produce valuable petroleum-like products. Polym. Degrad. Stab. 195, 109770. https://doi.org/10.1016/j.polymdegradstab.2021.109770

Klein, A., Bockhorn, O., Mayer, K., Grabner, M., 2016. Central European wood species: characterization using old knowledge. J. Wood Sci. 62, 194–202. https://doi.org/10.1007/s10086-015-1534-3

Kumagai, S., Fujita, K., Kameda, T., Yoshioka, T., 2016. Interactions of beech wood–polyethylene mixtures during co-pyrolysis. J. Anal. Appl. Pyrolysis 122, 531–540. https://doi.org/10.1016/j.jaap.2016.08.012

Kumagai, S., Fujita, K., Takahashi, Y., Nakai, Y., Kameda, T., Saito, Y., Yoshioka, T., 2019. Beech Wood Pyrolysis in Polyethylene Melt as a Means of Enhancing Levoglucosan and Methoxyphenol Production. Sci. Rep. 9, 1955. https://doi.org/10.1038/s41598-018-37146-w

Liu, X., 2021. 9.3 Stability of Alkyl Radicals.

Longley, C.J., Fung, D.P.C., 1993. Potential Applications and Markets for Biomass-Derived Levoglucosan, in: Bridgwater, A.V. (Ed.), Advances in Thermochemical Biomass Conversion. Springer Netherlands, Dordrecht, pp. 1484–1494. https://doi.org/10.1007/978-94-011-1336-6_120

Mohabeer, C., Abdelouahed, L., Marcotte, S., Taouk, B., 2017. Comparative analysis of pyrolytic liquid products of beech wood, flax shives and woody biomass components. J. Anal. Appl. Pyrolysis 127, 269–277. https://doi.org/10.1016/j.jaap.2017.07.025

Mohabeer, C., Reyes, L., Abdelouahed, L., Marcotte, S., Buvat, J.-C., Tidahy, L., Abi-Aad, E., Taouk, B., 2019a. Production of liquid bio-fuel from catalytic de-oxygenation: Pyrolysis of beech wood and flax shives. J. Fuel Chem. Technol. 47, 153–166. https://doi.org/10.1016/S1872-5813(19)30008-8

Mohabeer, C., Reyes, L., Abdelouahed, L., Marcotte, S., Taouk, B., 2019b. Investigating catalytic de-oxygenation of cellulose, xylan and lignin bio-oils using HZSM-5 and Fe-HZSM-5. J. Anal. Appl. Pyrolysis 137, 118–127. https://doi.org/10.1016/j.jaap.2018.11.016

Plastics - the Facts 2021 [WWW Document], 2021. URL https://www.plasticseurope.org/fr/resources/publications/1804-plastics-facts-2019 (accessed 5.15.20).

Uddin, M.A., Koizumi, K., Murata, K., Sakata, Y., 1997. Thermal and catalytic degradation of structurally different types of polyethylene into fuel oil. Polym. Degrad. Stab. 56, 37–44. https://doi.org/10.1016/S0141-3910(96)00191-7

U.S. Energy Information Administration (EIA) [WWW Document], 2022. URL https://www.eia.gov/energyexplained/us-energy-facts/ (accessed 2.3.21).

Wang, J., Abdelouahed, L., Xu, J., Brodu, N., Taouk, B., 2021. Catalytic Hydrodeoxygenation of Model Bio-oils Using HZSM-5 and Ni2P/HZM-5 Catalysts: Comprehension of Interaction. Chem. Eng. Technol. 44, 2126–2138. https://doi.org/10.1002/ceat.202100239

Yang, J., Rizkiana, J., Widayatno, W.B., Karnjanakom, S., Kaewpanha, M., Hao, X., Abudula, A., Guan, G., 2016. Fast co-pyrolysis of low density polyethylene and biomass residue for oil production. Energy Convers. Manag. 120, 422–429. https://doi.org/10.1016/j.enconman.2016.05.008

Zhao, C., Jiang, E., Chen, A., 2017. Volatile production from pyrolysis of cellulose, hemicellulose and lignin. J. Energy Inst. 90, 902–913. https://doi.org/10.1016/j.joei.2016.08.004

CHAPTER 4:

Upgrading pyrolytic oil by catalytic co-pyrolysis of beechwood and polystyrene

4. UPGRADING PYROLYTIC OIL BY CATALYTIC CO-PYROLYSIS OF BEECHWOOD AND POLYSTYRENE

4.1. Introduction

The previous chapter discussed the co-pyrolysis of BW and plastic without the use of a catalyst. It has been shown that PS showed the best performance with BW and the quality of the bio-oil could be further improved via the use of a catalyst. The catalytic pyrolysis of polystyrene was not extensively studied under metal-modified zeolites. Several researchers investigated the latter only over H-ZSM5, which recorded a further improvement in the quality of the bio-oil towards valuable aromatic products (Dorado et al., 2014; Hassan et al., 2016; Li et al., 2014). To propose a new catalyst modification in catalytic co-pyrolysis this study used both iron and nickel incorporated with H-ZSM-5. Iron-based zeolites prove to be active in the catalytic pyrolysis of biomass. Compared with a series of catalysts, it has been stated that 1.4 wt.% Fe conducted to the largest decrease in oxygen content from lignocellulosic to about 14 wt.% (Mohabeer et al., 2019). Furthermore, nickel-incorporated HZSM-5 was considered in the catalytic pyrolysis of biomass to increase aromatic yield while increasing the hydrothermal stability of the catalyst (Valle et al., 2010). The combination between Ni and the acids sites provides a reactive environment for improving aromatic formation (Ding et al., 2020). This chapter aims to present a detailed analysis of catalytic co-pyrolysis of polystyrene (PS) and beechwood (BW, *Fagus sylvatica*) as lignocellulosic-forestry residue, under iron and nickel modified zeolites (Fe/Ni-ZSM-5). The influence of different parameters such as metal loading of the catalyst, biomass/plastic ratio, and pyrolysis temperature on the quality and quantity of co-pyrolysis oil was investigated. At first, each feedstock (BW and PS) was used independently and as a mixture to produce a database reference of pyrolytic oils under the several catalysts synthesized. The best catalyst was chosen, then other parameters such as temperature and biomass to plastics ratio were investigated to improve the best pyrolytic oils.

4.2. Experimental Section

4.2.1. Materials

The virgin polystyrene (PS) was supplied by Goodfellow company (Huntingdon, UK) and beech wood was supplied by ETS Lignex Company (Patornay, France). PS was milled and sieved with a 2 mm average mesh, whereas the average particle size of beech wood was about 0.4 mm as supplied. The conventional HZSM-5 in its proton form (SiO_2/Al_2O_3 ratio of 38, specific surface area of about 250 m^2/g, and 5 nm of pore size) was acquired from ACS materials (Pasadena CA, USA) as 3 mm diameter pellets. The catalyst was milled and sieved to 0.6 mm and 1.18 mm particle size. The upper range ensures the proper stacking of adequate quantities of catalyst in the reactor whereas the lower range ensures gas flow without the risk of clogging and pressure buildup. Iron nitrate salt, ferric (III) nonahydrate ($Fe(NO_3)_3.9H_2O$), and nickel nitrate salt, Nickel (II) nitrate hexahydrate ($Ni(NO_3)_2.6H_2O$), were purchased from Panreac AppliChem (Darmstadt, Germany) and Alfa Aesar (Kandel, Germany), respectively.

The elemental analysis was obtained under oxidizing atmosphere by the combustion of the samples in the presence of tungstic anhydride at a high temperature for about 20 s using a CHN elemental analyzer Flash 2000 (Thermofisher Scientific). The calculation of the percentage of each element was analyzed by the "Eager 300" software (**Table 4.1**).

Thermogravimetric (TGA) measurements were achieved using an SDT/Q600-TA analyzer for the ultimate analysis (**Table 4.1**). The heating rate was 5 °C.min^{-1} under a nitrogen flow rate of 50 mL.$min^{-1}$and at atmospheric pressure.

Table 4.1. Ultimate and proximate analysis of used raw materials (wt.%).

Name	Ultimate analysis			Proximate analysis			
	% C	% H	% O	Moisture	Fixed Carbon	Volatile	Ash
PS	92.6	7.4	-	-	0.3	99.7	-
BW	47.4	6.1	46.5	5.7	17.5	75.9	0.9

4.2.2. Catalyst preparation

A set of Fe/Ni-modified ZSM-5 was prepared by impregnating around 50 g of ZSM-5. Iron and nickel nitrate salts were used to prepare three metal loading: 1.4 wt.% Fe/ZSM-5, 1.4 wt.% Ni/ZSM-5, and (1.4 wt.% Fe and 1.4 wt.% Ni) /ZSM-5. Then the weighed nitrates were dissolved in a 40 ml deionized water solution. Impregnation with 50 g of ZSM-5 was carried out using incipient wetness impregnation method. Impregnation was performed at ambient temperature for about 4 h. The 3 impregnated samples were then dried overnight at 105 °C. Finally, the obtained catalysts along with the parent ZSM-5 were calcinated at 550 °C for 4 h, with a heating rate of 2 °C.min^{-1} in an oxidative atmosphere (air). The catalysts were then noted as ZSM-5, 1.4 % Ni-ZSM-5, 1.4 % Fe-ZSM-5 and 1.4/1.4 % Fe/Ni-ZSM-5. For better understanding, a detailed schema concerning the catalyst preparation steps is described in **Fig. 4.1**.

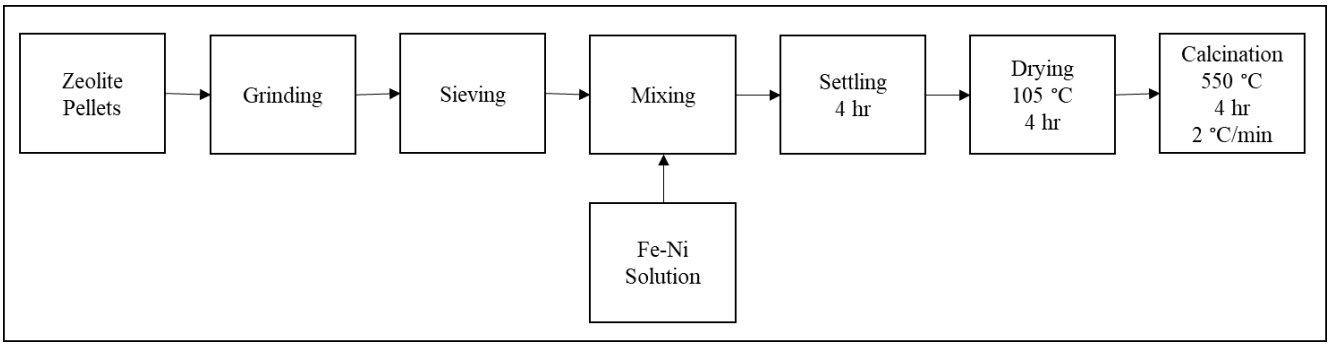

Fig. 4.1. Catalysts preparation procedure.

4.2.3. Catalysts characterization

The actual Fe and Ni contents were computed using inductively coupled plasma optical emission spectroscopy (ICP-OES) from Thermo-fisher Scientific (Waltham, USA) and further verified by X-ray fluorescence (XRF) technique using Thermo-fisher scientific Niton™ XL2. X-ray diffraction (XRD) patterns were recorded by a D5000 diffractometer at 40 kV and 40 mA with CuKα radiation (λ = 0.1542 nm) in the range of 2θ from 5 to 100 degrees. Particle size distribution was analyzed using Horiba Partica laser scattering LA-950V2 (Kyoto, Japan).

The textural properties, BET surface area, and pore size of the catalysts were characterized by N_2 adsorption-desorption at -196 °C on a Micromeritics Gemini VII (Georgia, USA). Before analysis, the samples were degassed overnight at 200 °C. Nitrogen adsorption-desorption isotherms were obtained over a wide range of relative pressure (P/P_0) from 0.01 to 0.99.

4.2.4. Experimental methods

4.2.4.1. Pyrolysis experimental setup

The pyrolysis reactions were performed in a semi-continuous tubular reactor with a quartz tube (ϕ= 50 mm, L=1050 mm) inserted horizontally (**Fig. 4.2**) (Pyrolysis zone). The catalyst was placed downstream in the narrower part of the reactor. The catalyst bed was 1 cm in length and 2.5 cm in diameter and weighed around 3.7 g (5 cm^3 volume catalysis zone). To insert the samples, a stainless-steel sample carrier "spoon" was placed and pushed at the inlet of the reactor, while the other side was connected to a flask and a condenser for liquid collection. The non-condensable gases were also collected using a Tedlar gas bag. At first, the catalyst and BW were dried in an oven at 105 °C for 2 h to eliminate excessive moisture. Then, a typical 3 g sample of plastic and/or biomass was loaded into the sample carrier (1.2:1 catalyst-to-feed ratio). After the required temperature is attained, the sample carrier was pushed inside the heating zone to achieve isothermal conditions. Liquid oil was recovered from the condenser and the flask using acetone as solvent. For a typical trial, the experiment was repeated 3 times with a maximum error not to exceed 1 % both for temperature and experimental results. All the experimental conditions done with a catalyst were also done without a catalyst for comparison purposes. Ultimately one catalyst (Fe/Ni-ZSM-5) was chosen to carry on feedstock ratio and temperature analysis. This catalyst was chosen since it gave the best results during catalytic co-pyrolysis. The performed experiments are summarized in **Table 4.2.**

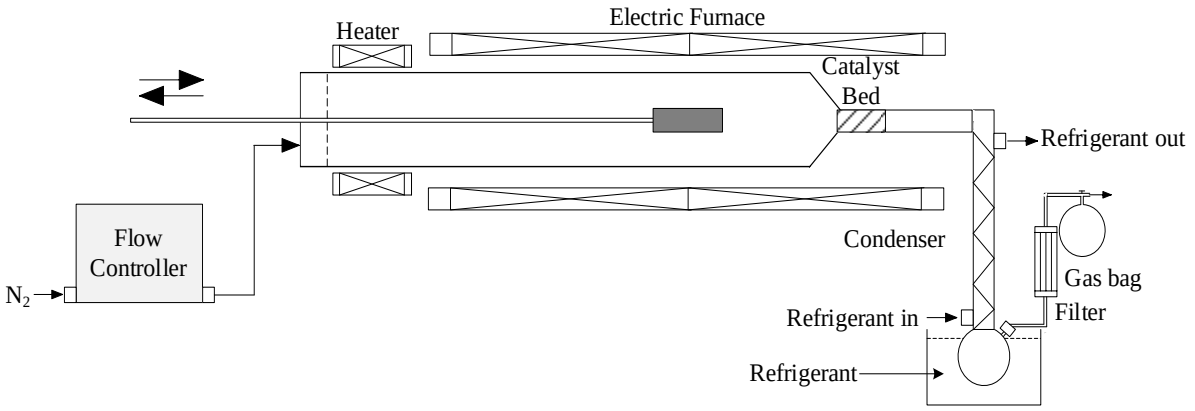

Fig. 4.2. Schematic setup of the tubular reactor.

Table 4.2. Summary of the performed experiments.

Reaction	Catalyst	BW-PS percentage (wt.%)	Temperature (°C)
Biomass pyrolysis	No catalyst	100-0	500
	ZSM-5		
	Fe-ZSM-5		
	Fe/Ni-ZSM-5		
	Ni-ZSM-5		
Plastic pyrolysis	No catalyst	0-100	500
	ZSM-5		
	Fe-ZSM-5		
	Fe/Ni-ZSM-5		
	Ni-ZSM-5		
Co-pyrolysis	No catalyst	25-50-75	500
	No catalyst	50	450-500-550-600
	ZSM-5	50	500
	Fe-ZSM-5	50	
	Fe/Ni-ZSM-5	25-50-75	
	Ni-ZSM-5	50	
	Fe/Ni-ZSM-5	50	450-500-550-600

4.2.4.2. Liquid oil and non-condensable gas analysis

The technique used for the liquid and gas product analysis has been already detailed previously (**Chapter 2, sections 2.2.2.2, 2.2.2.3, 2.2.2.4, 2.2.2.5**)

4.2.4.3. Synergy between biomass and plastic

The technique used for synergy analysis has been already detailed previously (**Chapter 3, section 3.2.2.3)**

4.3. Results and discussion

4.3.1. Catalyst characterization

The chemical and textural properties of the synthesized catalyst are summarized in **Table 4.3.** It is noticed that there are no major variations in the SiO_2/Al_2O_3 ratios due to the mild modifications and low metal loading. The actual Fe and Ni loading were slightly close to the planned percentages.

Table 4.3. Characterization of the parent, Fe-, Fe/Ni-, Ni- modified ZSM-5 zeolites.

	ZSM-5	Fe-ZSM-5	Fe/Ni-ZSM-5	Ni-ZSM-5
SiO_2/Al_2O_3	38.0	38.4	38.9	38.5
Fe (wt.%)[a]	0.04	1.46	1.32	0.04
Ni (wt.%) [a]	-	-	1.22	1.21
BET surface area (m^2/g)[b]	282.0	299.1	284.9	274.0
Micropore surface area (m^2/g)[c]	109.5	135.5	123.8	126.8
External surface area (m^2/g)[c]	172.5	163.6	161.1	147.3
Specific pore volume (cm^3/g)[c]	0.24	0.24	0.23	0.22
Micropore volume (cm^3/g)[c]	0.05	0.06	0.06	0.06

[a] Actual Fe and Ni loading measured by ICP-OES and XRF

[b] From N_2 adsorption/desorption (BET)

[c] From N_2 adsorption/desorption (tplot)

The BET surface area attained an average value between 274-299 m^2/g with no significant variation after impregnation. The elevated surface area of all catalysts could have a good impact on the performance of the catalyst. In most cases, the higher the surface area, the better the activity. It has been shown that after impregnation, the surface area would be reduced (Yao et al., 2015). It was not the case in this study due to the low metal loading, thus keeping the surface activity of the zeolites high. This observation was in accordance with the work of Li et al. (2020), where no significant change in BET surface area was observed for a Fe/ZSM-5 content of around 3 wt.%. N_2 adsorption-desorption isotherms of the used catalysts are illustrated in **Fig. 4.3**. The adsorption-desorption isotherms observed for the catalysts exhibited a hysteresis loop corresponding to a type IV isotherm (Thommes et al., 2015). However, the

isotherms showed a broad loop at p/p^0=0.5–1.0, which can indicate the co-existence of both micropores and mesopores. This hypothesis is further verified by **Fig. 4.4 (a)**, which describes the distribution of the cumulative pore volume relative to pore size. All catalysts showed similar behavior so only Fe/Ni-ZSM-5 figure is illustrated. There was no variation in the specific pore volume of the modified ZSM-5 relative to the parent after impregnation. The pore volume was approximately 0.23 m^2/g. This could suggest that Fe and Ni were deposited mainly on the edges and external surface area of ZSM-5 (Botas et al., 2014). The derivative of the pore volume relative to pore width was further investigated in **Fig. 4.4 (b)**. The curve showed 2 maximum refereeing to around 2 nm and 6 nm, further verifying the previous deduction of both micro and mesopores of the prepared ZSM-5.

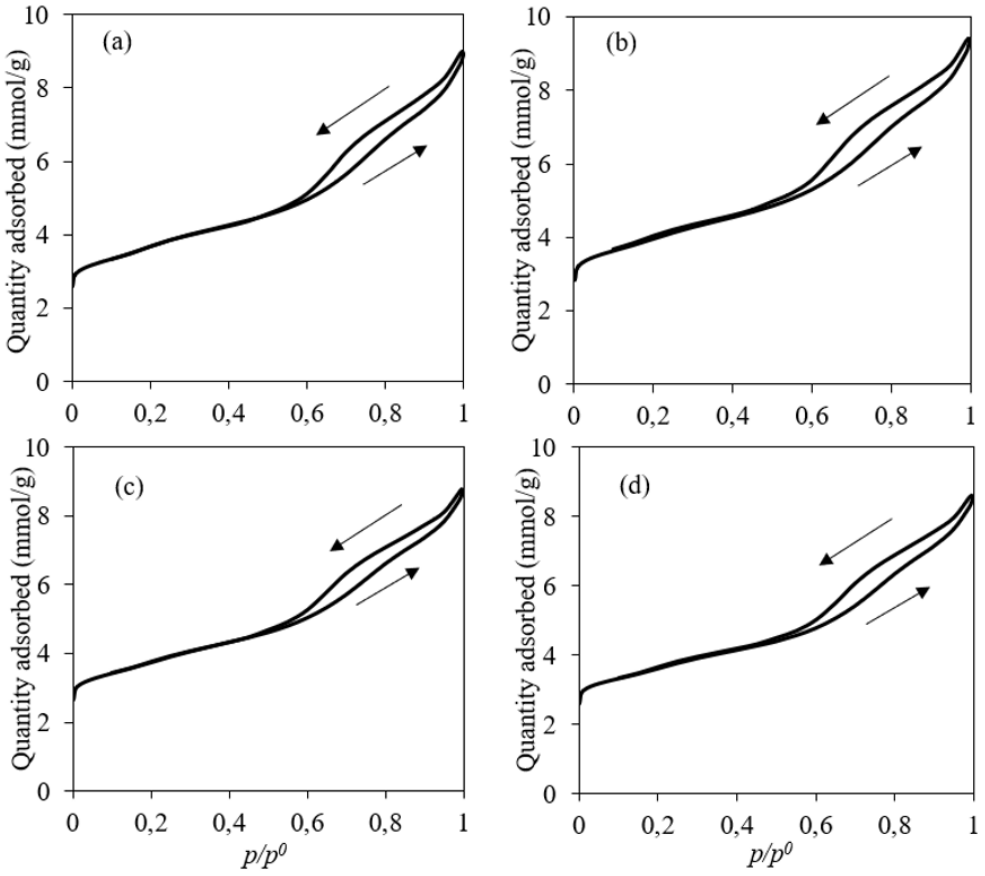

Fig. 4.3. N_2 adsorption/desorption isotherms. (a): ZSM-5; (b): Fe-ZSM-5; (c): Fe/Ni-ZSM-5; (d): Ni-ZSM-5

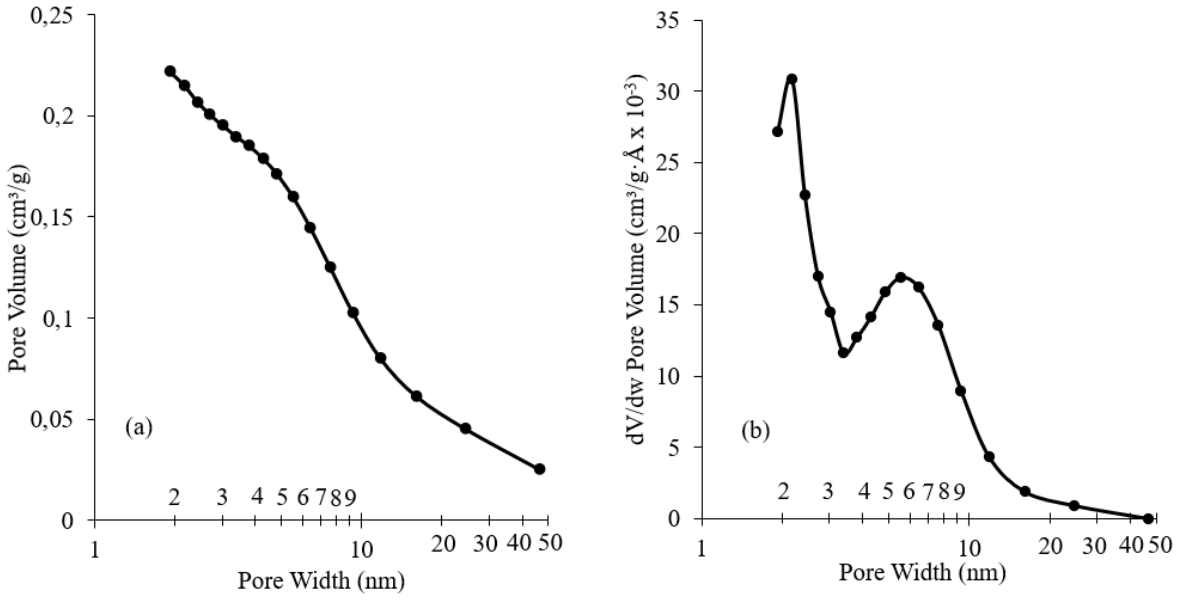

Fig. 4.4. Barrett–Joyner–Halenda (BJH) pore size distributions of Fe/Ni-ZSM-5. (a): Cumulative pore volume, (b): Differential pore volume

The size population distribution followed a monomodal distribution with a mean size diameter of about 1.3 mm ± 0.4 by granulometric analysis as shown in **Fig. 4.5**. As for the XRD analysis, the patterns of the parent ZSM-5 showed a typical MFI zeolite structure as shown in **Fig. 4.6**. The results showed that the modification with Fe and Ni did not affect the framework structure of ZSM-5. All samples exhibited peaks at 2θ 9° and 27° with no additional peaks after modification. Furthermore, the intensity of the diffraction peaks was reduced slightly after impregnation implying a slight reduction in crystallinity. This could be because during impregnation some chemical changes may occur in the pores of the catalyst, especially after chemical impregnation followed by calcination at 550 °C (Zhu et al., 2019).

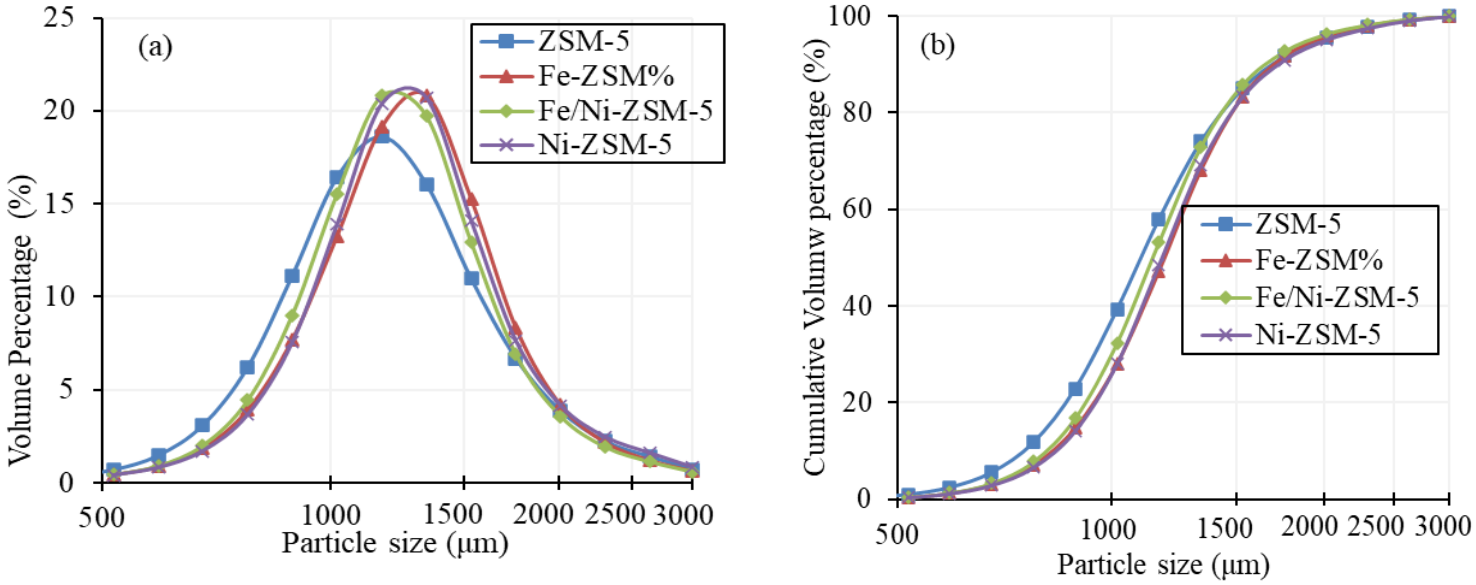

Fig. 4.5. (a): Particle size distribution of catalyst used; (b): Cumulative particle size distribution of the catalyst used.

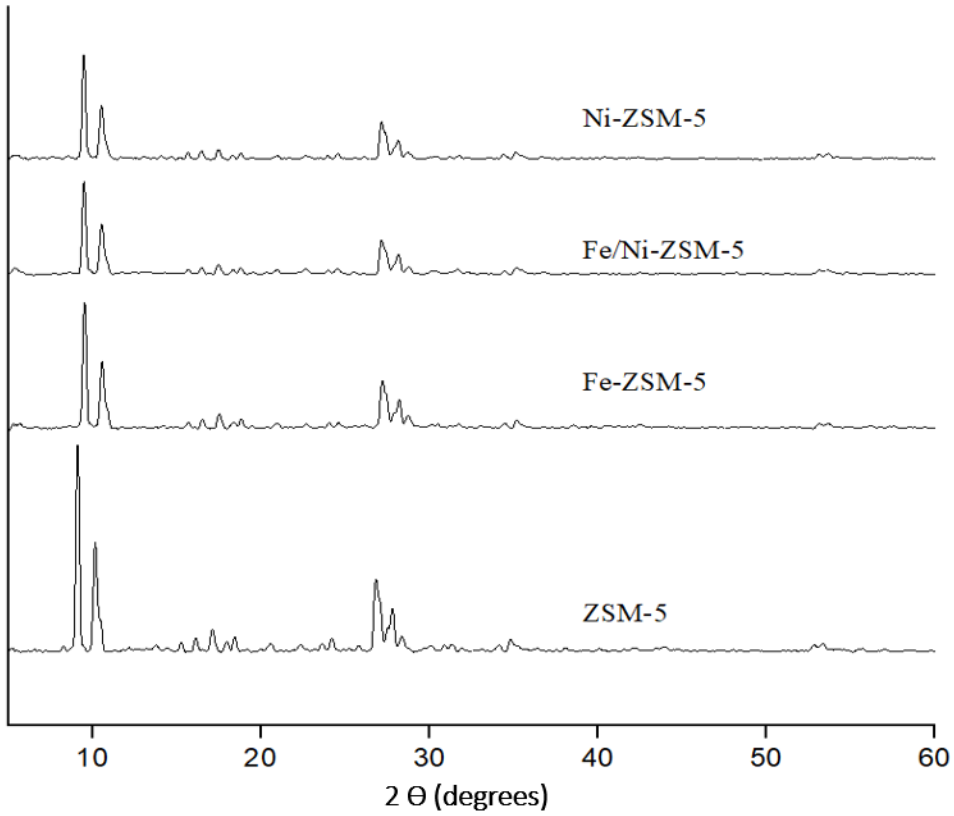

Fig. 4.6. X-Ray diffractograms of the parent, Fe-, Fe/Ni-, Ni- modified ZSM-5 zeolites.

4.3.2. Catalytic pyrolysis of individual biomass and plastic

At first, GC-MS analysis of various pyrolytic oils was carried out to identify the present compounds in each pyrolytic oil obtained at 500 °C. The analysis was conducted for BW and PS alone and as a mixture without and with every synthesized catalyst. For instance, around 120 and 100 compounds were identified for PS and BW, respectively. The compounds identified for PS with and without a catalyst were similar and all the compounds were aromatic hydrocarbons. However, for BW, the majority of the compounds were oxygenated compounds, yet after catalysis, new aromatic hydrocarbons were further identified as benzene, toluene, xylene, styrene, and indene.

The identified compounds were grouped into the most relevant organic families divided between oxygenated and hydrocarbon compounds to better visualize further analysis (Jaafar et al., 2022; Mohabeer et al., 2017). The families and major products for calibration are illustrated in **Table 3.3.**

Table 4.4. Chemical families of the pyrolytic oil with their corresponding reference compound.

RT (min) *	Chemical family	Reference compound
6.63	Furans	Furan
11.15	Carboxylic acids	Acetic acid
12.13	Aromatics	Toluene
18.39	Esters & Ethers	Allyl butyrate
19.52	Aldehydes	Furfural
21.63	Ketones	2-methyl-2-cyclopenten-1-one
31.82	Phenols	p-cresol
40.76	PAH	Bibenzyl
41.74	Guaiacols	4-methylcatechol
42.74	Nitrogenates	Benzamide
49.58	Carbohydrates	Levoglucosan

* GC-FID retention time

Beech wood pyrolysis produces an oil rich in acids, ketones, and carbohydrates (levoglucosan). The distribution can be observed in **Fig. 3.2 (a)**. Carboxylic acids constituted around 35 wt.% followed by carbohydrates and ketones with respective percentages of 17 wt.% and 15 wt.%. It was considered that BW was chemically composed of 42 wt.% cellulose, 37 wt.%

hemicelluloses, and 19 wt.% lignin (Gucho et al., 2015). This would explain the domination of carbohydrates and acids on the liquid bio-oil since they are the dominant species in the independent pyrolysis of cellulose and hemicellulose, respectively; whereas phenols and guaiacols are derived from lignin (Zhao et al., 2017). As it can be seen, BW pyrolysis has no hydrocarbon aromatic production, thus leaving the oil with high oxygen content and low LHV of around 41 wt.% and 18 MJ/kg, respectively, as shown in **Table 4.5. Fig. 3.2 (b)** and **Table** 4.5 show the variation of the properties of the bio-oil after catalysis. In contrast to BW pyrolysis, catalytic pyrolysis showed the formation of aromatic compounds. The total aromatics were around 7 wt.% for the catalytic pyrolysis under the parent HZSM-5. This production of aromatics mainly came at the expense of levoglucosan (derived from cellulose) without any major variation of the other compounds. This can be explained by the transformation of the latter compound into aromatic compounds via catalytic decarbonylation, decarboxylation, dehydration, oligomerization, and isomerization on the surface of the catalysts as explained in **Fig. 4.8** (R. Carlson et al., 2011). On the other hand, phenolic compounds and guaiacols seemed to increase after catalysis. The reason for that lies in the aromatic selectivity and pore structure of ZSM-5. Phenols and guaiacols have a similar structure as monoaromatic compounds, so an increase in those compounds can be due to the transformation of aldehydes, ketones, carbohydrates, and furans into oxygenated aromatics in the pores of the catalyst without the deoxygenation step. The LHV and oxygen content varied slightly to be around 20 MJ/kg and 36 wt.% respectively. This variation can be due to catalytic oxygen elimination mainly into CO and CO_2 represented by an increase in gas yield that is mainly CO, CH_4, and CO_2.

The effect of the different metal loading on the performance of catalytic pyrolysis of BW was investigated and the results are shown in **Table 4.5.** The parent HZSM-5 showed the best selectivity towards aromatics and PAH compared to other modifications. This suggests that the modification by metals on the original zeolite inhibits aromatic formation (Mohabeer et al.,

2019), yet the inhibition is minimal due to low metal loading. The char yield was not affected since it was produced before catalysis, also coking was somehow similar.

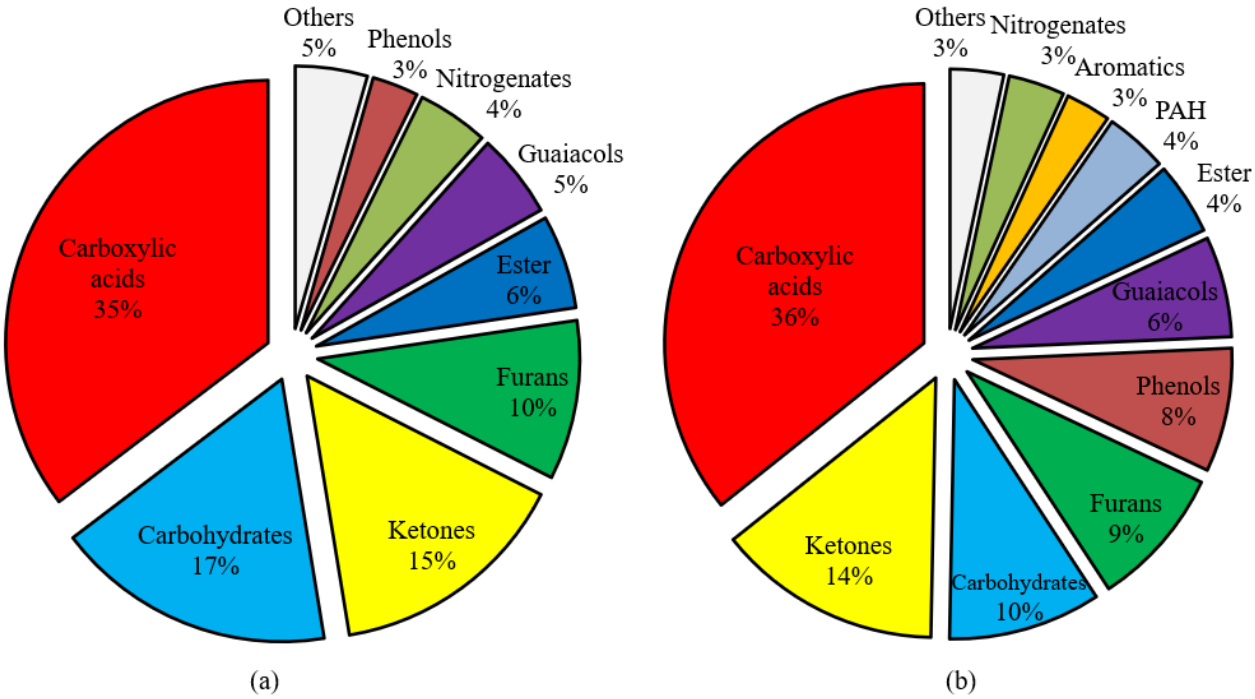

Fig. 4.7. Chemical families in BW bio-oil at 500 ˚C. (a): Without catalyst; (b): HZSM-5.

Table 4.5. Catalyst effect on chemical family distribution and properties of BW bio-oil.

	Percentages (wt.%)				
	no catalyst	ZSM-5	Fe-ZSM-5	Fe/Ni-ZSM-5	Ni-ZSM-5
Carboxylic acids	35.3	35.7	33.5	36.1	35.3
Ester	5.8	4.5	4.4	4.7	4.4
Ether	0.7	1.0	0.9	0.9	0.9
Nitrogenates	4.4	3.5	3.8	4.3	4.1
Ketones	15.0	14.0	14.0	13.8	14.7
Furans	9.8	8.8	8.5	8.8	9.6
Aldehydes	2.4	0.5	0.5	0.7	0.8
Carbohydrates	17.3	9.5	11.7	12.5	12.4
Phenols	2.8	7.7	8.0	5.0	3.9
Guaiacols	5.2	6.3	7.0	6.6	6.9
Aromatics	-	2.8	2.6	2.6	2.7
PAH	-	3.9	3.3	2.3	2.1
Oxygen content	41.3	36.4	37.3	39.0	38.9
LHV (MJ/kg)	18.4	20.4	20.3	19.4	19.4
Liquid yield	70.0	56.2	56.0	47.9	56.3
Char yield	20.0	21.3	20.7	21.3	20.0
Coke	-	3.0	3.3	3.3	2.3
Gaz yield	15.0	19.5	20.0	27.5	21.4

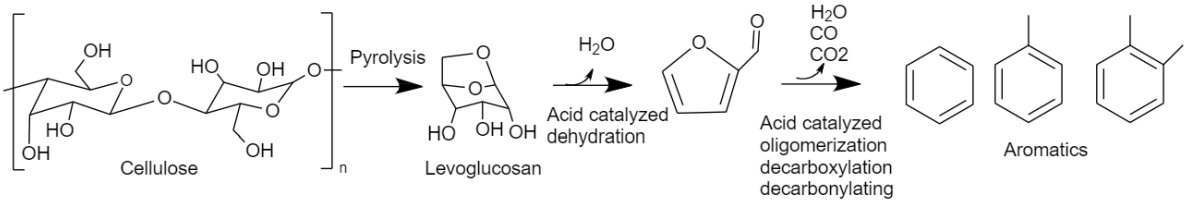

Fig. 4.8. Reaction pathway of catalytic pyrolysis of biomass over ZSM-5 at 400-600 °C, adapted from (R. Carlson et al., 2011).

As for the individual catalytic pyrolysis of polystyrene (**Table 4.6**), the effect was like a typical cracking reaction. At first, the pyrolytic oil was mainly composed of monoaromatic hydrocarbons of about 77 wt.%, mainly the styrene monomer. The heating value was elevated (about 40 MJ/kg) with no oxygen due to the hydro-carbonaceous nature of polystyrene. The liquid yield was almost total with no gases nor char, which was confirmed in a previous study (Jaafar et al., 2022). On the other hand, the catalytic effect on polystyrene liquid oil enhanced cracking and dissociation reaction, thus the lighter hydrocarbon was higher for all 4 catalysts with an advantage to the parent zeolite. This reinforces the former deduction that the selectivity of the parent zeolites towards aromatics was reduced through impregnation. However, PAH was transformed into lighter aromatics yet not gases. The gas yield was still minimal, this would further support the high selectivity of zeolites toward aromatics (Mihalcik et al., 2011). Ultimately, the reduction in liquid yield was at the expense of coke.

Table 4.6. Catalyst effect on chemical family distribution and properties on PS pyrolytic oil.

	Percentages (wt.%)				
	no catalyst	ZSM-5	Fe-ZSM-5	Fe/Ni-ZSM-5	Ni-ZSM-5
Aromatics	76.7	82.2	77.7	81.7	77.8
PAH	23.3	17.8	22.3	18.3	22.2
LHV (MJ/kg)	40.6	40.6	40.0	40.6	40.5
Liquid yield	99.9	96.2	96.1	96.6	96.3
Char yield	0.0	0.0	0.0	0.0	0.0
Coke	0.0	3.3	3.1	3.0	3.3
Gaz yield	0.1	0.5	0.8	0.4	0.4

4.3.3. Catalytic co-pyrolysis of biomass and plastic

The catalytic co-pyrolysis of biomass and plastic was investigated as shown in **Fig. 4.9**. The effect of metal loading and the distribution of main properties were also studied. At first, the non-catalytic co-pyrolysis of biomass and plastics yielded an oil rich in aromatics with low oxygen content and high heating value of around 8 wt.% and 37 MJ/kg, respectively. However, the oxygen content should be further reduced to have the potential to be used as fuel directly. On the other hand, despite the oxygen content, the total acids and oxygenated compounds could cause several problems such as corrosion and chemical instability. For instance, biomass bio-oil exhibits a pH value of around 2-3, the value differs between each type of biomass but in general, the oil is highly acidic (Qi, 2007). Although the percentage of acids is reduced significantly yet the pH would not reach neutral levels.

After catalysis, for all the prepared catalysts, the liquid yield was significantly reduced from 85 wt.% to 70 wt.% at the expense of coking and gas production, which is typical for any catalytic cracking. On the other hand, the polycyclic aromatic hydrocarbons (PAH) increased after catalysis. This increase was followed in general by a decrease in single aromatic and other oxygenated compounds. This increase in PAH can be supported by the mechanism shown in **Fig. 4.10**. The reaction pathway was proposed between PS and biomass components (cellulose) in the presence of an HZSM-5 catalyst in a temperature range of 300-650 °C (Cheng and Huber, 2012; Dorado et al., 2015). Naphthalene formation and other PAH could be obtained through Diels-Alder reactions of monoaromatics and furans (originated from levoglucosan) through a series of alkylation reactions (Cheng and Huber, 2012). The mechanism suggests the reaction pathway of cellulose with PS, which is considered one of the main constituents of BW.

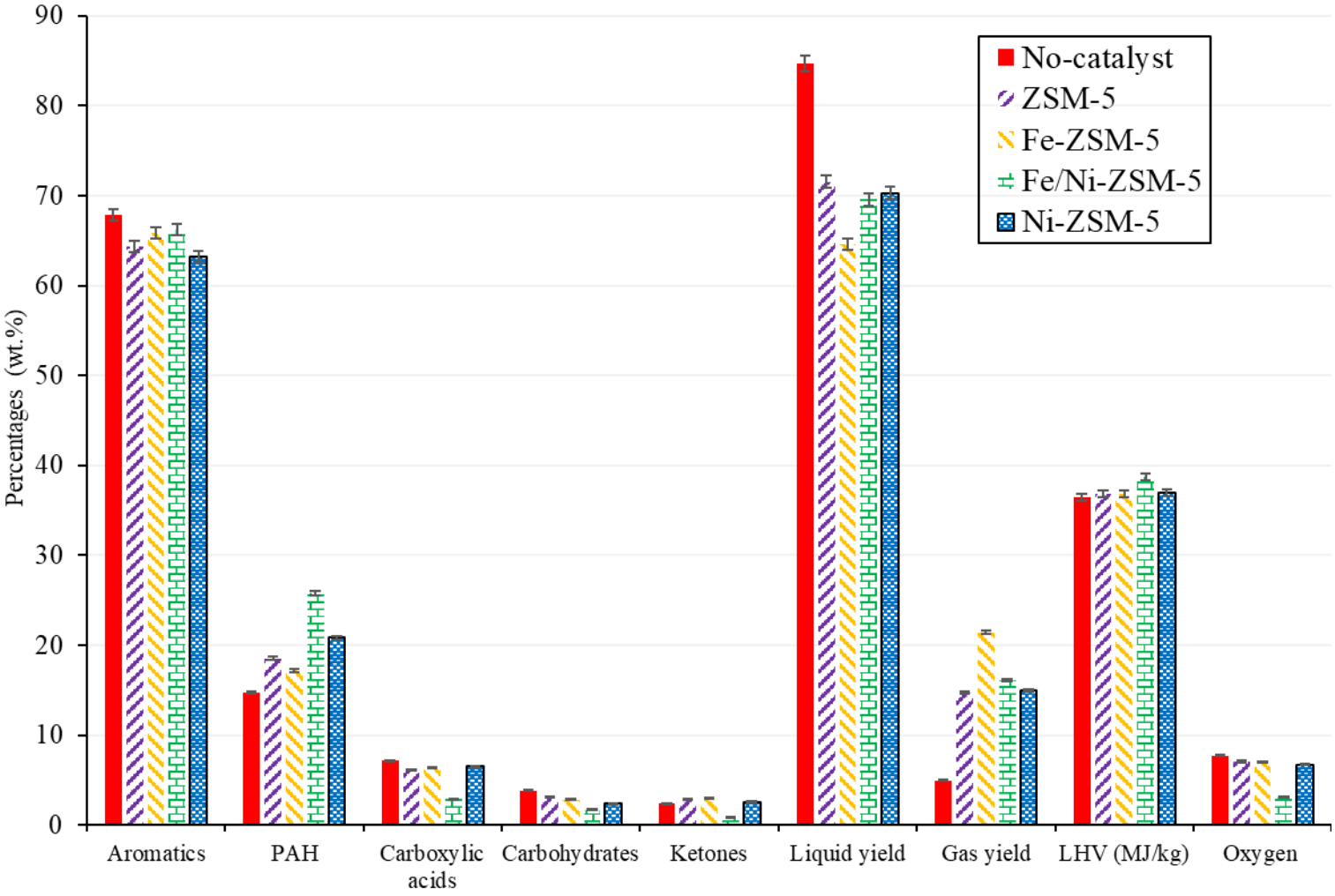

Fig. 4.9. Comparison of the catalyst used relative to the major families and main properties of BW-PS (50-50) liquid oil (wt.%) 500 °C.

Regarding the metal loading of the catalyst, all the metal loading yielded approximately the same outcome, except for the Fe/Ni-ZSM-5, regarding de-oxygenation. For instance, the latter catalyst exhibited a slight reduction in oxygen with no major change within the compositional analysis of the pyrolytic oil. The co-impregnation of iron and nickel onto the surface of the catalyst had a great effect on the oxygen content of the pyrolytic oil during co-pyrolysis. The oxygen content reached very low values of around 3 wt.% with a decrease in acids and other oxygenated compounds. The reduction in oxygen content was close to that of Dyer et al., 2021 who studied the catalytic co-pyrolysis of waste wood with polystyrene under HZSM-5. The oxygenated compounds reached 2 % relative to the total ion chromatography

peak. The value is low but it is not accurate for comparison since there was no calibration to get the real value. The effect of Fe/Ni-ZSM-5 catalyst was seen in co-pyrolysis but not in the pyrolysis of BW, which would imply that the catalyst further reinforces the synergy between PS and BW. The hydrogen supply from the plastics was best utilized for this catalyst. This could be due to the interaction between both metals (Fe and Ni) and the higher metal loading compared to the other catalysts.

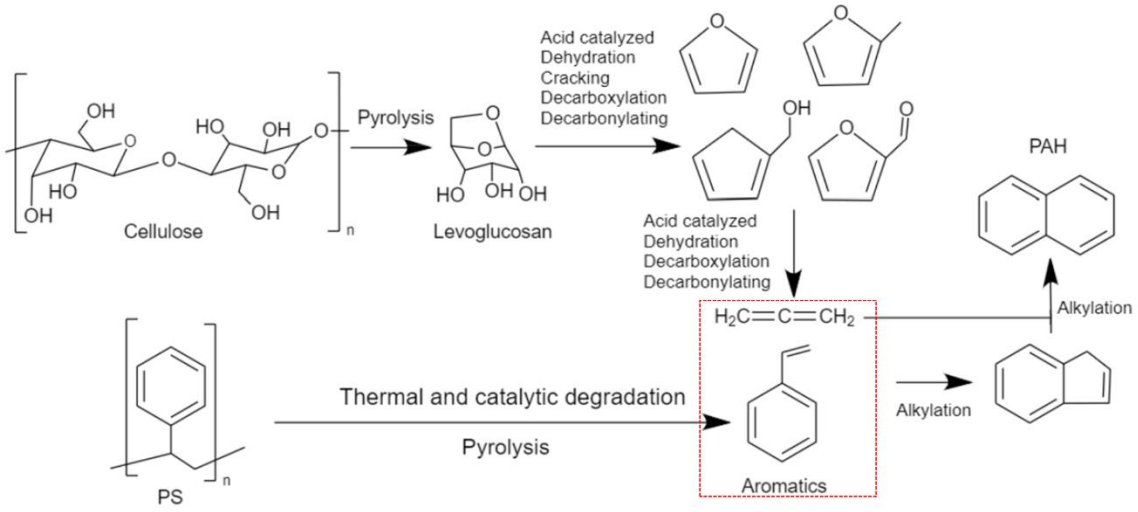

Fig. 4.10. Reaction pathway of catalytic co-pyrolysis of polystyrene and biomass over ZSM-5, adapted from (Cheng and Huber, 2012; Dorado et al., 2015).

4.3.4. Catalytic co-pyrolysis over Fe/Ni-ZSM-5

To delve deeper into the quality of the bio-oil produced, several parameter tests were done on the pyrolytic oil derived from Fe/Ni-ZSM-5 catalyst. The oil was mainly composed of aromatics of around 92 wt.%, of which 66 wt.% are monoaromatics and 26 wt.% are PAH **(Fig. 4.11)**. The oil exhibited very low acid and other oxygenated compound content. For this reason, this type of oil could be used as a possible substitute for petroleum fuel due to its high heating value and low oxygen and acids content. However, several parameters should be investigated before recommending the oil for automotive fuels (gasoline and diesel) as octane and cetane number, viscosity, density, distillation profile, etc. (Aitani, 2004). These parameters could not be calculated in this study since a solvent was used to collect the oil; the derived oil should be pure

to be able to calculate the latter properties. Yet, regarding the octane number, the oil should have a high octane number due to the dominance of aromatics (Jaafar et al., 2022). Nevertheless, PAH (26 wt.%) should be removed so that the oil could be used as gasoline or as a gasoline blend, otherwise it could be burned directly as heating fuel.

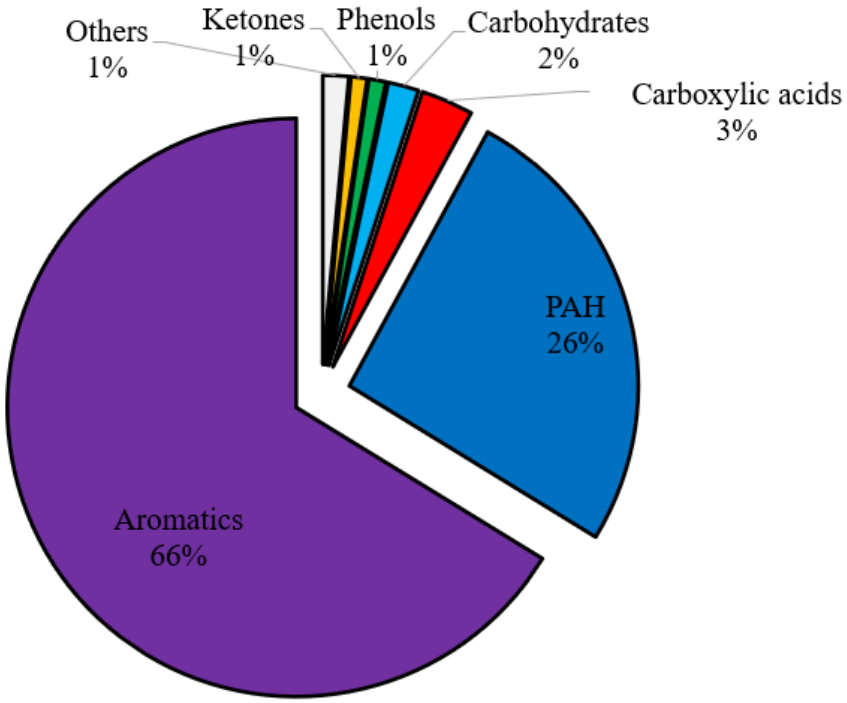

Fig. 4.11. Chemical families of BW-PS 50-50 (Fe/Ni-ZSM-5) liquid oil at 500 °C.

Effect of BW/PS ratio on synergy and chemical families

The effect of the BW/PS ratio on the family's distribution is shown in **Fig. 4.12.** The synergetic effect was also discussed by representing the experimental and theoretical values of each family computed by ***Eq. 3.1***. The theoretical values vary relative to each BW percentage in the feed. The synergy gave a positive effect by increasing aromatics and reducing the oxygenated compounds. For instance, for the total aromatic percentages, the effect of adding plastics improved the yield by around 24 wt.% for the 50-50 mix. This effect was better observed for higher BW content. The synergy showed an increasing trend as BW content increased. For example, the difference between the theoretical and experimental percentages of

total aromatics was around 10 wt.% for the 25-75 BW/PS mix compared with 34 wt.% for the 75-25 BW/PS mix. Therefore, this was good to conclude since the objective of catalytic co-pyrolysis is to enhance the properties of bio-oil from biomass pyrolysis, so the more one uses a natural, renewable, reliable, and carbon-neutral source, the greater the advantage towards the environment.

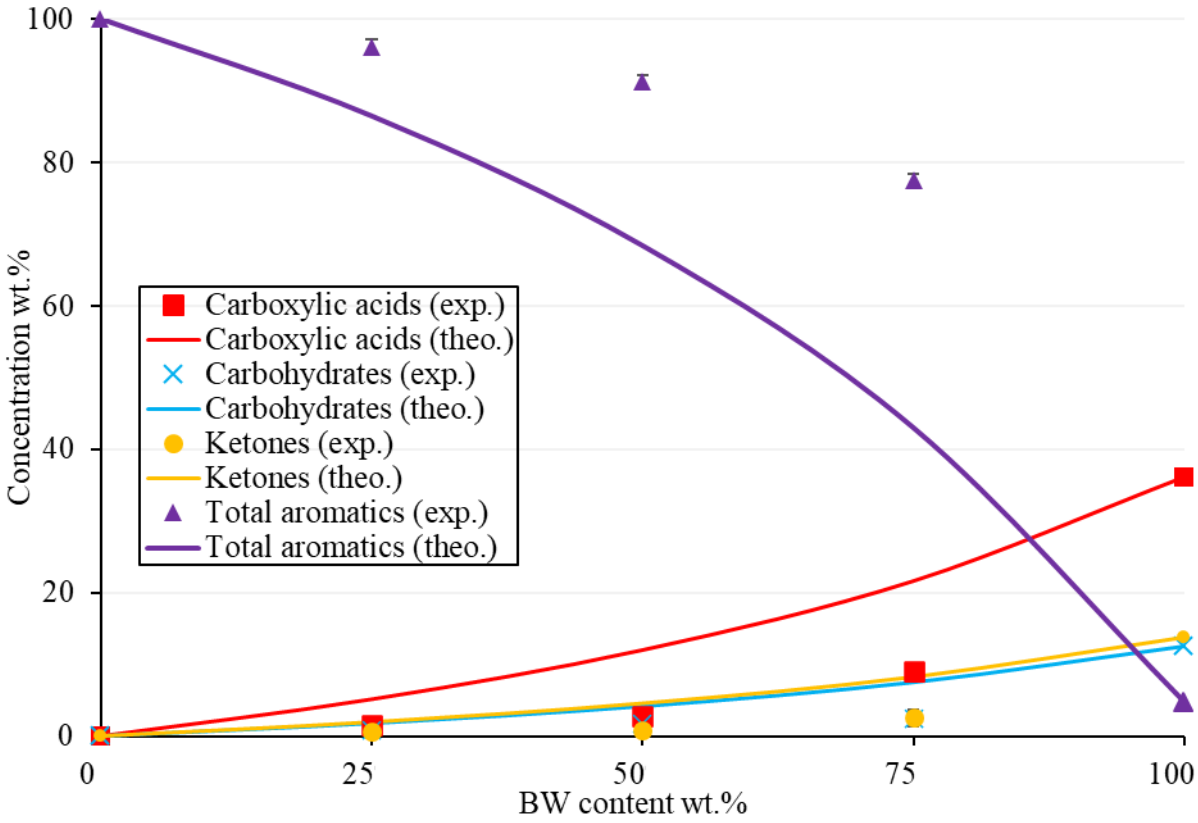

Fig. 4.12. Distribution of the major families of BW-PS (Fe/Ni-ZSM-5) liquid oil as experimental and theoretical concentrations relative to BW content at 500 °C (wt.%)

LHV and oxygen content

The synergetic and catalytic effects on the LHV and oxygen content were further discussed in **Fig. 4.13** and **Table 4.7**. The synergetic effect was also evident regarding the calorific value of liquid oil. The latter conclusion was further reassured; the synergy was greater realized at high BW content. On the other hand, compared to co-pyrolysis without catalyst, the trend showed that the LHV and oxygen content of the liquid oil for the 50-50 mix without catalyst was like that of 75-25 mix with catalyst and the 25-75 mix without catalyst was like

that of the 50-50 mix with catalyst. For instance, the LHV and oxygen content were around 37 MJ/Kg and 8 wt.%, respectively for the 50-50 mix without catalyst, which was similar compared to 36 MJ/Kg and 9 wt.% for the 75-25 mix with catalyst. Hence, the addition of a catalyst mimicked the effect of increasing hydrocarbon feed to the mixture without any significant change in the properties of the liquid oil. Referring to **Table 4.7**, the percentage increase in LHV from BW virgin bio-oil attained its maximum for the catalytic pyrolysis with Fe/Ni-ZSM-5 for the 50-50 mix. The latter increase was about 111 %, accompanied by deoxygenation of around 92 %.

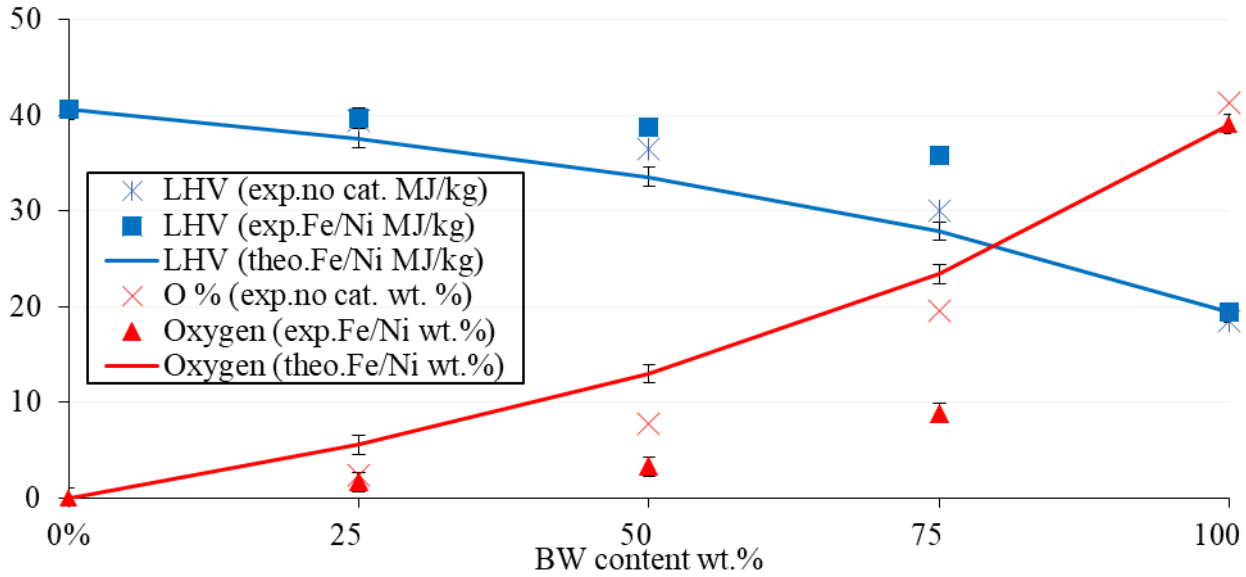

Fig. 4.13. The evolution of LHV (MJ/kg) and O % (wt.%) in BW-PS (Fe/Ni-ZSM-5) liquid oil as per BW content at 500 °C.

The derived liquid oils were then compared to conventional petroleum fuels to study the possible end-use of each product. The most promising liquid fuel was from the catalytic co-pyrolysis of 2 different feedstock proportions 50-50 and 75-50. The first showed a further decrease in oxygen content making the oil more suitable to be used as automotive fuel. However due to the high percentages of aromatics, the oil cannot be used as diesel oil so it should be fractionated to match the gasoline carbon range, then it could be used with some minor modifications (Kamrin, 2014). The latter pathway equally favors PS and BW consumption as feedstock, yet to fully benefit from the word's forestry residue, the second option is still

feasible. Furthermore, the bigger the use of a renewable carbon-neutral energy source such as BW, the more sustainable and environmental the process becomes. The oxygen content is higher compared to that of the 50-50 mix, still, it could be used in furnaces for burning or to be blended with gasoline with adequate proportions.

Table 4.7. Comparison within the pyrolytic oils and between conventional fuels.

Name	LHV (MJ/kg)	LHV change (%)	O % (wt.%)	O % change (%)	Ref.
BW (No cat.)	18.4	n.a	41.3	n.a	This work
BW (HZSM-5)	20.4	+10.9 [a]	36.4	− 11.9 [a]	
BW-PS 50-50 (No cat.)	36.5	+ 98.4	7.8	− 81.1	
BW-PS 50-50 (Fe/Ni-ZSM-5)	38.8	+ 110.9	3.2	− 92.3	
BW-PS 75-25 (No cat.)	30.0	+ 63.0	19.6	− 52.5	
BW-PS 75-25 (Fe/Ni-ZSM-5)	35.8	+ 94.6	8.8	− 78.7	
PS	40.6	n.a	-	n.a	
Gasoline	43.4-46.5		~ 2.7		(Anuar Sharuddin et al., 2017; Imam and Capareda, 2012; "U.S. energy facts explained," 2022)
Kerosene	43.0-46.2		n.a.		
Diesel	42.8-45.8		~ 1.8		

[a] Catalyst and/or synergetic improvement on the LHV/O% relative to BW bio-oil

Effect of temperature on liquid oil properties

Ultimately, a temperature analysis was carried out to specify the optimum operating temperature. The main composition and properties of the 50-50 catalytic co-pyrolysis oil relative to temperature are summarized in **Table 4.8.** Regarding the product yield, liquid and char yield decreased as per temperature, accompanied by an increase in the gaseous yield. This behavior is typical for cracking reactions. Nevertheless, coking on the catalyst surface increased with temperature, and the oxygen content also increased, especially from the temperature form

550 °C and above. This suggests that the catalyst deactivated and lost its de-oxygenation potential at higher temperatures (≥ 550 °C). This behavior could be attributed to the catalyst's performance. The catalyst was calcined at a temperature of 550 °C, therefore it is expected to have a decrease in performance at higher temperatures. The same behavior was reported by Zhang et al.(2014) for the co-pyrolysis of pine sawdust and polyethylene. They reported lower catalytic performance when co-pyrolysis was conducted at a temperature of 650 °C, above the calcination temperature of 600 °C. Ultimately, the optimum operating temperature for the catalytic co-pyrolysis would be 500 °C, where the liquid oil had the best quality, and the liquid yield was relatively high.

Table 4.8. Evolution of BW-PS 50-50 (Fe/Ni-ZSM-5**)** liquid oil composition and properties relative to temperature (wt.%).

Chemical Families	Operating Temperature (°C) ±5 °C			
	450	500	550	600
Carboxylic acids	3.6	2.9	4.1	5.6
Ketones	1.3	0.9	1.5	2.1
Furans	0.7	0.8	1.2	1.5
Carbohydrates	1.3	1.7	2.7	3.0
Aromatics	68.9	66.2	68.4	74.0
PAH	22.5	25.8	20.3	12.2
Gas yield	14.5	16.1	17.9	23.0
Liquid yield	70.2	69.9	66.1	61.0
Char yield	12.7	10.3	10.0	9.0
Coke	2.7	3.6	6.0	7.0
O %	3.6	3.2	4.7	6.0
LHV*****	38.7	38.8	38.0	37.5

***** Lower heating value (MJ/kg)

4.4. Conclusion

The catalytic co-pyrolysis of beech wood and polystyrene creates a good opportunity for the valorization of a widely known forestry product and the reduction of an environmentally hazardous plastic such as polystyrene. After deeper analysis, the derived oil mainly constituted about 92 wt.% of aromatics for the 1:1 mixture of beechwood and polystyrene with a remarkable high heating value of around 39 MJ/kg compared to 18 MJ/kg for beechwood bio-oil.

The liquid oil experienced a great reduction in the oxygen content from 41 wt.% (beechwood) to just 3 wt.% for the polystyrene-beechwood 50-50 mixture, which is a great reduction of about 92 %.

The catalytic and synergetic effects showed to be more effective with high biomass proportions. This could increase the utilization of a renewable and reliable carbon-neutral energy source in an economically feasible process. The derived oil could be used as alternative gasoline after further testing or it could be blended with gasoline due to its high aromaticity and low oxygen content. In the end, using these wastes to produce valuable energetic oil is one step forward in the long journey towards ensuring energy security away from petroleum sources, besides the major contribution to waste management and landfill reduction.

4.5. References

Aitani, A.M., 2004. Oil Refining and Products, in: Cleveland, C.J. (Ed.), Encyclopedia of Energy. Elsevier, New York, pp. 715–729. https://doi.org/10.1016/B0-12-176480-X/00259-X

Anuar Sharuddin, S.D., Abnisa, F., Wan Daud, W.M.A., Aroua, M.K., 2017. Energy recovery from pyrolysis of plastic waste: Study on non-recycled plastics (NRP) data as the real measure of plastic waste. Energy Convers. Manag. 148, 925–934. https://doi.org/10.1016/j.enconman.2017.06.046

Botas, J.A., Serrano, D.P., García, A., Ramos, R., 2014. Catalytic conversion of rapeseed oil for the production of raw chemicals, fuels and carbon nanotubes over Ni-modified nanocrystalline and hierarchical ZSM-5. Appl. Catal. B Environ. 145, 205–215. https://doi.org/10.1016/j.apcatb.2012.12.023

Cheng, Y.-T., Huber, G.W., 2012. Production of targeted aromatics by using Diels–Alder classes of reactions with furans and olefins over ZSM-5. Green Chem. 14, 3114. https://doi.org/10.1039/c2gc35767d

Ding, Y.-L., Wang, H.-Q., Xiang, M., Yu, P., Li, R.-Q., Ke, Q.-P., 2020. The Effect of Ni-ZSM-5 Catalysts on Catalytic Pyrolysis and Hydro-Pyrolysis of Biomass. Front. Chem. 8.

Dorado, C., Mullen, C.A., Boateng, A.A., 2015. Origin of carbon in aromatic and olefin products derived from HZSM-5 catalyzed co-pyrolysis of cellulose and plastics via isotopic labeling. Appl. Catal. B Environ. 162, 338–345. https://doi.org/10.1016/j.apcatb.2014.07.006

Dorado, C., Mullen, C.A., Boateng, A.A., 2014. H-ZSM5 Catalyzed Co-Pyrolysis of Biomass and Plastics. ACS Sustain. Chem. Eng. 2, 301–311. https://doi.org/10.1021/sc400354g

Dyer, A.C., Nahil, M.A., Williams, P.T., 2021. Catalytic co-pyrolysis of biomass and waste plastics as a route to upgraded bio-oil. J. Energy Inst. 97, 27–36. https://doi.org/10.1016/j.joei.2021.03.022

Gucho, E.M., Shahzad, K., Bramer, E.A., Akhtar, N.A., Brem, G., 2015. Experimental Study on Dry Torrefaction of Beech Wood and Miscanthus. Energies 8, 3903–3923. https://doi.org/10.3390/en8053903

Hassan, E.B., Elsayed, I., Eseyin, A., 2016. Production high yields of aromatic hydrocarbons through catalytic fast pyrolysis of torrefied wood and polystyrene. Fuel 174, 317–324. https://doi.org/10.1016/j.fuel.2016.02.031

Imam, T., Capareda, S., 2012. Characterization of bio-oil, syn-gas and bio-char from switchgrass pyrolysis at various temperatures. J. Anal. Appl. Pyrolysis 93, 170–177. https://doi.org/10.1016/j.jaap.2011.11.010

Jaafar, Y., Abdelouahed, L., Hage, R.E., Samrani, A.E., Taouk, B., 2022. Pyrolysis of common plastics and their mixtures to produce valuable petroleum-like products. Polym. Degrad. Stab. 195, 109770. https://doi.org/10.1016/j.polymdegradstab.2021.109770

Kamrin, M.A., 2014. Gasoline, in: Wexler, P. (Ed.), Encyclopedia of Toxicology (Third Edition). Academic Press, Oxford, pp. 700–701. https://doi.org/10.1016/B978-0-12-386454-3.00391-2

Li, X., Dong, W., Zhang, J., Shao, S., Cai, Y., 2020. Preparation of bio-oil derived from catalytic upgrading of biomass vacuum pyrolysis vapor over metal-loaded HZSM-5 zeolites. J. Energy Inst. 93, 605–613. https://doi.org/10.1016/j.joei.2019.06.005

Li, X., Li, J., Zhou, G., Feng, Y., Wang, Y., Yu, G., Deng, S., Huang, J., Wang, B., 2014. Enhancing the production of renewable petrochemicals by co-feeding of biomass with plastics in catalytic fast pyrolysis with ZSM-5 zeolites. Appl. Catal. Gen. 481, 173–182. https://doi.org/10.1016/j.apcata.2014.05.015

Marlair, G., Cwiklinski, C., Tewarson, A., 1999. An analysis of some practical methods for estimating heats of combustion in fire safety studies. Interflam 99 Jun 1999 Edimbourg U. K. Ineris-00972167.

Mihalcik, D.J., Mullen, C.A., Boateng, A.A., 2011. Screening acidic zeolites for catalytic fast pyrolysis of biomass and its components. J. Anal. Appl. Pyrolysis 92, 224–232. https://doi.org/10.1016/j.jaap.2011.06.001

Mohabeer, C., Abdelouahed, L., Marcotte, S., Taouk, B., 2017. Comparative analysis of pyrolytic liquid products of beech wood, flax shives and woody biomass components. J. Anal. Appl. Pyrolysis 127, 269–277. https://doi.org/10.1016/j.jaap.2017.07.025

Mohabeer, C., Reyes, L., Abdelouahed, L., Marcotte, S., Buvat, J.-C., Tidahy, L., Abi-Aad, E., Taouk, B., 2019. Production of liquid bio-fuel from catalytic de-oxygenation: Pyrolysis of beech wood and flax shives. J. Fuel Chem. Technol. 47, 153–166. https://doi.org/10.1016/S1872-5813(19)30008-8

Qi, Z., 2007. Review of biomass pyrolysis oil properties and upgrading research. Energy Convers. Manag. 48, 1, 87–92.

R. Carlson, T., Cheng, Y.-T., Jae, J., W. Huber, G., 2011. Production of green aromatics and olefins by catalytic fast pyrolysis of wood sawdust. Energy Environ. Sci. 4, 145–161. https://doi.org/10.1039/C0EE00341G

Scanlon, J.T., Willis, D.E., 1985. Calculation of Flame Ionization Detector Relative Response Factors Using the Effective Carbon Number Concept. J. Chromatogr. Sci. 23, 333–340. https://doi.org/10.1093/chromsci/23.8.333

Thommes, M., Kaneko, K., Neimark, A.V., Olivier, J.P., Rodriguez-Reinoso, F., Rouquerol, J., Sing, K.S.W., 2015. Physisorption of gases, with special reference to the evaluation of surface area and pore size distribution (IUPAC Technical Report). Pure Appl. Chem. 87, 1051–1069. https://doi.org/10.1515/pac-2014-1117

Topaloğlu Yazıcı, D., Bilgiç, C., 2010. Determining the surface acidic properties of solid catalysts by amine titration using Hammett indicators and FTIR-pyridine adsorption methods: Determining the surface acidic properties of solid catalysts. Surf. Interface Anal. 42, 959–962. https://doi.org/10.1002/sia.3474

U.S. Energy Information Administration (EIA) [WWW Document], 2022. URL https://www.eia.gov/energyexplained/us-energy-facts/ (accessed 2.3.21).

Valle, B., Gayubo, A.G., Aguayo, A.T., Olazar, M., Bilbao, J., 2010. Selective Production of Aromatics by Crude Bio-oil Valorization with a Nickel-Modified HZSM-5 Zeolite Catalyst. Energy Fuels 24, 2060–2070. https://doi.org/10.1021/ef901231j

Yao, W., Li, J., Feng, Y., Wang, W., Zhang, X., Chen, Q., Komarneni, S., Wang, Y., 2015. Thermally stable phosphorus and nickel modified ZSM-5 zeolites for catalytic co-pyrolysis of biomass and plastics. RSC Adv. 5, 30485–30494. https://doi.org/10.1039/C5RA02947C

Zhang, H., Nie, J., Xiao, R., Jin, B., Dong, C., Xiao, G., 2014. Catalytic Co-pyrolysis of Biomass and Different Plastics (Polyethylene, Polypropylene, and Polystyrene) To Improve Hydrocarbon Yield in a Fluidized-Bed Reactor. Energy Fuels 28, 1940–1947. https://doi.org/10.1021/ef4019299

Zhao, C., Jiang, E., Chen, A., 2017. Volatile production from pyrolysis of cellulose, hemicellulose and lignin. J. Energy Inst. 90, 902–913. https://doi.org/10.1016/j.joei.2016.08.004

Zhu, L., Lv, X., Tong, S., Zhang, T., Song, Y., Wang, Y., Hao, Z., Huang, C., Xia, D., 2019. Modification of zeolite by metal and adsorption desulfurization of organic sulfide in natural gas. J. Nat. Gas Sci. Eng. 69, 102941. https://doi.org/10.1016/j.jngse.2019.102941

CHAPTER 5:

Catalytic co-pyrolysis of polystyrene and beech wood in a continuous fluidized bed reactor

5. CATALYTIC CO-PYROLYSIS OF POLYSTYRENE AND BEECH WOOD IN A CONTINUOUS FLUIDIZED BED REACTOR

5.1. Introduction

The previous chapter discussed the catalytic co-pyrolysis of BW and PS in a semi-batch reactor. To better simulate an upscale production, a continuous reactor must be considered to get considerable quantities of oil. Therefore, this chapter describes an extensive study of biomass/PS catalytic co-pyrolysis under the previously chosen catalyst (Fe/Ni-ZSM-5) in a fluidized bed reactor. The influence of different parameters such as metal loading of the catalyst (1.4%Fe-1.4%Ni and 5%Fe-5%Ni), biomass/plastic ratio (1:3, 1:1, 3:1), and pyrolysis temperature (450-600 °C) on the quality and quantity of co-pyrolysis oil was investigated.

5.2. Materials and methods

5.2.1. Materials

The materials used in the previous chapters are also used in this chapter. BW was ground and seized to yield a particle size of 200-300 µm for fluidization purposes. Polystyrene was milled to obtain a mixture of different plastic sizes ranging from 2mm to 100mm.

The conventional HZSM-5 in its proton form (SiO_2/Al_2O_3 ratio of 38, specific surface area of about 250 m^2/g and 0.5 nm of pore size) was acquired from ACS materials (Pasadena CA, USA) in the form of pellets (Ø = 3 mm, L = 30 mm). The SiO_2/Al_2O_3 ratio was 38, the specific surface area was about 250 g/m^2 and the pore size was about 5 Å. Catalyst pellets were ground and sieved to obtain a particle size between 0.1 and 0.2 mm before the modification.

5.2.2. Methods

5.2.2.1. Catalyst preparation

Two Fe/Ni modified ZSM-5 were prepared by using the wetness impregnation method of 50 g of the previously prepared ZSM-5 as described in **chapter 4**. Iron and nickel nitrate salts were

used to prepare two metal loading: (1.4 wt.% Fe and 1.4 wt.% Ni) /ZSM-5 and (5 wt.% Fe and 5 wt.% Ni) /ZSM-5. The catalysts were then noted as 1.4/1.4 % Fe/Ni-ZSM-5 and 5/5 % Fe/Ni-ZSM-5.

5.2.2.2. Fluidized bed set-up

Co-pyrolysis of biomass and plastics was performed in a fluidized bed reactor (**Fig. 5.1**). The reactor and furnace were acquired from MTI Corporation (Ref. OTF-1200X-S-FB). The reactor is made from stainless steel with a 42 mm inner diameter and 45 mm external diameter with a 125 mm reaction zone length. The carrier N_2 gas enters from the bottom of the reactor. The pyrolysis process was considered isothermal. The catalyst was placed inside the reactor before the furnace is started. After that, the reactor is heated to the desired temperature with a constant flow of N_2 to ensure fluidization and an inert atmosphere.

Before pyrolysis, the catalyst and BW were dried in an oven at 105 °C for 2 h to eliminate excessive moisture. 5 g of catalyst were introduced into the reactor and carrier gas flowed through the system for 30 min before feeding to create an inert atmosphere. The N_2 gas entered the reactor at a flow rate of 1 $L.min^{-1}$ to ensure catalyst fluidization (Kunii and Levenspiel, 1991). Under such flow, the real residence time was calculated to be around 4-7 s.

The biomass/plastic feed entered from the top of the reactor to the reacting zone through a stainless-steel tube. Pyrolysis products exited the reactional area through a second stainless steel tube placed at the top of the reactor. Solid particles were collected in the cyclone that was placed right after the reactor. The tube and the cyclone were each covered by a heat exchanger to maintain a temperature of 300 °C and avoid condensation in the system. Gaseous products entered a condenser, which was kept at a temperature of 5 °C using a refrigerant cooler by Julabo (Ref. 1.953.0800-V3) and the oil was accumulated in a flask at the end of the condenser. Non-condensable gases were purged from the condenser after passing through a cotton filter to

retain any remaining solid particles. The gases were then collected in a Tedlar gas bag.

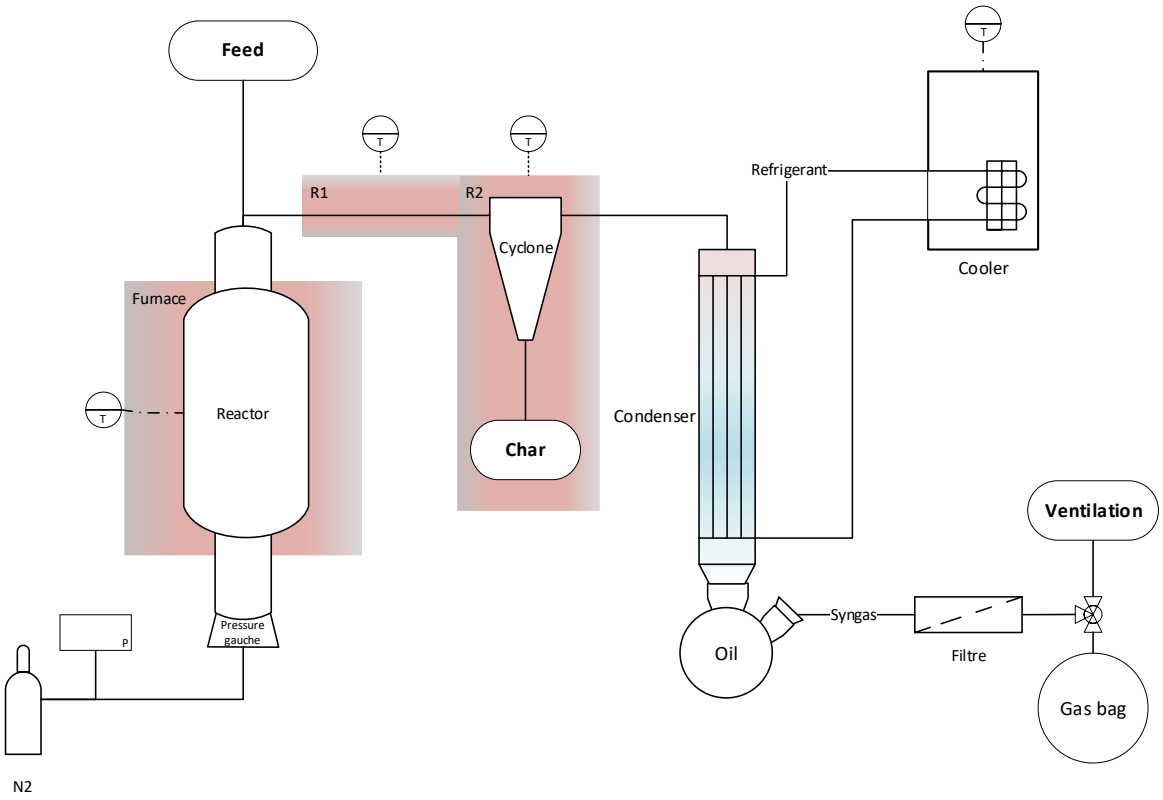

Fig. 5.1. Fluidized catalytic bed reactor setup.

Different temperatures (450–600 °C) and biomass/plastic ratios (1:3–3:1) were tested to obtain the optimum reaction conditions for co-pyrolysis. Pyrolysis of 100 % BW and 100 % PS was performed for comparison. A feed rate of 1 g every 3 min was used. All the experimental conditions done with a catalyst were also achieved without a catalyst (using sand as fluidizing agent) for comparison purposes. **Table 5.1** lists all the experiments performed in this study.

Table 5.1. Summary of the performed experiments

Temperature (°C)	Fluidized bed	Feedstock	Poportion
500	Sand	BW	100
		BW-PS	50-50
		PS	100
450	1.4/1.4 % Fe/Ni-ZSM-5	BW-PS	50-50
500			
550			
600			

500	1.4/1.4 % Fe/Ni-ZSM-5	BW	100
		BW-PS	75-25
			50-50
			25-75
		PS	100
500	5/5 % Fe/Ni-ZSM-5	BW-PS	50-50

5.2.2.3. Product analysis

The same analytical methods were used as in the previous chapters in addition to moisture content analysis of the liquid products (oil), which was analyzed using Karl-Fischer titration technique: volumetric (870, Metrohm, Switzerland) for liquid products with high water content (10-100%) and coulometric (899, Metrohm, Switzerland) for low water content (0-10%).

5.3. Results and discussion

5.3.1. Co-pyrolysis of BW and PS in different proportions over sand

5.3.1.1. Product yield analysis

For this set of experiments, pyrolysis of PS, BW, and co-pyrolysis in equal parts of these 2 feedstocks were performed over sand at 500 °C. The obtained results serve as a reference to compare with those from pyrolysis over catalyst. **Table 5.2** shows oil, char, and gas yields (wt.%) for these experiments.

For the pyrolysis of PS, all the feedstock was converted into a liquid product, as seen before in the fixed bed reactor. Pyrolysis of BW produces a higher char yield (22 wt.%) due to the nature of the biomass, thus a lower oil yield. Despite the production of some gases, the yield was too low be of have interest in this study. When co-pyrolysis was performed, a high oil yield was obtained (89 wt.%), and compared to the pyrolysis of BW, a reduction of 54 wt.% of char yield was obtained. For the synergy calculation by **Eq. 3.1**, it can be concluded that experimental co-pyrolysis values are very close to the theoretical ones, confirming an absence of any synergy for the product yield, just like in the fixed bed reactor.

Table 5.2. Product yields (wt.%) of pyrolysis of PS and BW, and co-pyrolysis of BW-PS 50-50 over sand at 500 °C.

Feedstock	**PS**	**BW-PS 50-50**	**BW**
Oil yield	99.9	89.3	76.2
Oil yield theo.	-	88.1	-
Char yield	0.1	9.8	21.5
Char yield theo.	-	10.8	-
Gas yield	0.0	0.9	2.3
Gas yield theo.	-	1.2	-

5.3.1.2. Liquid product composition

Fig. 5.2 illustrates the composition (wt.%) of the pyrolysis oil of PS and BW over sand as well as the co-pyrolysis oil of these two feedstocks over sand. These 3 experiments were carried out at a temperature of 500 °C. For PS, just aromatics were produced, with around 20 wt.% of PAH. For BW, logically no aromatics were obtained. BW produced mostly carboxylic acids, carbohydrates, and other families like furans, esters, and aldehydes (noted under "others"). A more detailed composition of these oils is listed in **Table A.8.**

A theoretical calculation of the co-pyrolysis yields was made based on the results of the pyrolysis of BW and PS over sand. This calculation was noted as theoretical (theo.) in **Fig. 5.2**. Compared to the experimental results, it was estimated to have around 15 wt.% of carboxylic acids but the experimental result was higher (23 wt.%). More aromatics were also estimated for co-pyrolysis, around 57 wt.%, however, a total of 46 wt.% in aromatics was observed when the experiment was performed. This shows the synergistic nature of the co-pyrolysis of plastics and biomass. The theoretical results seemed more attractive because more aromatics were estimated. This difference in the experimental results could be related to the variation in residence time and the reactor setup of 4-7 s compared with that of the fixed bed reactor of about 15-20 s. This problem could be solved by using a catalyst. The comparison between the experimental and theoretical PS and biomass has rarely been investigated. However, Zhang et

al. (2014) investigated the catalytic co-pyrolysis of biomass (pine sawdust) with PE, PS, and PP in a fluidized bed reactor using different catalysts including FCC, which is mainly constituted of zeolites (Komvokis et al., 2016). The study focused on PE and pine sawdust and they found a 86 % improvement in aromatic yield from 20 wt.% to 37 wt.% with the 1:1 ratio of PE/PS at 600 °C. The overall petrochemical yield was also improved from 33 wt.% to 57 wt.%. From here, it was believed that catalysis has a remarkable effect on aromatic and petrochemical production.

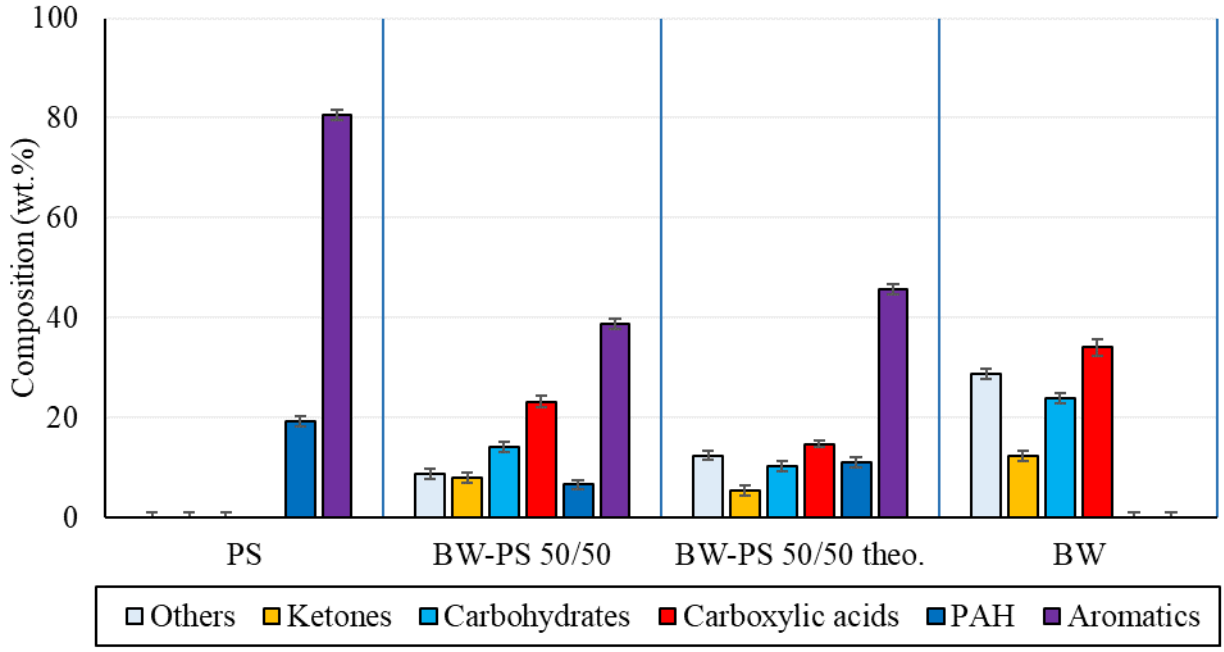

Fig. 5.2. Oil composition (wt.%) of pyrolysis of PS, BW-PS 50-50, and BW over sand at 500 °C.

5.3.1.3. LHV and oxygen content

The Lower Heating Value (LHV) and oxygen content (wt.%) are two key factors for co-pyrolysis oil. High LHV and low oxygen content is the most desirable outcome but due to the nature of the biomass, this is usually not the case. On top of the importance of the effect of the catalyst in this study, these two factors will be discussed as well. The curves of these results are illustrated in **Fig. 5.3**.

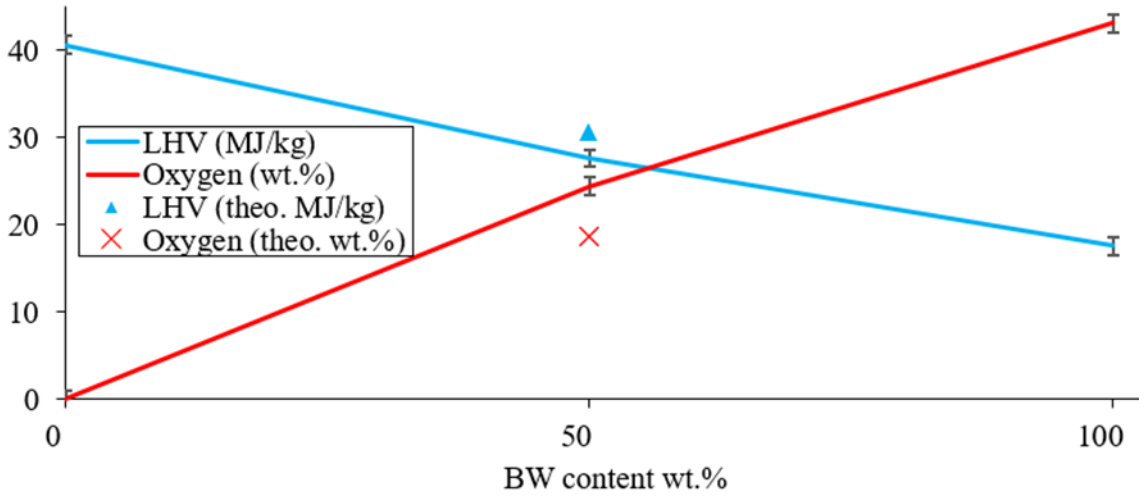

Fig. 5.3. LHV (MJ/kg) and oxygen content (wt.%) of co-pyrolysis experiments over sand at 500 °C.

As before, an estimation was made for the co-pyrolysis based on the results from the pyrolysis of PS and BW, separately. For LHV, the estimated value was a bit higher but close to the value obtained when co-pyrolysis of BW-PS (50-50) was conducted. The estimated oxygen content was lower than the observed for the experiment. This difference is related to the increased production of acids and other oxygenated compounds relaying no or negative synergy between PS and BW in this type of reactor and operating conditions.

5.3.2. Co-pyrolysis of BW and PS at different temperatures over 1.4/1.4 % Fe/Ni-ZSM-5

5.3.2.1. Product yield analysis

High liquid yields were obtained, where the minimum was 80 wt.% at 450 °C and a maximum of 89 wt.% at 600 °C. In this case, a clear tendency was observed, as the temperature increased, so did the oil and gas yields while the char yield decreased. The oil, gas, and char yields expressed in wt.% can be seen in **Table 5.3.**

5.3.2.2. Liquid product composition

The composition of the pyrolytic oils obtained in this set of experiments is illustrated in **Fig. 5.4**. For comparison, the composition of the oil obtained from the co-pyrolysis over sand of BW-PS in equal parts (ref.) at 500 °C is also shown in the same figure.

The oils presented a higher aromatics composition and lower carboxylic acids due to the presence of the catalyst; 55 wt.% of aromatics were obtained at 450 °C, then for 500, 550, and 600 °C, the total aromatics were about 94 wt.% of the composition. A decrease in PAH was observed going from 18 wt.% at 500 °C to 12 wt.% at 600 °C, which resulted in an increase in aromatics due to thermal cracking. The quantity of other components like carbohydrates, phenols, and ketones decreased significantly from performing the co-pyrolysis at 450 °C to 500 °C.

The results obtained at 500 °C and higher did not show a significant difference. This means 500 °C is the optimum temperature for co-pyrolysis of BW and PS over 1.4/1.4 % Fe/Ni-ZSM-5 to obtain the best oil quality with the minimum cost possible.

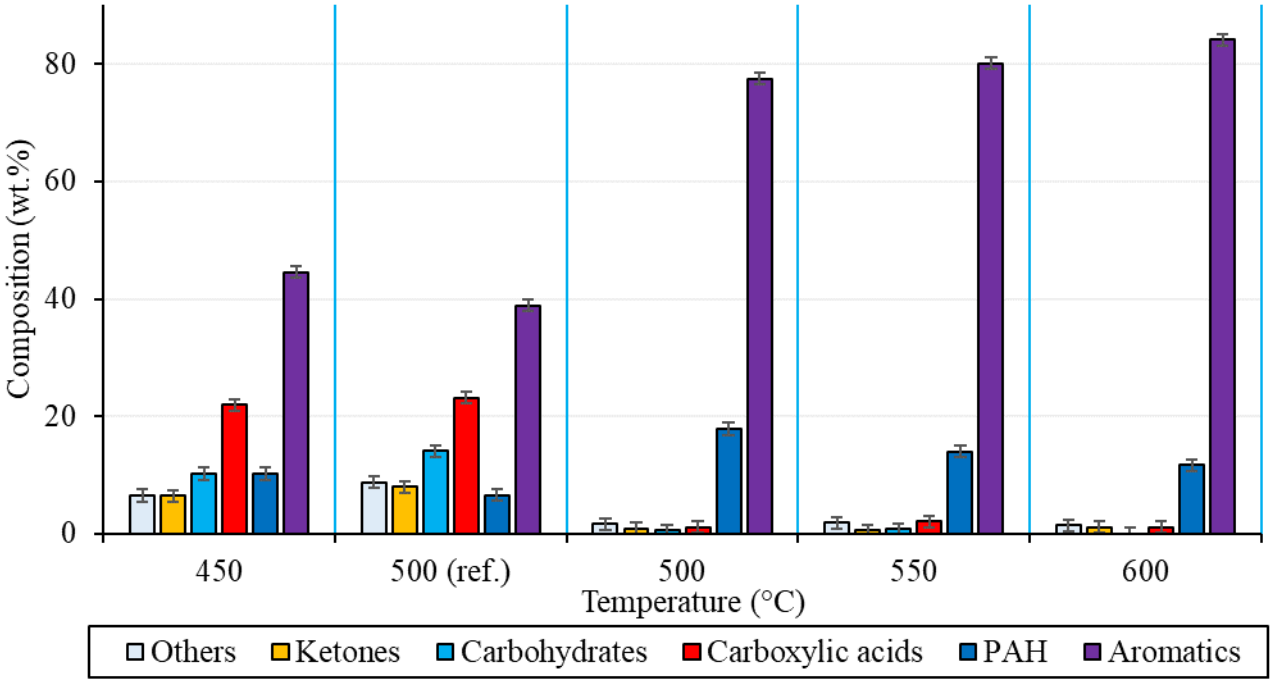

Fig. 5.4. Oil composition (wt.%) from co-pyrolysis of BW-PS 50-50 over 1.4/1.4 % Fe/Ni-ZSM-5 at different temperatures and comparison with reference at 500 °C.

5.3.2.3. LHV and oxygen content

Fig. 5.5 shows the evolution of the LHV as well as the oxygen content (wt.%) of the oils obtained from co-pyrolysis at different temperatures. A notable difference is observed from 450 °C to 500 °C after a more stable evolution for these curves, which is consistent with the behavior discussed for the compositions.

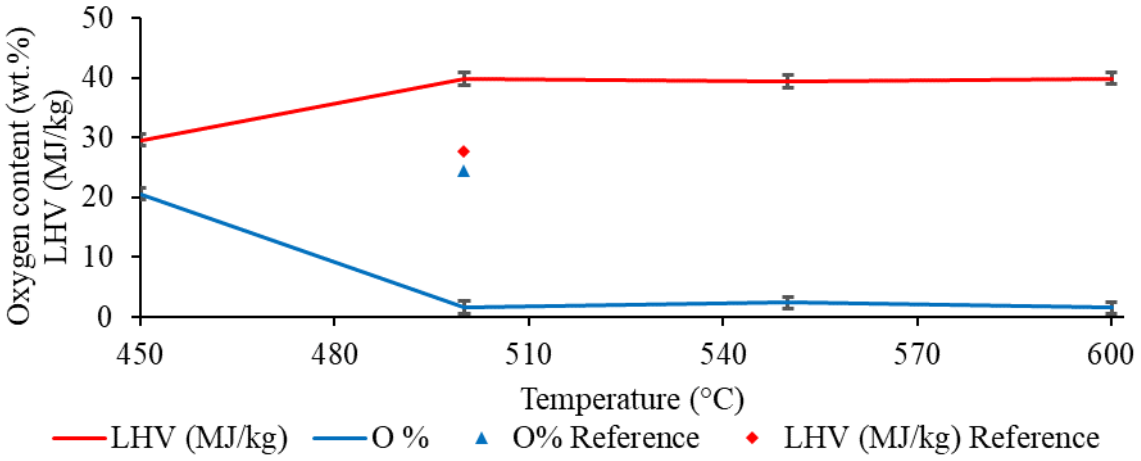

Fig. 5.5. LHV (MJ/kg) and oxygen content (wt.%) of co-pyrolysis oils from BW-PS 50-50 over 1.4/1.4 % Fe/Ni-ZSM-5 at different temperatures and comparison with reference at 500 °C.

In comparison with the reference experiment (co-pyrolysis over sand), the presence of the catalyst significantly increased the LHV and reduced the oxygen content. Co-pyrolysis over sand at 500 °C produced a liquid product with 28 MJ/kg and 24 wt.% of oxygen while the co-pyrolysis over 1.4/1.4 % Fe/Ni-ZSM-5 at the same temperature produced oil with 40 MJ/kg and 2 wt.% of oxygen.

5.3.3. Co-pyrolysis of BW and PS in different proportions over 1.4/1.4 % Fe/Ni-ZSM-5

5.3.3.1. Product yield analysis

A set of 5 experiments followed the previous set to study the influence of different feedstock ratios in the co-pyrolysis of BW and PS. Co-pyrolysis was performed at 500 °C, which was

previously stated as an optimum temperature over the modified catalyst: 1.4/1.4 % Fe/Ni-ZSM-5. **Table 5.3** provides the product yields (wt.%) obtained for this set of experiments.

Table 5.3. Product yield (wt.%) for co-pyrolysis over 1.4/1.4 % Fe/Ni-ZSM-5 at 500 °C with different proportions of BW and PS.

Feedstock	**PS**	**BW-PS 25-75**	**BW-PS 50-50**	**BW-PS 75-25**	**BW**
Oil yield	98.5	93.9	85.9	81.2	71.6
Oil yeild theo.	-	91.8	85.1	78.3	-
Char yeild	1.4	5.5	13.1	17.4	26.6
Char yeild theo.	-	7.7	14	20.3	-
Gas yield	0.1	0.6	1.0	1.4	1.8
Gas yeild theo.	-	0.5	0.9	1.4	-

The highest liquid yield was observed when the highest quantity of PS was fed into the reactor. Char yield increased with the increase of BW in the feedstock. Gas yield remained low in comparison to oil and char yields. The theoretical values for the composition based on PS and BW alone for the mixtures: theoretical values for oil yield (%) were 92 wt.% for BW-PS 25/75, 85 wt.% for 50/50, and 78 wt.% for BW/PS 75/25. Compared to the experimental values, the values were close to 50/50 and slightly higher for 75/25 and 25/75. The catalytic co-pyrolysis showed some positive synergy in oil yield compared to the fixed bed reactor. This can be due to the intimate interaction between the volatiles and the surface of the catalyst.

This positive synergy is described by the desirable increase in oil yield and reduction in char yield.

5.3.3.2. Liquid product composition

Fig. 5.6 illustrates the composition of the oils obtained from the co-pyrolysis over 1.4/1.4 % Fe/Ni-ZSM-5 feeding different proportions of BW and PS and the results obtained in the reference experiments. These experiments were performed at 500 °C.

These results were not clear and did not follow the logical tendency of the other experiments in this study. For instance, for co-pyrolysis of 75 % BW, 28 wt.% of carboxylic acids was obtained when it has been confirmed that the catalyst can properly crack these molecules. Fewer aromatics were therefore reported, which did not follow the expected tendency since co-pyrolysis of BW-PS in equal parts produced a higher percentage of aromatics and fewer carboxylic acids.

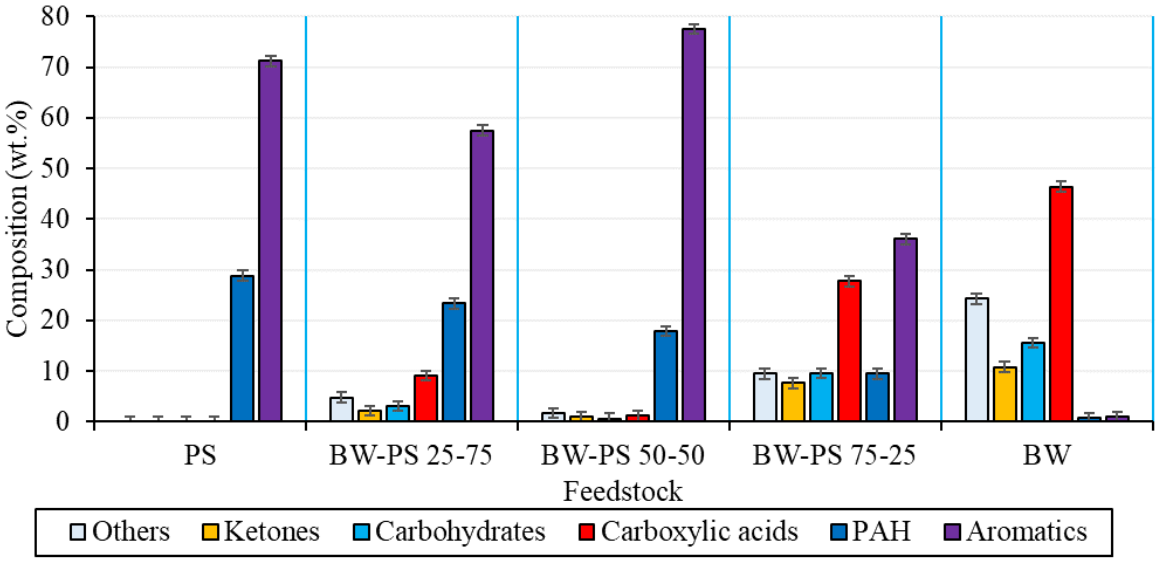

Fig. 5.6. Oil composition (wt.%) from co-pyrolysis of BW-PS over 1.4/1.4 % Fe/Ni-ZSM-5 with different proportions of BW and PS at 500 °C.

If a comparison was made for these results with the reference experiments for the pyrolysis of BW over sand and over 1.4/1.4 % Fe/Ni-ZSM-5 (see **Fig. 5.7**), the content of the carboxylic acid was higher (46 wt.%) when the catalyst was used. The aromatics composition was higher than expected but because of the value of carboxylic acids, the percentages of aromatics obtained are believed to be correct. The results obtained for co-pyrolysis in equal parts do seem logical: high aromatics, and low carboxylic acids. Compared to the reference, it shows the benefit of the catalyst on the final liquid product.

In general, the difference between the reference experiments and those performed with the catalyst was not significant nor positive from the point of view of the catalyst's performance for some of these experiments. After a rigorous review of the procedures, this issue was highlighted and might have originated from oil sampling for the GC analysis. As two phases were part of the oil collected, pre-homogenization had to be done to obtain a proper sample for chromatography. The results for co-pyrolysis of 75 wt.% BW, for example, seem more logical when assuming they are just for the aqueous phase of the oil or when the sample is mostly this phase since it is expected to have fewer aromatics and therefore more carboxylic acids, ketones, aldehydes, etc.

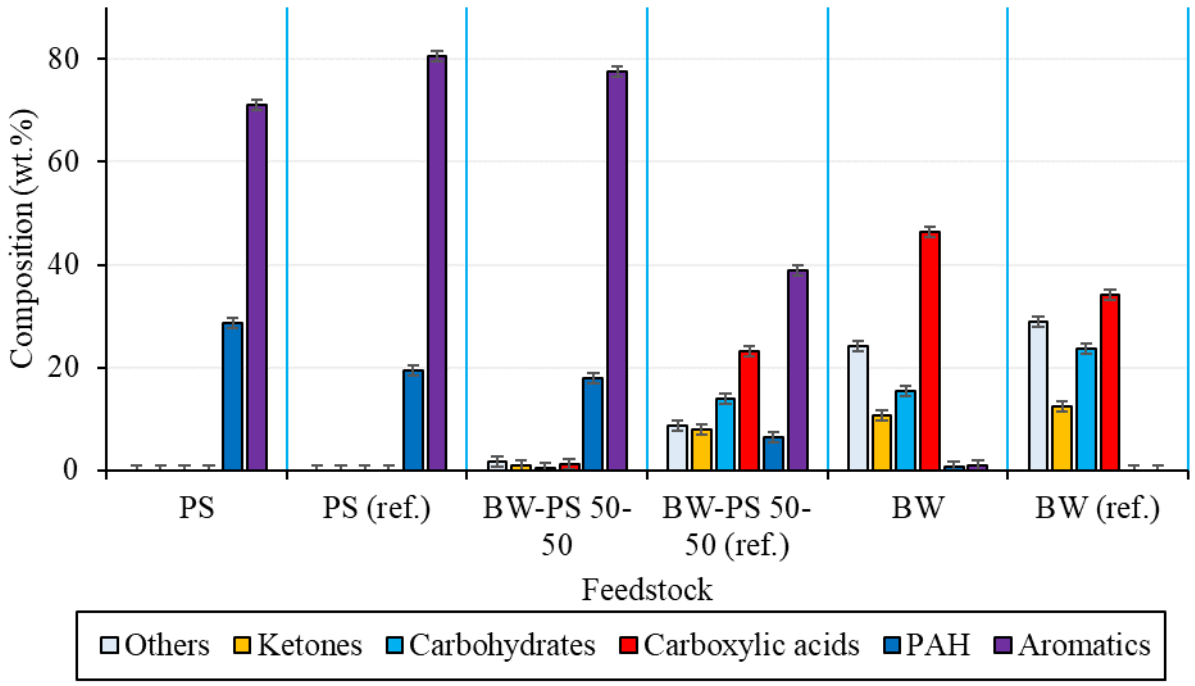

Fig. 5.7. Comparison of oil composition (wt.%) from co-pyrolysis of BW-PS over 1.4/1.4 % Fe/Ni-ZSM-5 with different proportions of BW and PS at 500 °C with reference experiments over sand.

It is believed that this set of experiments should be repeated and before the chromatography analysis, good chemical homogenization or independent analysis of each phase is necessary to obtain the correct results. High-purity acetone as a solvent is recommended to be used for the two phases.

5.3.3.3. LHV and oxygen content

For LHV and oxygen content, an estimation was made for co-pyrolysis based on the feedstock proportions of BW and PS and the results obtained from the pyrolysis of PS and BW separately. These are noted as theoretical (theo.) results in **Fig. 5.8**.

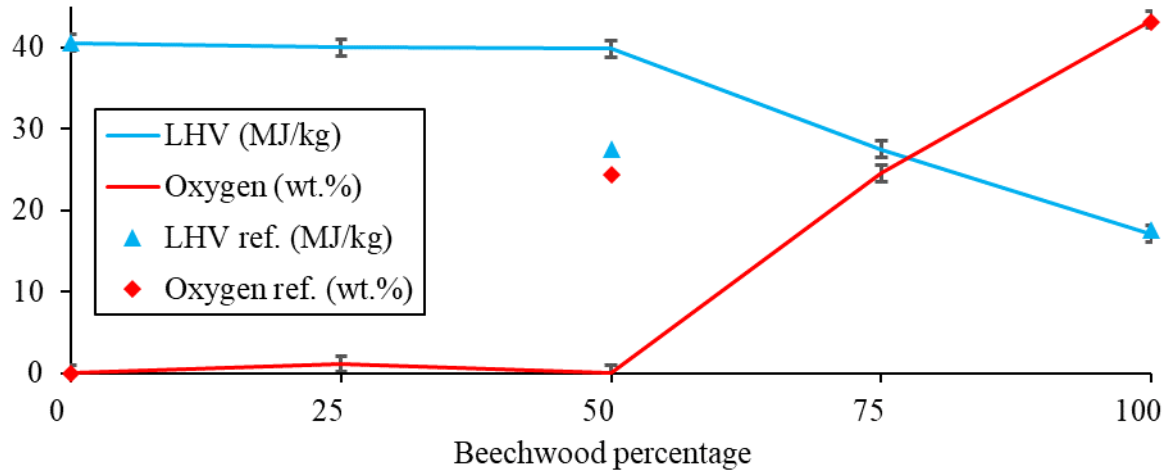

Fig. 5.8. LHV (MJ/kg) and oxygen content (wt.%) of oils from co-pyrolysis of different ratios of BW-PS over 1.4/1.4 % Fe/Ni-ZSM-5 at 500 °C.

The LHV value ranged between 39 and 41 MJ/kg for the pyrolysis of PS, BW-PS 25-75, and BW-PS 50-50 then it started to decrease to 17 MJ/kg for BW pyrolysis. A more notable difference was expected since the feedstock portion changed considerably. As previously noticed, the highest oxygen content is reported with the highest feed of BW. However, the result obtained (43 wt.%) is far from the reality since it is almost double the value obtained in the reference experiment for co-pyrolysis of BW-PS 50-50, and in fact, the values are extremely close to those of the reference for the pyrolysis of PS and BW, which implies no influence of the catalyst on the final product.

This might be due to the issue discussed in the previous section. LHV and oxygen content are calculated based on the GC-MS results, so it is believed these results are inconclusive until confirmed by experimentation and analysis.

5.3.4. Co-pyrolysis of BW and PS over 5/5 % Fe/Ni-ZSM-5

5.3.4.1. Product Yield Analysis

Only one experiment was conducted using 5/5 % Fe/Ni-ZSM-5 for co-pyrolysis of BW-PS 50-50 at 500 °C. The intention was to compare these results and see if an increase in metal loading would also improve the quality of the oil. This section will discuss and compare the results of the same experiment, co-pyrolysis of BW-PS 50-50 at 500 °C, over the two catalysts used and the reference (sand). These results are listed in **Table 5.4**.

The maximum oil yield was obtained when sand was used (89 wt.%). 1.4/1.4 % Fe/Ni-ZSM-5 produced the minimum with 88 wt.%. For char, 1.4/1.4 % Fe/Ni-ZSM-5 produced the highest yield with 13 wt.%, however, the difference from the other catalysts was not significant in comparison.

Table 5.4. Product yields (wt.%) from co-pyrolysis of BW-PS in equal parts over different catalysts at 500 °C.

Catalyst	**5/5 % Fe/Ni-ZSM-5**	**1.4/1.4 % Fe/Ni-ZSM-5**	**Sand**
Oil yield	88.5	85.9	89.3
Char yield	10.6	13.1	9.8
Gas yield	0.9	1.0	0.9

5.3.4.2. Liquid product composition

Fig. 5.9 illustrates the composition of the oils produced when co-pyrolysis of BW and PS in equal proportions conducted at 500 °C. 1.4/1.4 % Fe/Ni-ZSM-5 provided the best results when comparing the compositions. The oil obtained was rich in aromatics and poor in oxygenated compounds. Some carbohydrates and furans were obtained but the value was close to 0.6 wt.% for each of these two.

In comparison, 5/5 % Fe/Ni-ZSM-5 showed less catalytic performance, which resulted in higher content of carboxylic acids, ketones, carbohydrates, and furans. This can be explained by the

reduction of the active catalytic surface of the ZSM-5 due to a higher metal surface loading. This also reduced the acidity of the catalyst and therefore, the catalytic performance. A similar outcome was reported by Balasundram et al. (2017) for the catalytic pyrolysis of sugarcane bagasse over molybdenum (Mo) modified HZSM-5. They tested three different loadings (0.5, 1.0, and 1.5 wt.%) of Mo where the highest loading (1.5 wt.%) presented less catalytic activity.

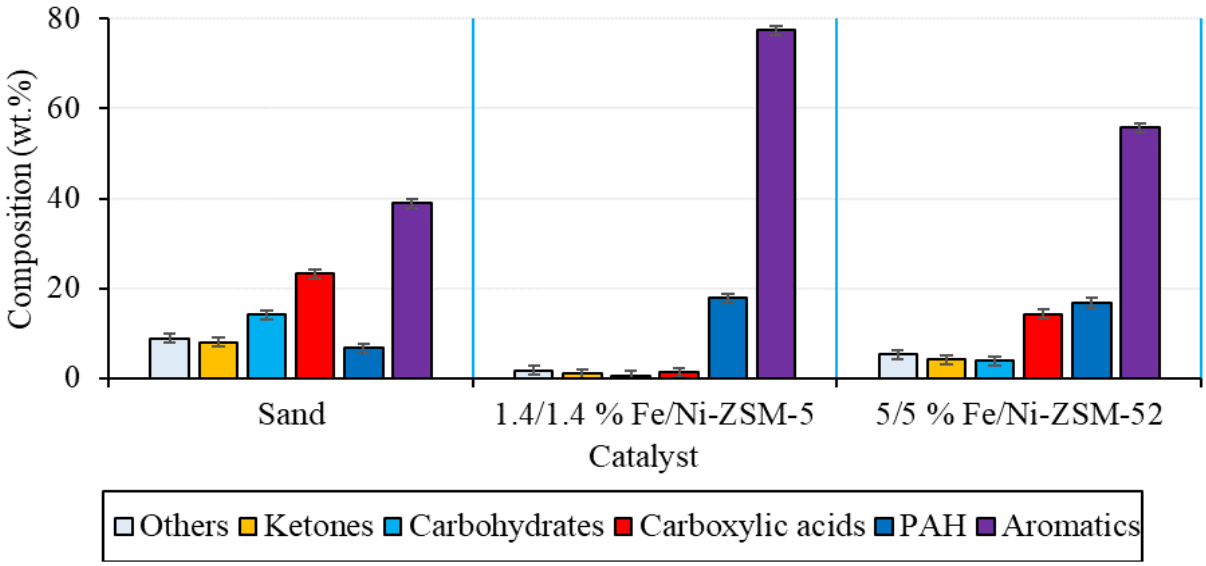

Fig. 5.9. Oil composition (wt.%) from co-pyrolysis at 500 °C of BW-PS in equal parts over different catalysts and sand.

5.3.4.3. LHV and oxygen content

For comparison purposes, these values have been re-tabulated in **Table 5.5**. The same behavior was observed for these two factors as well. 1.4/1.4 % Fe/Ni-ZSM-5 produced the best results with the highest LHV (40 MJ/kg) and the lowest oxygen content (2 wt.%). 5/5 % Fe/Ni-ZSM-5 resulted in close values but less positive since higher oxygen content and lower LHV were observed.

These results further confirm the reduction of catalytic performance due to the high metal loading. This allows the verification that 1.4/1.4 % Fe/Ni-ZSM-5 is as of now, the most suitable loading for co-pyrolysis of BW and PS.

Table 5.5. LHV (MJ/kg) and oxygen content (wt.%) of oils from co-pyrolysis of BW and PS in equal parts over different catalysts at 500 °C.

Catalyst used	5/5 % Fe/Ni-ZSM-5	1.4/1.4 % Fe/Ni-ZSM-5	Sand
LHV (MJ/kg)	34.1	39.8	27.6
Oxygen (wt.%)	12.3	1.6	24.4

5.3.5. Water content analysis

When co-pyrolysis was performed, two miscible phases were always observed in the liquid product. High water content (> 30 wt.%) leads to phase separation, hence the appearance of 2 phases which was observed in this study (Chiaramonti et al., 2007). For water content analysis, these phases were separated by decantation and analyzed based on the expected water percentage. By optical inspection, it was suggested that the volume of each phase was proportional to the quantity of BW and/or PS that was fed to the reactor, to support this claim, Brebu et al. (2010) found that the aqueous phase of the liquid product from the pyrolysis of lignocellulosic biomass (pine cone in their study) constituted mainly of a water-miscible phase, yet the liquid produced from plastics polymers were mainly oil products (water immiscible). Therefore, the estimated water content of the final liquid product was made taking into consideration the fraction BW-PS (X_{PS} & X_{BW}) of each experiment as shown in ***Eq. 5.1***:

$$Water\%_{estimated} = X_{PS} * Water\%_{light\ phase} + X_{BW} * Water\%_{heavy\ phase} \qquad \textit{Eq. 5.1}$$

5.3.5.1. Influence of catalyst in co-pyrolysis

The water content of the liquid products from co-pyrolysis of BW-PS 50-50 using both synthesized catalysts as well as the reference with sand is tabulated in **Table 5.6**. Higher water content was found when 1.4/1.4 % Fe/Ni-ZSM-5 was used, resulting in 34 wt.% of water. When 5/5 % Fe/Ni-ZSM-5 catalyst was used, less water was collected in the final product (31 wt.%). This can be due to the reduced catalytic performance caused by the high loading of metals and

the reduction of active surface in the catalyst, as previously discussed. This signifies that the main deoxygenation is via dehydration reactions. This idea is supported by Mohabeer et al. (2019), who studied the catalytic pyrolysis of beechwood over metal-modified zeolites in a semi-batch reactor. Their results showed that the water content in the bio-oil tripled after the use of the catalyst.

The quantity of water in the oil phase was low enough to confirm that most, if not all of it, can be found just in the aqueous phase. Therefore, the estimated values follow the same tendency as the aqueous phase. These results corroborated the results of Brebu et al. (2010), who studied the co-pyrolysis of pine cone and plastics polymers. The finding showed that the oil phase exhibited very low water content as low as 0.02-0.45 wt.% and very high-water content in the aqueous phase of around 62-69 wt.% of water in the co-pyrolysis liquid product between pine cone and plastics. However, the latter study showed the separation into 2 phases of pine cone bio-oil with a majority in the aqueous phase. Yet in this study, there was no phase separation of the independent BW bio-oil, which can be due to the difference in the type of lignocellulosic biomass used.

Table 5.6. Water content (wt.%) for co-pyrolysis of BW and PS in equal parts at 500°C using the different catalysts and reference experiment (sand).

Catalyst	**Estimated**	**Oil phase**	**Aqueous phase**
Sand	25.2	0.4	50.0
1.4/1.4 % Fe/Ni-ZSM-5	34.2	0.4	68.0
5/5 % Fe/Ni-ZSM-5	30.8	0.4	61.1

5.3.5.2. Influence of temperature

The results obtained for co-pyrolysis of BW-PS 50-50 at temperatures ranging from 450 to 600 °C are illustrated in **Fig. 5.10**. The lowest value was obtained at 450 °C. The highest one was

obtained at 550 °C. The water content seemed to increase as the pyrolysis temperature increased. However, when co-pyrolysis was conducted at 600 °C, the water content slightly decreased. These results corroborated the findings in the previous chapter that the catalyst deactivated rapidly at a temperature above the calcination temperature (Zhang et al., 2014). Studies about the water content in catalytic co-pyrolysis of lignocellulosic biomass and plastics seemed rare but the trend of the curve could be compared to the individual catalytic pyrolysis of biomass. This trend of increasing water content with temperature corroborated the results of Naqvi et al. (2014). Their study talked about the effect of temperature and catalyst on the bio-oil properties of paddy husk (lignocellulosic biomass) pyrolysis. The temperature range studied was between 350-600 °C. Their result showed high water content for the bio-oil of about 60-65 wt.%, which is comparable to the values of BW bio-oil of this study of 54 wt.%. Despite the slight decrease in water content from 350 °C to 450 °C, the trend was similar to the behavior in this study with an increase of water content in the range of 450-600 °C.

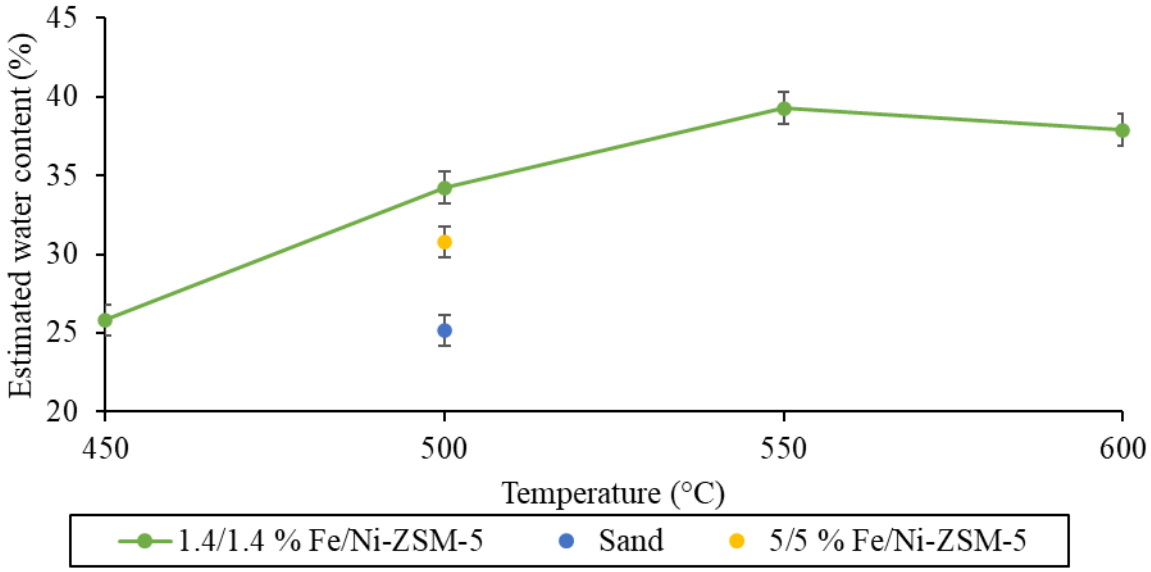

Fig. 5.10. Water content for co-pyrolysis of BW and PS in a 1:1 ratio at different temperatures.

5.3.5.3. Influence of BW-PS proportions

The water content for catalytic co-pyrolysis of BW and PS alone and with different ratios (25:75, 50:50, and 75:25) over 1.4/1.4 % Fe/Ni-ZSM-5 is tabulated in **Table 5.7**. The estimated value was taken for comparison since it can show some analogy with the actual total water yield. The expected tendency was confirmed: the higher the quantity of PS in the mixture, the less water would be found in the final liquid product. This was predicted based on the ultimate and proximate analysis of the feedstock. Water can only come from BW, if its quantity decreased, water decreased. As shown in **Table 5.7**, the oil phase has very low water content and thus, high calorific value, so this phase should be studied further for fuel purposes and the aqueous phase can be used to extract certain water-soluble chemicals such as levoglucosan, carboxylic acids, and esters (Rover et al., 2014; Sadaka and Boateng, 2009).

Table 5.7. Water content (wt.%) of Oil and aqueous phases for co-pyrolysis experiments of different feedstock ratios over 1.4/1.4 % Fe/Ni-ZSM-5 at 500^{o}C.

Feedstock	**Estimated**	**Oil Phase**	**Aqueous Phase**
BW	54.0	-	54.0
BW-PS 75-25	43.8	1.1	58.1
BW-PS 50-50	34.2	0.4	68.1
BW-PS 25-75	17.7	0.2	70.0
PS	-	-	-

5.4. Conclusion

Co-pyrolysis of lignocellulosic (beechwood) and thermoplastic (polystyrene) mixtures over iron and nickel modified zeolite and the influence of different parameters was carried out in a fluidized bed reactor.

Co-pyrolysis temperature ranged between 450 and 600 °C for the first part of the study. 500 °C showed to be the optimum temperature for co-pyrolysis of BW-PS 50-50 since the difference in the liquid product composition and yield at higher temperatures did not have significant variation. A decrease in aromatics selectivity and catalytic performance at temperatures over the catalyst's calcination temperature was observed.

The biomass/plastic ratio was then varied (25:75, 50:50, and 75:25) to study the influence of different proportions on the feedstock. The results show that there are some positive synergistic effects between the two feedstocks, especially under catalysis.

HZMS-5 zeolite was modified by the wetness impregnation method with two metal loadings (1.4%Fe-1.4%Ni and 5%Fe-5%Ni). 1.4/1.4 % Fe/Ni-ZSM-5 proved to be the most suitable loading for co-pyrolysis of BW and PS producing a liquid product with low oxygen content (1.6 wt.%) and highest LHV (39 MJ/kg). The 5% Fe / 5% Ni loading showed limited catalytic performance, which was also seen with water content (wt.%) results since co-pyrolysis over 5/5 % Fe/Ni-ZSM-5 resulted in less water on the final liquid product.

5.5. References

Balasundram, V., Ibrahim, N., Kasmani, R.Md., Isha, R., Abd. Hamid, Mohd.K., Hasbullah, H., 2017. Catalytic pyrolysis of sugarcane bagasse using molybdenum modified HZSM-5 zeolite. Energy Procedia, Proceedings of the 9th International Conference on Applied Energy 142, 793–800. https://doi.org/10.1016/j.egypro.2017.12.128

Brebu, M., Ucar, S., Vasile, C., Yanik, J., 2010. Co-pyrolysis of pine cone with synthetic polymers. Fuel 89, 1911–1918. https://doi.org/10.1016/j.fuel.2010.01.029

Chiaramonti, D., Oasmaa, A., Solantausta, Y., 2007. Power generation using fast pyrolysis liquids from biomass. Renew. Sustain. Energy Rev. 11, 1056–1086. https://doi.org/10.1016/j.rser.2005.07.008

Komvokis, V., Tan, L.X.L., Clough, M., Pan, S.S., Yilmaz, B., 2016. Zeolites in Fluid Catalytic Cracking (FCC), in: Xiao, F.-S., Meng, X. (Eds.), Zeolites in Sustainable Chemistry: Synthesis, Characterization and Catalytic Applications, Green Chemistry

and Sustainable Technology. Springer, Berlin, Heidelberg, pp. 271–297. https://doi.org/10.1007/978-3-662-47395-5_8

Kunii, D., Levenspiel, O., 1991. Fluidization Engineering. Butterworth-Heinemann.

Mohabeer, C., Reyes, L., Abdelouahed, L., Marcotte, S., Buvat, J.-C., Tidahy, L., Abi-Aad, E., Taouk, B., 2019. Production of liquid bio-fuel from catalytic de-oxygenation: Pyrolysis of beech wood and flax shives. J. Fuel Chem. Technol. 47, 153–166. https://doi.org/10.1016/S1872-5813(19)30008-8

Naqvi, S.R., Uemura, Y., Yusup, S.B., 2014. Catalytic pyrolysis of paddy husk in a drop type pyrolyzer for bio-oil production: The role of temperature and catalyst. J. Anal. Appl. Pyrolysis 106, 57–62. https://doi.org/10.1016/j.jaap.2013.12.009

Rover, M.R., Johnston, P.A., Whitmer, L.E., Smith, R.G., Brown, R.C., 2014. The effect of pyrolysis temperature on recovery of bio-oil as distinctive stage fractions. J. Anal. Appl. Pyrolysis 105, 262–268. https://doi.org/10.1016/j.jaap.2013.11.012

Sadaka, S., Boateng, A.A., 2009. Pyrolysis and bio-oil. [Cooperative Extension Service], University of Arkansas, US Department of Agriculture, and County Governments Cooperating, https://www.academia.edu/4469223/Pyrolysis_and_Bio_Oil.

Zhang, H., Nie, J., Xiao, R., Jin, B., Dong, C., Xiao, G., 2014. Catalytic Co-pyrolysis of Biomass and Different Plastics (Polyethylene, Polypropylene, and Polystyrene) To Improve Hydrocarbon Yield in a Fluidized-Bed Reactor. Energy Fuels 28, 1940–1947. https://doi.org/10.1021/ef4019299

Conclusion and Perspectives

CONCLUSIONS AND PERSPECTIVES

Conclusions:

The objective of this work was to provide a detailed analysis of the pyrolysis and co-pyrolysis products obtained from plastics and lignocellulosic biomass as beech wood with and without the use of a catalyst. The process was carried out in two different reactors: a semi-continuous reactor (tubular reactor) and a continuous reactor (fluidized bed reactor). The main aim was to improve the quality of the produced oil from biomass via the synergy between plastics and the de-oxygenation capacity of the catalyst.

At first, the individual pyrolysis of plastics (PS, HDPE, LDPE, PP) and their mixture were carried out in a semi-continuous reactor at different temperatures. It was found that all plastics exhibited a high heating value similar to that of diesel and gasoline, however, the possible utilization of each oil was different. For instance, PS yielded high percentages of styrene, which is useful in petrochemical industries. HDPE and LDPE yielded similar pyrolytic oil of consecutive triplet series of linear aliphatic hydrocarbons at each carbon number, alkane, 1-alkene, 1, (N-1)-alkadiene. The products can be fractionated into valuable products. For PP, the pyrolysis oil could be used as a fuel after treatment or blended with conventional fuels. Finally, the mixing of the plastics yielded better quality, without any additional post-treatment, oil to be used as fuel.

Plastics were then mixed with BW to study the possible synergistic interactions between them. BW bio-oil was mainly composed of acetic acid, levoglucosan, and ketones with very low heating value and high oxygen content of around 18 MJ/Kg and 41 wt.%, respectively. It was concluded that all plastics improved the latter properties after mixing due to the plastic pyrolytic oil's good properties. However, additional analysis required the testing of the synergistic interaction between the 2 feedstocks. Olefinic polymers showed a negative synergy between

beechwood with an increase in oxygenated compounds. The case was different for the aromatic polymer PS, where a great increase in aromatic production was followed by a reduction of oxygen content to reach a low value of about 8 wt.% for the 50-50 BW-PS blend. The liquid oil produced could be still blended with gasoline to reduce its production and boost the octane number due to the high aromatic content.

Unfortunately, it cannot be used directly as fuel without treatment. The catalytic co-pyrolysis of BW and PS creates a good opportunity for the valorization of a widely known lignocellulosic biomass and to reduce the environmental hazard of PS. Several metal-modified zeolites (ZSM-5) were prepared and tested for the latter purpose. At first, the experiment was carried out as the previous experiment in a fixed bed reactor. The oil derived constituted mostly of aromatic compounds with a remarkable heating value of around 40 MJ/kg and a great reduction in oxygen content to just around 2 wt.% for the 50-50 BW-PS blend. These results led to conclude that the derived oil could be used as alternative gasoline after further testing or could be blended with gasoline due to its high aromaticity and low oxygen content. The study then went forward to describe a continuous reactor. A fluidized bed setup was established and the catalytic co-pyrolysis of PS and BW was also studied. A high-grade liquid oil was produced in high quantities and a continuous manner. The liquid product split into 2 different phases: an oil phase and an aqueous phase. The oil phase has low water content and has the most energetic value and thus can be used as fuel. However, the aqueous phase is considered to be in the majority of water (>50 wt.%) along with carboxylic acids, levoglucosan, and esters which can be extracted to be used as chemicals. In the end, using plastics and biomass to produce highly energetic oil is one step forward in the long journey toward energy security and waste management.

Perspectives:

The previously described work in this thesis provided a complete experimental lab-scale analysis of the pyrolysis and co-pyrolysis of plastics and lignocellulosic biomass. Some future recommendations will be proposed henceforth.

A. *Understanding the catalytic co-pyrolysis mechanisms of model molecules from each family to be able to establish a more detailed reaction pathway.*

While there is yet still controversy and ambiguity on how the 2 feedstocks interact, a further investigation of the mechanism is essential. To make such a mechanism model, at first model compounds should be specified. Usually, volatile compounds are the main reason for the interaction between plastics and biomass thus the main compounds of each chemical family in the volatile fraction should be considered to establish the reaction model. For this purpose, the fluidized bed setup would be ideal to test the interaction since most of the compounds would be liquid compounds.

B. *Setting up a model to describe the overall scale-up process of catalytic co-pyrolysis in a fluidized bed reactor coupled with a continuous regeneration unit.*

The previous work should be developed into an industrial-scale process to truly touch the impact of such a process. An exergetic and energetic balance followed by a kinetic study should be conducted for reactor scaling and design. Modeling could help researchers to have tangible parameter variation for any future plant design purposes. For the use of catalysts in a fluidized bed reactor, deactivation is considered to be a major problem. The technology is widely known especially in the petroleum industry through fluidized catalytic cracking (FCC). The technology is divided into a reaction section and a regeneration section. The regeneration usually takes place at a high temperature by direct burning of the catalyst. This model could be achieved and it also could be further studied to achieve regeneration at ambient temperature by using several solvents. Experimental tests are required in this matter to investigate its full potential.

Annexes

A. ANNEXES

This part presents supplementary data gathered in different tables that are related to the different results discussed in the text.

Table A.1. Overview experiments realized for pyrolysis of plastic.

Polymer	Temperature (°C)	Mass used (g) ±0.01
PP	450	3.0
	500	3.0
	550	3.0
	600	3.0
HDPE	450	3.0
	500	3.0
	550	2.5
	600	2.5
LDPE	450	2.5
	500	2.5
	550	2.5
	600	2.5
PS	450	3.0
	500	3.0
	550	3.0
	600	3.0
MP (34% PP-32% LDPE-21% HDPE-13% PS)	450	3.0
	500	3.0
	550	3.0
	600	3.0

Table A.2. LHV of different molecules (Perry's Handbook 7th 1997).

Component	LHV (MJ/kg)
N2	-
H2	112.0
CO	10.1
CH4	50.0
CO2	-
C2H2	48.3
C2H4	47.2
C2H6	47.5
C3H4	46.1
C3H6	45.8
C3H8	46.3

Table A.3. (a), (b), (c), (d), and (e): Correlations existing between and within pyrolytic oil chemical groups of (a) Mixed Plastic (b) Polypropylene, (c) Low-density polyethylene, (d) High-density polyethylene, (e) Polystyrene.

(a) Mixed Plastic

Families	Temperature	Paraffin Gasoline	Iso-Paraffin Gasoline	Olefin Gasoline	+Diolefin Gasoline	Naphthene Gasoline	Paraffin Diesel	Iso-Paraffin Diesel	Olefin Diesel	+Diolefin Diesel	Naphthene Diesel	Fuel Oil	BTX	Styrene monomer	Mono-Aromatics	Di-Aromatics	Tri-Aromatics
Temperature	1.00																
Paraffin Gasoline	0.73	1.00															
Iso-Paraffin Gasoline	-0.74	-0.09	1.00														
Olefin Gasoline	0.99	0.64	-0.81	1.00													
+Diolefin Gasoline	0.99	0.80	-0.67	0.97	1.00												
Naphthene Gasoline	-0.94	-0.53	0.87	-0.93	-0.92	1.00											
Paraffin Diesel	-0.99	-0.81	0.65	-0.97	-1.00	0.90	1.00										
Iso-Paraffin Diesel	-0.99	-0.69	0.76	-1.00	-0.98	0.91	0.98	1.00									
Olefin Diesel	-0.50	-0.87	-0.15	-0.45	-0.56	0.19	0.60	0.52	1.00								
+Diolefin Diesel	0.99	0.70	-0.78	0.98	0.99	-0.97	-0.98	-0.98	-0.42	1.00							
Naphthene Diesel	0.95	0.60	-0.82	0.94	0.94	-1.00	-0.92	-0.92	-0.26	0.98	1.00						
Fuel Oil	-0.92	-0.93	0.45	-0.86	-0.96	0.81	0.96	0.89	0.69	-0.91	-0.86	1.00					
BTX	0.88	0.96	-0.35	0.82	0.93	-0.73	-0.93	-0.85	-0.78	0.86	0.79	-0.99	1.00				
Styrene monomer	0.76	1.00	-0.13	0.68	0.82	-0.54	-0.83	-0.73	-0.89	0.72	0.61	-0.93	0.97	1.00			
Mono-Aromatics	0.99	0.78	-0.69	0.96	1.00	-0.94	-0.99	-0.97	-0.51	0.99	0.96	-0.96	0.92	0.80	1.00		
Di-Aromatics	-0.99	-0.64	0.82	-0.99	-0.97	0.97	0.97	0.98	0.38	-1.00	-0.98	0.88	-0.82	-0.67	-0.98	1.00	
Tri-Aromatics	-0.61	-0.98	-0.07	-0.53	-0.69	0.37	0.71	0.59	0.94	-0.56	-0.45	0.84	-0.90	-0.98	-0.66	0.51	1.00

(b) Polypropylene

Families	Temperature	Iso-Paraffin Gasoline	Olefin Gasoline	+Diolefin Gasoline	Naphthene Gasoline	Aromatics Gasoline	Iso-Paraffin Diesel	Olefin Diesel	+Diolefin Diesel	Acetylene Diesel	Naphthene Diesel	BTX	Fuel Oil
Temperature	1.00												
Iso-Paraffin Gasoline	0.79	1.00											
Olefin Gasoline	-0.07	0.56	1.00										
+Diolefin Gasoline	0.61	0.96	0.72	1.00									
Naphthene Gasoline	-0.22	-0.43	-0.44	-0.32	1.00								
Aromatic Gasoline	0.92	0.96	0.31	0.87	-0.30	1.00							
Iso-Paraffin Diesel	0.91	0.97	0.34	0.89	-0.32	1,00	1.00						
Olefin Diesel	-0.63	-0.53	0.01	-0.55	-0.52	-0.65	-0.64	1.00					
+Diolefin Diesel	-0.03	-0.42	-0.66	-0.39	0.95	-0.22	-0.24	-0.54	1.00				
Acetylene Diesel	-0.77	-0.47	0.29	-0.40	-0.46	-0.67	-0.65	0.94	-0.58	1.00			
Naphthene Diesel	-0.84	-0.81	-0.16	-0.77	-0.15	-0.90	-0.89	0.92	-0.20	0.89	1.00		
BTX	0.83	0.97	0.44	0.94	-0.20	0.98	0.98	-0.72	-0.18	-0.66	-0.93	1.00	
Fuel Oil	-0.08	-0.54	-0.75	-0.75	-0.19	-0.41	-0.43	0.58	0.03	0.27	0.55	-0.60	1.00

Olefin Gasoline	Temperature	2,4-Dimethyl-1-heptene	5-Ethyl-1-nonene	1-Undecene	Cyclohexane, 1-methyl-4-(1-methylethylidene)-
Temperature	1.00				
2,4-Dimethyl-1-heptene	-0.57	1.00			
5-Ethyl-1-nonene	0.70	0.04	1.00		
1-Undecene	0.19	0.56	0.83	1.00	
Cyclohexane, 1-methyl-4-(1-methylethylidene)-	0.97	-0.36	0.78	0.33	1.00

Olefin diesel	Temperature	3-Tetradecene, (Z)-	7-Tetradecene, (Z)-	4-Tetradecene, (Z)-	9-Octadecene, (E)-	3-Hexadecene, (Z)-	1-(isopropylidenecyclopropyl)-Hexane	1-Undecene, 8-methyl-
Temperature	1.00							
3-Tetradecene, (Z)-	-0.60	1.00						
7-Tetradecene, (Z)-	-0.90	0.89	1.00					
4-Tetradecene, (Z)-	-0.88	0.84	0.96	1.00				
9-Octadecene, (E)-	-0.93	0.86	0.99	0.95	1.00			
3-Hexadecene, (Z)-	0.31	0.56	0.14	0.04	0.07	1.00		
1-(isopropylidenecyclopropyl)-hexane	0.97	-0.60	-0.88	-0.80	-0.92	0.24	1.00	
1-Undecene, 8-methyl-	0.94	-0.38	-0.74	-0.67	-0.79	0.46	0.97	1.00

(c) Low-density polyethylene

Families	Temperature	Paraffin Gasoline	Olefin Gasoline	+Diolefin Gasoline	Paraffin Diesel	Olefin Diesel	+Diolefin Diesel	Fuel Oil
Temperature	1.00							
Paraffin Gasoline	0.32	1.00						
Olefin Gasoline	0.74	0.44	1.00					
+Diolefin Gasoline	0.65	0.37	0.99	1.00				
Paraffin Diesel	-0.78	-0.11	-0.94	-0.93	1.00			
Olefin Diesel	0.79	0.21	0.97	0.96	-0.99	1.00		
+Diolefin Diesel	0.74	0.29	0.99	0.99	-0.98	0.99	1.00	
Fuel Oil	-0.73	-0.41	-0.99	-0.99	0.94	-0.97	-0.99	1.00

Paraffin Gasoline	Temperature	Undecane	Decane	Nonane	Octane
Temperature	1.00				
Undecane	-0.67	1.00			
Decane	-0.63	0.99	1.00		
Nonane	-0.67	0.99	0.99	1.00	
Octane	0.73	-0.51	-0.52	-0.58	1.00

Olefin Gasoline	Temperature	1-Decene	1-Undecene	1-Nonene
Temperature	1.00			
1-Decene	0.75	1.00		
1-Undecene	0.74	0.99	1.00	
1-Nonene	0.76	0.99	0.99	1.00

Paraffin Diesel	Temperature	Dodecane	Tridecane	Tetradecane	Pentadecane	Heptadecane	Hexadecane	Octadecane	Nonadecane
Temperature	1.00								
Dodecane	-0.62	1.00							
Tridecane	-0.78	0.97	1.00						
Tetradecane	-0.81	0.96	0.99	1.00					
Pentadecane	-0.82	0.94	0.98	0.99	1.00				
Heptadecane	-0.81	0.93	0.97	0.99	0.99	1.00			
Hexadecane	-0.82	0.94	0.99	0.99	0.99	0.99	1.00		
Octadecane	-0.79	0.95	0.98	0.99	0.99	0.99	0.99	1.00	
Nonadecane	-0.78	0.96	0.98	0.99	0.99	0.99	0.99	0.99	1.00

Olefin Diesel	Temperature	1-Dodecene	1-Tetradecene	1-Pentadecene	Cetene	1-Heptadecene	1-Octadecene	1-Nonadecene	1-Eicosene	1-Tridecene
Temperature	1.00									
1-Dodecene	0.73	1.00								
1-Tetradecene	0.71	0.99	1.00							
1-Pentadecene	0.70	0.99	0.99	1.00						

Cetene	0.69	0.99	0.99	0.99	1.00					
1-Heptadecene	0.68	0.98	0.99	0.99	0.99	1.00				
1-Octadecene	0.66	0.98	0.99	0.99	0.99	0.99	1.00			
1-Nonadecene	0.62	0.96	0.98	0.99	0.99	0.99	0.99	1.00		
1-Eicosene	0.52	0.91	0.94	0.96	0.96	0.97	0.97	0.99	1.00	
1-Tridecene	0.89	0.90	0.92	0.92	0.92	0.91	0.91	0.90	0.85	1.00

(d) High-density polyethylene

Families	Temperature	Paraffin Gasoline	Olefin Gasoline	+Diolefin Gasoline	Paraffin Diesel	Olefin Diesel	+Diolefin Diesel	Fuel Oil
Temperature	1.00							
Paraffin Gasoline	-0.18	1.00						
Olefin Gasoline	0.80	0.41	1.00					
+Diolefin Gasoline	0.84	0.34	0.99	1.00				
Paraffin Diesel	-0.54	0.89	0.07	-	1.00			
Olefin Diesel	0.71	-0.67	0.17	0.23	-0.93	1.00		
+Diolefin Diesel	0.88	-0.58	0.43	0.49	-0.87	0.95	1.00	
Fuel Oil	-0.86	-0.34	-0.99	-0.99	0.05	-0.32	-0.54	1.00

Paraffin Gasoline	Temperature	Undecane	Decane	Octane	Nonane
Temperature	1.00				
Undecane	-0.96	1.00			
Decane	-0.67	0.45	1.00		
Octane	0.66	-0.82	0.11	1.00	
Nonane	-0.77	0.58	0.98	-0.03	1.00

Olefin Gasoline	Temperature	1-Decene	1-Undecene	1-Nonene
Temperature	1.00			
1-Decene	0.77	1.00		
1-Undecene	0.93	0.95	1.00	
1-Nonene	0.70	0.99	0.91	1.00

Paraffin Diesel	Temperature	Dodecane	Tridecane	Tetradecane	Pentadecane	Hexadecane	Heptadecane	Octadecane	Nonadecane	Eicosane
Temperature	1.00									
Dodecane	-0.91	1.00								
Tridecane	-0.95	0.99	1.00							
Tetradecane	-0.97	0.98	0.99	1.00						
Pentadecane	-0.98	0.96	0.99	0.99	1.00					
Hexadecane	-0.99	0.95	0.98	0.99	0.99	1.00				
Heptadecane	0.46	-0.06	-0.16	-0.25	-0.29	-0.36	1.00			
Octadecane	0.47	-0.07	-0.17	-0.26	-0.31	-0.37	0.99	1.00		
Nonadecane	0.40	-	-0.10	-0.19	-0.24	-0.30	0.99	0.99	1.00	
Eicosane	-0.99	0.94	0.97	0.99	0.99	0.99	-0.40	-0.41	-0.34	1.00

Olefin Diesel	Temperature	1-Tetradecene	1-Dodecene	1-Tridecene	1-Pentadecene	Cetene	1-Heptadecene	1-Octadecene	1-Nonadecene	1-Eicosene
Temperature	1.00									
1-Tetradecene	0.98	1.00								
1-Dodecene	0.98	0.96	1.00							
1-Tridecene	0.99	0.98	0.99	1.00						
1-Pentadecene	0.96	0.99	0.92	0.95	1.00					
Cetene	0.92	0.96	0.85	0.89	0.99	1.00				
1-Heptadecene	-0.61	-0.58	-0.76	-0.71	-0.47	-0.34	1.00			
1-Octadecene	-0.63	-0.60	-0.78	-0.73	-0.49	-0.36	0.99	1.00		
1-Nonadecene	-0.67	-0.64	-0.81	-0.76	-0.54	-0.41	0.99	0.99	1.00	
1-Eicosene	0.19	0.25	-	0.07	0.37	0.50	0.65	0.63	0.59	1.00

(e) Polystyrene

Families	Temperature	BTX	Mono-Aromatics (Low BP)	Di-Aromatics (Medium BP)	Tri-Aromatics (High BP)	Styrene monomer
Temperature	1.00					
BTX	0.94	1.00				
Mono-Aromatics (Low BP)	0.95	0.99	1.00			
Di-Aromatics (Medium BP)	-0.92	-0.99	-0.99	1.00		
Tri-Aromatics (High BP)	-0.76	-0.52	-0.55	0.47	1.00	
Styrene monomer	0.97	0.99	0.99	-0.99	-0.61	1.00

Di-aromatics	Temperature	2,4-Diphenyl-1-butene	Bibenzyl	2,5-Diphenyl-1,5-hexadiene	1,2-Diphenylcyclopropane	Benzene, 1-methyl-3-(2-phenylethenyl)-, (E)-	1-(4-Methylphenyl)-4-phenylbuta-1,3-diene	Benzene, 1,1'-(1-butene-1,4-diyl)bis-, (Z)-	Benzene, 1,1'-(1-methyl-1,2-ethanediyl)bis-	(E)-Stilbene	Benzene, 1,1'-(1,3-propanediyl)bis-
Temperature	1.00										
2,4-Diphenyl-1-butene	-0.98	1.00									
Bibenzyl	0.65	-0.56	1.00								
2,5-Diphenyl-1,5-hexadiene	-0.51	0.64	0.26	1.00							
1,2-Diphenylcyclopropane	-0.87	0.91	-0.19	0.86	1.00						
Benzene, 1-methyl-3-(2-phenylethenyl)-, (E)-	-0.75	0.60	-0.68	-0.02	0.48	1.00					
1-(4-Methylphenyl)-4-phenylbuta-1,3-diene	-0.85	0.87	-0.83	0.28	0.59	0.50	1.00				
Benzene, 1,1'-(1-butene-1,4-diyl)bis-, (Z)-	0.19	-0.31	-0.61	-0.92	-0.65	0.22	0.12	1.00			
Benzene, 1,1'-(1-methyl-1,2-ethanediyl)bis-	0.44	-0.31	0.96	0.52	0.07	-0.63	-0.65	-0.80	1.00		
(E)-Stilbene	0.95	-0.99	0.49	-0.71	-0.92	-0.50	-0.85	0.39	0.23	1.00	
Benzene, 1,1'-(1,3-propanediyl)bis-	0.53	-0.34	0.55	0.22	-0.26	-0.96	-0.25	-0.32	0.58	0.23	1.00

Table A.4. Percentage of chemical groups in pyrolytic oil recovered.

Plastic Type		Polypropylene				High-density polyethylene				Low-density polyethylene			
Temperature (°C)		450	500	550	600	450	500	550	600	450	500	550	600
Chemical families (%)	Paraffin Gasoline	-	-	-	-	1.9	1.0	0.8	1.7	2.4	1.5	2.3	2.5
	Iso-Paraffin Gasoline	2.7	2.3	2.8	4.3	-	-	-	-	-	-	-	-
	Olefin Gasoline	28.0	21.2	21.2	27.4	3.4	3.3	3.6	7.6	4.7	5.1	4.4	10.6
	+Diolefin Gasoline	2.3	1.8	1.9	3.6	0.3	0.5	0.6	2.8	0.7	0.8	0.3	2.3
	Acetylene Gasoline	-	-	-	0.1	-	-	-	0.2	-	-	-	-
	Naphthene Gasoline	2.3	7.9	1.6	2.8	-	-	-	-	0.1	0.1	0.1	-
	Aromatic Gasoline	0.2	0.3	0.8	2.1	-	-	-	-	-	-	-	-
	Paraffin Diesel	0.1	0.2	0.3	-	10.6	8.2	6.4	8.8	11.0	9.0	10.5	6.5
	Iso-Paraffin Diesel	0.9	0.9	1.1	1.7	-	0.1	-	-	0.1	0.1	0.1	-
	Olefin Diesel	26.5	22.3	25.8	21.1	15.2	16.3	18.9	17.2	13.4	17.3	14.5	25.0
	+Diolefin Diesel	2.1	7.8	3.4	3.4	2.0	3.4	5.0	4.5	2.0	3.1	1.9	6.9
	Acetylene Diesel	1.0	0.6	0.8	0.5	-	-	-	-	-	-	-	-
	Naphthene Diesel	1.9	1.5	1.7	1.1	0.1	0.2	0.1	0.1	1.1	0.2	0.1	0.1
	Aromatic Diesel	0.2	-	-	-	-	-	-	-	-	-	-	-
	PAH	0.1	0.1	0.1	0.5	-	-	-	-	-	-	-	-
	BTX	-	0.1	0.3	2.3	-	-	-	0.2	-	-	-	0.5
	Fuel Oil	31.7	32.9	38.3	29.2	66.7	67.1	64.7	57.0	64.5	62.9	65.9	45.7
		Mixed Plastic (Experimental)				Mixed Plastic (Theoretical)							
	Paraffin Gasoline	3.2	3.0	3.0	4.6	1.2	0.7	0.9	1.2				
	Iso-Paraffin Gasoline	1.2	1.1	1.0	1.1	0.9	0.8	0.9	1.4				
	Olefin Gasoline	12.3	13.9	14.8	15.7	11.7	9.4	9.1	13.9				

	+Diolefin Gasoline	1.1	2.1	3.4	5.1	1.1	1.0	0.9	2.5
	Naphthene Gasoline	1.4	1.2	0.6	0.6	0.8	2.7	0.6	0.9
	Paraffin Diesel	4.9	4.3	3.6	2.5	5.8	4.7	4.9	3.9
	Iso-Paraffin Diesel	1.1	0.7	0.5	0.2	0.3	0.4	0.4	0.5
	Olefin Diesel	18.6	18.1	19.3	17.0	16.4	16.5	17.0	18.5
	+Diolefin Diesel	1.6	2.7	4.7	5.8	1.8	4.3	2.8	4.2
	Naphthene Diesel	0.5	0.6	1.0	1.1	1.0	0.6	0.6	0.4
	Fuel Oil	28.1	27.9	24.9	19.0	45.4	45.4	47.5	36.1
	BTX	0.8	0.9	1.3	3.0	-	0.1	0.3	1.4
	Styrene monomer	12.2	12.2	12.1	15.6	5.3	5.8	6.9	8.6
	Mono-Aromatics	0.7	1.2	2.4	3.4	0.2	0.2	0.7	1.6
	Di-Aromatics	11.6	9.4	6.5	5.2	6.7	6.4	5.8	3.5
	Tri-Aromatics	0.5	0.6	0.7	0.2	1.3	1.0	0.7	1.1
		Polystyrene							
	BTX	0.2	0.5	1.3	3.0				
	Mono-Aromatics (Low BP)	0.6	1.0	3.1	6.3				
	Di-Aromatics (Medium BP)	50.0	48.0	41.5	24.4				
	Tri-Aromatics (High BP)	9.5	7.4	4.9	6.6				
	Styrene monomer	39.7	43.2	49.3	59.7				

Table A.5. Composition of gas products and the yield of gas, liquid, and char of plastic pyrolysis as a function of temperature.

Plastic	Temp.(°C) ±5°C	Gas component (vol %)						Yield (wt.%)		
		H_2	CH_4	C_2H_4	C_2H_6	C_3H_6	C_3H_8	Gas	Liquid	Char
	450	5.8	12.5	15.3	18.4	25.0	23.1	1.1	97.3	1.6
	500	3.6	16.6	27.2	15.8	23.7	13.2	2.3	97.3	0.4
LDPE	550	4.3	19.1	33.6	13.1	23.4	6.6	5.3	94.7	-
	600	5.4	20.4	36.0	11.2	23.4	3.6	10.1	89.9	-
	450	5.3	8.9	13.8	13.4	27.3	25.6	0.6	99.4	-
	500	7.0	13.8	24.4	12.8	23.6	11.6	1.9	98.1	-
HDPE	550	4.6	18.2	34.0	12.0	24.5	5.7	5.2	94.8	-
	600	5.8	18.8	34.6	10.0	24.4	3.1	10.1	89.9	-
	450	1.9	8.6	1.8	14.5	69.5	3.7	2.4	97.6	-
PP	500	1.6	10.6	5.8	15.5	63.4	3.3	4.2	95.9	-
	550	2.8	15.4	11.5	15.0	52.6	2.7	10.9	89.1	-
	600	3.8	19.0	13.7	14.0	46.9	2.6	13.8	86.2	-
	450	37.3	12.7	44.7	5.3	-	-	-	100.0	-
PS	500	39.1	13.6	45.3	2.1	-	-	-	100.0	-
	550	41.8	13.8	37.1	1.5	5.8	-	0.1	99.9	-
	600	41.3	17.3	34.8	1.4	5.0	0.1	0.1	99.9	-
	450	14.8	10.9	9.2	13.7	40.7	10.7	2.2	97.8	-
MP	500	8.3	14.6	18.8	13.9	37.3	7.2	4.7	95.3	-
(Experimental)	550	15.2	16.6	22.5	11.8	30.1	3.7	11.2	88.8	-
	600	15.5	19.2	24.4	10.8	27.5	2.7	20.5	79.5	-
	450	4.6	10.1	6.8	15.5	52.8	10.2	1.3	98.2	0.5
MP	500	3.4	13.1	14.8	15.3	46.4	7.0	2.6	97.3	0.1
(Theoretical)	550	5.7	16.6	19.8	13.8	40.1	3.9	6.5	93.5	-
	600	7.2	19.5	23.7	12.3	34.4	3.0	10.1	90.0	-

Table A.6. List of the major products in BW-PP pyrolytic oil.

Compound	Percentages (wt %)		
	BW	BW-PP 50-50	PP
Furan	2.7	2.6	-
3,5-hexadien-2-ol	-	1.3	-
2,5-dimethylfuran	3.6	-	-
Acetic acid	33.6	16.3	-
1-hydroxy-2-propanone	8.0	3.7	-
1.2-ethanediol, monoacetate	3.5	2.3	-
1-propen-2-ol, acetate	-	2.6	-
Furfural	2.1	0.7	-
1.2-cyclopentanedione	1.8	-	-
Levoglucosan	8.4	5.3	-
2,4-dimethyl-1-heptene	-	16.4	29.5
5-ethyl-1-nonene	-	3.6	5.4
1,3,5-trimethyl-cyclohexane	-	0.5	1.6
Gas yield	15.0	7.6	4.2
Liquid yield	65.0	77.1	95.9
Char yield	20.0	15.3	-

Table A.7. List of the major products in BW-PS pyrolytic oil.

Compound	Percentages (wt %)		
	BW	BW-PS 50-50	PS
Furan	2.7	1.0	-
2,5-dimethylfuran	3.6	0.6	-
Acetic acid	33.6	6.3	-
1-hydroxy-2-propanone	8.0	1.5	-
1.2-ethanediol, monoacetate	3.5	-	-
Furfural	2.1	0.4	-
1.2-cyclopentanedione	1.8	0.3	-
Levoglucosan	8.4	2.7	-
Ethylbenzene	-	4.7	0.2
Styrene	-	57.5	73.8
α-methylstyrene	-	3.5	1.3
Bibenzyl	-	0.8	1.3

2,4-diphenyl-1-butene	-	5.1	12.5
1,3,5-triphenyl-cyclohexane	-	1.5	2.9
Gas yield	15.0	5.0	0.02
Liquid yield	65.0	84.7	99.9
Char yield	20.0	10.3	-

Table A.8. Oil composition (wt.%) of co-pyrolysis experiments over sand at 500 °C.

Feedstock	PS	BW-PS 50-50	BW
Carboxylic acids	-	23.2	34.1
Ester	-	0.3	5.2
Ether	-	-	0.6
Nitrogenates	-	-	0.7
Ketones	-	8.0	12.4
Furans	-	6.6	16.0
Aldehydes	-	1.5	4.1
Carbohydrates	-	14.1	23.8
Phenols	-	0.6	0.9
Alcohols	-	0.4	1.2
Guaiacols	-	-	1.1
Paraffins	-	-	-
Olefins	-	-	-
Aromatics	-	38.9	-
PAH	-	6.6	-